

**THE ROLE OF SOME CHROMATIN COMPONENTS IN
CHROMOSOME DYNAMICS IN PLANTS AND HUMANS**

By

Alghamdi Saeed Abdullah

A thesis submitted to
The University of Birmingham
for the degree of

DOCTOR OF PHILOSOPHY

Supervisor: Dr Eugenio Sanchez-Moran

**School of Biosciences
University of Birmingham
January 2015**

UNIVERSITY OF
BIRMINGHAM

University of Birmingham Research Archive

e-theses repository

This unpublished thesis/dissertation is copyright of the author and/or third parties. The intellectual property rights of the author or third parties in respect of this work are as defined by The Copyright Designs and Patents Act 1988 or as modified by any successor legislation.

Any use made of information contained in this thesis/dissertation must be in accordance with that legislation and must be properly acknowledged. Further distribution or reproduction in any format is prohibited without the permission of the copyright holder.

ABSTRACT

The chromatin provides a structural organization in which the DNA can be compacted up to 10,000-20,000 fold. Nevertheless, this compaction achieved by the chromatin structure has to be highly dynamic and controlled in order to allow the different vital processes of the DNA to occur such as transcription, replication, DNA repair, chromosome segregation and recombination (mitosis and meiosis). Nucleosomes are the basic unit of chromatin compaction that are positioned throughout the vast genomic DNA in higher eukaryotes. A nucleosome consists of a pair of each histone protein H2A, H2B, H3 and H4 and the associated 147 base pairs (bp) of DNA. They are important contributors to overall chromatin organization.

In this study we have analysed different histone H2A isoforms in *Arabidopsis thaliana*. We have analysed in more detailed the role of *HAT1* or *AtH2A1* (*RAT5*) gene which encodes for a histone H2A isoform which has been reported to be essential for the T-DNA integration by *Agrobacterium tumefaciens* into the *Arabidopsis* genome by root transformation. The mutant *Ath2a1/rat5* in *Arabidopsis* has showed chromosome fragmentation and anaphase bridges in mitosis. Furthermore, different connections between non-homologous and homologous chromosomes have been identified during diakinesis and the presence of anaphase bridges has also been observed at meiotic anaphase I.

We have also analysed different chromatin components named High Mobility Group proteins. Structure Specific Recognition Protein 1 (SSRP1) is an HMG protein that has been investigated in *Arabidopsis thaliana*. It has reported to play an important role in DNA repair response, in DNA replication, and elongation and regulation of the transcription machinery.

In an *Arabidopsis Atssrp1* mutant we have observed defects during the meiotic anaphase I and anaphase II that led to errors in chromosome segregation and reduced fertility.

We have also carried out a Small interfering RNA (siRNA) strategy to reduce the expression of hSSRP1 in endothelial cells. The knocked down cells showed a clear reduction of beta-tubulin microtubules in the mitotic spindle and errors in their organization that led to a poor alignment of the chromosomes and missegregation. Furthermore, DNA repair and cytokinesis were also affected in the siRNA knockdowns. Immunolocalization of hSSRP1 and hSPT16 have shown that both could be involved in DNA repair when localising to the chromatin forming the FACT complex but also they could be deeply involved in spindle formation and organization in higher eukaryotes. Especially, since hSSRP1 localises in the centrioles.

ACKNOWLEDGEMENTS

The author would like to thank his supervisors Eugenio Sanchez-Moran and Sue Armstrong for providing him with the best guidance to achieve this thesis and also for their support of gaining the basic knowledge and skills to get me to this position. I would also like to thank all the lab technicians and students for their friendship and support.

I would like to acknowledge Karen Staples for keeping my plants growing at the best optimum conditions and being always looking after them. Furthermore, I am very pleased to thank Klarke Sample, a PhD student at the UoB Medical School, who facilitated the delivery of the studies in human cells (with the aid of his supervisor Roy Bicknell) and for his expertise in human cytological and molecular techniques. I am of course grateful to the Saudi government who kindly funded and supported me since I started my PhD project.

Table of Contents

ABSTRACT	2
ACKNOWLEDGEMENTS	4
LIST OF ABBREVIATIONS	13
CHAPTER ONE	18
INTRODUCTION	18
1.1 Chromatin	19
1.1.1 Classical model of chromatin structure.....	19
1.1.2 Nucleosome structure and Histone proteins.....	21
1.1.3 Some histone variants	22
1.1.4 Histone H1 and linker DNA.....	23
1.1.5 Chromatin Scaffold	24
1.1.6 Structure-specific recognition protein 1 (SSRP1).....	25
1.1.6.1 Role of FACT complex in chromatin	26
1.1.6.2 The role of SSRP1 in Microtubule development	27
1.1.7 Microtubules (MTs)	27
1.1.7.1 Microtubule Nucleation	28
1.1.7.2 γ -tubulin organization in <i>Arabidopsis thaliana</i>	29
1.1.8 <i>Arabidopsis</i> Kinesin.....	32
1.1.8.1 Microtubules organization in ATK1 and ATK5	33
1.2 Mitosis and meiosis	34
1.2.1 Kinetochore Assembly at Centromeres.....	39
1.2.2 Chiasmata formation in <i>Arabidopsis</i>	42
1.3 DNA double strand breaks and homologous recombination	42
1.3.1 Meiotic Homologous Recombination (HR).....	44
1.3.1.1 Initiation of DNA DSBs.....	44
1.3.1.2 The processing of meiotic DNA DSBs.....	46
1.3.1.3 Synthesis-dependant strand annealing (SDSA)	50
1.3.1.4 The first class (class I) of COs pathway	50
1.3.1.5 The second class (class II) of COs pathway	51
1.3.2 Non Homologous End Joining (NHEJ)	52
1.4 Project aims	54
CHAPTER TWO	56
Material and methods	56
2.1 Plant material	57
2.1.1 Plant growth conditions	59

2.2 Bacteria growth media	59
2.2.1 Lysogeny Broth (LB media)	59
2.2.2 Lysogeny Broth Agar (LBA Media).....	59
2.2.3 Required growth conditions for bacteria.....	60
2.2.4 Bacteria culture	60
2.3 Molecular genetics	60
2.3.1 Plant DNA extraction (<i>Arabidopsis leaves</i>).....	60
2.3.2 Polymerase chain reaction (PCR)	61
2.3.3 Preparation of gel electrophoresis.....	61
2.3.4 Gel purification	62
2.3.5 Restriction enzyme digestion	63
2.3.6 Ligation of DNA fragments into a vector	63
2.3.7 Isolation of plasmid from bacteria	64
2.3.8 RNA purification from plant tissues	65
2.3.9 Reverse transcriptase-polymerase chain reaction (RT-PCR).....	65
2.4 Cytological analysis of <i>Arabidopsis thaliana</i> chromosomes	67
2.4.1 Chromosome fixation.....	67
2.4.2 Chromosome spreading.....	67
2.4.3 DAPI staining.....	68
2.4.4 Fluorescence microscopy	68
2.4.5 Imaging	68
2.5 Immunolocalization	68
2.5.1 Slides washing.....	68
2.5.2 Phosphate buffer solution (PBS).....	69
2.5.3 Block solution	69
2.5.4 Spreading technique	69
2.5.5 Squash technique.....	70
2.5.6 FLUTAX1 technique	71
2.6 T-DNA Transformation	73
2.6.1 Floral Dipping T-DNA Transformation.....	73
2.6.2 Selection of BASTA resistant <i>Arabidopsis</i> transformants.....	74
2.7 Immunolocalization for the human cells	75
2.7.1 Human Cell Culture	75
2.7.2 HUVEC Isolation	76
2.7.3 Cell culture.....	76
2.7.4 siRNA Transfection and Knockdown of ncRNAs	77

2.7.5 Real Time Quantitative Polymerase Chain Reaction.....	78
2.7.6 Immunocolization in human cells.....	79
CHAPTER THREE	81
Characterisation of histone AtH2A1 (RAT5).....	81
3.1 INTRODUCTION.....	82
3.1.1 Histone H2A1/RAT5.....	82
3.2 RESULTS	83
3.2.1 <i>In silico</i> identification of histone AtH2A isoforms.....	83
3.2.2 Fertility of <i>Ath2a</i> mutant isoforms.....	86
3.2.3 Identification and characterisation of an <i>Ath2a1/rat5</i> T-DNA insertion mutant line.....	91
3.2.4 Phenotype of <i>Ath2a1/rat5</i> mutant line.....	93
3.2.5 Meiotic and mitotic cytogenetic analysis of wild-type and <i>Ath2a1/rat5</i> mutant plants	94
3.2.6 Quantification of the meiotic and mitotic chromosome abnormalities in <i>Ath2a1/rat5</i> mutant	101
3.3 Immunolocalisation of different meiotic proteins in <i>Ath2a1/rat5</i> mutant	102
3.3.1 AtASY1 and AtRAD51 immunolocalisation in <i>Ath2a1/rat5</i> mutant.....	102
3.4 Genetic analysis of the T-DNA transformation of <i>Arabidopsis</i> by Floral Dipping	105
3.5 DISCUSSION	111
3.5.1 Histone H2A isoforms in <i>Arabidopsis thaliana</i>	111
3.5.2. Different roles for AtH2A1/RAT5 histone protein in <i>Arabidopsis</i>	113
3.5.3 Anaphase bridges/chromosome lagging in <i>Ath2a1/rat5</i> mutant.....	114
3.5.4 <i>Agrobacterium tumefaciens</i> T-DNA integration during Floral Dipping is not dependent of AtH2A1/RAT5 but on DSB formation and processing by HR and NHEJ pathways	120
CHAPTER FOUR.....	130
Characterisation of <i>AtSSRP1</i>	130
4.1 INTRODUCTION.....	131
4.1.1 High mobility group proteins (HMG).....	131
4.2. RESULTS	135
4.2.1 Fertility characterisation in <i>Athmg</i> mutants in <i>Arabidopsis</i>	135
4.2.2 Characterisation of <i>Atssrp1</i> mutant.....	141
4.2.3 Plant phenotype for <i>Atssrp1</i> mutant.....	144
4.2.4 Expression of AtSSRP1 in <i>Arabidopsis thaliana</i>	146
4.2.5 Cytogenetic analysis of the male meiosis in <i>Atssrp1</i> mutant.....	147
4.2.6 Cytogenetic analysis of the mitotic division in <i>Atssrp1</i> mutant.....	149
4.2.7 Quantification of meiotic chromosome missegregation in <i>Atssrp1</i>	151
4.2.8 Immunolocalization of AtASY1 and AtZYP1 on both wild-type and <i>Atssrp1</i> mutant	152

4.2.9 Localization and distribution of microtubule spindles during meiosis and mitosis in <i>Arabidopsis</i>	155
4.2.10 Immunolocalisation of AtSSRP1 in wild-type and <i>Atssrp1</i> mutant	157
4.2.11 Immunolocalisation of AtSPT16 in the wild-type	161
4.2.12 Dual immunolocalisation of AtSPT16 and AtSSRP1 in the wild-type	164
4.2.13 Characterization of <i>Atk1</i> mutant	168
4.3 DISCUSSION	173
4.3.1 HMG proteins roles.....	173
4.3.2 AtSSRP1 role in microtubule and spindle stability and organization is important for accurate chromosome segregation	175
4.4 Kinesin AtK1 might have also an important role in accurate organization of the <i>Arabidopsis</i> spindle in mitosis and meiosis.....	179
CHAPTER FIVE.....	182
Characterisation of human <i>hSSRP1</i> gene function.....	182
5.1 INTRODUCTION.....	183
5.2 RESULTS	185
5.2.1 <i>In silico</i> analysis of SSRP1 protein in different species	185
5.2.2 hSSRP1 and hSPT16 localisation in different human somatic cells.....	187
5.2.2.1 hSSRP1 localisation in human endothelium cells.....	187
5.2.2.2 hSSRP1 localisation in human fibroblast cells	191
5.2.2.3 hSPT16 localisation in human endothelium cells	192
5.2.2.4 Co-localisation of hSSRP1 and hSPT16 in human endothelium cells.....	193
5.2.3 Characterisation of siRNA <i>hssrp1</i> knockdown mutants in human endothelium cells.....	194
5.2.3.1 Design of siRNA constructs for <i>hSSRP1</i>	194
5.2.3.2 Q-PCR analysis of <i>hssrp1</i> knockdown mutant cells	195
5.2.3.3 Cytological analysis of <i>hssrp1</i> knockdown mutant cells	196
5.3 DISCUSSION	199
5.3.1 hSSRP1 and hSPT16 localise on chromatin and centrosome regions	199
5.3.2 siRNA <i>hssrp1</i> knockdown mutant cells possess an aberrant spindle and chromosome segregation	202
CHAPTER SIX	204
General Discussion and Conclusions.....	204
6.1 The importance of studying chromatin components.....	205
6.2 <i>Arabidopsis</i> Histone AtH2A isoforms	206
6.3 AtH2A1 (RAT5) is involved in DNA repair and recombination.....	209
6.4 Decoding the mechanisms of T-DNA integration using Floral Dipping	210
6.5 High Mobility Group (HMG) proteins and their role in plant fertility	212

6.6 <i>Arabidopsis</i> AtSSRP1 is involved in DNA repair and chromosome segregation during mitosis and meiosis.....	214
6.7 Human hSSRP1 localises in the centrioles and is essential for the correct mitotic spindle formation and organization	215
6.8 Evolutionary differences in spindle organization between plants and mammals	216
6.9 GENERAL CONCLUSIONS.....	218
6.10 Future Work.....	222
REFERENCES.....	223
APPENDIX.....	242
Appendix A: Full genomic DNA of H2A1 gene (RAT5).....	243
Appendix B: pEarleGate PEG205 vector	244
Appendix C: Full genomic DNA of SSRP1 gene (At3g28730).	245
Appendix D: Full genomic DNA of <i>hSSRP1</i> gene in human	246
Participation in International Scientific Conferences:	248
Other scientific activities	249

LIST OF FIGURES

Figure 1. The classical model of chromatin compaction.	20
Figure 2. Model of the structure and components of a nucleosome.	21
Figure 3. Schematic representation of the SSRP1 protein structure.	25
Figure 4. Schematic representation of the structure of MTs and g-TuRC complex in <i>A. thaliana</i>	31
Figure 5. Structure of kinesin motor protein.	33
Figure 6. Model of mitosis and meiosis.	35
Figure 7. Cohesin Complex Structure in budding yeast.	36
Figure 8. Graphic diagram to show the different stages of meiosis I.	38
Figure 9. Centromere and kinetochore structure in higher eukaryotes.	41
Figure 10. Multiprotein complexes involved in the formation of meiotic DSBs.	46
Figure 11. Pathways of homologous recombination.	47
Figure 12. Multiple alignments of histone H2A isoforms identified in <i>Arabidopsis thaliana</i>	85
Figure 13. Fertility evaluation of the different <i>Ath2a</i> isoform mutants evaluated.	90
Figure 14. Identification of an <i>AtH2A1/RAT5</i> gene and a T-DNA insertion mutant line.	92
Figure 15. Fertility reduction and delayed growth and development in <i>rat5</i> mutant plants.	94
Figure 16. Meiotic stages in <i>Arabidopsis thaliana</i> wild-type (Columbia).	96
Figure 17. Mitotic cell cycle in wild-type (Col) plants.	97
Figure 18. Meiotic stages in <i>Ath2a1/rat5</i> mutant (SALK-040809).	99
Figure 19. Anaphase-Telophase Mitotic stages in wild-type and <i>Ath2a1/rat5</i> mutant plants.	100
Figure 20. Diagrams representing the quantification of chromosome abnormalities observed in meiotic and mitotic divisions in <i>Ath2a1/rat5</i> mutant.	102
Figure 21. Dual immunolocalisation of AtASY1 (green) and AtRAD51 (red) during meiotic Prophase I in the wild-type and <i>Ath2a1/rat5</i> mutant.	104
Figure 22. Evaluation of T-DNA transformants by herbicide treatment.	107
Figure 23. Evaluation of the T-DNA integration in different mutants.	110
Figure 24. Schematic representation showing a proposed model to produce anaphase bridges, chromosome lagging and fragmentation.	116
Figure 25. Diagram representing different DSB repair pathway mutants involved in T-DNA integration by Floral Dipping.	129
Figure 26. Fertility evaluation for <i>Athmg</i> mutants.	140
Figure 27. Schematic representation of the structure of <i>AtSSRP1</i> gene and the location of the T-DNA insertion in the mutant analysed.	143
Figure 28. Plant phenotype in <i>Atssrp1</i> mutant.	145
Figure 29. RT-PCR electrophoresis photograph showing the expression of <i>AtSSRP1</i> gene in wild-type and <i>Atssrp1</i> mutant tissues.	146
Figure 30. Meiotic stages of PMCs in <i>Atssrp1</i> mutant line (SALK-001283).	149
Figure 31. Cytological analysis of the mitosis in wild-type and <i>Atssrp1</i> mutant.	150
Figure 32. Proportion of normal and abnormal meiotic chromosome segregation in the wild-type and <i>Atssrp1</i> mutant.	151
Figure 33. immunolocalisation of AtASY1 and AtZYP1 in both wild-type and <i>Atssrp1</i> mutant.	154
Figure 34. Staining of beta-tubulin in meiosis and mitosis in wild-type and <i>Atssrp1</i> mutant.	157
Figure 35. Dual immunolocalisation of beta-tubulin (green) and AtSSRP1 (red) during meiosis.	161
Figure 36. Dual immunolocalisation of beta-tubulin (green) and AtSPT16 (red) in wild-type meiosis.	163

Figure 37. Dual immunolocalisation of AtSSRP1(green) and AtSPT16 (red) in wild-type pollen mother cells.	167
Figure 38. <i>ATK1</i> gene structure, T-DNA insertion location and plant genotyping.	169
Figure 39. Semi-sterile phenotype in <i>Atk1</i> mutant.	171
Figure 40. Cytological analysis of the meiotic process in <i>atk1</i> mutant (SALK-043587).	172
Figure 41. Multiple amino acid sequence alignment of SSRP1 homologues in <i>Arabidopsis</i> , <i>Drosophila</i> and other mammalian species (human, mouse and rat).	187
Figure 42. Dual immunolocalisation for hSSRP1 and Beta-Tubulin in Human endothelium cells. ..	189
Figure 43. Immunolocalisation of hSSRP1 using a Z-stack acquisition of images for SSRP1 in endothelium cells.	191
Figure 44. Immunolocalisation of hSSRP1 on human fibroblasts.	191
Figure 45. Dual immunolocalisation for hSPT16 and Beta-Tubulin in human endothelium cells.	192
Figure 46. Immunolocalisation of hSSRP1 and hSPT16 in human endothelium cells.	193
Figure 47. Schematic representation of the structure of <i>hSSRP1</i> gene and the target location for the designed siRNAs.	194
Figure 48. Relative Expression of <i>hSSRP1</i> by qPCR in HUVEC.	196
Figure 49. Dual immunolocalisation of hSSRP1 and beta-tubulin in <i>hssrp1</i> knockdown and control cells (HUVEC).	198

LIST OF TABLES

Table 1. Components of some of MT associated proteins and their functions.	30
Table 2. T-DNA insertion mutant lines and their primers used for genotyping and for RT-PCR.	58
Table 3. Floral Dipping T-DNA transformation results.....	109
Table 4. <i>Arabidopsis</i> Histone AtH2A isoforms.	112
Table 5. Proportion of plants with T-DNA integration compared to the wild-type in different mutants of key components of HR and NHEJ.....	127
Table 6. Localization of AtSPT16 and AtSSRP1 during the <i>Arabidopsis</i> meiotic process.	179
Table 7. siRNA oligo sequences to target <i>hSSRP1</i>	195

LIST OF ABBREVIATIONS

3D-SIM	Three-dimensional structural illumination microscopy
Ab	Antibody
ADP	Adenosine 5'-Diphosphate
AE	Axial elements
ASY1	Asynaptic 1
<i>At</i>	<i>Arabidopsis thaliana</i>
ATP	Adenosine tri-phosphate
<i>AT-rich</i>	Adenine and Thymine-rich
ATK1	<i>Arabidopsis</i> Kinesin-1
ATK5	<i>Arabidopsis</i> Kinesin-5
ATM	Ataxia Telangiectasia Mutated
ATR	Ataxia Telangiectasia and Rad3-related protein
<i>AtPS1</i>	<i>Arabidopsis thaliana</i> Parallel Spindle 1
TAM	Tardy Asynchronous Meiosis
APC	Anaphase Promoting Complex
BRCA2	Breast Cancer type 2
BrdU	Bromodeoxyuridine
BSA	Bovine serum albumin
CE	Central Element
CenH3	Centromeric histone3
CAP	Chromosome associated protein
Cdc	Cell-division-cycle protein
cDNA	Copy DNA
CENP	Centromere protein
CO	Crossover
Col-0	<i>Arabidopsis</i> Columbia ecotype
D-loop	Displacement loop

DAPI	4, 6-diaminido-2-phenylindole
DEPC	Diethylpyrocarbonate
dHj	Double Holliday junction
DIG	Digoxygenin
D-loop	Displacement loop
DMC1	Disruption of meiotic control 1
DNA	Deoxyribonucleic acid
DNA-PK	DNA-Protein Kinase
DNA-PKcs	DNA-dependent Protein Kinase catalytic subunit
DYP	Dumpy chromosomes
DSB	Double strand break
EM	Electron microscope
FACT	FAcilitates Chromatin Transcription
FISH	Fluorescent <i>in situ</i> hybridisation
FITC	Fluorescein isothiocyanate
GAPD	Glyceraldehyde-3-phosphate dehydrogenase
GCP	Gamma-Tubulin Complex
GDP	Guanosine 5'-Diphosphate
GTP	Guanosine 5'-Triphosphate
g-TuRC	Gamma-Tubulin Ring Complex
HOP1	Homologue Pairing 1
H2AX	Histone 2AX
HMG	High Mobility Group Proteins
HR	Homologous Recombination
HUVEC	Human Umbilical Vein Endothelial Cells
LE	Lateral elements
Mer	Meiotic recombination defective

MLH	MutL homologue 1
MLH3	MutL homologue 3
MMS4	Methyl methanesulfonate sensitive 4
MRE11	Meiotic recombination 11
mRNA	Messenger RNA
MSH	MutS homologue
MUS81	MMS and UV sensitive 81
MTs	Microtubules
MTOCs	Microtubules Organization Centres
M/SARs	Matrix/Scaffold Attachment Regions
NASC	National <i>Arabidopsis</i> stock centre
NBS1	Nijmegen breakage syndrome 1
NCO	Non crossover
NCD	Non Claret Disjunctional
NHEJ	Non-Homologous End Joining
OSD1	Omission of Second Division
PBS	Phosphate buffered saline
PMC	Pollen mother cell
PCM	Pericentriolar Material
P53	Suppressor protein 53
qPCR	Reverse Transcriptase Quantitative PCR
rDNA	Ribosomal DNA
RNA	Ribonucleic acid
RNAi	RNA interference
RPA	Replication protein A
RT	Room temperature

RT-PCR	Reverse-transcription polymerase chain reaction
RAT	Resistance to <i>Agrobacterium</i> Transformation
SEI	Single-end invasion
SC	Synaptonemal complex
SDSA	Synthesis-dependant strand annealing
SDW	Sterile distilled water
SMC	Structural maintenance of chromosomes
SPO11	Sporulation specific protein 11
ssDNA	Single-stranded DNA
S-phase	Synthesis phase
SSRP1	Structure Specific Recognition Protein 1
SMG7	Suppressor with Morphogenetic Effect on Genitalia7
SPT16	SuPpressor of Ty 16
SYCP	Synaptonemal complex protein
T-DNA	Transfer DNA
Ti	Tumour Inducer
TF	Transverse filament
Topo	Topoisomerase
TFs	Transcription Factor
TUBG1	Bovine Tubulin gamma-1
<i>TUA</i>	<i>α-Tubulin</i> gene
<i>TUB</i>	<i>β-Tubulin</i> gene
<i>TUG</i>	<i>γ-Tubulin</i> gene
TDM	Three-Division Mutation
<i>vir</i>	Virulence gene

WT	Wild-type
γ -TuSC	γ -tubulin Small Complex
ZYP1	Synaptonemal Complex Protein 1

CHAPTER ONE

INTRODUCTION

1.1 Chromatin

An individual human body is normally built by around sixty trillion cells (Inoue *et al.*, 2005). Interestingly, each single cell in one individual contains the same genetic information (coded in the DNA) which is mainly organised inside the cell nucleus (Maeshima *et al.*, 2010). There are two main problems for the DNA: space and accessibility. First of all, DNA has to be accommodated into the nucleus. For instance, in humans, the different DNA molecules (chromosomes) are around 2 meters long and they have to be packed into a nucleus of 10 μm of diameter. Secondly, DNA has to be accessible for the different biological processes of the nucleus such as DNA replication, recombination, repair, gene expression, mitotic division and meiosis to produce sexual gametes (Maeshima *et al.*, 2010). The natural solution for these problems has been provided by the association of the DNA with different proteins forming a structure denominated chromatin. Chromatin is the fundamental component for DNA organization (Maeshima *et al.*, 2010) because of its dynamic structure which allows the correct packaging and the complete accessibility required for the different vital processes carried out by the DNA.

1.1.1 Classical model of chromatin structure

The classical model of the chromatin structure for higher eukaryotes can be divided in different hierarchical levels of DNA compaction (Luger *et al.*, 1997). Thus, the first level of chromatin compaction is the nucleosomal fibre also known as 10 nm fibre or ‘beads on a string’ due to its appearance that can be achieved when the double strand of DNA is wrapped around histones forming the nucleosome (Varga-Weisz and Becker, 2006). A further structure level is achieved by the compaction of the nucleosome fibre into a Higher Order

Chromatin fibre also known as the 30 nm fibre which compaction nature seems to be highly polymorphic among species, among different cell types and along different regions on the chromosomes (Luger *et al.*, 1997; Maeshima *et al.*, 2010). Furthermore, this Higher Order Chromatin fibre can be further compacted by attaching itself into organised loops attached to a proteinaceous structure or chromosome axis scaffold (Luger *et al.*, 1997) (**Figure 1**).

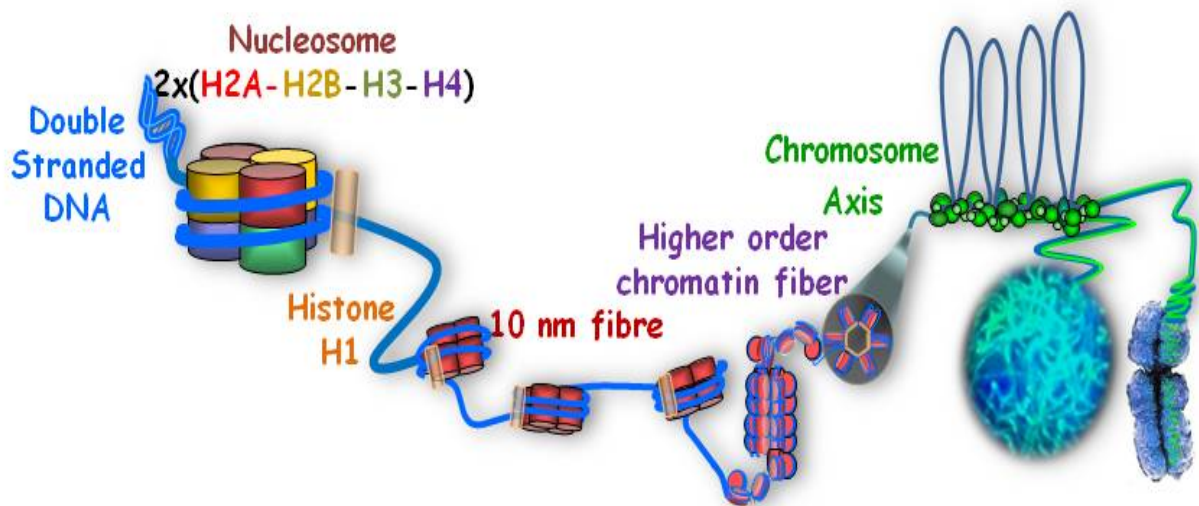


Figure 1. The classical model of chromatin compaction.

The figure shows the different levels of chromatin compaction: from the double stranded DNA, nucleosome fibre, Higher order chromatin fibre, chromosome axis, up to the mitotic metaphase chromosome. The first level of chromatin compaction is the nucleosomal fibre, also known as “10 nm” fibre or ‘beads on a string’ because of its appearance at the electron microscope (see image by Victoria Foe in Essential Cell Biology 4th ed. Page 185 Figure 5-20). The second level is the higher order chromatin fibre also known as 30 nm fiber. The next level is the association of chromatin loops into a chromosome axis or scaffold. The chromatin fibres attach to the scaffold by forming loops (Diagram drawn and conceived by E. Sanchez-Moran).

1.1.2 Nucleosome structure and Histone proteins

The nucleosome is the basic unit of the chromatin which consists of two pairs of each histone molecule: H2A, H2B, H3 and H4 (also known as core histones) wrapped by approximately 147 base pairs (bp) of DNA (Luger *et al.*, 1997) (**Figure 2**).

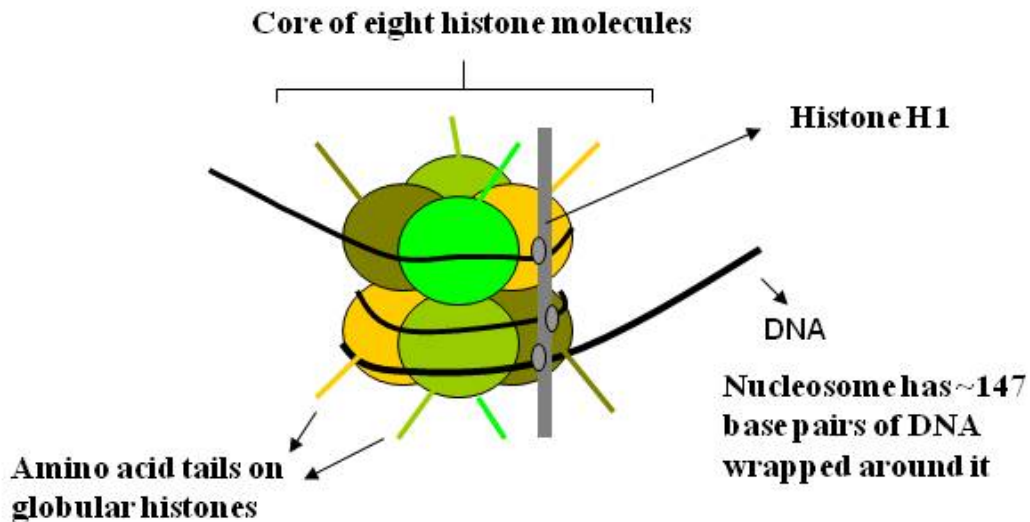


Figure 2. Model of the structure and components of a nucleosome.

The core histone octamer (2X H2A/H2B/H3/H4) is shown together with the double strand of DNA and linker histone H1 (Adapted from Belmont, 2006 and Hirs and Marra, 2009).

Histone proteins have a low molecular weight of approximately, 11,000-16,000 Dalton and between 102-135 amino acids. They are rich in lysine and arginine (20% of the amino acid composition) that gives a highly positive charge and contributes to the binding of the DNA (negatively charged by the phosphate groups). The DNA wraps around the histone octamer by approximately 1.75 turns. Core histones have a conserved structure with different folding domains that consist of 3 α -helices linked by two loops. It is thought that histone folding domains play an important role in the interaction between the histones themselves and with the DNA. Furthermore, the amino terminal regions of histones (N-terminal tails) contain a

high amount of lysines that protrude from the histone octamer (Bonenfant *et al.*, 2007). It is thought that these N-terminal tails are the target sites for post-translation modifications. Moreover, these N-terminal tails can provide a site for other protein interactions which may contribute to form the next level of chromatin compaction: the higher order chromatin (Valls *et al.*, 2005).

Chemical *in vitro* studies have shown that histones H2A and H2B appear to be a stable dimer (H2A/H2B) while histones H3 and H4 appear to be stable enough to form a tetramer ((H3/H4)²) (Kamakaka and Biggins, 2005). The association of DNA to these histones provide the stabilization of the octamer (Kamakaka and Biggins, 2005). *In vitro*, it has been observed that exposure to high salt concentrations (like 1M NaCl), can separate the histones from the octamer and from the DNA. On the other hand, when the concentration gets reduced gradually to about 650 mM and 300 mM NaCl, the core histones start joining to the naked DNA. Moreover, “beads on a string” structures can also be formed at a more reduced salt concentration of 50 mM (Zhang *et al.*, 2003).

1.1.3 Some histone variants

All eukaryotic histones are part of a large family of genes with several copies for each histone. Some are identical or nearly in sequence (core histones) and others are similar but with specific differences (histone variants). Core histones are deposited during DNA replication at the S-phase whereas histone variants can be deposited during different stages of the cell cycle (Kamakaka and Biggins, 2005). These histone variants have precise roles and are usually located at specific locations. For example, centromeric histone 3 (CenH3) also known as CENP-A in mammals is a histone variant for H3. This variant has an exclusive N-

terminus that does not exist within the core histone H3. CENP-A is located entirely at the centromere region and has not been discovered at any other regions of the chromosome. CENP-A has a particular role during cell cycle of facilitating the attachment of microtubules to the kinetochore (Sarma and Reinberg, 2005). Consequently, chromosomal centromeres can be properly functional and achieve the accurate chromosome segregation. On the other hand, H2A histone variants have been studied extensively. H2AX is a histone H2A variant which contains a conserved residue (Ser 139) at its C-terminus that gets rapidly phosphorylated as a result of responding to a DNA double strand break (Kamakaka and Biggins, 2005; Sarma and Reinberg, 2005).

It has been reported that 33 different histone proteins found in *A. thaliana* are encoded by 47 genes. Thirteen of these genes (*HTA1-13*) encode different H2A proteins, 11 different proteins of H2B have been found to be encoded by 11 *HTB* genes. A total of 8 different H3 proteins have been found to be encoded by 15 *HTR* genes and only one isoform of H4 protein have been found to be encoded by 8 *HFO* genes (Tenea *et al.*, 2009). *HTA1* is one of these genes that has been studied extensively because it seems to be necessary for the T-DNA transformation of *Agrobacterium tumefaciens*. It is reported that the disruption of this gene contributes to the resistance to *Agrobacterium* transformation (RAT) (Tenea *et al.*, 2009).

1.1.4 Histone H1 and linker DNA

Higher eukaryotic cells also have a linker histone (H1/H5). Histone H1 binds to the linker DNA that is located between the nucleosomes with a changeable length of 10-90 bp (Woodcock and Dimitrov, 2001). The linker histone proteins contain 2 globular domains located in their C- and N-terminal regions. They also contain 3 α -helix domains that may play

an important role in stabilizing the interaction between core histones and the associated DNA (Horn and Peterson, 2002). Moreover, it has been supposed that the linker histone proteins might play an important function in facilitating the chromatin folding to a higher order compaction and they are considered to be a target for post-translation modifications during cell cycle and development (Horn and Peterson, 2002).

1.1.5 Chromatin Scaffold

Non-histone proteins can also provide the structure of the chromatin by forming a chromosome axis and participating in the formation and attachment of the higher order chromatin loops. Particular DNA sequences (AT-rich DNA) are the base for the attachment of the chromatin loops to the protein scaffold also called matrix/scaffold attachment regions (M/SARs). These attachments comprise the anchor domains. M/SARs can contain around 70% of A/T nucleotides and be from 300bp up to 2kb in length in higher eukaryotes. The attachment between M/SARs and the scaffold is thought to play important functions such as the regulation of gene expression (De, 2002).

Arabidopsis thaliana possesses around 2,000 M/SARs that may influence gene expression. It has been estimated that 15% of transcription factor (TF) genes possess these attachment regions to the scaffold. Most of these TFs are involved in gene expression which is necessary for tissue and organ development. Several protein families have been located throughout the chromosome axis such as, stability maintenance of chromosomes proteins (SMC) and high mobility group proteins (HMG) (De, 2002).

1.1.6 Structure-specific recognition protein 1 (SSRP1)

Structure specific recognition protein 1 (SSRP1) is one component of the HMG protein family (Zeng *et al.*, 2010). It is an abundant protein that binds to chromatin and has been found to play a crucial role in the DNA repair response, DNA replication and the elongation and regulation of transcription machinery (Kumari *et al.*, 2009; Zeng *et al.*, 2010).

SSRP1 contains two conserved domains, the N-terminal that interacts with SPT16 protein (SuPpressor of Ty 16) and a tubulin binding domain. The association of SSRP1 and SPT16 forms the heterodimeric protein complex FACT (FACilitates Chromatin Transcription). The C-terminal domain of SSRP1 also includes an HMG domain which might play a key role in binding to DNA (**Figure 3**) (Kumari *et al.*, 2009; Zeng *et al.*, 2010). According to Zeng and collaborators (2010), the co-immunoprecipitation and mass spectrometry analysis for SSRP1 conducted to check the protein interactions of SSRP1 showed that α -tubulin is another protein that might associate with SSRP1 in addition to SPT16.

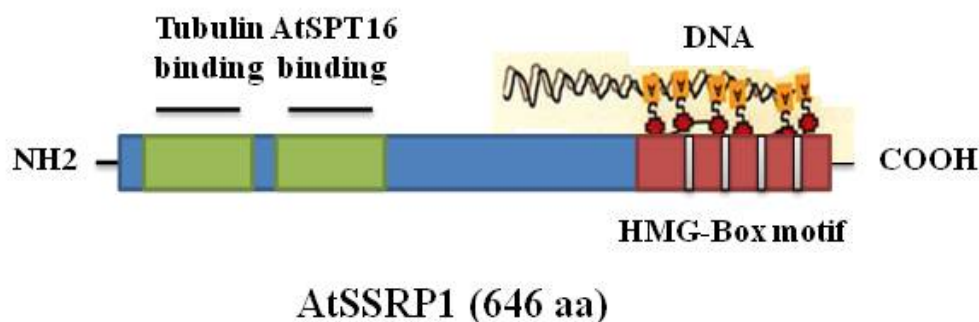


Figure 3. Schematic representation of the SSRP1 protein structure.

The diagram illustrates the structure of SSRP1 protein in *Arabidopsis thaliana* of which the red boxes include the AT-hook regions (HMG domain) that produce a high affinity of binding to DNA and the green box domains that bind into tubulin and SPT16 (Adapted from Zeng *et al.*, 2010; Kumari *et al.*, 2009).

1.1.6.1 Role of FACT complex in chromatin

Chromatin is comprised of DNA, histones and non-histone proteins that interact in a dynamic way in order to allow the several biological processes of the DNA. FACT is a complex of two proteins including SSRP1 and SPT16. FACT has been found to have a key function in chromatin condensation by the assembling and disassembling of some chromatin components like histone proteins (Laurentino *et al.*, 2011).

In 1998, the human FACT complex (hFACT) was revealed to be a necessary component for elongation of transcription throughout chromatin (Orphanides *et al.*, 198; Winkler *et al.*, 2011). The heterodimer proteins SSRP1 and SPT16 are essential for the FACT complex to allow cell division to take place correctly (Winkler *et al.*, 2011).

FACT has been described as a histone chaperone that plays a vital role of nucleosome organization over the chromatin (histone assemble and disassemble). Consequently, the DNA can be unwound and freed of histone proteins and in some cases to be accessible for several biological processes such as DNA replication, recombination, repair and gene transcription (Winkler *et al.*, 2011; Laurentino *et al.*, 2011). It has been found that FACT seems to have an important role in DNA repair and seems to be correlated with the activation of histone variant H2AX and P53 protein (Suppressor protein 53 in humans) as a response to DNA damage (Winkler *et al.*, 2011). Impacts on human cell viability have been observed when FACT is depleted (Laurentino *et al.*, 2011). FACT complex might also be playing a crucial role for gamete formation and development in human (Laurentino *et al.*, 2011).

The assembly of nucleosomes over the DNA take place gradually, (H3-H4)₂ tetramer firstly bind and rearrange along the DNA and (H2A-H2B) dimers join afterwards into the nucleosome structure (Winkler *et al.*, 2011). The FACT complex is capable of positioning and removing the nucleosomes along the DNA (Winkler *et al.*, 2011). The binding between

the complexes of hFACT and the histone dimers (H2A-H2B) can enable the release of nucleosomes to allow gene transcription machinery to access the DNA (Winkler *et al.*, 2011).

1.1.6.2 The role of SSRP1 in Microtubule development

The formation of microtubules (MTs) is a crucial process for chromosome movement and segregation during mitotic and meiotic divisions. SSRP1 protein seems to play a basic role of MT regulation and could even assist the polymerization of tubulin. Null mutants for *SSRP1* result in irregular chromosome segregation during mitosis in which the spindle structure and formation are defective (Zeng *et al.*, 2010).

1.1.7 Microtubules (MTs)

MTs are cylindrical structures that consist of a stable heterodimer of proteins including α - and β -tubulin subunits. The α - and β -tubulin dimers polymerize end to end producing a specific polarity. Thus, one end will have the α -tubulin exposed (- end) and the opposite end will have the β -tubulin exposed (+ end). The elongation of microtubules only occurs in the (+) ends (Struck and Dhonukshe, 2013; Hashimoto, 2013; Liu *et al.*, 1993). The α - and β -tubulin subunits bind to Guanosine 5'-Triphosphate (GTP). There is no hydrolysis of GTP when this is bound to α -tubulin but the GTP can be hydrolysed to GDP when it is bound to β -tubulin, therefore, indicating its involvement in MT polymerisation (Struck and Dhonukshe, 2013).

α - and β -tubulin dimers polymerize into protofilaments. The association of these protofilaments will form a MT. MTs are long cylinders of about 24 nm in diameter which are

hollow in the middle, formed by 13 globular protofilaments that are attached to each other (Hashimoto, 2013).

Several functions have been ascribed for MTs in eukaryotes (Eckardt, 2006). MTs are necessary for several biological processes including cell division, cell polarity, phragmoplast assembly, homologous chromosomes and sister chromatid segregation as well as being considered as a fundamental element for propagation in higher eukaryotic organisms (Eckardt, 2006).

1.1.7.1 Microtubule Nucleation

Different polymers can be formed by the interactions between MTs themselves; consequently, keeping them organized in arrays and bundles (Hashimoto, 2013). In animals, MTs are polymerized from microtubules organization centres (MTOCs) like centrosomes, while in plants MTs assemble in the absence of centrosomes (Pastuglia *et al.*, 2006). Nevertheless, it has been found that γ -tubulin works as an anchor for the nucleation and the organization of MTs in the plant kingdom (Liu *et al.*, 1993).

In the animal and fungi kingdoms, the γ -tubulin acts as a factor for the MTs nucleation which localizes in the MTOCs. In animals, MTs need to be growing in bundles and arrays that are organised by the centrosomes (animals) or the spindle pole body (fungi). The centrosome contains a pair of centrioles and pericentriolar material (PCM) that surrounds the centrioles. PCM contains several associated proteins including γ -tubulin, pericentrin and ninein (Eckardt, 2006). Furthermore, it has been found that the structure of γ -tubulin in animals is like a ring which helps form of the α - and β -tubulin heterodimer as well as maintaining their

stability. Additionally it helps MTs polymerization from (-) ends and it is a regulator of mitotic checkpoints (Eckardt, 2006).

However, in the plant kingdom there are not MTOCs. Instead, MTs in plants polymerise from a dispersed complex of proteins; these complexes of proteins include γ -tubulin that is found to be localised along MTs arrays (Eckardt, 2006). γ -tubulin plays an important role of MTs organization and nucleation in the plant kingdom. It is reported that when γ -tubulin is inhibited by using a specific antibody, it results in a failure of MT nucleation. Moreover, depletion of this protein can affect the mitotic process. For example loss of the protein is lethal during cotyledon growth, producing incorrect formation of phragmoplast and cell shape organization. In addition, using RNAi knockdown technology for both γ -tubulin genes (*TUBG1* and *TUBG2*), showed defects in the polarity formation of cells. Consequently, these observations confirm that this protein is necessary for MTs organization and distribution in plants (Eckardt, 2006).

1.1.7.2 γ -tubulin organization in *Arabidopsis thaliana*

The *A. thaliana* genome encodes for 6 α -Tubulin genes (*TUAs*), 9 β -Tubulin genes (*TUBs*) and 2 γ -Tubulin genes (*TUGs*) (Struck and Dhonukshe, 2013). MTs are developed from small polymerizing regions known as the gamma-tubulin ring complex (g-TuRC). Furthermore, the formation of MTs is dependent on the presence of the g-TuRC. It has been found that in plants the g-TuRC is made up of γ -tubulin and five other gamma-tubulin complex proteins (GCP2/3/4/5/6). Budding yeast has GCP2-3 that attaches to γ -tubulin to form a small complex known as γ -TuSC (Hashimoto, 2013; Struck and Dhonukshe, 2013). However, GCP4, GCP 5 and GCP 6 do not exist in budding yeast.

The abundance of these GCP proteins in *A. thaliana* is diverse, in which γ -tubulin is the highest abundance molecule compared to GCP2-3 while the lowest abundant proteins are GCP4, GCP5 and GCP6 (Liu *et al.*, 1993). **Table (1)** presents some different functions of tubulin components and their phenotypes when mutated in *A. thaliana*:

Protein	Function	Mutant phenotype
α-tubulin (1-6)	<ul style="list-style-type: none"> ✓ Essential for MT organization ✓ Attaches to GTP irreversibly ✓ MTs stability and orientation 	<ul style="list-style-type: none"> ✓ Alteration of MT polymerization ✓ Dwarf plant ✓ Reduction of root elongation ✓ Defect of MT orientation
β-tubulin (1-9)	<ul style="list-style-type: none"> ✓ Basic element for MT organization ✓ GTP was hydrolysed to GDP when bound to β-tubulin ✓ MT stability 	<ul style="list-style-type: none"> ✓ Helical MT arrangement
γ-tubulin (1-2)	<ul style="list-style-type: none"> ✓ Maintains MT formation ✓ essential for the development of mitotic spindle, phragmoplast and cortical microtubules 	<ul style="list-style-type: none"> ✓ Lethal to embryos (gametophytic or seeding stage) ✓ unbalance of MT array formation ✓ Disruption of both genes leading to abnormal phragmoplast formation ✓ Variation of nuclear division during gametophytes

Table 1. Components of some of MT associated proteins and their functions.

(Struck and Dhonukshe, 2013).

The g-TuRC includes two molecules (GCP2-GCP3) that join together to form the g-tubulin small complex (gTuSC) (**Figure 4**). However, other components (GCP4-GCP6) can create g-TuSC-like complexes (**Figure 4**); consequently, the assembly between two complexes (g-TuSC and g-TuSC-like sub-complex) would result in the production of inactive g-TuRC. Therefore, in the presence of other activating proteins and other targeting factors (sub-cellular molecules) to gTuRC, this leads to activation and polymerization of MTs (**Figure 4**) (Pastuglia, 2006; Hashimoto, 2013).

All GCPs have 2 motifs called GRIP1 and GRIP2 which play a crucial role by interacting between g-TuRC associated proteins. GRIP1 motif is the main component for all GCPs interactions. Furthermore, the GRIP2 motif assists binding between γ -tubulin and GCPs (Hashimoto, 2013).

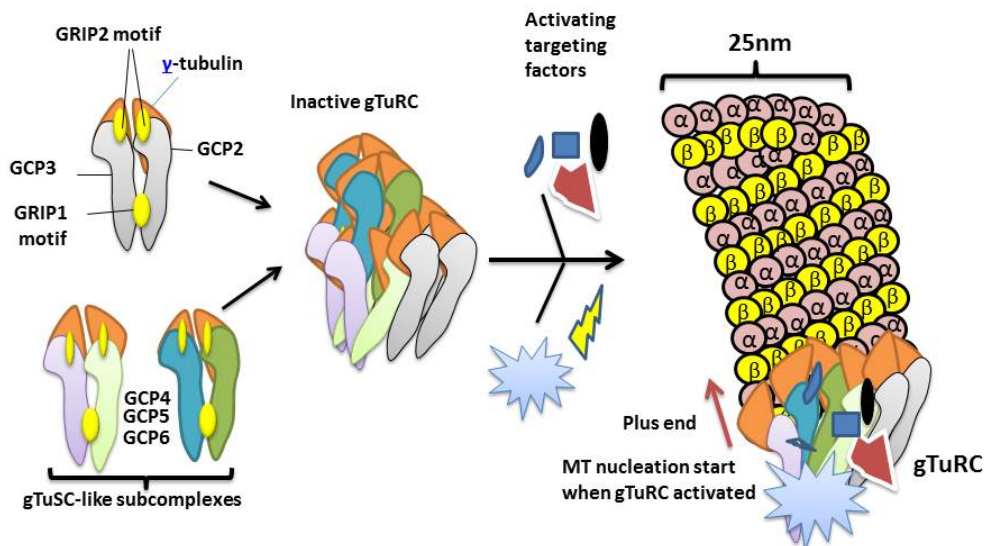


Figure 4. Schematic representation of the structure of MTs and g-TuRC complex in *A. thaliana*.

This model shows the structure of MTs and the assembly of g-TuRC that eventually plays a role for MTs nucleation (adapted from Hashimoto, 2013).

1.1.8 *Arabidopsis* Kinesin

The kinesin protein superfamily includes microtubule associated motor proteins that play a crucial role in the intracellular transport of proteins. Kinesin motor proteins are evolutionary conserved among all eukaryotic species. The kinesin motor proteins include a conserved domain that is essential for the movement of several cargo materials such as mRNA, organelles, signals and other protein mixtures (Li *et al.*, 2012; Zhu *et al.*, 2012).

Surprisingly, it is observed that the kinesin motor proteins are the target protein for microtubules within the cells. Therefore, it is found that kinesins also have a role in other biological processes such as microtubule attachment to the chromosome centromeres, sister chromatid separation to different poles (polarity), alignment of all chromosomes along the metaphase plate in both meiosis and mitosis and the nucleation of spindles (Li *et al.*, 2012). Moreover, the occurrence of the kinesin motor proteins facilitate cross-linking between MTs resulting in a parallel formation as well as focussing MTs to the minus (-) poles (Ambrose, 2007).

Kinesins have been categorized into two classes; the first class are the kinesins that are responsible for microtubule organization allowing microtubule mobility and cross-linking between microtubules. The second class are kinesins that maintain microtubule activity such as movement of cellular elements and are also responsible for linking between chromosomes and microtubules (Zhu *et al.*, 2012).

Kinesin motor proteins include a N-terminal domain that consists of two globular heads (attached to beta-tubulin), nick (target domains for the ATP hydrolysis that is essential for kinesin movement), two alpha helical coiled-coil tails (stalk) and C-terminals (light chains) that are responsible for cargo attachments (**Figure 5**) (Chen *et al.*, 2002; Ambrose, 2007).

Kinesins link to adenosine triphosphate (ATP) causing its hydrolysis that produces the energy to allow the kinesin movement. The kinesin family contains a distinctive catalytic core domain. This core domain consisting of 350 amino acids attaches to the microtubules binding domains and ATP. So when they attach with each other, the ADP is released resulting in a directional movement and orientation of the kinesin heads throughout microtubules (Zhu *et al.*, 2012).

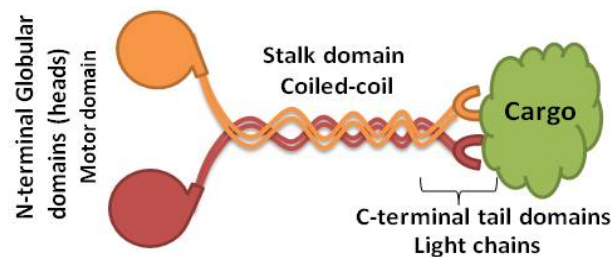


Figure 5. Structure of kinesin motor protein.

In *Arabidopsis*, it is estimated that kinesin is encoded by 61 genes classified into 14 different kinesin families (Ambrose, 2007; Chen *et al.*, 2002; Zhu *et al.*, 2012). In contrast, the human genome is predicted to have 45 kinesin genes (Zhu *et al.*, 2012). Bioinformatic analysis has been conducted on plant kinesins, and it has been found that plants have unique kinesins compared to animals. Therefore, it is predicted that kinesin motor proteins have a particular role in the plant kingdom such as microtubule assembly and organization (Zhu *et al.*, 2012).

1.1.8.1 Microtubules organization in ATK1 and ATK5

It has been determined that ATK1 and ATK5 are (-) end motor proteins that have a role of focusing microtubules in bundles toward to the (-) ends. It has been reported that these two proteins are localising at both spindle poles and at the midzone (Zhu *et al.*, 2012). By protein

sequence alignment, it has been found that the identity between these proteins is 83%. These proteins seem to be very important for the maturation of gametophytes (Zhu *et al.*, 2012).

Kinesin-5 family proteins are necessary for spindle development, and they arrange the spindle into anti-parallel microtubules and they localize on the midzone. The kinesin-5 family includes AtKRP125a, AtKRP125b and AtKRP125c proteins. The function of AtKRP125c seems to be a role in spindle organization. Furthermore, mutation of this gene leads to irregular mono-polar spindle formation as well as spindle fragmentation. The same phenotype has been observed in animals and fungi when kinesin-5 is mutated. In contrast, there was no defective spindle assembly or organization when *AtKRP125a* and *AtKRP125b* were mutated (Bannigan *et al.*, 2007; Zhu *et al.*, 2012).

Mutation of *atk1-1* produces unfocused spindles as well as defects in the bipolarity which leads to abnormalities in chromosome segregation (Zhu *et al.*, 2012). However, when *atk5-1* was mutated, spindle pole positions spread out during mitosis.

1.2 Mitosis and meiosis

The mitotic cycle is the biological process that allows one cell to produce two genetically identical daughter cells (**Figure 6**). These daughter cells share the same genetic information to that of the parental cell. For this to be possible, before the mitotic process is started, DNA replication is needed to take place during the S phase. Consequently, a pair of sister chromatids is produced for every chromosome (Blow and Tanaka, 2005). During the early mitotic stage (prophase), the sister chromatid pair is held to each other by the cohesin complex proteins, also known as sister chromatid cohesion (**Figure 7**).

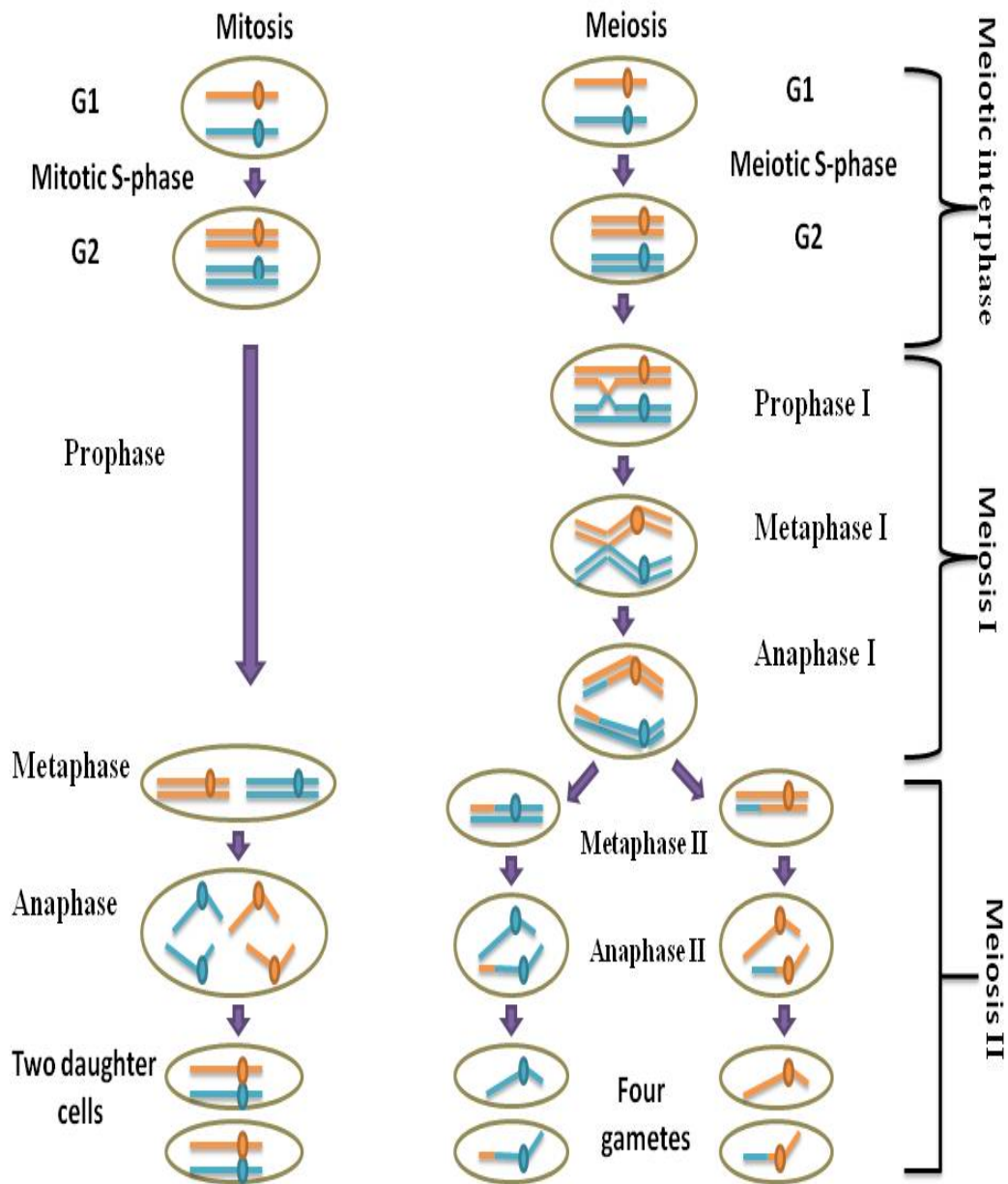


Figure 6. Model of mitosis and meiosis.

Diagram representation of mitosis and meiosis showing two homologous chromosomes differentiated by different colour: Paternal (orange) and maternal (blue).

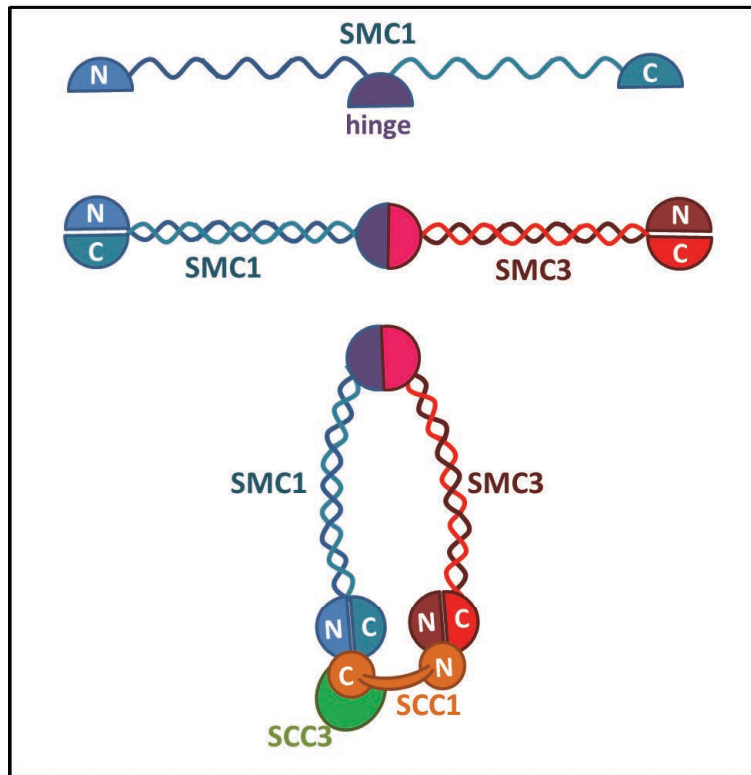


Figure 7. Cohesin Complex Structure in budding yeast.

Cohesin is an essential complex for facilitating the equal segregation between chromatids during mitosis and meiosis. The complex of cohesin in *Saccharomyces cerevisiae* includes four subunits: Smc1, Smc3, Scc1 and Scc3 which form a ring structure around the sister chromatids.

At the end of prophase, the mitotic spindle fibres start polymerising and the nuclear membrane breaks. The spindle attaches to the chromosome kinetochores at the centromeric regions. Consequently, at metaphase, chromosomes are aligned at the centre of cells known as metaphase plate or equatorial plate (Chan, 2003; Winey *et al.*, 1995). During anaphase, chromatid cohesion is released and chromatids are separated and pulled off from each other to opposite poles (Miller, 2000). Eventually, at telophase, chromatids begin to decondense, spindle disappears and the nuclear membrane is reformed around the chromosomes. At the end of telophase, cytokinesis occurs and the cytoplasm division occurs to produce two daughter cells. In plants, the cell wall can be constructed to form separate two daughter cells

whereas in mammalian cytoplasm is cleaved (Albertson *et al.*, 2005; Glotzer, 2005) (**Figure 6**).

Meiosis is the biological process that allows sexual reproduction to exist in higher eukaryotes. The purpose from meiosis is to generate four haploid gamete cells from a diploid cell. Thus, gametes carry half the quantity of the genetic material of the parental diploid cells of the organism (Ma, 2006).

Meiosis and gametogenesis in general, take place in a specific tissue of every organism to produce gametes (Hamoir, 1992). Meiosis involves two rounds of nuclear divisions, meiosis I (or first meiotic division) and meiosis II (or second meiotic division). During meiosis I, homologous chromosomes separate to different poles in a reductional division. Meiosis I stages include: prophase I, metaphase I, anaphase I and telophase I. Moreover, meiosis prophase I can be divided under five cytological sub-stages that include: leptotene, zygotene, pachytene, diplotene and diakinesis (Stack and Anderson, 2001; Zickler and Kleckner, 1999).

At the beginning of S-phase, cohesion is established between sister chromatids. The cohesin complex plays a very important role in keeping sister chromatids held together (Lee and Orr-Weaver, 2001; Nasmyth and Haering, 2005). During mitosis, cohesion is released between metaphase/anaphase stages which lead to proper segregations between sister chromatids to opposite poles. However during meiosis, cohesion is actually released at two different times. The first cohesion is released along the chromosome arms during anaphase I which contributes to the proper homologue segregation. Cohesin complex is maintained at the centromeres to hold the sister chromatids together until anaphase II. The second release occurs at the end of anaphase II in which cohesion is totally released from centromeres and sister chromatids are able to completely separate to opposite poles (Nasmyth and Haering, 2005).

After S-phase, DNA replication is completed and a pair of sister chromatids hold by cohesins formed each chromosome. Leptotene is the first visible stage of meiosis that can be identified. During leptotene, each chromosome starts to condense within the cell nucleus and appears as a thin and a long thread (La Cour and Wells, 1971). During zygotene, the homologous chromosomes start to align side by side. At the same time chromosome synapsis begins by the polymerisation of a special multiprotein structure (the synaptonemal complex or SC). Chromosome pairing and synapsis are fully completed at pachytene. During this stage, fully synapsed homologous chromosome pairs appear as thick threads. At diplotene, homologous chromosomes start to separate from each other as a result of the gradual depolymerisation of the SC. The homologous chromosomes start separating from each other excluding the regions where homologous recombination has taken place, crossovers (COs) also known cytologically as chiasmata (Albini and Jones 1984; Sanchez Moran *et al.*, 2001). Diakinesis is the last stage of prophase I. During this stage, homologous chromosome pairs, also known as bivalents, are further condensed (**Figure 8**).

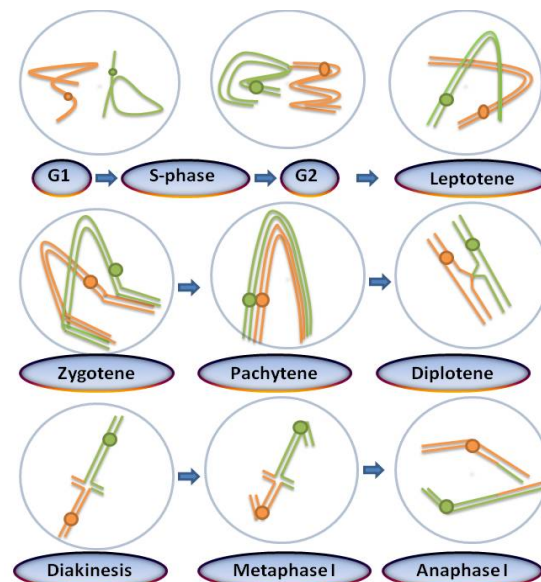


Figure 8. Graphic diagram to show the different stages of meiosis I.

Green chromosome (paternal) and Orange chromosome (maternal) are duplicated throughout S-phase.

During metaphase I, the nuclear membrane breaks and the spindle attaches to the kinetochores of each homologous chromosome connected with each other by the chiasmata (Crossovers) allowing the bivalents to orientate at the equatorial plate (Chan, 2003; Winey *et al.*, 1995). Consequently, this correct alignment of bivalents at the metaphase I plate leads to the accurate separation of the homologous chromosomes at anaphase I. During this stage, each one of the homologous chromosomes moves to the opposite poles of the cell. Eventually, at telophase I the nuclear membrane reforms into two haploid nuclei and the chromosomes get decondensed. The second nuclear division (meiosis II) is very similar to a mitotic division where the sister chromatids get separated. Consequently, in male meiosis four gametes are produced in which every cell has one haploid genome (Hamant *et al.*, 2006; Pawlowski *et al.*, 2004; Zickler and Kleckner, 1999).

1.2.1 Kinetochores Assembly at Centromeres

There are three key structures which allow the correct chromosome segregation during cell cycle and meiosis: the centromere (kinetochore), the sister chromatid cohesion and the spindle (MTs).

The centromere is a fundamental component for the correct chromatid segregation during mitosis (and second meiotic division) and for the segregation of homologous chromosomes during the first meiotic division. The chromatin around centromeres contains specific DNA sequences (tandem arrays of repeat sequences) and associated proteins which have been found to have an essential role of kinetochore assembly and sister chromatid cohesion. Abnormal behaviour of the centromere or the associated kinetochore can lead to aberrant chromosome divisions.

Kinetochores are complex dynamic structures which are composed of several different proteins. These proteins are assembled and disassembled during the cell cycle and play a crucial role for the accurate chromosome segregation during mitosis and meiosis. Some of these proteins are part of the centromeric chromatin as CENP-A which is a centromeric histone H3 variant included in the centromeric nucleosomes. CENP-A determines the localisation of the kinetochore proteins at the centromere connecting the centromeric DNA to and the kinetochore proteins (Sullivan *et al.*, 2001). The kinetochore protein complex forms at mitotic prophase or meiotic prophase I in order to attach the mitotic and meiotic spindle's MTs to the chromosome centromere. The kinetochore is formed by over 80 different proteins which are localised in three different regions: inner plate, outer plate and fibrous corona **(Figure 9)**.

The different roles of the kinetochore include: to establish the site for attachment of the MTs and associated motor proteins, to monitor the correct MT attachment by sensing the tension provided by the spindle, to remove the MTs which are incorrectly attached, to provide a checkpoint control and to ensure that all chromosomes are correctly aligned at metaphase.

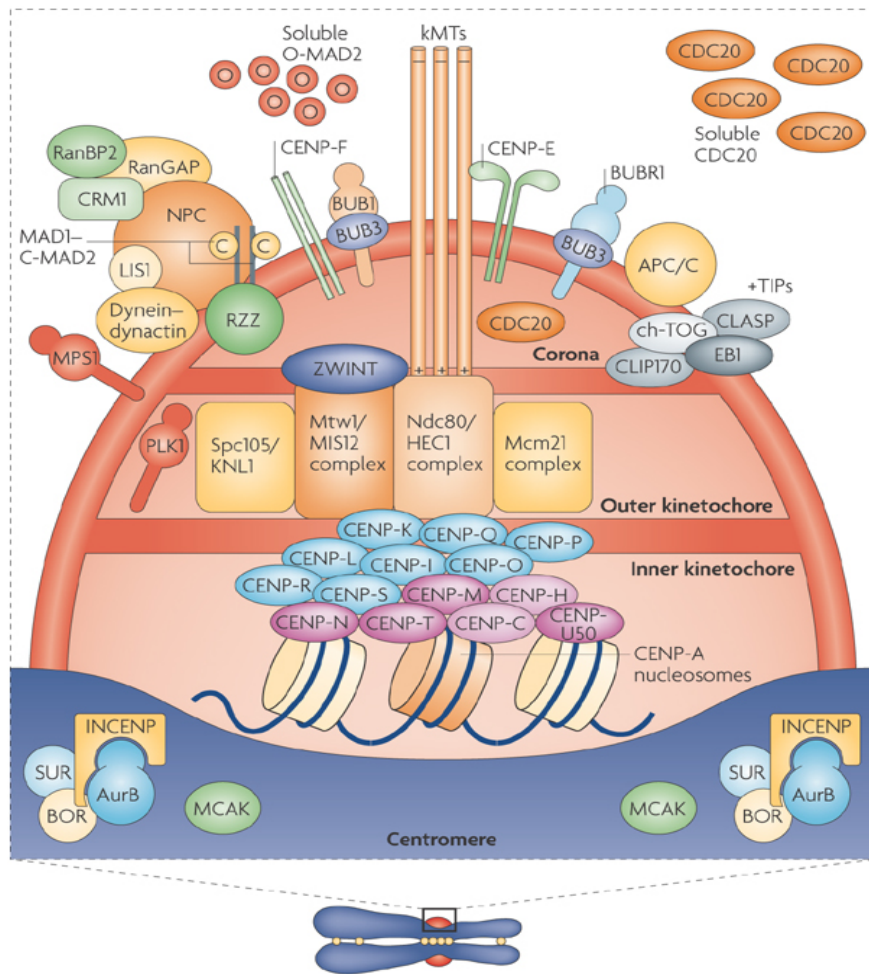


Figure 9. Centromere and kinetochore structure in higher eukaryotes.

The inner centromere regions include protein complex Chromosome Passenger Complex (CPC) which includes the proteins BOR, SUR, Aurora B (AurB), MCAK and INCENP. CPC is involved in the correction of errors in the attachment of MTs and centromeres and in the activation of the spindle assembly checkpoint monitoring the tension. The kinetochore consists of a unique nucleosome which includes the histone H3 variant CENP-A protein. The Inner-kinetochore includes several proteins which associate at different stages of the cell cycle. The spindle pole component (SPC105/KNL-1) seems to be essential in organizing and recruiting the outer layer in the kinetochore. The Outer-kinetochore provides a multiprotein platform for different spindle-assembly checkpoint proteins like Mtw1/Mis12 and proteins involved in the attachment of MTs like Ndc80/Hec1 complex. The corona region contains proteins like the Anaphase Promoting Complex/Cyclosome (APC/C) which is an E3 ubiquitin ligase which gets activated when the correct MTs tension is achieved at metaphase. This activation allows APC/C to ubiquitinate the Securin attached to the Separase and thus allowing this last protein to cleave the cohesion complexes and allow the separation of sister chromatids at anaphase (Diagram drawn and conceived by Andrea Musacchio & Edward D. Salmon. 2007).

1.2.2 Chiasmata formation in *Arabidopsis*

A chiasma can be described as the cytological observation of a crossover that has been formed by homologous recombination (Rhoades, 1961). Chiasma formation is necessary to produce an equal tension between the homologous chromosomes at metaphase I during meiosis, so they can separate towards opposite poles at anaphase I. However, the absence of chiasmata can lead to an unequal segregation of chromosomes at anaphase I. Consequently, random segregation of chromosomes throughout meiosis II would appear (Rhoades, 1961).

Analysing chiasmata allows the proper evaluation of the global homologous recombination that occurs at a specific meiotic event. The goal of examination of the chiasma frequency at metaphase I is to quantify the amount of recombination in individual meiotic events (Moran *et al.*, 2000 or 2001). The mean of chiasma frequency is variable through the *Arabidopsis* chromosomes. Chromosome 1 which is the largest chromosome in size has a high mean chiasma frequency of 2.14, whereas chromosomes 2 and 4 which are the smallest chromosomes have a lower mean chiasma frequency of 1.54 and 1.56, respectively (Moran *et al.*, 2001).

1.3 DNA double strand breaks and homologous recombination

Living organisms are frequently exposed to different factors which can produce DNA damage. These factors can be exogenous like radiation and chemical mutagens or endogenous like errors during DNA replication or compounds produced by cellular metabolisms (West *et al.*, 2004). These damages can be repaired by different DNA repair pathways which maintain the genome integrity in higher eukaryotes. One of the major lesions

for DNA are DNA double strand breaks (DSBs). Two major, evolutionary conserved, repair pathways are constantly competing to repair DSBs: homologous recombination (HR) and non-homologous end joining (NHEJ) (West *et al.*, 2004).

HR depends on the presence of a homologous sequence of DNA, either in a sister chromatid or in a non-sister chromatid. HR is an error-free accurate repair pathway. However, ectopic recombination may take place during this process as a result of an abundance of other homology sequences along the whole genomic DNA. Consequently, rearrangement of the eukaryotic genome can be occurred. On other hand, NHEJ is another evolutionarily conserved DSB repair pathway (Ferdous *et al.*, 2012; Molinier *et al.*, 2004). Unsuccessful repair of DSBs may lead to gross genetic instabilities and eventually might cause cell death (Tamura *et al.*, 2002).

The initiation of meiotic homologous recombination in most eukaryotic organisms is preceded by the formation of DSBs (Osman *et al.*, 2011; Peoples *et al.*, 2002; Burgess, 2002 ; Celerin *et al.*, 2000; Scott *et al.*, 2004). The formation of DSBs precedes chromosome pairing, synapsis and recombination between homologous chromosomes during prophase I (Osman *et al.*, 2011). However, in organisms such as *Drosophila melanogaster* and *Caenorhabditis elegans*, pairing can be completed in the absence of DSBs formation (Dernburg *et al.*, 1998; McKim *et al.*, 1998).

1.3.1 Meiotic Homologous Recombination (HR)

1.3.1.1 Initiation of DNA DSBs

HR is initiated by key particular proteins which role is to induce DSBs. The mechanism and proteins involved in the initiation of DSBs have been found to be conserved between most species (Camerini-Otero, 2000 and Grelon *et al.*, 2001). The protein SPO11 (Sporulation Protein 11) is a topoisomerase-like type II protein that has been studied extensively in budding yeast (Keeney *et al.*, 1997). SPO11 have been found to play a key role of inducing DNA DSBs. DSBs are occurring randomly throughout the chromatin loops and physically move to the chromosome axis to be further processed (Keeney *et al.*, 1997).

S. cerevisiae was the first organism in which meiotic DSBs were found to be induced by SPO11 (Keeney *et al.*, 1997). Based on the DNA homology sequence, it was found that SPO11 sequence is similar to the archaeal TopoVI subunit (Bergerat *et al.*, 1997). Since then, different SPO11-associated proteins have been identified which play important roles in DSB formation together with SPO11 (De Massy *et al.* 1995; Keeney *et al.*, 1997). Several proteins (including RAD50, MRE11 and SAE2) bind covalently to the 5' DNA sites of the DSB in which they remain on both sides of the DSB before being removed by the resection proteins (MRN complex) (Keeney *et al.*, 1997).

SPO11 is a highly evolutionary conserved protein among higher eukaryotes showing its importance in meiotic recombination (Bowring *et al.* 2006; Keeney, 2011; Celerin *et al.* 2000). The *Arabidopsis thaliana* genome encodes for three SPO11 homologous genes: *AtSPO11-1*, *AtSPO11-2* and *AtSPO11-3* but only *AtSPO11-1* and 2 proteins are involved in DSB formation at meiosis (Hartung and Puchta, 2001). In fungi and *C. elegans*, *SPO11* genes have been identified mainly specifically express in meiotic cells (Keeney, 2011; Hartung and Puchta 2001; Ramesh *et al.* 2005; Hartung and Puchta 2000; Storlazzi *et al.*, 2003).

By using the protein sequence homology from yeast SPO11 protein it has been found that *A. thaliana* has three paralogues for SPO11 protein coded by three genes: *AtSPO11-1*, *AtSPO11-2* and *AtSPO11-3* (Hartung and Puchta, 2001; Ronceret *et al.*, 2009). *AtSPO11-1* and *AtSPO11-2* proteins apparently might be working as a heterodimer and are essential for the initiation of meiotic recombination. Each one of these proteins contain different tyrosine residues that seem to play a key role in inducing DSBs (Ronceret *et al.*, 2009).

Cytological analysis utilised to investigate the phenotype of *Atspoil1-1* and *Atspoil1-2* mutants in *A. thaliana* have shown their importance in the formation of DSBs. *Atspoil1-1* mutants have shown a severe reduction of fertility with no or a very limited number of bivalents at metaphase I (Grelon *et al.*, 2001). Moreover, *Atspoil1-2* mutants exhibited an extreme reduction of fertility like *Atspoil1-1* as well as a complete absence of bivalents at metaphase I. These observations emphasize that these proteins (*AtSPO11-1* and *AtSPO11-2*) are essential for DSBs formation (Stacey *et al.*, 2006; Ronceret *et al.*, 2009). Nevertheless, *AtSPO11-3* is the third paralogue protein which has been found to play other important cell roles such as cell growth and DNA replication in mitotic cells (Hartung *et al.*, 2007).

Furthermore, other proteins have been reported to be essential for DSBs formation in *A. thaliana* described as PRD proteins (Putative Recombination initiation Deficient): *AtPRD1* (homologue function of MEI1 protein in mammalian and found to be a partner to *AtSPO11-1*), *AtPRD2* (orthologue of MEI4 in mouse) and *AtPRD3* (homologue function of rice protein called PAIR1) (**Figure 10B**). Mutation of any one of these proteins results in the same phenotype as an *Atspoil1* mutant in which no DSBs are produced, not chiasmata formed and therefore univalents are only shown in metaphase I (Osman *et al.*, 2011).

In contrast, budding yeast requires for several other proteins to work together with SPO11 to be able to induce DSBs such as Mei4, Mre11, Rad50, Xrs2, Ski8, Mer2 Rec104, Rec114, and

Rec102 (**Figure 10A**). It is reported that some orthologues of these proteins have evolved different functions within the cell metabolism, for example, an orthologue of Ski8 in *Arabidopsis* seems to have a different function which is not related to meiotic processes (Jolivet *et al.*, 2006). There are also other proteins still involved in different roles in meiosis but which are not any longer required to induce DSBs like AtMRE11 and AtRAD50 (Osman *et al.*, 2011).

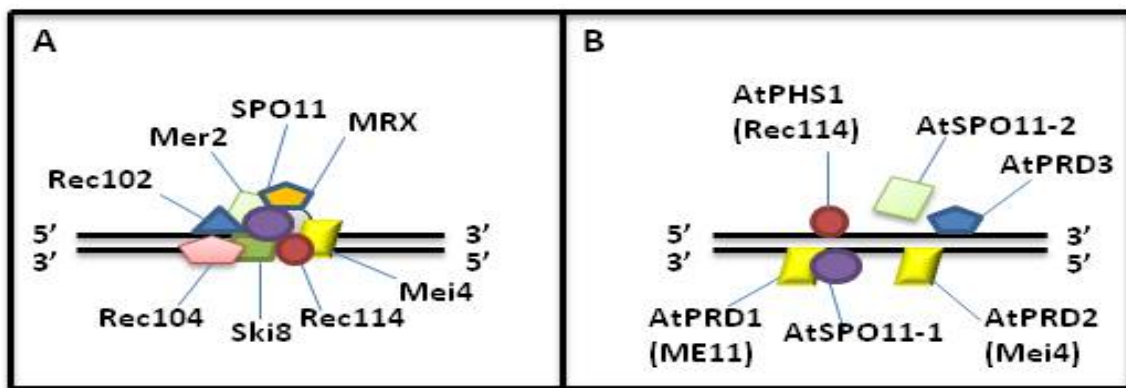


Figure 10. Multiprotein complexes involved in the formation of meiotic DSBs.

Schematic represent Proteins that are essential of inducing DNA DSBs of both budding yeast **A** and *A. thaliana* **B** (adapted from Edlinger and Schlogelhofer, 2011).

1.3.1.2 The processing of meiotic DNA DSBs

In budding yeast, meiotic recombination is initiated by the formation of DNA DSBs that is essential for proper synapsis of homologous chromosomes (Keeney *et al.*, 1997). These DNA breaks are taking place when the tyrosine chains of SPO11 attach to 5' phosphodiester bound of DNA. These attachments lead to form 3' OH tails (ssDNA). These tails are restricted to create free 3'OH single strands DNA. Resection processes from 5' to 3' are

performed by a multiprotein complex known as MRX (MRE11, RAD50 and NBS1/XRS2) (Figure 11).

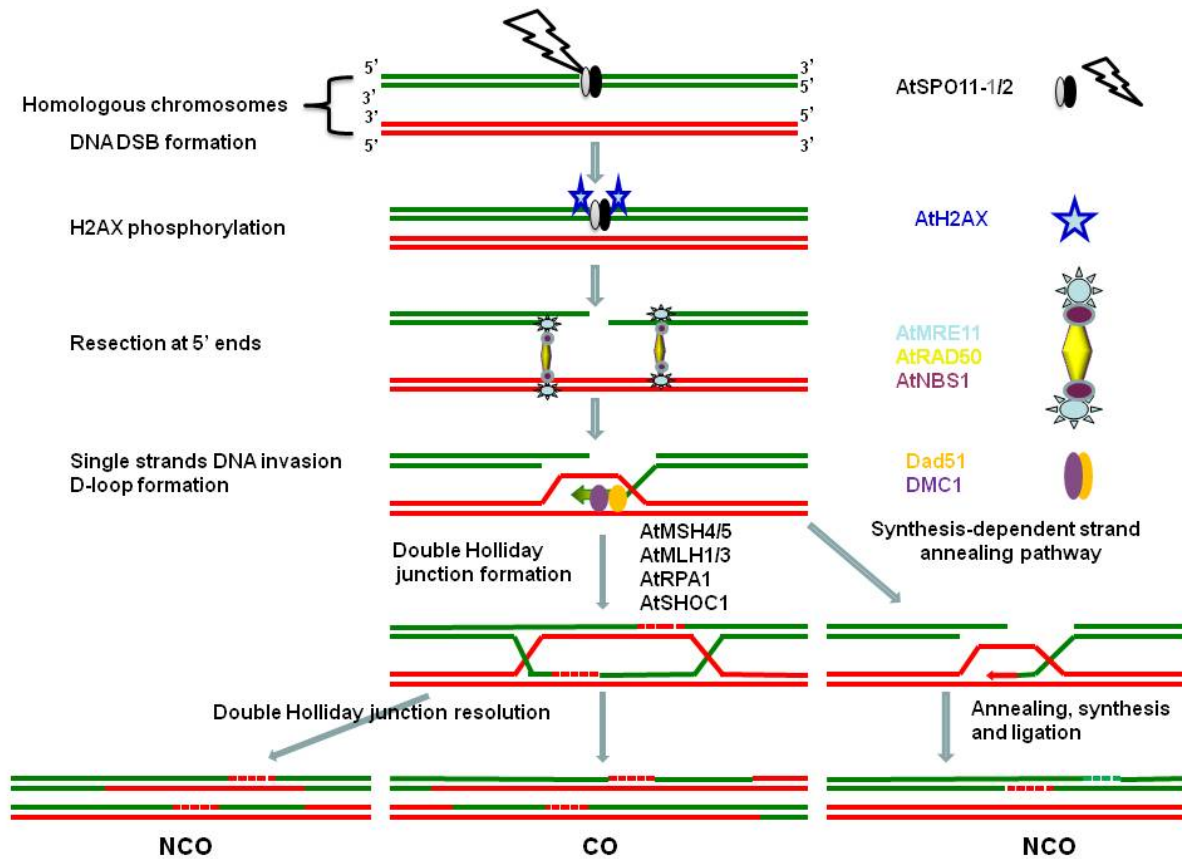


Figure 11. Pathways of homologous recombination.

Schematic representation of the events of meiotic recombination. DSBs are induced on the chromatin by SPO11. Broken DNA is processed by MRX protein complex to form 3'OH terminus of both sides of DNA. One of 3'OH tails are occupied by DMC1 and RAD51 proteins which main role is to search for the homology sequence of these tails in homologous chromosomes. By the end of this process, a D-loop can be established as a process known as a single end invasion (SEI). Eventually, COs and NCOs would form at the end of this processes (picture has been adapted from Osman *et al.*, 2011).

Arabidopsis possess orthologues for the budding yeast proteins forming the MRN complex named as AtMRE11, AtRAD50 and AtNBS1. Moreover, AtNBS1 has been recorded in *A. thaliana* to work as a heterodimer with AtMRE11 protein (Bundock and Hooykaas, 2002; Puizina *et al.*, 2004; Waterworth *et al.*, 2007; Uanschou *et al.*, 2007).

Mutations have been introduced to these genes in *A. thaliana* to understand their roles in meiotic recombination process. Chromosome fragmentation has been recorded in *Atmre11* or *Atrad50* mutants. It is important to emphasize that these proteins are essential for DNA DSB repair in somatic cells (Puizina *et al.*, 2004). These observations emphasize that these proteins (AtMRE11, AtRAD50 and AtNBS1) act as a complex after AtSPO11 induces DNA DSBs (Akutsu *et al.*, 2007; Waterworth *et al.*, 2007).

Following resection to form ssDNA by the MRX protein complex, nucleoprotein filaments form by RAD51 and DMC1 assembling on the 3' OH ssDNA. These two proteins accumulate on the side of ssDNA break (3'OH) and invade homologous sequences of non-sister chromatids. Consequently, a displacement loop (D-loop) is established and the polymerization of the D-loop depends on the size of the invasion (**Figure 11**).

In yeast, RAD51 protein is essential for mitotic and meiotic recombination while DMC1 protein is only necessary for meiotic recombination and for synaptonemal complex (SC) development (Symington *et al.*, 2004). *Arabidopsis* genome contains genes coding for *AtRAD51* and *AtDMC1* (Couteau *et al.*, 1999; Li *et al.*, 2004).

In *Atrad51* mutant meiotic cells, pairing and synapsis are defective and chromosome fragmentation has been recorded (Puizina *et al.*, 2004; Uanschou *et al.*, 2007). No chromosome fragmentation is detected in double *Atspo11-1* and *Atrad51* mutants (Siaud *et al.*, 2004). These observations emphasize that the AtRAD51 protein is necessary for DSB repair. However, *Atdmc1* mutants do not show chromosome fragmentation during meiosis, instead 10 univalents are detected showing that the DSBs can be repaired in absence of DMC1 in *Arabidopsis* but this does not produce COs. These observations showed that AtDMC1 protein play a vital role of meiotic chromosome recombination and synapsis but not in DNA DSBs repair (Couteau *et al.*, 1999).

Furthermore, in mammalian organisms, there are five paralogs for RAD51 including RAD51B, RAD51C, RAD51D, XRCC2 and XRCC3. In *Arabidopsis*, AtXRCC3 and AtRAD51C have been confirmed to have meiotic roles. AtXRCC3 act with AtRAD51C in a similar role to that of AtRAD51 (Albala *et al.*, 1997; Osakabe *et al.*, 2002; Schild *et al.*, 2000). *Atrad51c* and *Atxrcc3* mutants show chromosome fragmentation during meiosis. Furthermore, a double *Atspo11-1* and *Atrad51c* mutant has shown no chromosome fragmentation, thus the fragmentation observed in *Atrad51c* is dependent on DSBs from AtSPO11-1 (Bleuyard *et al.*, 2005; Li *et al.*, 2005; Vignard *et al.*, 2007).

Atxrcc3 mutant exhibit chromosome fragmentation and DNA bridges are detected at second meiotic division (Bleuyard and White, 2004). These observations show that AtXRCC3 protein might also be playing a vital function in double Holiday junction resolution (Beuyard *et al.*, 2004a; Li *et al.*, 2005). Furthermore, AtMND1 and AtHOP2 seem to have similar roles to RAD51 in ensuring synapsis and successful processing of DSBs repair (Osman *et al.*, 2011). Additionally, it was found that a tumour suppressor protein, known as BRCA2 (breast cancer type 2 susceptibility protein), could play a crucial role in homologous recombination as a recombination mediator (Islam *et al.*, 2012).

Apparently, the maintenance of DMC1 and RAD51 nucleoprotein filaments on the 3' ssDNA is achieved by another protein complex, Replication Protein A (RPA). This protein complex includes three subunits named as RPA1, RPA2 and RPA3. RPA1 protein is the largest subunit of the RPAs (around 70 kDa). Mutation in *RPA1* gene in budding yeast showed that recombination is extensively decreased. In *Arabidopsis* genome there are 5 genes coding for AtRPA1 (Shultz *et al.*, 2007). *Atrpa1* mutation reduces chiasmata formation (Osman *et al.*, 2009). These observations emphasize that this protein of both budding yeast and *Arabidopsis* is playing a crucial role of meiotic recombination processes (Iftode *et al.*, 1999; Osman *et al.*, 2011; Shultz *et al.*, 2007; Soustelle *et al.*, 2002). Furthermore, *rpa1* mutants in maize show

severe reduction of RAD51 foci, less than 1% of RAD51 foci reported comparing to the normal foci at mid-zygotene and around 95% reduction of synapsis between non-homologous chromosomes (Golubovskaya *et al.*, 2011).

1.3.1.3 Synthesis-dependant strand annealing (SDSA)

The D-loop is formed as a result of single strand invasion (SEI). Some of these SEIs might separate from the D-loop organization after the repair synthesis of DNA and be processed as a noncrossover (NCOs). This process is described as synthesis-dependant strand annealing (SDSA) which lead to non-crossovers between homologous chromosomes (**Figure 11**) (Borner *et al.*, 2004).

1.3.1.4 The first class (class I) of COs pathway

According to Borner and collaborators (2004), the class I interference sensitive CO pathway requires a group of proteins, called ZMM protein family which includes Zip1, Zip2, Zip3, Msh4, Msh5 and Mer3. This class of meiotic recombination is described as the interference-dependent pathway as the presence of one CO would interfere in the formation of another CO around that chromosomal region. This class represents approximately 85% of the total COs (**Figure 11**). MSH4 and MSH5 proteins act as a heterodimer and found to be homologs to the MutS in bacteria (Ross-Macdonald and Roeder, 1994; Zalevsky *et al.*, 1999; Osman *et al.*, 2011). It was proposed that the Human MSH4/5 heterodimer stabilizes the D-loop formation and therefore the formation of double Holliday Junctions (dHJs), the recombination

intermediate that leads to COs formation (Neale and Keeney, 2006). The processing of these dHJs could be resolved in COs or NCOs.

The MLH1 and MLH3 are orthologues of MutL in Bacteria ((Dion *et al.*, 2007; Nishant *et al.*, 2008; Osman *et al.*, 2011) and play important roles in stabilizing and maintaining the formation of COs throughout the resolution of dHJs (Osman *et al.*, 2011; Franklin *et al.*, 2006). In *Arabidopsis*, proteins involved in this class I pathway have been identified and characterised.

AtMER3 and AtSHOC1 proteins also contribute of class I COs formation in *Arabidopsis*. *Atmer3* mutation has revealed serious reductions in COs and SC formation (Chen *et al.*, 2005). These results revealed a similar reduction in CO frequency to those using these *Atmer3* and *Atshoc1* mutants in a *Atmsh4* or *Atmsh5* double mutant background. These results showed that AtSHOC1 play a vital role of class I COs formation pathway such as AtMSH4 and AtMSH5 (Macaisne *et al.*, 2008).

1.3.1.5 The second class (class II) of COs pathway

A second class pathway of COs representing around 15% of the total number of COs exist and is depending on the MUS81/MMS4 proteins. This second class of COs pathway is also known as the interference independent pathway (Berchowitz *et al.*, 2007; De Los Santos *et al.*, 2003; Franklin *et al.*, 2006; Higgins *et al.*, 2008b). In *Arabidopsis*, *Atmsh4* mutants presented a chiasma frequency of 1.25 per cell compared to the ~10 in the WT. Additional reduction of chiasma frequency was observed in the double mutants *Atmsh4xAtmus81* with an average of 0.85 chiasmata per cell. These observations revealed that around 0.4% of COs can be produced in absence of class I and class II pathways (Higgins *et al.*, 2008a).

Therefore, it has been postulated that another CO formation pathway could be present in *Arabidopsis*.

1.3.2 Non Homologous End Joining (NHEJ)

In higher eukaryotic organisms, NHEJ is the favour evolutionary conserved pathway to repair DSBs (Tamura *et al.*, 2004). Both, HR and NHEJ pathways need to be accessible to DSBs to keep the genome integrity in higher eukaryotes. Both pathways are in clear competition to access DSBs and repair them. The chosen pathway depends on different aspects such as of the species, the cell type, and even the stage of the cell cycle. For example, in budding yeast and bacteria the HR pathway is mainly used to repair DSBs while the NHEJ is the usual pathway used to repair DSBs in mammalian and higher plants, probably because these higher eukaryotes have a larger genomic size (Britt, 1996; West *et al.*, 2004). It has been suggested that NHEJ is prevalent from G1 to early S phases and HR is predominant in both S and G2 stages (Mao *et al.*, 2012).

NHEJ process requires the rejoining of the DNA strand ends broken on the DSBs throughout little or no homology of DNA sequences. Consequently, DNA can be fused back as the original template (Mao *et al.*, 2012). NHEJ main protein characters are evolutionary conserved and include the Ku heterodimer (Ku70 and Ku80 proteins), DNA-Protein Kinase (DNA-PK) and the DNA ligase protein (LigaseIV-Xrcc4) (Tamura *et al.*, 2004; West *et al.*, 2004). It has been found that following DSBs, both Ku70 and Ku80 are immediately localized along DNA breaks. This association of the Ku complex with the DSB leads to the recruitment of the DNA-PK (Tamura *et al.*, 2004). These mixtures of proteins are protecting DSBs ends from any nuclease activity on the nucleus. The DNA-PK catalytic subunit (DNA-PKcs) autophosphorylation seems to assist the endonuclease activity of Artemis to dissolve

the 5' and 3' overhanging ends in the DSB. Ultimately, the ligation of the DSB ends is taking place by XLF-IV-Xrcc4 proteins (Tamura *et al.*, 2004). However, NHEJ repair of DSB is error prone and thus 50-75% of the times. NHEJ will lead to small deletions/insertions in that region. Furthermore, genome instability may occur as a result of joining two non-matching ends (chromosome translocations and chromosome fusions). Consequently, anaphase bridges can be visualized during the cell cycle of these cells with chromosomal instabilities (Pfeiffer *et al.*, 2004).

Mutations in NHEJ proteins (*atku80*, *atku70*, *atlig4*) have been analysed to understand their role in DNA repair and plant fertility. It was revealed that plants showed a normal fertility phenotype while telomere defects could be observed in *atku70/80* mutants. These mutants showed hypersensitivity to mutagenic agents which induce DSBs including γ –irradiation and bleomycin. Nevertheless, the mutant plants still grow suggesting that other alternative pathway can be used as a backup to NHEJ when mutated (Menke *et al.*, 2001). It is suggested that plants have a backup pathway to NHEJ to repair DSBs compared to animals. In animals, NHEJ *ku70* and *ku80* homozygote mutants present severe abnormal development and *lig4* mutation seems to be lethal (West *et al.*, 2004).

1.4 Project aims

The aim of this project is to study the role of some chromatin components in different species such as *Arabidopsis* and humans. The strategy is to study different chromatin elements by analysing different mutant lines. The genetic analysis of these chromatin components would build an understanding of the relationship between these proteins and their roles in vital biological processes like DNA repair and chromosome condensation and segregation during mitotic and meiotic divisions. We have analysed different mutant lines using different molecular and cytological techniques to gain further insight into the role of these chromatin components.

It is possible to identify the function of several genes by producing mutants using T-DNA transformation. The transformation can be carried out using *Agrobacterium tumefaciens* which can transfer a molecule of DNA (T-DNA) into the genomic DNA of the plant cell. *Arabidopsis* meiotic stages have been characterised and analysed to study chromosome pairing, synapsis, recombination and segregation (Albini and Jones 1984; Swarbeck *et al.*, 2008; Zhang *et al.*, 2006).

This project will focus in the following:

1. Analysing different histone H2A isoform mutants in *Arabidopsis thaliana* to understand their roles in chromosome dynamics during mitosis and meiosis.
2. Further analysis of *Ath2a1* mutant to understand its role in the chromatin organization and T-DNA integration.
3. Evaluate the relationship between T-DNA integration and meiotic recombination using Floral Dipping approaches.
4. Studying different HMG mutants in *Arabidopsis* to understand their role in chromosome compaction and dynamics during mitosis and meiosis.
5. Analyse the role of SSRP1 in chromosome dynamics during mitosis and meiosis in *Arabidopsis*.
6. Analyse and compare the role of hSSRP1 in human cells using a siRNA knocking down strategy.

CHAPTER TWO

Material and methods

2.1 Plant material

The *Arabidopsis thaliana* wild-type (WT) accession used in this study was Columbia 0 (Col0). The different T-DNA mutant lines were obtained from the Salk Institute (<http://signal.salk.edu/cgi-bin/tdnaexpress>) (Alonso *et al.*, 2003) through the European *Arabidopsis* seed stock centre (NASC; <http://arabidopsis.info/>). The T-DNA insertion lines studied appear on (Table 2):

Gene locus	Mutant lines	Primers
AT5g54640 H2A1	Salk-040809	FP: CACACCACATTGACTGGTCTG RP: CCGAATTTGACATGCAAAAAT
AT4g27230 H2A2	N370949	LP: ACATCATAACCATCCCACCAC RP: CGCATAATTTAACGAAAGGCG
AT1g54690 H2A3	N55	FP: ATTTTCGGTTCAACATTGGATG RP: ATGTGGAACAGAGAGCCATG
AT1g08880 H2A5	N371389	FP: TTAGCGAGCTAATTCAGGTGC RP: CCCTAAAGCCCCTCATCTTC
AT5g59870 H2A6	N661871	FP: CAAAGCCAACAAGATCCAATC RP: CAAACAAAGCCCAATTGAAC
AT1g51060 H2A10	N582645	FP: CAGAGGAACGTAAGCAAAAACG RP: TTCCAAGGCATATTCAATTGG
AT5g02560 H2A12	N829140	FP: AGTTTCCTGTCTGGTAGGATCG RP: CCGATGGAAAAACAAAACCTGA
AT3g20670 H2A13	N658419	FP: TCATTTCAAAGTCAAAAACACATG RP: ACCAGCTTTCTTGGGAAGAAG
AT5g46640 HMGA-LIKE	Salk-002786	FP: TCAGAAACAAACGGGAAATTG RP: CACTTCCACATCTCAACCGAT
AT4G17950 HMGA-LIKE	Salk-014014	FP: ATCACCCTCATGGTTTCTGC RP: GGATGTGTTGTTGTTTCAGGG
AT1G14900 HMGA3	Salk-078240 078336	FP: GAGAAAGACTCCTCGGGATTG RP: TCCGAAATTGCATAAGTACCG
AT2G33620 HMGA2	Salk-010945C	FP: GTGCTGGCTGGAGAGGTATC RP: TGGTCCGAAAGTACCTCAAC
AT2G33620 HMGA2	Salk-073165C	FP: AGACAAGACACACACAGCACG RP: CTGCTAACACTTTTTGCCCTG
AT5G46640 HMGA1-LIKE	Salk-002786C	FP: TCAGAAACAAACGGGAAATTG RP: ATCGGTTGAGATGTGGAAGTG

AT5G46640 <i>HMGAI-LIKE</i>	Salk-110363	FP: ATGGTTCCACCAACAGAAGTG RP: CGACTGCACTTGATGATGATG
AT3G28730 <i>HMG-SSRP1</i>	Salk-001283C	FP: CCAGAAAAATTTAAGCCGGAG RP: TCCCAAATGGAAAGAGATGTG
AT1G20696 <i>HMGB3</i>	SALK-047872	FP: AGCCTTAGCCACATAAGGAGC RP: TCCTCTTGATTCTCTGCGTTG
AT4G35570 <i>HMGB5</i>	SALK-090616C	FP: ATCTCAATCGTCGTCTCTCCC RP: ATCCCACAGTTGACAGAAAGG
AT4G11080 <i>HMGB1</i>	GK-171F06.01	FP: TTCGCTTATTGATGGACCTTG RP: TTCCGACAAGTTCTTCCACTC
AT3G51880 <i>HMGB1</i>	GK-032E03.01	FP: CGACACTGACACTGAGAGACG RP: GAGGAGTACGCCATGCTAATG
AT4g10710 <i>SPT16</i>	Sail 294 E09	FP: TTGAGTCATGAGGGTTGAAGG RP: GAGAGTGCCATTGATGAGGAG
AT4g10710 <i>SPT16-A,B,C</i>	GK-193H04	FP: TGTTCATCATCACCTTAGG RP: TGATTTTTCTGTCTTCCCCC
AT2g28620 <i>AtKRP12SC</i>	Salk 104114 HM	FP: GCTTCTTCATAGTCAACGTGC RP: GAGAATTCAAAAACCGGAACC
AT2g28620 <i>AtKRP12SC</i>	SALK 118756	FP: GATGTTTCAAACCTGTTCGCC RP: TGCATATCTTCCTTTGCAACC
AT4g21270 <i>ATK1 (kinesin)</i>	Salk 043587	FP: ATTGCTAAGACAGCAAGCTGC RP: TTTTGAGAGCCGTGGATTATG
AT4g21270 <i>ATK1 (kinesin)</i>	SALK 146457	FP: TCCATATTGACAAAGGGATCG RP: ACCATTGAACGCAATGTTTTC
AT4g05190 <i>ATK5 (kinesin)</i>	Salk 001544	FP: TTGGTGCAGTAACAAAGGAATC RP: AAGTCCGTGATGATCGTGATC
AT5g57880 <i>MPS1</i>	Sail 94 D08	FP: AGCTCTAATTGTTGCGAGACG RP: TTAAAGGAAATGCAGCTCAGG
AT5g20930 <i>TSL1</i>	N8168	FP: CATACTTCTGCACCGTTCTG RP: CTTAGAGTAGGCAAGATATGG
AT5g20930 <i>TSL1</i>	SALK-082965	FP: TTTGGTCATGTCCAAAAGGTC RP: AGGAAGAGGAAGCTGTTTTGC
RT-PCR	Primers	
<i>ACTIN2</i> transcript	FP: 5'-CGTACAACCGGTATTGTGCTG-3' RP: 5'-AGGTTTCCATCTCCTGCTCGT-3'	
<i>AtH2AI/RAT5</i> transcript	FP: 5'-CCGCCGAGGTTCTTGAATTAG-3' RP: 5'-AGCCAAAAGAGAGACGTGTTC-3'	
<i>AtSSRP1</i> transcript	FP: 5'-TCTCAGCGGTCGCGGTGAAAAG-3' RP: 5'-TCGAGATCAGGATGTTCCAAGT-3'	

Table 2. T-DNA insertion mutant lines and their primers used for genotyping and for RT-PCR.

2.1.1 Plant growth conditions

Seeds were vernalized for around 48 hours at 4⁰C and then planted into a sterile mixture of sand and compost in a glasshouse with controlled temperature, humidity and light, at 18⁰C with a 16 hours light cycle.

2.2 Bacteria growth media

Sterile deionised water (SDW) was utilised for the preparation of media.

2.2.1 Lysogeny Broth (LB media)

It is a rich media with substances that are essential for bacteria growth including:

5.0% (w/v) bacto-yeast extracts (Difco)

10.0% (w/v) bacto-tryptone (Difco)

10% (w/v) NaCl

2.2.2 Lysogeny Broth Agar (LBA Media)

5.0% (w/v) bacto-yeast extracts (Difco)

10.0% (w/v) bacto-tryptone (Difco)

10% (w/v) NaCl

15.0% (w/v) bacto-agar

2.2.3 Required growth conditions for bacteria

Liquid culture was used to grow *E. coli* for approximately 19 hours at 37°C in a rotary shaker at 200rpm. *E. coli* was also grown on LBA plates for approximately 12 hours at 37°C.

2.2.4 Bacteria culture

Antibiotic was added to the media at the required concentration: Ampicillin-100 µL/50 ml (Sigma).

2.3 Molecular genetics

2.3.1 Plant DNA extraction (*Arabidopsis leaves*)

Leaf discs were taken from plants (mutant and wild-type plants) and placed inside 1.5ml sterile microtubes. Tubes were kept on ice during the procedure. Then, 40µL of extraction buffer was added to each tube. The extraction buffer consisted of 200mM Tris HCl Ph 7.5, 250mM NaCl, 25mM EDTA and 0.5%SDS and was freshly prepared. The leaves were grinded directly in the microtubes using sterile plastic grinders. Another 400µl of extraction buffer was added in each tube and then vortexed for about 5 seconds. Samples were centrifuged at 13,000 rpm for 5 minutes and the pellet containing the cellular remains was separated from the supernatant containing the genomic DNA. Pellets were discarded. A total of 400µl of the supernatant from all samples was transferred to new microtubes and 400µl of cold isopropanol was added to each sample to allow the DNA precipitation. Tubes were mixed gently and left on the bench for 2 minutes at room temperature. Samples were centrifuged at 13,000 rpm for 10 minutes and the supernatant was discarded. A total of 400µl

of 70% ethanol, freshly made, was added to wash the DNA pellet. Samples were centrifuged at 13,000 rpm for 5 minutes, the supernatant discarded and the pellet left to dry for 30 minutes on the bench. Then, 50µl of sterile deionised water (SDW) was added to each tube to dissolve the DNA pellet. Samples were incubated in an oven at 65⁰C for 10 minutes and then stored at -20⁰C.

2.3.2 Polymerase chain reaction (PCR)

PCR is used extensively in diagnostic testing and research. PCR technique is utilised to amplify one or more DNA templates throughout several cycles. Millions of DNA copies can be generated from one DNA molecule. PCR has been used for genotyping the mutant lines.

The PCR reaction final volume was 20µl per sample (7µl SDW, 1µl forward primer (LP), 1µl reverse primer (RP), 1µl of DNA and 10µl of 2xBiomix red (Bioline)). This reaction mixture (20µl) was transferred to a PCR machine and run for 30 cycles. The PCR programme for genotyping T-DNA insertion lines included: 1 cycle of 95⁰C for 2 minutes; 30 cycles of denaturation at 95⁰ C for 1 minute, annealing at 50⁰ C for 1 minute and then extension at 72⁰C for 2 minutes; a final extension cycle at 72⁰C for 4 minutes; and an unlimited cycle at 4⁰C. The samples were loaded in an agarose gel for DNA electrophoresis.

2.3.3 Preparation of gel electrophoresis

Gels were prepared by dissolving 0.8g of Agarose powder (Bioline) in 100ml of 0.5% electrophoresis buffer (100ml 5X TBE +900ml SDW), and heating in a microwave. After agarose was dissolved and cooled down (around 60⁰C), we added red safe stain (INtRON)

(2.5µl/100 agarose). Electrophoresis buffer (0.5% TBE) was added to fill the electrophoresis tank and approximately 15µL of each sample was loaded per well in the gel. Gene Ruler 1Kb DNA ladder (Fermentas) was used to mark the different molecular weights. The electrophoresis was carried out at 90V for approximately 50 minutes. The DNA bands were captured using a Biorad Gel DocXR imager and software.

2.3.4 Gel purification

The required DNA fragment was removed from the gel by cutting out the bands of interest using a clean sharp scalpel after exposure to UV light. The slice of gel containing the amplified DNA band was transferred into a colourless tube and weighed. QIAquick Gel extraction kit (QIAGEN) was used to dissolve the agarose gel. 3 volumes of QG buffer to 1 volume of gel slice were added together in one tube and incubated at 50⁰C for 10 minutes until gel dissolved completely (a vortex was used every 2-3 minutes during incubation period to help with gel dissolving). Isopropanol was added (equal to gel vol.) to the same tube and mixed. Mixture was transferred into a QIAquick spin column and centrifuged for 1 minute. The flow-through was discarded and the spin column put again into the collection tube. 750µL of buffer PE was added to the column and centrifuged for 1 minute and the flow-through discarded. The spin column was placed into a new 1.5ml microcentrifuge tube and DNA eluted by added 30µL of SDW and centrifuging for 1 minute. Another 20µL of SDW was added to the column and centrifuged for 1 minute to ensure elution of all DNA. Eventually, DNA is ready for ligation after extraction from agarose gel.

2.3.5 Restriction enzyme digestion

Restriction digestions were placed in their suitable buffer and correct digestion enzyme by the following steps:

Extracted DNA	10 μ L
BSA	0.5 μ L
10X buffer 4	5 μ L
Enzyme1/2	2 μ L
SDW	32.5 μ L

50 μ L

Mixtures were transferred to an incubator at 37⁰C for 1.5 hour or overnight. After this the mixture was incubated at 65⁰C for 20 minutes to deactivate the enzyme function.

2.3.6 Ligation of DNA fragments into a vector

pDrive cloning vector (QIAGEN) was used for cloning DNA fragments by the following steps:

pDrive vector (QIAGEN)	1 μ L
Extracted DNA	2 μ L
2X ligation Master Mix	5 μ L
SDW	2 μ L

10 μ L

The mixture was incubated at 15°C for overnight.

2.3.7 Isolation of plasmid from bacteria

5ml of an overnight grown bacterial culture was transferred to a microfuge tube and centrifuged at 5000rpm for five minutes. The supernatant was thrown away and the pellet was re-suspended in the remaining liquid using a vortex. Then, 200µL of solution I was added to the pellet. Solution I contains 50mM glucose, 10mM EDTA, 25mM Tris (Ph8). The sample was mixed gently (not using the vortex as it could damage the DNA) and placed onto ice for five minutes. 400µL of freshly prepared Solution II was added. Solution II contains 1% SDS and 0.2N NaOH. The samples stayed on ice for five minutes. The samples were mixed by gently inverting the tubes. 300µL of Solution III was added. Solution III contains 3M CH₃CO₂K. Samples were mixed gently and placed on ice for five minutes. The tubes were centrifuged for 15 minutes at a speed of 13,000 rpm. The supernatants were transferred to new tubes and 600 µL of cold isopropanol was added to each sample. Tubes were centrifuged for 15 minutes at 13,000 rpm and the supernatants removed. Pellets were washed with 70% EtOH at room temperature. Tubes were centrifuged for 10 minutes at 13,000 rpm, the supernatant removed and then pellets left to dry on the bench for a few minutes (~30 min). Once dried, 50µL of sterile distilled water (SDW) was added to dissolve each sample and transferred to a 65°C incubator for 10 minutes. The plasmid DNA samples were stored at -20°C.

2.3.8 RNA purification from plant tissues

RNA was extracted from *Arabidopsis thaliana* tissues (for example: leaves, flower buds, roots, siliques and stems) with no more than 100mg per sample using an accurate measuring machine. Sample was placed into liquid nitrogen for approximately 2 minutes and then ground using a mortar and pestle. 450 μ L of RLT mixture (1ml of RLT buffer with 10 μ L of β -Mercaptoethanol) was added to help with denaturing of proteins and RNase. Sample transferred into mini-spin column and centrifuged for 2 minutes. It is washed gently with around 250 μ L of 100 % ethanol and mixed carefully using a pipette. Sample was transferred into a new mini spin column and centrifuged for 15 seconds at 10,000 rpm. 700 μ L of RW1 buffer added and centrifuged for 15 seconds and discard the flow-through. After that 500 μ L of RPE buffer was added into the mini spin column and centrifuged at 10,000 rpm for 15 minutes and the flow- through discarded. The previous step was repeated but centrifuged for 2 minutes instead of 15 seconds. RNA was adsorbed on this silica membrane and this membrane was transferred to a new 1.5ml collection tube and RNA eluted using RNase free water. Eventually, sample was placed in liquid nitrogen and then stored at -80⁰C.

2.3.9 Reverse transcriptase-polymerase chain reaction (RT-PCR)

The aim of this technique is to evaluate the gene expression by converting mRNA into complementary DNA (cDNA) using RT-PCR enzymes of different plant tissues. After converting RNA into cDNA, specific primers were used to amplify a target template. The protocol was obtained from Promega and following these stages:

RAN ~500ng 4 μ L

Oligo-dT primer 1 μ L

Mixture was incubated at 70⁰C for 5 minutes and placed on ice for 5 minutes and then the following components added:

RNase free dH₂O (DEPC water) 5.5 μ L

5X Reaction buffer 4 μ L

MgCl₂ 3 μ L

Nucleotides mix (dNTP mix) 1 μ L

RNasin (RNase inhibitor) 0.5 μ L

RT 1 μ L

Sample was then placed at 42⁰C for 60 minutes and then 70⁰C for 15 minutes then 4⁰C to convert all mRNA into cDNA. Sample was ready to do a normal PCR using forward and reverse primers for the precise cDNA template to analyse the gene expression.

2.4 Cytological analysis of *Arabidopsis thaliana* chromosomes

2.4.1 Chromosome fixation

Arabidopsis inflorescences containing the flower buds were collected from wild-type and mutant plants and placed in approximately 15ml of fixative (3 parts of ethanol/1 part of glacial acetic acid). Buds were left around one week at room temperature and fixative was changed twice.

2.4.2 Chromosome spreading

Prior to the digestion, the flower buds were washed 3 times with citrate buffer, for 5 minutes each time. Citrate buffer consists of 5ml of 0.1M citric acid, 5ml of 0.1M sodium citrate and 40ml of SDW. Closed flower buds were transferred into a watched glass and separated from the inflorescence using forceps under a dissecting microscope. The flower buds were digested with a mixture of enzymes (0.33% w/v pectolyase, 0.33% w/v cytohelicase and 0.33% w/v cellulose in citrate buffer). 0.4ml of the enzyme mixture was added to the buds and then placed into a moist chamber and transferred into an incubator at 37⁰C for 1.5 hours. Cold water (4⁰C) was added to the buds to stop the enzyme digestion. A single bud was then transferred to a slide under a dissecting microscope with a tiny amount of buffer and macerated using a needle. A total of 10 μ L of 60% acetic acid was added and the slide was placed on at 45⁰C hotplate for 2 minutes. A diamond pen was used to mark the area where the macerated material was. An extra 10 μ L of 60% acetic acid was added and then, 100 μ L of fixative was added around the drop of acetic acid. Extra 100 μ L of fixative was added and the slide was dried using a hairdryer.

2.4.3 DAPI staining

Slides were stained using the DNA specific staining 4'-6-diamidino-2-phenylindole (DAPI) diluted in a Vectashield solution (Vector).

2.4.4 Fluorescence microscopy

Slides were checked using an epifluorescence microscope (Nikon ECLIPSE 90i).

2.4.5 Imaging

Images were acquired using a Hamamatsu Orca-ER digital CCD camera and analysed using NIS-Elements AR software (Nikon).

2.5 Immunolocalization

Material was prepared before beginning the immunolocalization protocol. The different materials are described below:

2.5.1 Slides washing

Slides were cleaned by dipping them in to the following:

Acetone 10 minutes

SDW 10 minutes

Ethanol 10 minutes

After that, slides can be left on bench until they dry and then kept on a clean pack.

2.5.2 Phosphate buffer solution (PBS)

1 tablet of PBS in 100 ml of SDW

0.1% Triton in 100ml PBS

2.5.3 Block solution

0.1g of Bovine Serum Albumin (BSA) added to 10ml of PBS+0.1% Triton. It was mixed gently until BSA was dissolved and then passed through a 0.2 μ M filter using a syringe into a clean falcon tube.

2.5.4 Spreading technique

Buds were selected of appropriate size (approximately 5-10 buds per slide) under a stereomicroscope to study the recombinant proteins structure and behaviour specifically during meiotic stages. After that, anthers were dissected from buds on a clean slide under stereoscope and 20 μ L of 0.1 % of cytohelicase (digestion enzyme for cell walls) on the same slides. Slides put in humid box at 37⁰C for 120 minutes. After this, slides were taken out of the humid box and anthers broken using a brass rod (keep anthers wet all the times by adding some of digestion enzyme). 10 μ L of 1% Lipsol was added to the broken anthers and spread carefully using plastic pipette and marked by a diamond pen. Slides were transferred to 37⁰C in a humid box that was put on the hot plate for around 5 minutes (avoid slides drying by adding drops of 1% Lipsol). Then, 20 μ L of 4% paraformaldehyde were added to the marked area and slides kept in fume hood for approximately 2 hours to dry and then washed 3 times for 5 minutes each with PBS (0.1%Triton). 50 μ L of blocking solution was added on a piece

of parafilm and put marked areas of slides upside down on the block solution and kept in humid box for 20mins at room temperature.

Primary antibody was diluted with blocking solution and put on the parafilm. Slides were placed upside down on this mixture and kept for 2 days at 4⁰C in a humid box. After two days, slides washed 3 times for 5 minutes each with PBS (0.1%Triton). Secondary antibody was mixed with blocking solution and added to the parafilm and the slides were kept in a dark area for 45 minutes. Slides were washed 4 times for 5 minutes each. Eventually Slides were stained with 7μL of DAPI added to the marked area and mounted under a cover slip.

2.5.5 Squash technique

This technique was used to obtain cells immunolocalisation in 3D. Specifically, this procedure was used to show the spindle polymerization of all stages in both mitotic and meiotic cells. Buffers were prepared as shown below:

The first buffer prepared was MTSB (microtubule staining buffer) 50mM PIPES, 5mM MgSO₄, 5mM EGTA pH 6.9. Preparing the 2X MTSB as below:

PIPES	15.12g
MgSO ₄	1.08g
EGTA	1.9g
SDW	500ml

And then, it was prepared 8% Paraformaldehyde to be added in 2XMTSB (to get 4% paraformaldehyde in MTSB buffer).

100ml of 8% Paraformaldehyde prepared and mixed with the 100ml of 2X MTSB to obtain 200ml of 4% Paraformaldehyde

The appropriate size of buds was selected (depending on which meiotic stage we were interested) with around 20 buds per slide. On the same slide, anthers were dissected from the buds and put in a drop of 1X MTSB on the same slide and make sure the anthers do not dry out. After obtaining all anthers in the 1X MTSB then dried this buffer using the edges of a tissue and quickly added the fixation buffer (4% Paraformaldehyde in MTSB) for 20 mins at room temperature. Then, the slide was washed by 1X MTSB 3 times and digestion enzyme added in the anthers (2.5% Cellulase, Cytohelicase and Pectolyase) for 30 mins at 37⁰C. After this digestion period, the slides were washed with 1X MTSB 3 times avoiding the slides to get dry out. These anthers were macerated quickly and a cover slip squashed onto the slide and immersed in liquid nitrogen. The cover slip was removed quickly using a razor blade and left on the bench to dry or 5 mins. Appropriate primary antibody was added after diluted with blocking buffer and put at 4⁰C in the fridge for 48 hours. After that, slides washed 2 times using PBS and incubated with a secondary antibody that has been diluted with blocking for 45 mins at room temperature in darkness. Finally, the slides were washed 3 times with PBS and then the DNA was stained with 7 μ L of DAPI.

2.5.6 FLUTAX1 technique

FLUTAX1 is a fluorescent taxol compound (Tocris) which binds to the taxol microtubule binding site with high affinity ($K_a \sim 10^7 M^{-1}$). This derivative is very useful for direct imaging of the microtubule cytoskeleton. The fluorescent has a maximum Excitation of ~ 495 nm and Emission of ~ 520 nm. The concentration used was of 1 μ L/1ml.

The flower buds were fixed for 3 days and the fixative was changed twice. After three days, the fixed material was prepared by the chromosome spreading technique shown earlier. After that, the slides were washed 3 times by PBS and then FLUTAX1 (1 μ M) was added for 1 hour at room temperature in darkness. Then, slides were washed twice for 1 min each with PBS. Followed by added DAPI stain to slides and stored at 4⁰C until observation at the epifluorescence microscope.

2.6 T-DNA Transformation

2.6.1 Floral Dipping T-DNA Transformation

This is a technique that can be used to transfer the T-DNA from *Agrobacterium tumefaciens* into the genome of a host plant cell, in our case *Arabidopsis thaliana*. The T-DNA vector used was PEG205 kindly donated by Zongcheng Lin with a kanamycin resistance gene to select in bacteria and a herbicide (Basta) resistance gene to select in plants. *Agrobacterium* cells carrying the T-DNA were grown on fresh LBA plates that include:

Rifampicin 10 mg/mL

Kanamycin 50 mg/mL

Gentamycin 30 mg/mL

Agrobacterium was spread on the fresh LBA plates including all antibiotics and incubated for 1 day at 28⁰C in incubator. After, 2-3 colonies were added to independent 20ml LB cultures which contained all the antibiotics and put on shaker incubator at 200 rpm at 28⁰C until the next day. A total of 125 μ L of each culture was added to a fresh 500ml of LB media that also contained all the needed antibiotics with the correct concentration and put on shaking incubator till the next day at 28⁰C. The optical density (OD) was measured by using a spectrophotometer until achieving an OD₆₀₀ between 1.5 and 2.0 to be able to continue with the procedure. Once the correct density was obtained, the culture was centrifuged in sterile tubes for 10 minutes at 5000 rpm and the supernatant was discarded. A solution of 50g/1L of sucrose was prepared and the pellet cells were dissolved in about a correct volume to get the *Agrobacterium* OD₆₀₀ at 0.8. A total of 200-250ml of this solution was added to a beaker and just previous to the floral dipping a solution of 50g/1L of Silwet (Sigma) was added (a detergent that helps with T-DNA integration). The mixture was then ready for floral dipping

of *A. thaliana* inflorescences. The *Arabidopsis* plants used were healthy and producing flowers. Plants were dipped in the mixture for around 3 to 5 seconds and covered by cling film in the dark or low light. The next day, cling film was removed and the plants were allowed to grow under perfect conditions.

2.6.2 Selection of BASTA resistant *Arabidopsis* transformants

BASTA herbicide's active ingredient is glufosinate or its ammonium salt DL-phosphinothricin which interferes with ammonia detoxification and the biosynthesis of glutamine then killing the plant (bleaching phenotype). The BASTA resistance can be used for plant transformation selection. The Wilco Complete Weedkiller as a source of glufosinate-ammonium (37.5g/l solution. *Arabidopsis thaliana* transformant plants can be made resistant when sprayed with the glufosinate-ammonium solution (**0.1g/l**). The best period for spraying BASTA is when the first proper leaves appear. The spraying was taking place within 8-10 day intervals. The resistant transformed plants only grew. The following dilution has to be used for the spraying:

2.70ml weedkiller in 1L water.

The spray period can be summarised as:

1 st Spray	True Leaves
2 nd Spray	8 days after 1 st spray
3 rd Spray	2 days after 2 nd Spray

2.7 Immunolocalization for the human cells

Human cells (endothelial cells and fibroblast cells) were obtained and cultured by Mr Klarke Sample a PhD student at the Medical School at the University of Birmingham following the required ethical and legal controls required.

2.7.1 Human Cell Culture

Materials	Source
Human umbilical vein endothelial cells (HUVEC)	Birmingham Women's Hospital, Birmingham
Media 199	Cancer research UK and Sigma, UK
DMEM	Sigma, UK
Bovine brain extracts	Pel-Freez, USA. and prepared as described by Maciag <i>et al.</i> (1979)
Fetal calf serum	PAA, The Cell Culture Co., UK
L-glutamine	Sigma, UK
Porcine skin gelatine	Sigma, UK
Trypsin-EDTA	Sigma, UK
FastRead Haemocytometer	Immune Systems, UK
Tryphan Blue	Sigma, UK
Leica DM IL inverted microscope	Leica Microsystems, USA

2.7.2 HUVEC Isolation

Human umbilical vein endothelial cells (HUVECs) were isolated from three human umbilical cords from Birmingham women's health care NHS trust were isolated using a standard protocol (Klarke Sample).

2.7.3 Cell culture

The HUVEC were subsequently cultured to confluence in collagen coated (0.1% w/v) sterile plastic culture dishes at 37°C in a humidified atmosphere (with 5% CO₂). Media 199 containing 10% (v/v) foetal calf serum (FCS), 4mM L-glutamine and supplemented with bovine brain extract and 90 µg/ml heparin was used. The fibroblasts were also cultured on plastic culture dishes (non-coated), but were maintained in DMEM supplemented with 10% (v/v) foetal calf serum (FCS) and 4mM L-glutamine.

Once confluent the cells were split after washing with 1x phosphate-buffered saline (PBS) and incubated in pre-warmed 1xtrypsin-EDTA solution for 5 minutes at 37°C. Once detached, Media 199 containing 10% FCS was added before centrifuging at 250 RCF for 5 minutes.

The pellet was resuspended in fresh supplemented Media 199 and re-plated at a ratio of 1:3 for further cultivation.

2.7.4 siRNA Transfection and Knockdown of ncRNAs

Materials	Source
OptiMEM	Invitrogen, UK
Lipofectamine RNAi MAX	Invitrogen, UK
SSRP1 D0 (S13490)	Invitrogen, UK
SSRP1 D1 (S13491)	Invitrogen, UK
Negative control duplex	Invitrogen, UK
20mm Coverslips	Fisher Scientific, UK
Ethanol	Sigma, UK
1M HCl	Sigma, UK
Sterile H ₂ O	n/a

Four coverslips per condition were exposed to 1M HCl and rotated for 10 minutes before being washed in sterile H₂O, 70% ethanol and finally in three times in sterile H₂O. 360,000 HUVECs were seeded onto the four gelatine coated glass coverslips in a 6cm dish the day before the cells were transfected with siRNA. 360,000 HUVECs per condition were also seeded onto gelatine coated 6cm dishes to be used for the qPCR validation. The knockdown was performed by adding 0.72 μ L of the 20 μ M siRNA duplexes to 244.28 μ L of opti-MEM (per plate) to give a final concentration of 10nM. Furthermore 10% (v/v) lipofectamine RNAi MAX was added to opti-MEM to obtain a total volume of 43 μ L. The two mixtures were mixed gently and incubated at room temperature for 10 minutes. Once this was complete the two mixtures were combined, flicked and incubated again at room temperature for 10 minutes. The cells were washed twice with PBS, before adding 1.2mL of opti-MEM. Finally the transfection mix was added to the cells, mixed by tilting and incubated for 4 hours at 37°C in a humidified atmosphere with 5% CO₂. After the incubation the transfection mix was

replaced with fresh media 199 without antibiotics and the cells were incubated again for 48 hours in the conditions stated above.

2.7.5 Real Time Quantitative Polymerase Chain Reaction

Materials	Source
QIASHredder	Qiagen, UK
RNeasy mini kit	Qiagen, UK
2-mercaptoethanol	Sigma-Aldrich, UK
70% ethanol (in RNase-free water)	n/a
High-Capacity cDNA Archive Kit	Invitrogen, UK
Sensimix™	Quantace, UK
Universal Probe Library set, Human	Roche Applied Science, UK
PCR Primers	Eurogenetec, UK
Rotor-Gene RG-3000 qPCR machine	Corbett Research Ltd, Australia
Rotor-Gene 6 software	Corbett Research Ltd, Australia

The HUVECs plated for the qPCR analysis were lysed and RNA was isolated using the RNeasy mini kit (an optional DNase step was performed) according to the manufacturer's instructions. The isolated RNA was then used to generate cDNA using a high-capacity cDNA archive kit according to the manufacturer's instructions.

Real time quantitative polymerase chain reaction (qPCR) was performed using the Roche universal probe library. A reaction mix totalling 25µL was used:

- 12.5µL Sensimix™
- 1µL forward primer (10 µM)
- 1µL reverse primer (10 µM)
- 0.25µL of the appropriate probe
- 0.25µL deionised water
- 10µL of cDNA

A Rotor-gene RG-3000 was used to conduct the qPCR with the following program:

1. 92°C for 10 minutes
2. 92°C for 15 seconds
3. 60°C for 45 seconds
4. Steps 2 and 3 were repeated for a total of 40 Cycles

2.7.6 Immunolocalization in human cells

Human cells (endothelium and fibroblasts) were obtained from Klarke Sample (Medical School). These cells were placed on 20mm round coverslips (coated with 0.1% gelatin) and put into 6 cm dishes containing supplemented media 199. Afterwards the coverslips were washed with PBS 3 times and fixed with 4% Paraformaldehyde for 10 minutes at room temperature. Following this incubation the coverslips were washed 3 times with PBS and incubated with 0.1% triton and 2X PBS for 4 minutes (if incubated for more than 4 minutes the cells may be lysed). The cells then washed 3 times with PBS and put in blocking buffer for 1 hour or overnight at 4°C.

The next day the cells were incubated with a total of 50 µL primary antibody diluted with blocking buffer for 1 hour at room temperature upside-down on parafilm in an opaque box.

The cells were then washed 3 times with PBS and incubated with the secondary antibody, which was again diluted with blocking buffer for 1 hour in an opaque box at room temperature before washing the cells with PBS 3 times. Finally 7 μ L of DAPI were added to each coverslip, which were put upside-down on slides and stored at 4°C.

CHAPTER THREE

Characterisation of histone AtH2A1 (RAT5) and T-DNA integration in Arabidopsis

3.1 INTRODUCTION

3.1.1 Histone H2A1/RAT5

Eukaryotic chromatin consists of genomic DNA associated to abundant proteins like histone and non-histone proteins forming different molecules named chromosomes compacting the DNA up to 10,000-20,000 times (Woodcock and Ghosh, 2010). Chromosomes replicate and are divided into identical cells during mitosis. During the mitotic process, the cell has to produce two identical cells which contain identical genetic material (chromosomes). To allow sexual reproduction during meiosis, a diploid cell produces four haploid gametes which contain half of the genetic material.

The first level of compaction of the DNA into chromatin involves the formation of nucleosomes. A nucleosome consists of two pairs of histones H2A, H2B, H3, and H4 that bind around 146 bps (base pairs) of DNA (Luger *et al.*, 1997). *AtH2A1* (*HTA1*; *Histone Two A1*) is one of histone *H2A* genes that seem to be necessary for T-DNA integration from *Agrobacterium tumefaciens* into the *Arabidopsis* genome. It has been reported that mutations in the *H2A1* gene might cause a significant reduction in T-DNA root transformation frequency into the plant genome (Mysor *et al.*, 2000). On the other hand, over expression of this gene seems to contribute to increase the T-DNA root transformation frequency in plants (Yi *et al.*, 2002).

The efficiency of the T-DNA integration in *rat5* has been scored to be around 7% to that of WT *Arabidopsis* ecotype (WS) (Mysor *et al.*, 2000). Furthermore, the expression pattern of *AtH2A1/RAT5* gene has been shown to correlate with the root cells that are most susceptible to T-DNA transformation (Yi *et al.*, 2002). Similarly, increasing the expression of this gene using a treatment with phytohormones also correlates with an increase in T-DNA root transformation (Yi *et al.*, 2002).

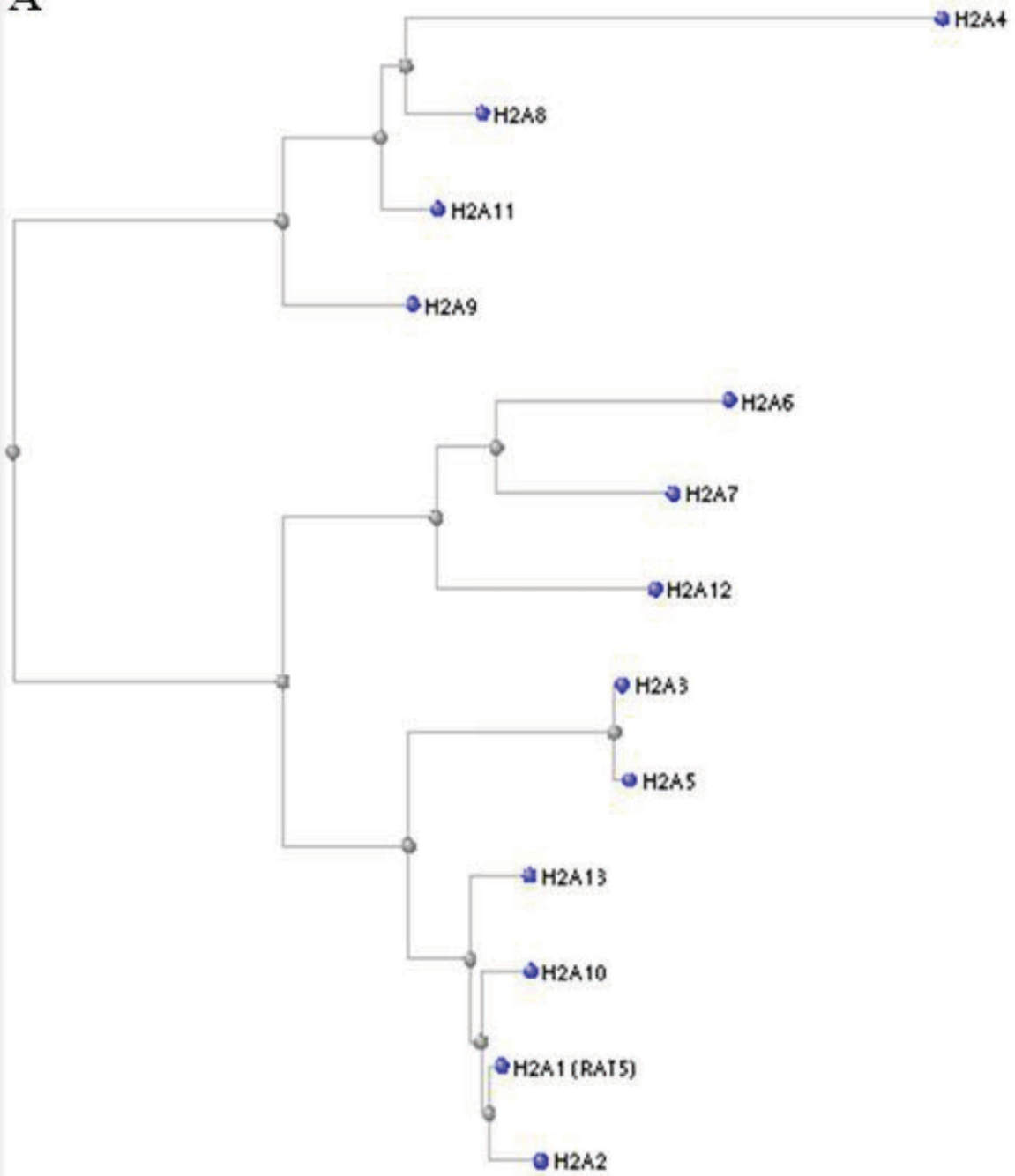
In this study, we have identified an *Ath2a1* mutant which has showed meiotic abnormalities at the level of recombination and chromosome segregation. Connections between chromosomes have been observed as early as prophase I stages and chromosome bridges have been observed at anaphase I as well as some chromosome fragmentations. Additionally, anaphase bridges have also been observed in the mitotic division.

3.2 RESULTS

3.2.1 *In silico* identification of histone AtH2A isoforms

Arabidopsis genome codes for 13 histone AtH2A protein isoforms. The predicted protein length for these isoforms varies between 119-153 amino acids. These isoforms have been categorized into four groups according to their amino acid sequence similarity (**Figure 12A**). Histones H2A1, 2, 10 and 13 have been grouped together as H2A core histones because they share around 92% identity at the level of amino acid sequences. Whereas, H2A3 and H2A5 have very similar amino acid sequence but they share only around 76% identity to the H2A1 amino acid sequence. H2A6, 7 and 12 have similar amino acid sequences but share around 70% identity to H2A1. H2A8, 9 and 12 histone protein isoforms are similar but only share around 52% with H2A1. The lowest amino acid sequence identity found among the histones H2A isoforms is between H2A4 and H2A1, with only around 35% identity in which H2A4 has the shortest amino acid length of all different H2A isoforms (119 amino acid) (**Figure 12B**).

A



B

H2A1	1	M----	----AGRGKTLGSGGAKKAT---SRSSKA	GLQFPVGR IARFLKAGKYA-ERVGAGAPVYLA AVLEYLAA	62
H2A2	1	M----	----AGRGKQLGSGAAKST---SRSSKA	GLQFPVGR IARFLKAGKYA-ERVGAGAPVYLA AVLEYLAA	62
H2A3	1	MS-SG	----AGSGTTKGGRGKPKATksvSRSSKA	GLQFPVGR IARFLKAGKYA-ERVGAGAPVYLS AVLEYLAA	68
H2A4	1	-----	MVCNT---NILKDVSTKISA---FENVRM[4]	GEMFQVAR IHKQLKNRVSAhSSVGATDVVYMTSILEYLT	67
H2A5	1	MS-TG	----AGSGTTKGGRGKPKATksvSRSSKA	GLQFPVGR IARFLKSGKYA-ERVGAGAPVYLS AVLEYLAA	68
H2A6	1	ME-S-[2]	KVKKAFGGRKPPGAPKTKSV---SKSMKA	GLQFPVGR ITRFLKKGKYA-QLGGGAPVYMA AVLEYLAA	70
H2A7	1	ME-SS[4]	KPTRGAGGRK--GGDRKKS---SKSVKA	GLQFPVGR IARYLKKGRYA-LRYGSGAPVYLA AVLEYLAA	71
H2A8	1	MAGKG[4]	LAAKTAAAAANKDSVKKKSI---SRSSRA	GIQFPVGR IHRQLKQVSAhGRVGATAAVYTASILEYLT	75
H2A9	1	MSgKG[4]	IMGKP--SGSDKDKDKKKPI---TRSSRA	GLQFPVGR VHRLLKTRSTAhGRVGATAAVYTAAILEYLT	73
H2A10	1	M----	----AGRGKTLGSGSAKKAT---TRSSKA	GLQFPVGR IARFLKKGKYA-ERVGAGAPVYLA AVLEYLAA	62
H2A11	1	MAGKG[4]	VAAKTMAANKDKDKKKKPI---SRSARA	GIQFPVGR IHRQLKTRVSAhGRVGATAAVYTASILEYLT	75
H2A12	1	MD-SG[1]	KVKKGAAGRSGGGPKKPV---SRSVKS	GLQFPVGR IGRYLLKGRYS-KRVGTGAPVYLA AVLEYLAA	70
H2A13	1	M----	----AGRGKTLGSGVAKKST---SRSSKA	GLQFPVGR IARFLKNGKYA-TRVGAGAPVYLA AVLEYLAA	62
H2A1	63		EVLELAGNAARDNKKTRIVPRHIQLAVRNDEELSKLLGDVTTIANGGVMPNIHNL L L P K K A	GASK P-QED-	130
H2A2	63		EVLELAGNAARDNKKTRIVPRHIQLAVRNDEELSKLLGDVTTIANGGVMPNIHNL L L P K K A	GSSK PTEED-	131
H2A3	69		EVLELAGNAARDNKKTRIVPRHIQLAVRNDEELSKLLGSVTTIANGGVLPNIHQ T L L P S K V	GKNK[4] SASQEF	142
H2A4	68		EVLQLAENTSKDLKVKRITPRHLQLAIRGDEELDTLIGK-TIIGGSVIPHIH-----	-----	118
H2A5	69		EVLELAGNAARDNKKTRIVPRHIQLAVRNDEELSKLLGSVTTIANGGVLPNIHQ T L L P S K V	GKNK[4] SASQEF	142
H2A6	71		EVLELAGNAARDNKKSR I I PRHLLLAIRNDEELGKLLSGVTTI AHGGVLPNINSVLLPKKS[2] KPAE[3] TKSPVK[5]		150
H2A7	72		EVLELAGNAARDNKKNRINPRHLCLAIRNDEELGRL LHGVTTI ASGGVLPNINPVLLPKKS[2] SSSQ[4] --SATK[5]		150
H2A8	76		EVLELAGNASKDLKVKRITPRHLQLAIRGDEELDTLIGK-TIAGGGVIPHIH KSLVNKVT	-----[2]	136
H2A9	74		EVLELAGNASKDLKVKRISPRHLQLAIRGDEELDTLIGK-TIAGGGVIPHIH KSLINKSA	-----[2]	134
H2A10	63		EVLELAGNAARDNKKTRIVPRHIQLAVRNDEELSKLLGDVTTIANGGVMPNIHNL L L P K K T	GASK PSAEDD	132
H2A11	76		EVLELAGNASKDLKVKRITPRHLQLAIRGDEELDTLIGK-TIAGGGVIPHIH KSLINKTT	-----[2]	136
H2A12	71		EVLELAGNAARDNKKNR I I PRHVLLAVRNDEELGTL LKGVTTI AHGGVLPNINPILLPKKS[4] STTK[4] PSKATK[5]		153
H2A13	63		EVLELAGNAARDNKKTRIVPRHIQLAVRNDEELSKLLGDVTTIANGGVMPNIHNL L L P K K A	GASK PSADED	132

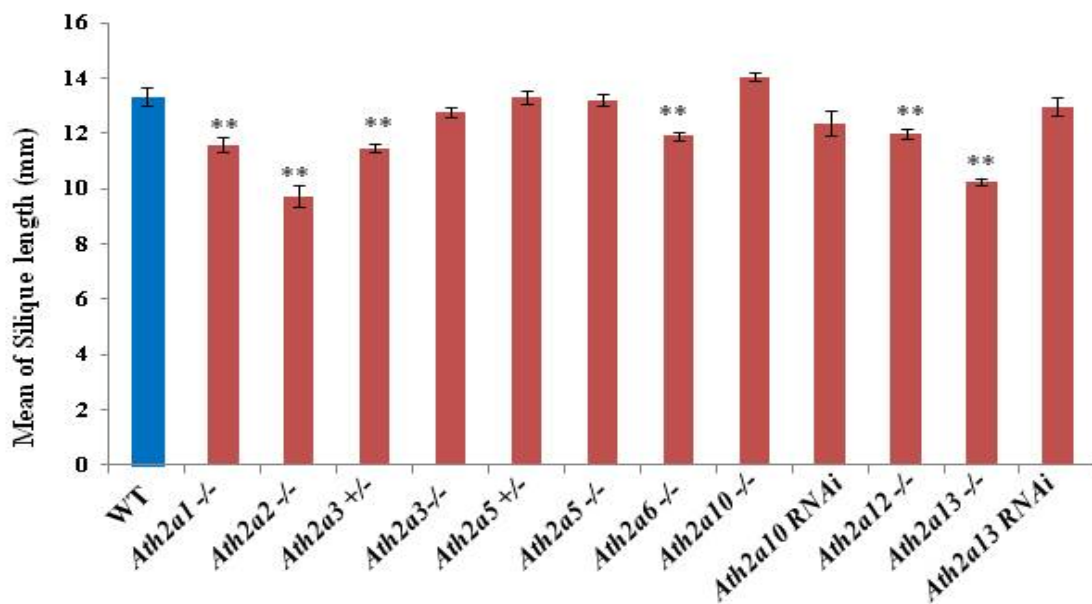
Figure 12. Multiple alignments of histone H2A isoforms identified in *Arabidopsis thaliana*.

A total of 13 genes have been characterised in the *Arabidopsis* genome to code for histone H2A protein isoforms. *Arabidopsis* amino acid sequence databases (TAIR) and multiple sequence alignment sequences tools (NCBI) have been utilised. **A** Phylogenetic tree representing the amino acid similarity found in the *Arabidopsis* histone H2A isoforms. **B** Amino acid sequences from the different histone H2A protein isoforms coded in the *Arabidopsis* genome. The amino acid residues highlighted in red colour are identical among all these H2A isoforms while the amino acid residues highlighted in blue colour indicate some similarities between some of these isoforms.

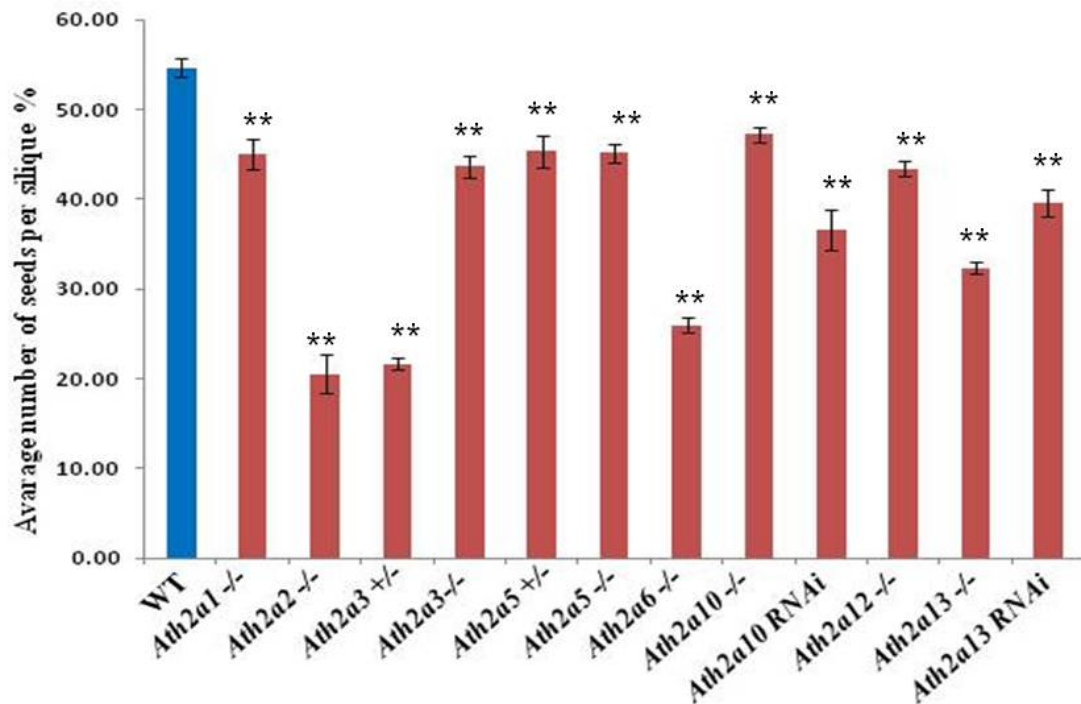
3.2.2 Fertility of *Ath2a* mutant isoforms

In order to assess the plant fertility, we have measured the silique (fruit) length and quantified the number of seeds per silique in different *Ath2a* isoform mutants and we have compared them to the wild-type plants. The mean length of the silique for some of the *Ath2a* isoform mutants is significantly reduced (marked with 2 stars (**)) compared to the average 13.34 mm of the wild-type (*t*-test, $p < 0.005$) (**Figure 13A**). Furthermore, the mean number of seeds per silique for all of these *Ath2a* isoform mutants are significantly reduced (marked with 2 stars (**)) compared to the 54.68 seeds/silique observed in the wild-type (*t*-test, $p < 0.005$) (**Figure 13B**).

A

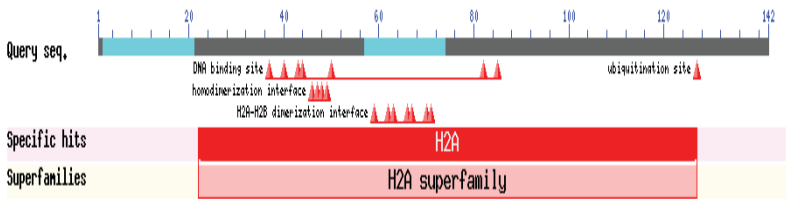
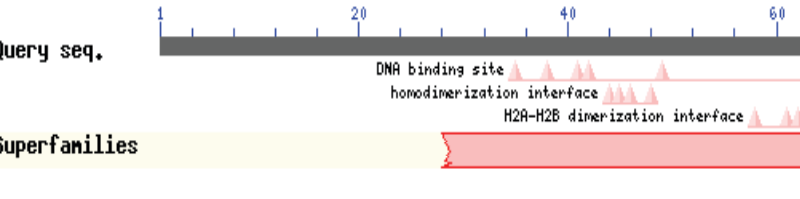
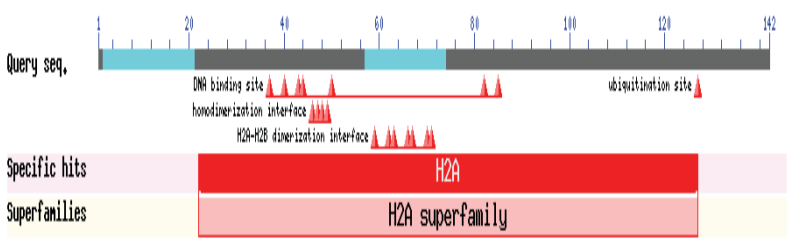
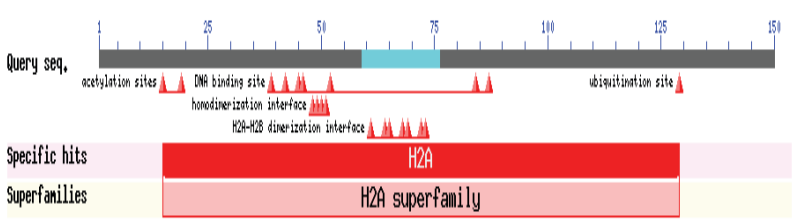
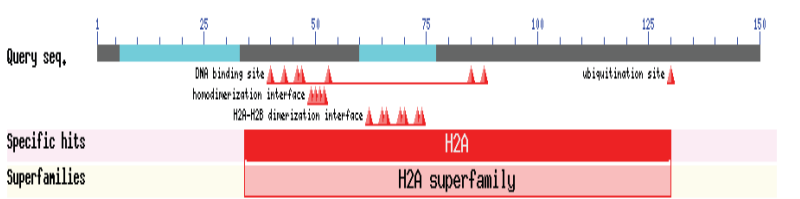


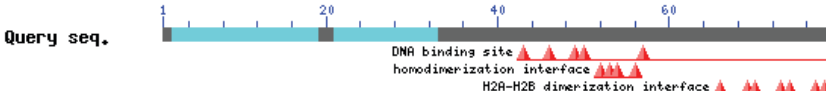
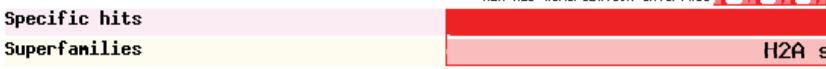
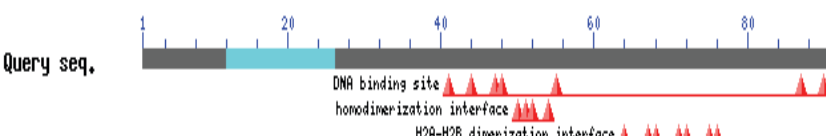
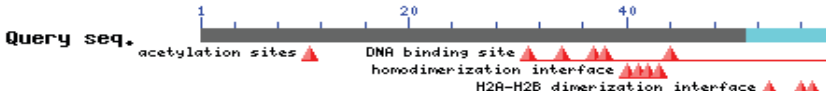
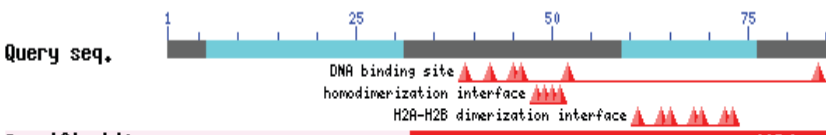
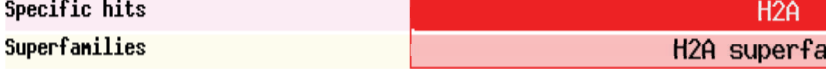
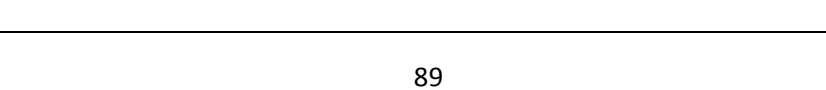
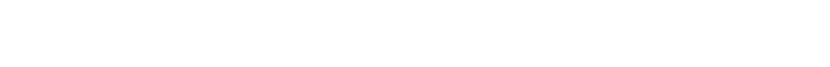
B



C

Gene locus	Conserved domain	P-value of seeds number per silique
At5g54640 <i>AtH2A.1/</i> <i>RAT5</i> N540809	<p>MAGRGKTLGSGGAKKATSRSSKAGLQFPVGRIARFLKAGKYAERVGAGAPVYLAADVLEYLAAEVLELAGNAARD NKKTRIVPRHIQLAVRNDEELSKLLGDVTIANGGVMPIHNLNLLPKKAGASKPQED</p>	8.58E-06
<i>AtH2A2</i> At4g27230 N370949	<p>MAGRKQLGSGAANKSTSRSSKAGLQFPVGRIARFLKAGKYAERVGAGAPVYLAADVLEYLAAEVLELAGNAARD NKKTRIVPRHIQLAVRNDEELSKLLGDVTIANGGVMPIHNLNLLPKKAGSSKPTTEED</p>	3.46E-25

<p><i>H2A3</i> At1g54690</p>	<p>MSSGAGSGTTKGGRGKPKATKSVSRSSKAGLQFPVGRIARFLKAGKYAERVGAGAPVYLSAVLEYLAAEVL ELAG NAARDNKKTRIVPRHIQLAVRNDEELSKLLGSVTIANGGVL PNIHQTL LPSKVGKNGDIGSASQEF</p> 	
<p><i>H2A4</i> At4g13570 No mutant</p>	<p>MVCNTNILKDVSTKISAFENVRMIMVEGEMFQVARIHKQLKNRVSASHSSVGDV VYMTSILEYLTTEVLQAENT SKDLKVKRITPRHLQLAIRGDEELDTLKGTHIGGSVIPHH</p> 	
<p><i>H2A5</i> At1g08880</p>	<p>MSTGAGSGTTKGGRGKPKATKSVSRSSKAGLQFPVGRIARFLKSGKYAERVGAGAPVYLSAVLEYLAAEVL ELAG NAARDNKKTRIVPRHIQLAVRNDEELSKLLGSVTIANGGVL PNIHQTL LPSKVGKNGDIGSASQEF</p> 	
<p><i>H2A6</i> At5g59870 N661871</p>	<p>MESTGKVKKAFGGRRKPPGAPKTKSVSKSMKAGLQFPVGRITRFLKKG RYAQRLGGGAPVYMAAVLEYLAAEVL ELAGNAARDNKKSRIPRHL LLAIRNDEELGKLLSGVTIAHGGVLPNINSVLLPKKSATKPAEEKATKSPVKSPPKA</p> 	<p>1.02E-37</p>
<p><i>H2A7</i> At5g27670 N371389 No mutant</p>	<p>MESSQATTKPTRGAGGRKGGDRKKS VSKSVKAGLQFPVGRIARV LKKGRYALRYGSGAPVYLA AVLEYLAAEVL ELAGNAARDNKNRINPRHLCLAIRNDEELGRLLHGVTIASGGVLPNINPVLLPKKSTASSQA EKASATKSPKKA</p> 	

<p><i>H2A8</i></p> <p>At2G38810</p> <p>No mutant</p>	<p>MAGKGGKGLLAAKTTAAAANKDSVKKKSISRSSRAGIQFPVGRHRQLKQRVSAHGRVGGATAAAVYTASILEYLTA EVLELAGNASKDLKVKRITPRHLQLAIRGDEELDTLKGTIAGGGVPIPHIKSLVNVKTKD</p> <p>Query seq. </p> <p>Specific hits </p> <p>Superfamilies </p>	
<p><i>H2A9</i></p> <p>At1g52740</p> <p>N644722</p> <p>No mutant</p>	<p>MSGKGAKGLIMGKPSGSDKDKDKKKPITRSSRAGLQFPVGRVHRLKTRSTAHGRVGGATAAAVYTAILEYLTAEV LELAGNASKDLKVKRISPRHLQLAIRGDEELDTLKGTIAGGGVPIPHIKSLINKSAKE</p> <p>Query seq. </p> <p>Specific hits </p> <p>Superfamilies </p>	
<p><i>H2A10</i></p> <p>AT1G51060</p> <p>N582645</p>	<p>MAGRGKTLGSGSAKATTRSSKAGLQFPVGRIARFLKKGKYAERVGAGAPVYLAADVLELAAEVLELAGNAARD NKKTRIVPRHIQLAVRNDDELSKLLGDVTIANGGVMPIHNLKPKKTKGASKPSAEDD</p> <p>Query seq. </p> <p>Specific hits </p> <p>Superfamilies </p>	8.49E-07
<p><i>H2A11</i></p> <p>At3g54560</p>	<p>MAGKGGKGLVAAKTMANKDKDKDKKPKISRSARAGIQFPVGRHRQLKTRVSAHGRVGGATAAAVYTASILEYL AEVLELAGNASKDLKVKRITPRHLQLAIRGDEELDTLKGTIAGGGVPIPHIKSLINKTTKE</p> <p>Query seq. </p> <p>Specific hits </p> <p>Superfamilies </p>	
<p><i>H2A12</i></p> <p>At5g02560</p> <p>N829140</p>	<p>MDSGKTKVKKGAAGRRSGGPKKPKVSRVSKGLQFPVGRIGRYLKKGRYSKRVGTGAPVYLAADVLELAAEVLE LAGNAARDNKKNRHPRHVLAVRNDDEELGTLKGVTAHGGVLPNINPILLPKKSEKAASSTKTPKSPSKATKSPK S</p> <p>Query seq. </p> <p>Specific hits </p> <p>Superfamilies </p>	2.34E-12
<p><i>H2A13</i></p> <p>At3g20670</p>	<p>MAGRGKTLGSGVAKKSTSRSSKAGLQFPVGRIARFLKNGKYATRVGAGAPVYLAADVLELAAEVLELAGNAARD NKKTRIVPRHIQLAVRNDDELSKLLGDVTIANGGVMPIHNSLLPKKAGASKPSADED</p> <p>Query seq. </p> <p>Specific hits </p> <p>Superfamilies </p>	2.75E-31

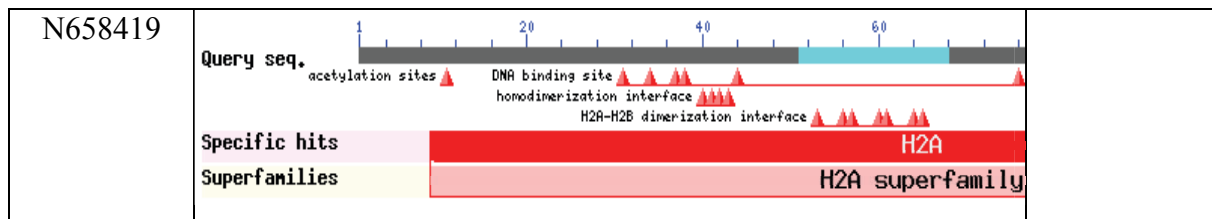


Figure 13. Fertility evaluation of the different *Ath2a* isoform mutants evaluated.

A Mean silique length for the different mutant isoforms (100 silique; N=10 plants). **B** Mean number of seeds per silique for the different histone *Ath2a* isoform mutants. **C** Protein Conserved Domains of the different histone AtH2A isoforms in *Arabidopsis* and their p value for the number of seeds per silique observed in each mutant compared to the wild-type (*t*-test, $p < 0.005$); Error bars = Standard error for the means.

3.2.3 Identification and characterisation of an *Ath2a1/rat5* T-DNA insertion mutant line

AtH2A1/RAT5 gene is located in the long arm of chromosome 5 of *A. thaliana*. It consists of two exons and one intron in addition of both 3' and 5' UTRs. The T-DNA insertion in this line (SALK-040809) is located in the 5'UTR of the *AtH2A1/RAT5* gene (At5g54640). TAIR Databases and Sequence Viewer site has been utilised to reveal the DNA sequence, gene structure and the position of the T-DNA insertion (**Appendix A**). Seeds from the T-DNA insertion line (SALK-040809) were obtained from the SALK Institute (San Diego). Mutant and wild-type seeds were grown together in identical standard conditions and constantly monitored at our glasshouse. DNA was extracted from plant leaves in order to genotype them. Two primers were designed (LP and RP) (materials and method sections) using the genomic information available around the T-DNA insertion site in *RAT5* gene together with another specific primer for the left border of the T-DNA specific of this line (BP). The combination of these primers allowed us to confirm the presence or absence of the T-DNA insertion in different plants (**Figure 14A**).

PCR and gel electrophoresis was conducted to check the presence of the T-DNA insertion within the *RAT5* gene. Additionally, wild-type plants have been used as a control (**Figure 14B**). Wild-type plants showed one single amplified band with approximately 1kb in size as a result of amplifying the genomic sequence between LP and RP primers in the *RAT5* gene (**Figure 14B**). The other four plants were confirmed as homozygous mutants as a single amplified band of a 768bp in size was obtained as a result of amplifying the left border of the T-DNA up to the RP primer in the *RAT5* genomic sequence (**Figure 14B**).

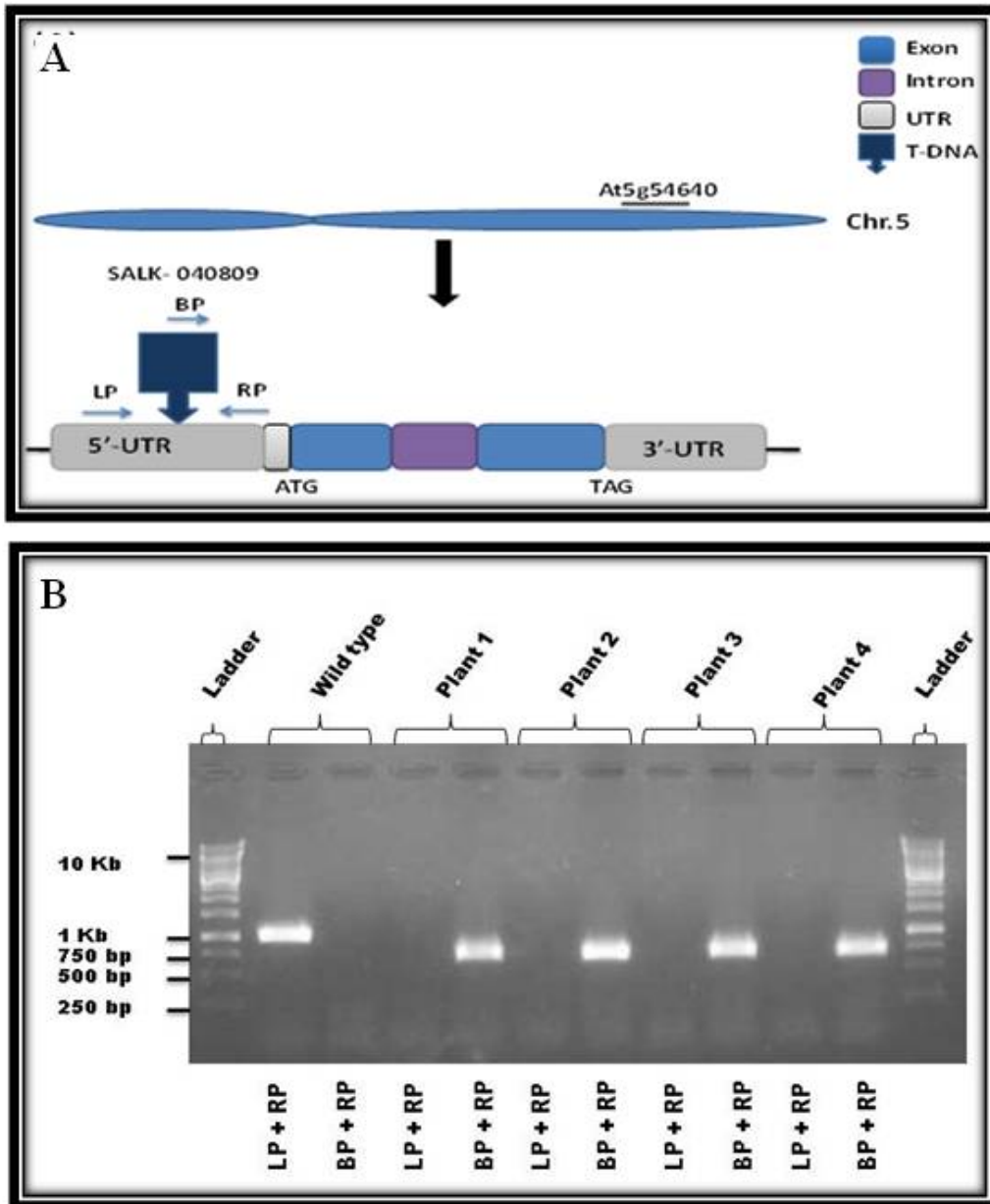


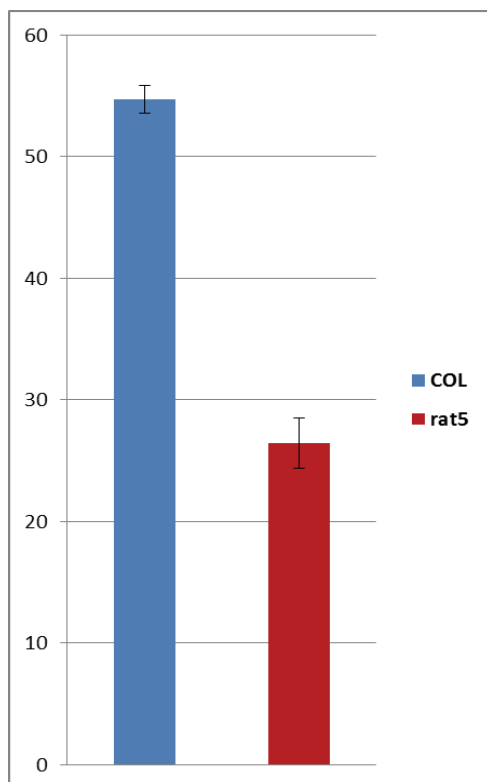
Figure 14. Identification of an *AtH2A1/RAT5* gene and a T-DNA insertion mutant line.

A Schematic representation of the structure of *RAT5* gene, and the location of the T-DNA insertion line (SALK-040809). The T-DNA is inserted in the 5'UTR (dark blue box) of *RAT5* gene on chromosome 5 in *Arabidopsis*. **B** Agarose gel electrophoresis was conducted to genotype both wild-type and mutated *A. thaliana* plants. Primer combination for the PCR and the size of the bands in the molecular marker are provided.

3.2.4 Phenotype of *Ath2a1/rat5* mutant line

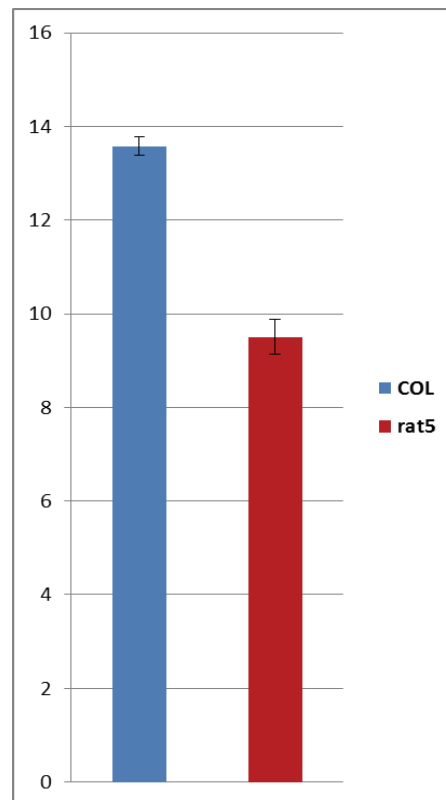
The measurement of the silique length and the quantification of the number of seeds per silique were carried out to assess the fertility of both, the mutant (Salk040809) and wild-type plants. The mean number of seeds per silique in *Ath2a1/rat5* mutant was significantly reduced to 26.44 seeds/silique compared to the 54.68 seeds/silique observed in the wild-type (ANOVA, $p=7.4 \times 10^{-22}$) (**Figure 15A**). The mean length of the silique for *rat5* mutant was also significantly reduced to 9.5 mm compared to the 13.58 mm of the wild-type (ANOVA, $p=2.63 \times 10^{-14}$) (**Figure 15B**). Furthermore, the plant growth and development in the mutant plants appeared to be delayed compared to the wild-type plants (**Figure 15C**).

A



Mean number of seeds per silique (N=100)

B



Mean silique length (mm) (N=100)

c



Figure 15. Fertility reduction and delayed growth and development in *rat5* mutant plants.

A Mean silique length in wild-type (Col) and *rat5* mutant plants. **B** Mean number of seeds per silique in wild-type (Col) and *rat5* mutant plants. **C** Plant phenotypes for *Ath2a1/rat5* mutant and wild-type (Col) plants.

3.2.5 Meiotic and mitotic cytogenetic analysis of wild-type and *Ath2a1/rat5* mutant plants

Cytological analysis was conducted using pollen mother cells to study the meiotic stages for both wild-type (Col; Columbia) and *Ath2a1/rat5* mutant (SALK-040809 line). Meiotic stages were analysed using DAPI-stained chromosome preparation spread.

At the beginning of meiosis, chromosomes appear like thin threads at leptotene (**Figure 16A**). Pairing and synapsis starts happening between homologous chromosomes (partial

synapsis) at zygotene (**Figure 16B**). Homologous chromosomes are completely synapsed and paired at pachytene (full synapsis) (**Figure 16C**). Homologous chromosomes become condensed and desynapsis takes place at diplotene (**Figure 16D**). Furthermore, chromosomes are further condensed and chiasmata are visible between homologous chromosomes at diakinesis (**Figure 16E**). During metaphase I, five condensed bivalents are align at the equatorial plate (**Figure 16F**). At anaphase I, separation between homologous chromosomes take place to different poles (**Figure 16G**). Homologous chromosomes are completely positioned in different poles at telophase I and the chromosomes start to condense again at prophase II (**Figure 16H**). Sister chromatids are aligned at metaphase II (**Figure 16I**) allowing the chromatids to segregate correctly at anaphase II (**Figure 16J**) and, thus, the formation of four haploid nuclei at telophase II (**Figure 16K**). Finally, tetrads are formed containing four gametes which would include half of the genetic material from the original diploid cell (**Figure 16L**). These four gametes will separate from the tetrad and form four pollen grains.

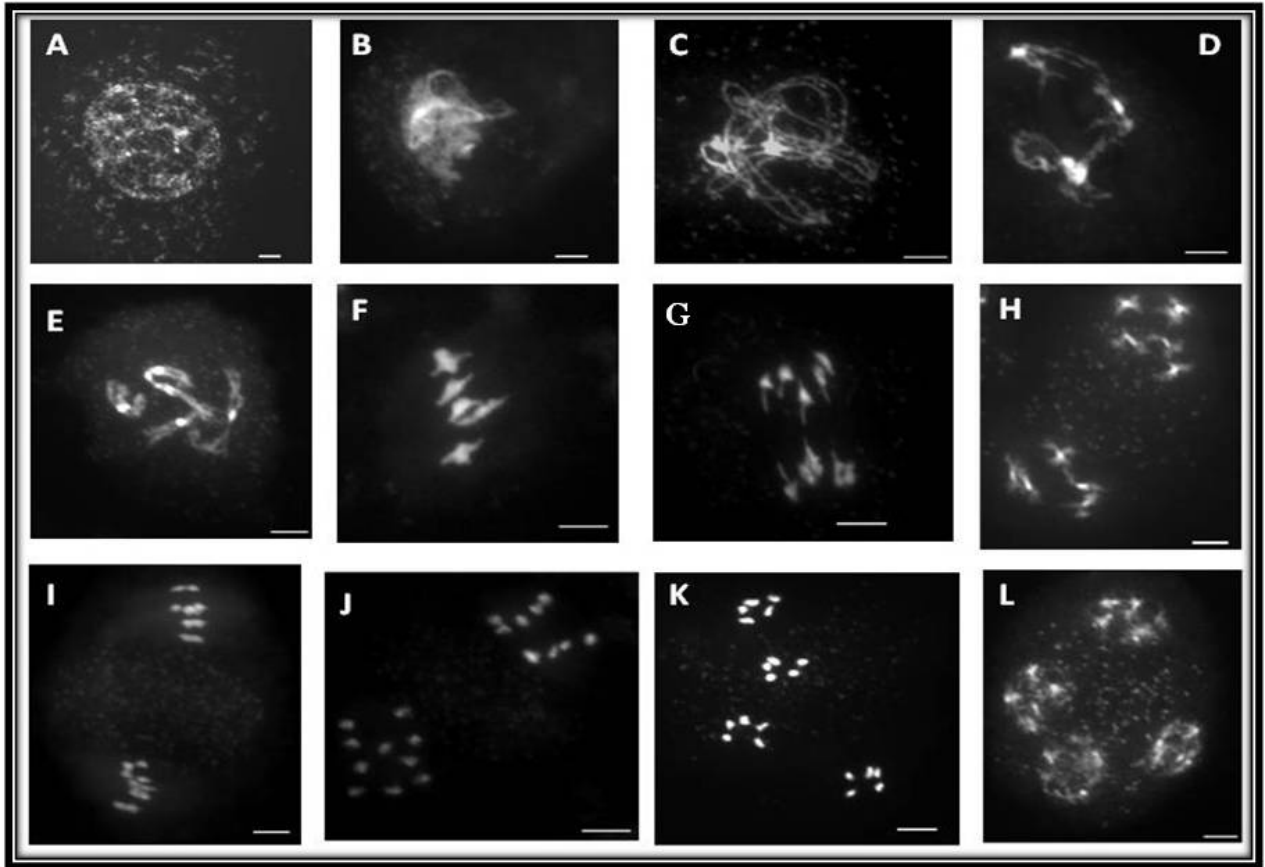


Figure 16. Meiotic stages in *Arabidopsis thaliana* wild-type (Columbia).

A Leptotene, homologous chromosomes appear as a thin thread. Each chromosome has two sister chromatids that are tightly bound to each other. **B** Zygotene, maternal and paternal chromosomes come together to form bivalents (they begin to pair and partially synapsed). **C** Pachytene, chromosomes are completely synapsed. **D** Diplotene, homologous chromosomes are separated but still joined together by chiasmata. **E** Diakinesis, bivalents become more condensed and chiasmata can be easily observed. **F** Metaphase I, bivalents are aligned at the metaphase plate and chiasmata can be counted. **G** Anaphase I, the separation of homologous chromosomes is taking place synchronously to different poles. **H** Telophase I, chromosomes are completely positioned on different poles followed by Prophase II in which chromosomes get more condensed. **I** Metaphase II, sister chromatids coorientation at the equatorial plate. **J** Sister chromatids separate at anaphase II. **K** Telophase II, each five chromatids positioned in different poles. **L** Telophase II, Tetrads get formed with four different nuclei enclosed in one cell. Each nucleus will produce one gamete (pollen grain). Scale bar = 5 μm .

Mitotic cytological analysis showed similarities with the meiotic second division with chromosomes condensing during prophase (**Figure 17**). Chromosomes with both sister chromatids aligned at metaphase allowing correct chromatid segregation at anaphase and, thus, allowing the identical chromosomes to be positioned at opposite poles at telophase. Consequently, both daughter cells have identical genetic material to the original cell (**Figure 17**).

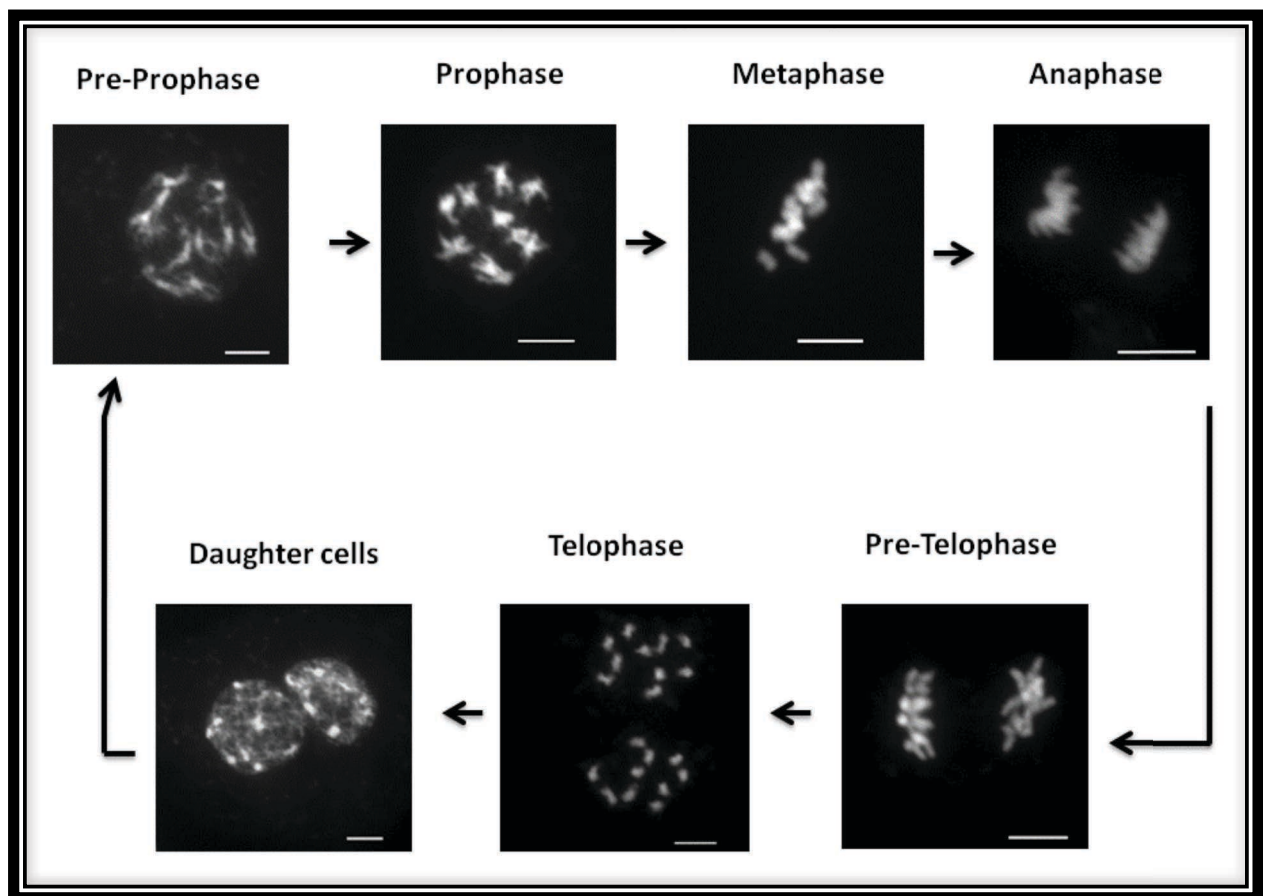


Figure 17. Mitotic cell cycle in wild-type (Col) plants.

The different stages are indicated. Scale bar =5 μ m.

In contrast, the T-DNA insertion line (SALK-040809) mutant in *RAT5* gene showed abnormalities in meiotic chromosome segregation. Pairing and synapses appeared to be normal between homologous chromosomes at prophase I (**Figure 18A, B, and C**). During diplotene and diakinesis, abnormal connections between non-homologous chromosomes could be observed (**Figure 18D and E**). Five bivalents were observed at the metaphase I plate but the transition to anaphase I of the five bivalent was not synchronised as it occurs in the wild-type. Also some lagging chromosomes and chromosome fragmentation was observed at this stage (**Figure 18F**). Furthermore, anaphase bridges and some chromosome fragmentation were observed at anaphase I (**Figure 18G and H, arrows**). Meiosis II (**Figure 18 I-L**) appeared to be normal with normal chromosome segregation in general with some exceptions of some fragmentation (**Figure 18L, arrows**).

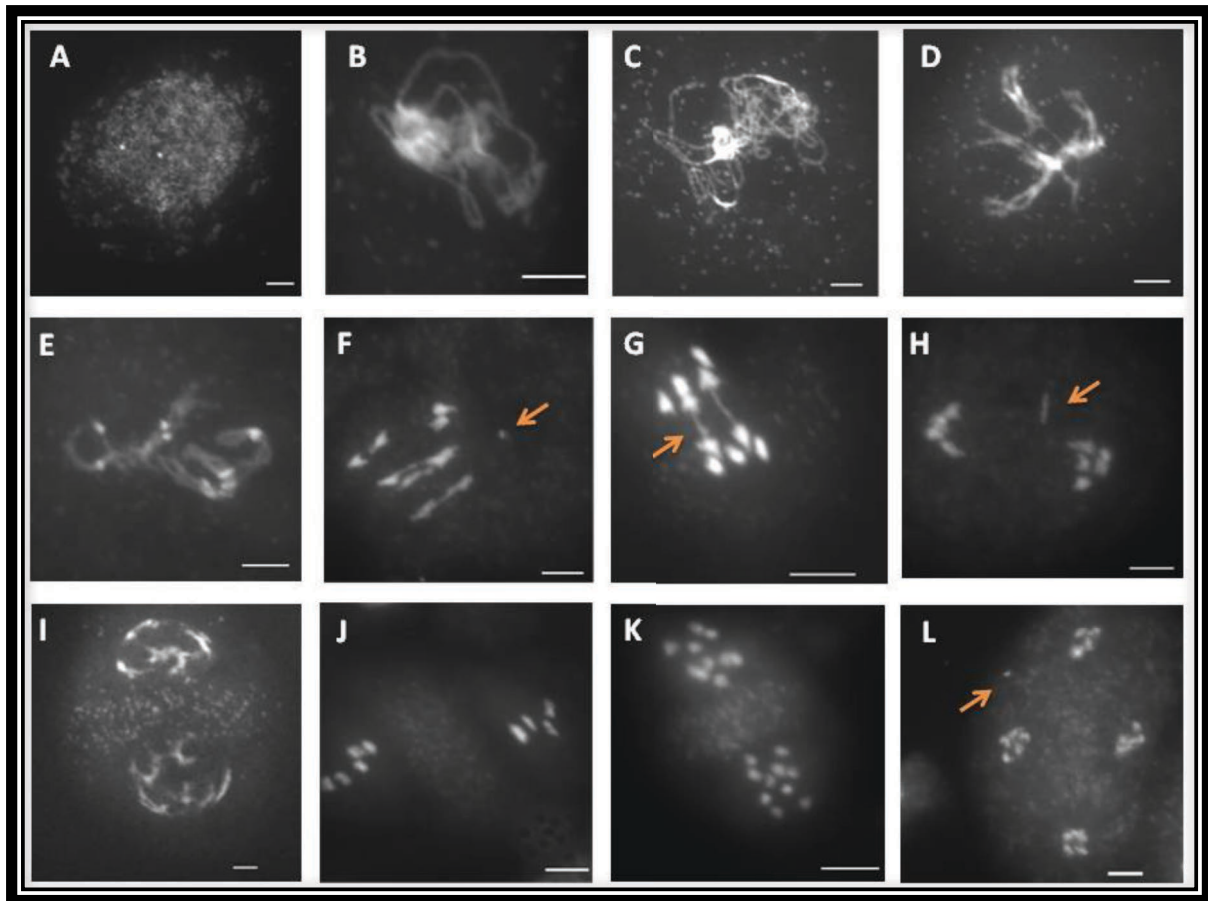


Figure 18. Meiotic stages in *Ath2a1/rat5* mutant (SALK-040809).

A Leptotene. **B** Synapsis is formed between homologous chromosomes at Pachytene. **C** Homologous chromosomes are fully synapsed at pachytene. **D** and **E** Homologous chromosomes are further condensed and connections are visible between non-homologous chromosomes at diplotene and diakinesis. **F** At metaphase I: five bivalents were observed aligning on the metaphase plate, in this cell three bivalents are not segregating the homologous chromosomes yet while in the other two bivalents the chromosomes have already migrated to opposite poles, in addition some chromosome fragmentation was observed (arrow). **G** Anaphase bridges can be observed at anaphase I (arrow). **H** Anaphase I with a chromosome fragment (arrow). **I** Prophase II. **J** Metaphase II. **K** Anaphase II. **L** Telophase II with a chromosome fragment (arrow). Scale bar = 5 μ m.

Furthermore, during mitosis in the *rat5* mutant line we could observe also some anaphase bridges and lagging chromosomes were observed. At telophase, we also observed some chromosome fragmentation (Figure 19). These errors could lead to genomic instability in the mutant and have effects in the growth and development of the mutant plants.

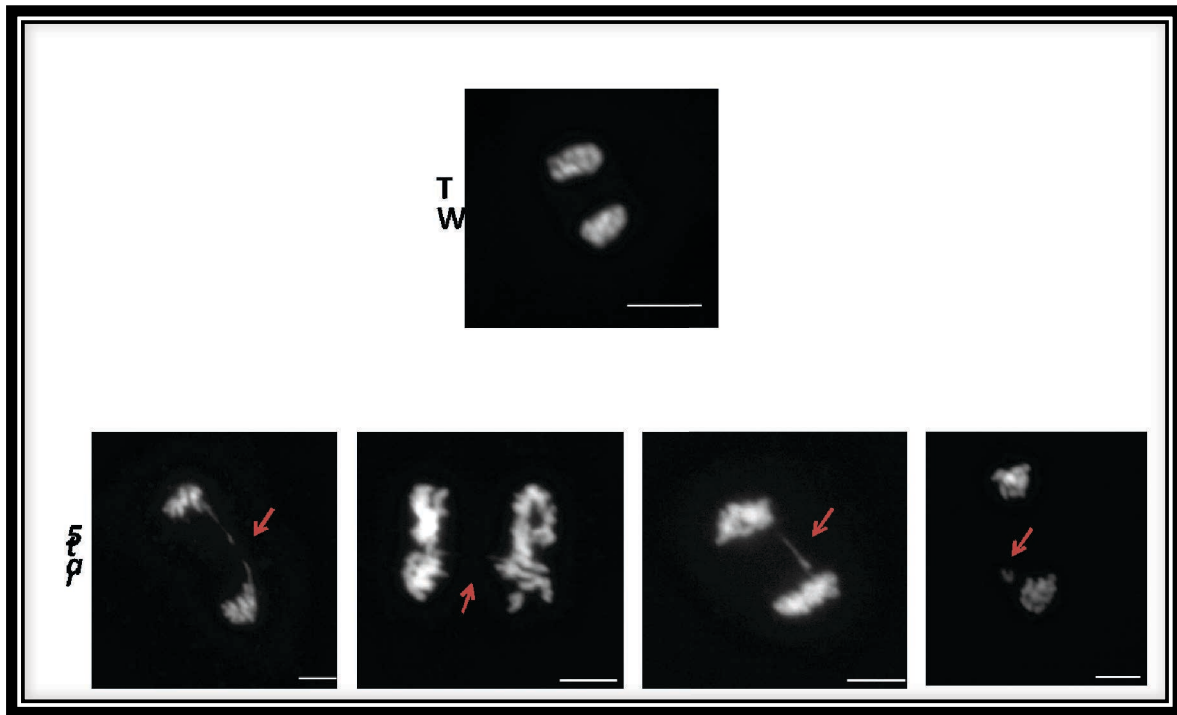


Figure 19. Anaphase-Telophase Mitotic stages in wild-type and *Ath2a1/rat5* mutant plants.

Arrows indicate anaphase bridges/lagging chromosomes and chromosome fragmentation. Scale bar = 5 μ m.

3.2.6 Quantification of the meiotic and mitotic chromosome abnormalities in *Ath2a1/rat5* mutant

The characterization of the T-DNA insertion *Ath2a1/rat5* mutant has showed some chromosome abnormalities. The quantification of these abnormalities is shown in **Figure 20**, indicating the percentage of chromosome abnormalities in meiotic and mitotic cell divisions of *Ath2a1/rat5*. The frequency of cells in the mutant showing anaphase bridges was of around 50% in mitosis and around 87% of the cells in meiosis (**Figure 20A and C**). Additionally, around 16% of the mutant meiocytes presented chromosome connections at Diakinesis (**Figure 20B**). The average number of anaphase bridges per cell observed during meiosis was around 2.5 bridges per cell whereas during mitosis was only around 1% anaphase bridge per cell (N=100) (**Figure 20D**).

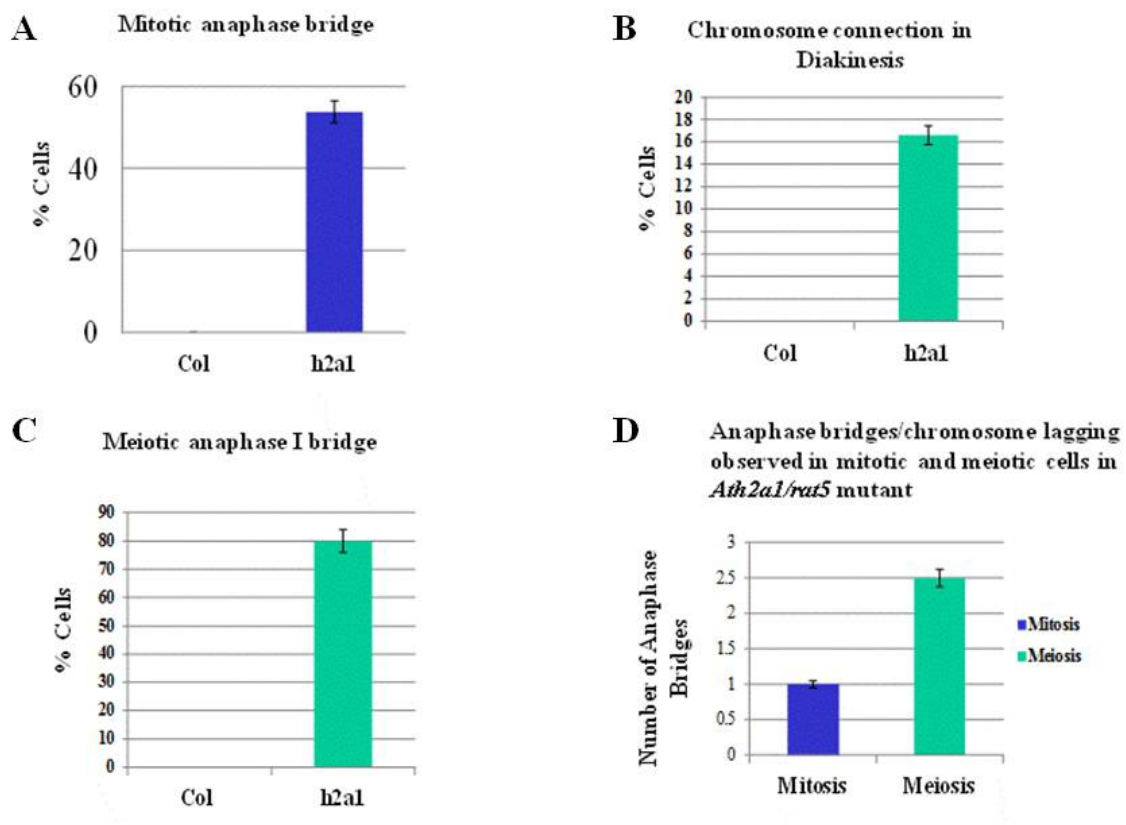


Figure 20. Diagrams representing the quantification of chromosome abnormalities observed in meiotic and mitotic divisions in *Ath2a1/rat5* mutant.

A Percentage of cells presenting mitotic anaphase bridges/chromosome lagging in wild-type (Col) and *Ath2a1/rat5* mutant. **B** Percentage of cells presenting abnormal chromosome connections during Diakinesis (between non-homologous chromosomes). **C** Percentage of cells presenting anaphase bridges/chromosome lagging during meiotic Anaphase I. **D** Mean number of anaphase bridges/chromosome lagging observed during mitosis and meiosis in *Ath2a1/rat5* mutant (N=100).

3.3 Immunolocalisation of different meiotic proteins in *Ath2a1/rat5* mutant

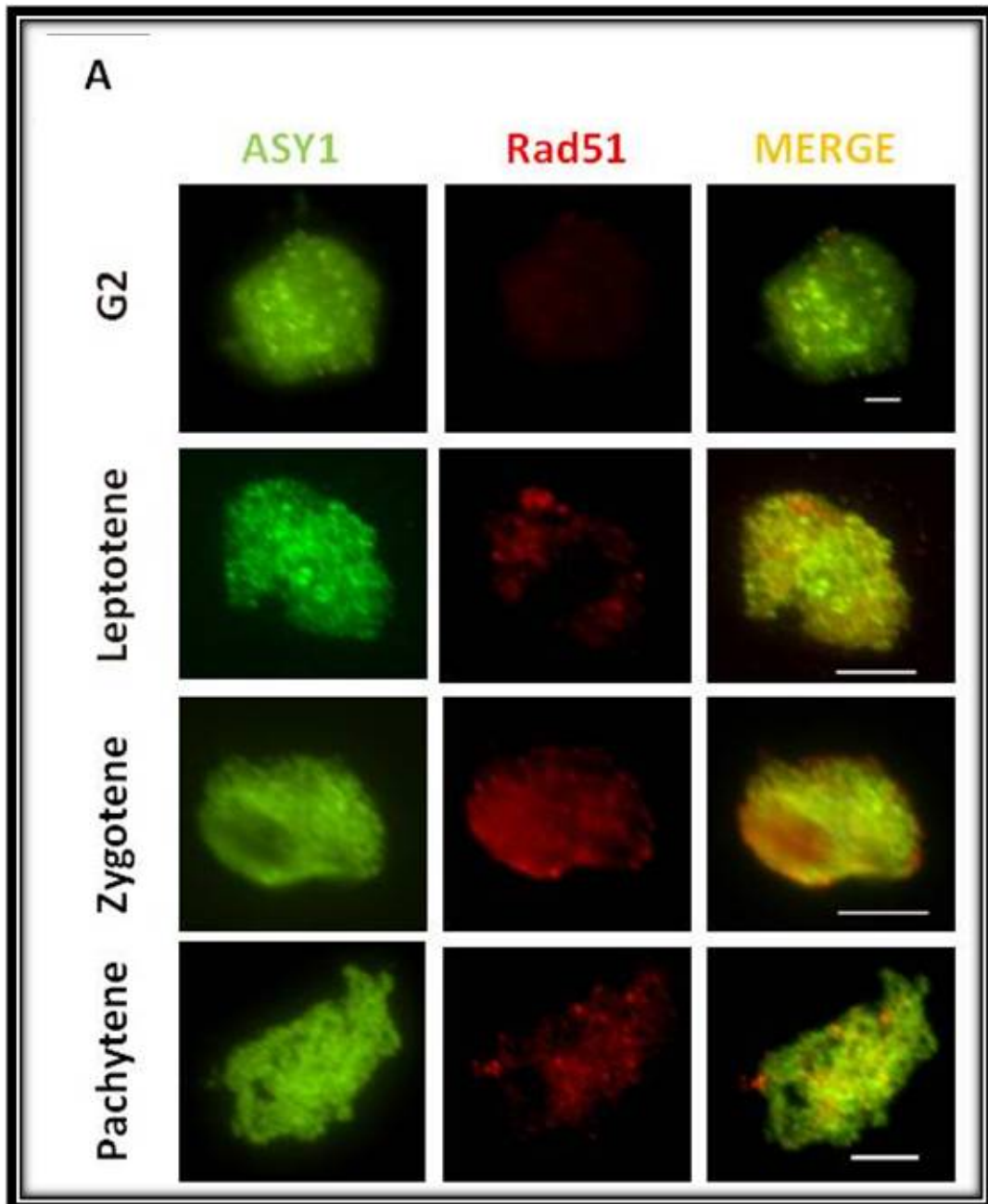
The *Arabidopsis* mutant *Ath2a1/rat5* showed some chromosome abnormalities during meiosis. Different chromosome connections between non-homologous chromosomes identified during prophase I, especially during diakinesis. Furthermore, the presence of anaphase bridges or chromosome lagging during metaphase I/anaphase I was also observed. Therefore, it is important to analyse the localisation of some of the meiotic proteins involved in chromosome recombination using immunocytological techniques in this mutant.

3.3.1 AtASY1 and AtRAD51 immunolocalisation in *Ath2a1/rat5* mutant

The immunolocalisation of meiotic specific chromosome axis protein AtASY1 and the recombinase AtRAD51 has been conducted at early Prophase I in pollen mother cells in wild-type (Col) and *Ath2a1/rat5* PMCs using spreading technique.

The wild-type and mutant localisation of AtASY1 appeared identical with the signal polymerizing along the chromosome axis from G2 stage until zygotene/pachytene (**Figure 21 A and B**). AtRAD51 was detected as foci which accumulated in the meiotic nucleus during early prophase I in a similar pattern in the wild-type and the *Ath2a1/rat5* mutant. The AtRAD51 signal co-localised with AtASY1 chromosome axis signal as a clear foci at leptotene/zygotene for both wild-type and *Ath2a1/rat5* mutant (**Figure 21A and B**). These

observations indicate that AtASY1 and AtRAD51 are localising accurately in the *Ath2a1/rat5* mutant.



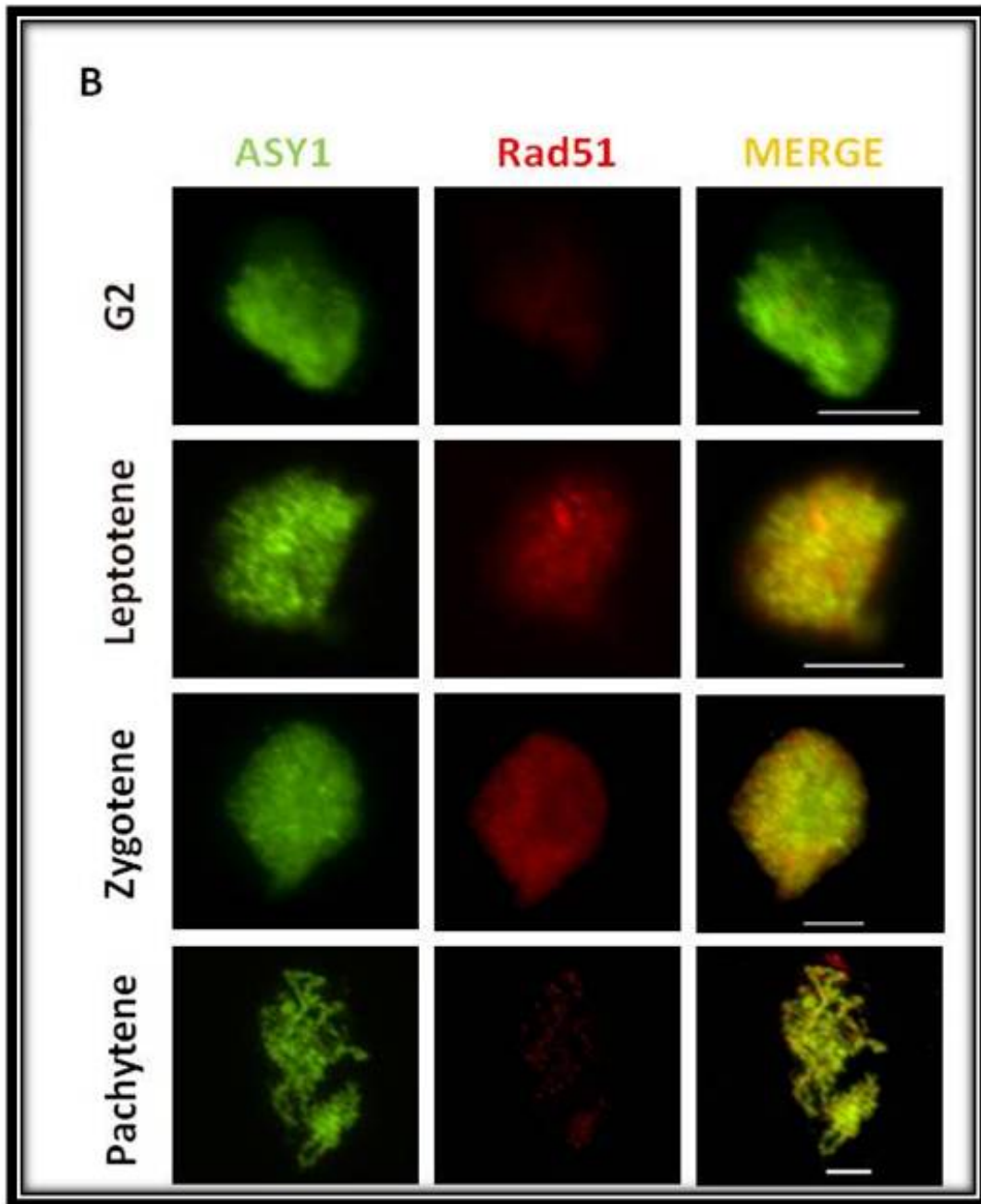


Figure 21. Dual immunolocalisation of AtASY1 (green) and AtRAD51 (red) during meiotic Prophase I in the wild-type and *Ath2a1/rat5* mutant.

A AtASY1 - AtRAD51 co-localisation in wild-type pollen mother cells. B Dual immunolocalisation of AtASY1 and AtRAD51 in the *Ath2a1/rat5* mutant. Scale bar = 5 μ m.

3.4 Genetic analysis of the T-DNA transformation of *Arabidopsis* by Floral Dipping

The histone isoform AtH2A1 has been related to the T-DNA transformation efficiency in *Arabidopsis*. Mutants for *AtH2A1* locus have been named *rat5* or *resistance to Agrobacterium transformation 5* because they showed a reduced frequency of T-DNA transformation. Furthermore, the over-expression of this locus also increases the frequency of T-DNA transformation in plants (Tenea *et al.*, 2009). Thus, it seems that AtH2A1/RAT5 might be playing an important role in the T-DNA integration in plants. All these analysis have been done in root-based T-DNA transformation methodologies but not in the most frequently used method of floral dipping. Thus, we decided to conduct a genetic analysis with several mutants to quantify their role in the T-DNA transformation using the floral dipping methodology.

Different mutants were selected to characterise their role in T-DNA transformation by floral dipping: the histone *Ath2a1/rat5* mutant, different meiotic mutants involved in Homologous Recombination (HR): *Atspo11.2*, *Atmre11*, *Atrad51*, *Atmsh4* and *Atmlh3*, and different mutants involved at different levels of DSB repair by Non-Homologous End Joining (NHEJ): *Atku70*, *Atku80* and *Atlig4*.

The selected HR mutations were done because their proteins play an essential role in DSBs repair. SPO11 proteins play a basic role inducing DSBs at early stages of meiosis (Zicher and Kleckner, 1999). The presence of these DSBs during meiotic division could be utilised for the T-DNA integration. Furthermore, AtMRE11 is involved in the processing of these DSBs and AtRAD51 in ssDNA invasion (for more details see chapter one) (Uanschou *et al.*, 2007; Waterworth *et al.*, 2007). AtMSH4 and AtMLH3 are key proteins in the process of dHj and the formation of Class I COs (Couteau *et al.*, 1999; Li *et al.*, 2004; Osman *et al.*, 2011). On the other hand, NHEJ pathway has been shown to be very important in DSB repair in somatic cells in plants. We have analysed null mutants for AtKU80 and AtKU70 which recognise and

join the DSB ends and AtLIG4 which is the DNA ligase that will fill the gap created by the DSB (Tamura *et al.*, 2004; West *et al.*, 2004).

The T-DNA construct used in this experiment (**Appendix B**) contains a bacterial antibiotic resistance gene (kanamycin resistance) and a plant selection marker the phosphinothricin resistance gene or herbicide resistance (Basta®). The T-DNA transformation chosen was Floral Dipping Transformation and it was carried out in the wild-type (Col) and the different homozygous mutants at the same time and with the same conditions (see Material and Methods).

Several plants from each line were used to do the floral dipping transformations and no differences among them were observed afterwards. Seeds were collected only from the treated flower buds, other inflorescences that appear later on were cut to avoid contamination. Seeds from each mutant, wild-type and controls were grown on soil in mini-pots. After 2-3 weeks of standard controlled growth in the glasshouse when the first true leaves appeared they were treated with Basta® herbicide. The Basta® treatment consisted of spraying the herbicide (glufosinate-ammonium solution (0.1g/l)) onto the plants three times with a gap of 7-8 days between each spray. Plants transformed with the T-DNA containing the Basta resistance gene grew normally whereas plants without the resistance did not survive (**Figure 22**).

Different controls were included in this experiment: a negative control using wild-type (Col) seeds from a plant without Floral Dipping treatment which after the herbicide treatment not plant should survive. And a positive control using a T-DNA transformed line which T-DNA insertion site is known and therefore it is possible to genotype for homozygous seeds for the T-DNA insertion with the Basta® resistance which would allow to all the plants to be resistance to the herbicide and survive the treatment. A total of 600 germinated growing

plants from each material were evaluated for the herbicide resistance and therefore the T-DNA transformation. The negative control plants did not presented any survivors (**Figure 22E**), whereas the positive control showed all the plants to be resistant to the herbicide treatment (**Figure 22D**), as expected.

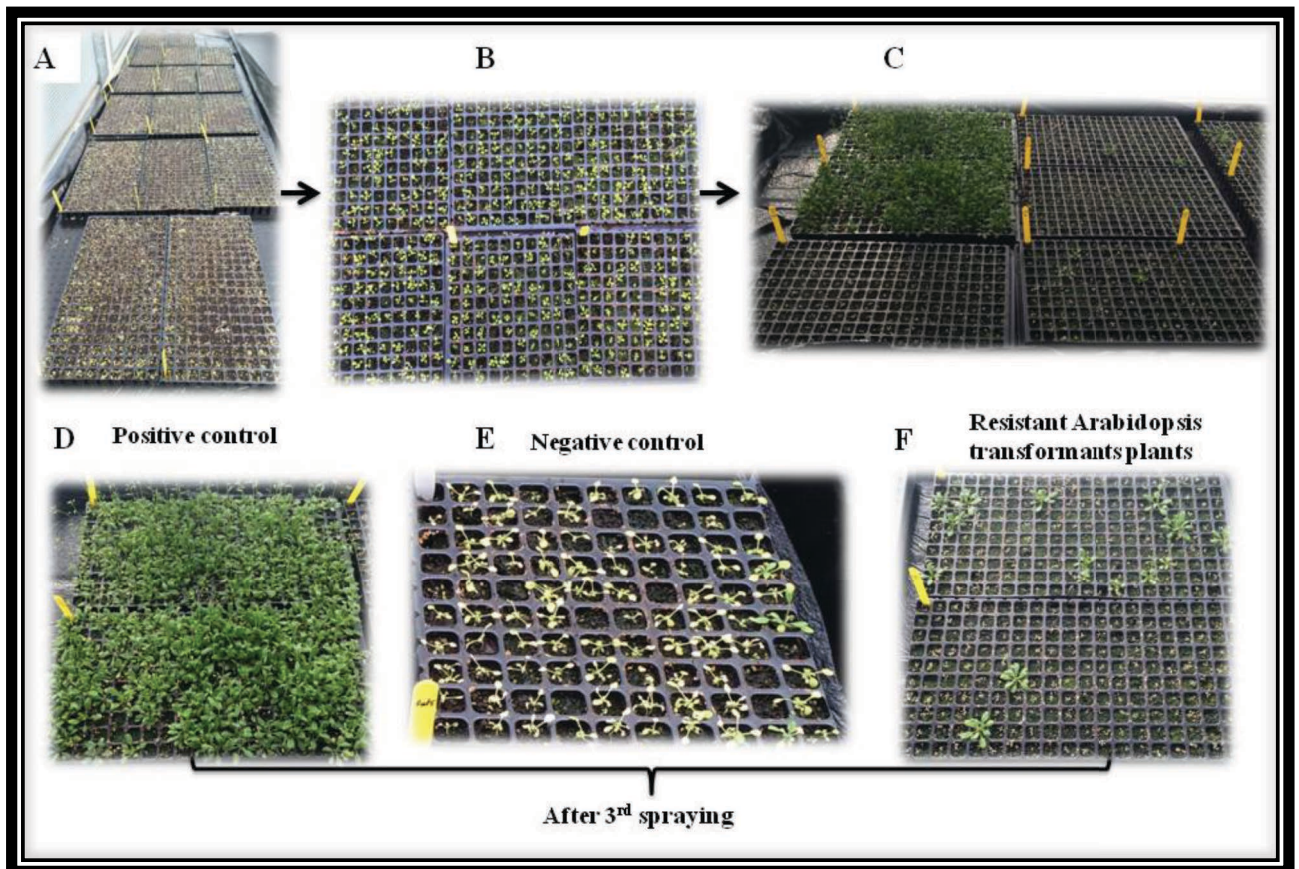


Figure 22. Evaluation of T-DNA transformants by herbicide treatment.

A Seeds were sowed in mini-pots. B Plants were let to grow until the first true leaves emerged and then a solution of glufosinate-ammonium was sprayed for 3 times with a 7-8 days interval. C Overview of the mini-pots after the third spray treatment, survivor (Basta® resistance) plants are obvious and can be counted accordingly. D Positive control with herbicide resistance transformed into the line by the T-DNA, all the plants survived. E Negative control, these plants were not transformed with the T-DNA including the Basta® resistance, after the herbicide treatment there were no survivors, all the plants were bleached by the herbicide. F Wild-type transformation by Floral Dipping, some plants were transformed (survivors) and others were not transformed (non survivors).

The number of transformant plants from the wild-type floral dipping offspring was 34/600 about a 5.6%. The survivors were counted for each gene type and a chi-square test (χ^2 test) that was conducted to calculate if their differences of statistically significant (**Table 3**). P-values were calculated: 0.100518 for *Ath2a1/rat5*, $6.7E^{-06}$ for *Atspo11.2*, $7.59E^{-07}$ for *Atmre11*, $1.78E^{-05}$ for *Atrad51*, 0.005581 for *Atmsh4*, 0.000474 for *Atmlh3*, 0.001778 for *Atku70*, 0.000941 for *Atku80* and $1.78E^{-05}$ for *Atlig4*. All p-values are significant except for *Ath2a1/rat5* which is non-significant (NS).

Floral Dipping T-DNA integration seems to require the formation of DSBs during meiosis as in absence of AtSPO11.2 the T-DNA transformants decrease 5.6 times compared to wild-type. T-DNA insertion seems to require DSB resection by AtMRE11 as in its absence the T-DNA insertion decreases 8.5 times that of the wild-type. In the absence of single strand invasion by AtRAD51, T-DNA integration gets reduced to 4.8 times compared to wild-type. Also, in the absence of double Holliday junction (dHj) maturation and resolution by AtMSH4 and AtMLH3, the T-DNA insertion reduced to 2.2 and 3 times respectively comparing to the wild-type. Thus, meiotic HR seems to play a highly important role in floral dipping T-DNA integration. Furthermore, NHEJ DSB repair pathway seems to be also playing an important role in Floral Dipping T-DNA integration as in absence of AtKU70, AtKU80 and AtLig4 the transformation decreased to 2.6, 2.8 and 4.8 times that of the wild-type, respectively (**Figure 23A and B**).

Material	No	Basta® Resistance Plants	χ^2 test P-values
Positive control	600	600	
Negative control	600	0	
Wild-type (Col)	600	34	
<i>Atspo11.2</i>	600	6	6.7E-06
<i>Atmre11</i>	600	4	7.59E-07
<i>Atrad51</i>	600	7	1.78E-05
<i>Atmsh4</i>	600	15	0.005581
<i>Atmlh3</i>	600	11	0.000474
<i>Atku70</i>	600	13	0.001778
<i>Atku80</i>	600	12	0.000941
<i>Atlig4</i>	600	7	1.78E-05
<i>Ath2a1/rat5</i>	600	22	0.100518

Table 3. Floral Dipping T-DNA transformation results.

The number of T-DNA transformants after Floral Dipping and the chi-square test p values are indicated.

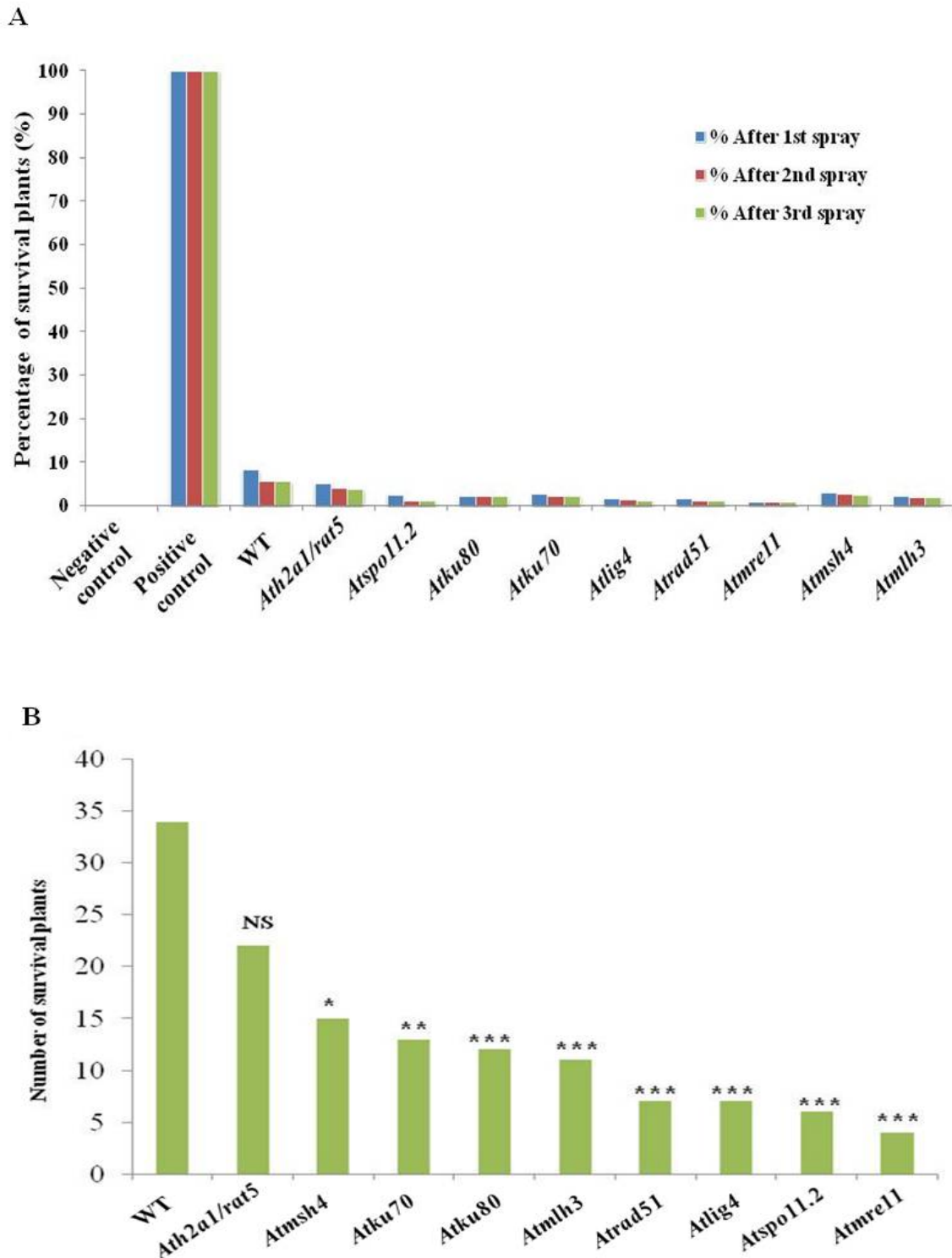


Figure 23. Evaluation of the T-DNA integration in different mutants.

Chi-square test was used to calculate which mutants were statistically significant from the wild-type. The *Ath2a1/rat5* values were not significant (NS) with respect to the wild-type. The (*) represents a significant reduction in transformed plants with $P < 0.1$, the (**) represents a highly significant reduction in transformed plants with $P < 0.05$. The (***) represents the higher significant reduction in transformed plants with $P < 0.0001$.

3.5 DISCUSSION

3.5.1 Histone H2A isoforms in *Arabidopsis thaliana*

Arabidopsis histone *AtH2A* loci are encoded in a family of genes that are distributed along the five chromosomes. These genes encode for 13 isoforms of AtH2A (including core histones and histone variants). Mammalian genomes include four isoforms for H2A proteins namely core H2A histone isoforms and histone variants macroH2A, H2A.F/Z and H2AX (Yi *et al.*, 2006). When *Arabidopsis* AtH2A isoforms are compared to the mammalian isoforms at their amino acid sequence level, the different isoforms can be classified: *Arabidopsis* AtH2A8, 9 and 11 histone isoforms are similar to the histone variant H2A.F/Z in mammals (**Table 4**). *Arabidopsis* AtH2A3 and 5 isoforms are similar to the histone variant H2AX in mammals. The *Arabidopsis* AtH2A3 and AtH2A5 (also known as AtH2AX1 and AtH2AX2, respectively) contain a conserved SQEF motif that is also found in mammals. The serine residue in *Drosophila* and yeast is the amino acid residue that is rapidly phosphorylated to signal the region where a DSB has occurred and initiates the processing/repair of this DSB and meiotic recombination (Yi *et al.*, 2006). The other *Arabidopsis* histone AtH2A6, 7 and 12 isoforms include a specific SPKK motif that is located at their C-terminal. It seems that these motifs are conserved in flowering plants and may play a role in sperm development. Phosphorylation of these motif contribute in chromatin condensation in which these motifs attach to A/T rich DNA minor groove (Yi *et al.*, 2006).

Histone H2A variants have been studied in different species showing several vital functions including regulation of gene expression and the proper segregation of chromosomes. For example, H2A.W seems to play a crucial role in chromatin condensation and heterochromatin

organization (Yelagandula *et al.*, 2014). Histone H2A variants seem to comprise identical conserved motifs between animals and plants that could suggest the conservation of similar functions like the role of H2A.W in organizing heterochromatin (Yelagandula *et al.*, 2014). The histone variant H2A.Z might play an important role in the maturation of meiotic crossovers in *Arabidopsis thaliana* (Choi *et al.*, 2013). Furthermore, H2A.Z has been suggested to have a thermo-sensing role, being affected at different temperatures at the nucleosome level. This is very important for the regulation of gene transcription during the temperature change response (Kumar and Wigge, 2010).

Protein	Domain position	Protein length (a.a)	function of protein
AtH2A1	At5g54640	130	T-DNA integration
H2A2	At4g27230	131	_____
H2A3	At1g54690	142	H2AX1 (SQEF) responding, marking DSBs
H2A4	At4g13570	118	_____
H2A5	At1g08880	142	H2AX2 (SQEF) responding, marking DSBs
H2A6	At5g59870	150	DNA binding motifs (SPKK)
H2A7	At5g27670	150	DNA binding motifs (SPKK)
H2A8	At2g38810	136	(H2A.F/Z) Transcription factor
H2A9	At1g52740	134	(H2A.F/Z) Transcription factor
H2A10	At1g51060	132	_____
H2A11	At3g54560	136	(H2A.F/Z) Transcription factor
H2A12	At5g02560	153	DNA binding motifs (SPKK)
H2A13	At3g20670	132	_____

Table 4. *Arabidopsis* Histone AtH2A isoforms.

Information obtained from TAIR (<http://www.arabidopsis.org/>).

3.5.2. Different roles for Ath2A1/RAT5 histone protein in *Arabidopsis*

HTA1 gene encodes for Ath2A1 (RAT5) protein that has been previously postulated to be important for the T-DNA integration from *Agrobacterium tumefaciens* into the plant genome (Tenea *et al.*, 2009; Yi *et al.*, 2006). *Agrobacterium tumefaciens* possesses a virulence (*VIR*) gene that encodes the VirD2 protein. This protein is attached to the single strand DNA (T-strand) which might prevent it from nuclease digestion when inserted into plant cells. The insertion of the T-DNA occurs randomly into the genomic plant DNA (Tenea *et al.*, 2009). The T-DNA integration into the genomic plant chromatin might be a consequence of the interaction between the VirD2 protein and some histones (Tenea *et al.*, 2009). Based on this, it has been speculated that the mutation of *HTA1* gene could lead to changes in chromatin structure and chromatin remodelling that could change the T-DNA integration (Tenea *et al.*, 2009). Nevertheless, in this study, we found no evidence that Ath2A1/RAT5 plays an important role in T-DNA integration using floral dipping.

However, we have identified chromosome abnormalities during mitotic and meiotic divisions in *Ath2a1/rat5* mutant. Chromosome lagging and anaphase bridges have been observed during anaphase-telophase stages in mitosis as well as some chromosome fragmentation. A reduction of fertility has been observed in an *Ath2a1/rat5* mutant with around 50% production of seeds. We have observed different connections between non-homologous chromosomes during prophase I, asynchronous anaphase I and the presence of anaphase bridges or chromosome lagging at anaphase I. Nevertheless, the frequency of chromosome mis-segregation is very small (1.5% of post anaphase I meiocytes). The seeds number reduction in the mutant cannot be explained just by such a small frequency of chromosome missegregation. Nevertheless, the connections and anaphase bridges/chromosome lagging and chromosome fragmentation observed during and after anaphase I could explain this

reduction in fertility. These bridges during anaphase I could be the result of a problem in the resolution of the chiasmata that could lead to different chromosome rearrangements such as deletions (chromosome fragments observed). These rearrangements may contribute in the loss of vital genetic information that could produce unviable gametes and therefore, the reduction on fertility (Acilan *et al.*, 2007).

3.5.3 Anaphase bridges/chromosome lagging in *Ath2a1/rat5* mutant

DNA damage can be induced by several endogenous or exogenous factors such as radiation. The majority of DNA double Strand Breaks (DSBs) can be repaired accurately and the original chromosome structure can be recovered (Acilan *et al.*, 2007). The major pathways to repair DSBs are the homologous recombination (HR) and the non-homologous end joining (NHEJ).

The ligation of non-homologous chromosome ends by NHEJ could create errors and thus, genomic instability. These errors can be visualised by cytological analysis as anaphase bridges/chromosome lagging/chromosome fragmentation. It has been suggested that NHEJ might play an important role in preventing anaphase bridge formation. Moreover, it has been reported that cohesin deficiency can also cause anaphase bridges (Acilan *et al.*, 2007).

Meiotic HR initiates with the production of DSBs by SPO11 and after these DSBs have to be repaired. The majority of these DSBs are processed through HR using the sequence homology between the homologous chromosomes and some of them will be repaired as crossovers (COs) and others as non-crossovers (NCOs). The connections observed during prophase I in *Ath2a1/rat5* mutants could be errors produced during the DSB processing and

could also explain the presence of anaphase bridges and chromosome lagging and fragmentation later on.

Anaphase bridges can be described as chromatin fibres that join between two chromosomes during the anaphase stage (Moa *et al.*, 2008). In human, anaphase bridges are considered as a hallmark of malignant cells and have been used as a diagnostic tool in oncology (Hoffelder *et al.*, 2004). Remarkably, the correlation between the formation of anaphase bridges and tumorigenesis has been described in human and mouse as a result of losing or gaining genes and thus altering the amount of oncogenic proteins. These alterations occur as a consequence of formation of breakage-fusion-bridges which would increase and get worse after every cell cycle division accumulating error (Hoffelder *et al.*, 2004).

Several studies have been proposed to explain how anaphase bridges can be produced. After DNA replication, fusion between sister chromatid ends or different chromosome ends may occur. Therefore, when spindle microtubule fibres pull from the chromosome centromeres in opposite directions during the anaphase stage these fusions would show as anaphase bridges (Hoffelder *et al.*, 2004; Moa *et al.*, 2008). Consequently, at the end of anaphase, chromosome breaks and fragmentation might take place which could lead to genomic instability (**Figure 24**).

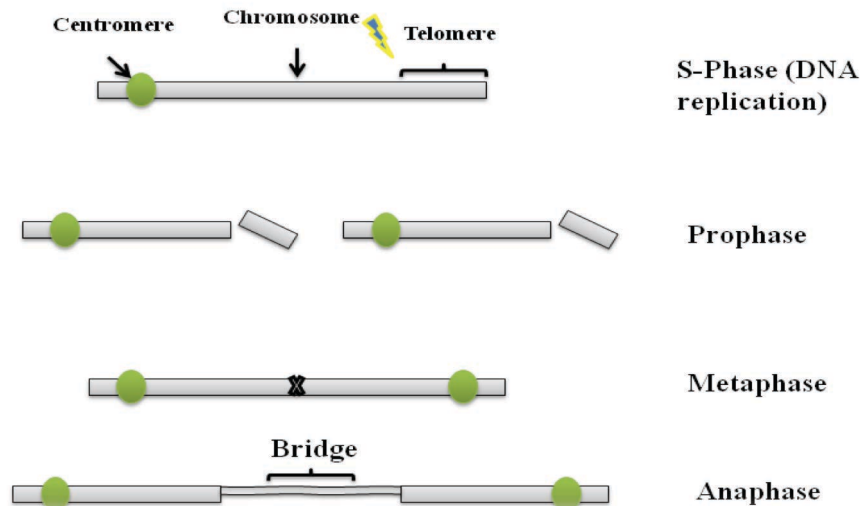


Figure 24. Schematic representation showing a proposed model to produce anaphase bridges, chromosome lagging and fragmentation.

A DSB might occur in one chromatid at S-phase or G2 phase. The process of the DSB might end up joining wrongly chromosome or chromatid ends, fusing chromatids or chromosomes and producing anaphase bridges that would consequently be processed by DNA brakes and visualize as chromosome fragments.

It has been found that NHEJ might play a predominant role of preventing the formation of anaphase bridges. Different studies have showed that mutations in NHEJ proteins could contribute to the formation of non-reciprocal translocation which normally forms anaphase bridges (Difilippantonio *et al.*, 2002).

Studies also showed that the fixation between the chromosomes ends during NHEJ require Ku80 protein (important protein for chromosome end joining). Deficiency of this protein leads to inappropriate fusion between chromosomes ends. However, another study proposed that when NHEJ is mutated, HR pathway is enhanced to form somatic CO intermediates which are not able to be resolved correctly, therefore contributing in the formation of chromatin anaphase bridges (Moa *et al.*, 2008).

By itself, HR pathway does not seem to be necessary for the production of anaphase bridges. However, some HR components might participate in repairing DSBs by other different

pathways that may lead to errors and thus the formation of anaphase bridges when some NHEJ proteins are not present. On the other hand, when both pathways (NHEJ and HR) are mutated, the number of anaphase bridges are significantly reduced which seems to suggest the previous hypothesis to be correct (Delacote *et al.*, 2002; Pierce *et al.*, 2001).

During each cell cycle division, chromosomes are compacted dramatically to reach higher condensation at metaphase stage. This organisation is monitored by several proteins to maintain the genomic integrity of the cell. Condensin is one of these major protein components that have been found to be involved in this during meiotic and mitotic cell divisions. Condensin is a multi-protein component that includes two basic elements described as the Structural Maintenance chromosomes family (SMC2 and SMC4) and other regulatory subunit proteins. Two types of condensins have been identified, Condensin I and Condensin II both of which contain SMC2 and SMC4 subunits. In wild-type, condensins start polymerizing along the chromosome arms and centromeres at the beginning of prophase and they disappear at anaphase. There is an interaction between the N-terminus of H2A/H2A.Z and CAP-H (CAP-H is a protein that is associated with SMC2 at the N-terminal and SMC4 at the C-terminal in Condensin I). It is suggested that in absence of H2A/H2AZ proteins the same phenotype to that when condensins are mutated should be observed.

It is reported that Aurora-B-dependent kinase is indispensable for the phosphorylation of CAP-H which is necessary for the attachment of the condensin complex to the H2A/H2AZ proteins. RNA interference was used to mutate *H2AZ* and it was found that the amount of condensins was significantly reduced. However, a limited amount of condensin still could be localised at the chromosome arms which may have occurred because of its interaction with other histone isoforms like H2A (Lipp *et al.*, 2007).

Remarkably, the phenotype found when condensins were mutated *Arabidopsis thaliana* was consistent with the presence of anaphase bridges during anaphase of both meiosis and mitosis

(Hirota *et al.*, 2004). In *A. thaliana*, *AtSMC4* gene was mutated by a T-DNA insertion but the mutation was lethal. Nevertheless, chromatin bridges have been reported in *Arabidopsis* when some *AtSMC4* could still be localised at the chromosome arms (Siddiqui *et al.*, 2003; Yu and Koshland, 2003; Yu and Koshland, 2005).

Topoisomerase II has been found to also play essential functions in resolving chromatin connections between chromosomes. Moreover, when anaphase bridges are formed, a failure to correct these structures between homologous chromosomes or sister chromatids has been reported. Hence, it was suggested that condensins and topoisomerase II proteins could be important for preventing the formation of anaphase chromatin bridges (Holmes and Cozzarelli, 2000; Chan *et al.*, 2004).

Other interesting studies reported that there is an indirect association between condensin and cohesin proteins. The cohesion complex is a multi-protein complex which is essential for the correct chromosome segregation during mitosis and meiosis. The condensin complex polymerizes along the chromosomes arms and disappears at anaphase to facilitate the separation of the sister chromatids to opposite poles during mitosis. However, defects in removing the cohesion complex proteins at the correct stage (anaphase) would contribute to inability to separate the sister chromatids accurately. A study has shown that condensin could play a crucial role of indirectly removing the cohesin complex at the correct stage (Yu and Koshland, 2005). Removing the cohesin proteins is the main role of the enzyme called Separase. The Separase activity is inhibited during prophase by the protein Securin. At metaphase, when all the chromosomes are at the equatorial plate of the spindle, the Chromosome Passenger Complex (CPC) recognise the appropriate tension and activates the Anaphase Promoting Complex/Cyclosome (APC/C) which will degrade the Securin and thus activating the Separase activity. The Separase will cleave the SCC1 cohesin subunit and

released the sister chromatid cohesion so the MTs of the spindle would be able to separate the sister chromatids into opposite poles (Uhlmann *et al.*, 2000).

Several studies have found that centromeric histone variant H3 (*CenH3*) is affected when condensins have been depleted in different organisms such as *Drosophila*, humans and budding yeast. Therefore, it was proposed that condensins are indispensable for *CenH3* maturation, organisation and maintaining (Yong-Gonzalez *et al.*, 2007; Jager *et al.*, 2005 and Samoshkin *et al.*, 2009).

Further studies have shown that budding yeast is enriched for condensin on the chromosome arms particularly on rDNA regions (highly repetitive regions) in order to keep genomic stability and avoid any fusions in these regions where ectopic recombination could occur (Yu and Koshland, 2005; Freeman *et al.*, 2000). Nevertheless, other studies showed that rDNA regions attach to the cell's nucleolus at the same time when condensin is polymerized and loaded into the cell nucleolus, so these attachments would have more of a role in preventing these repetitive domains from fusion (Koshland, 2005; Freeman *et al.*, 2000). The deficiency in condensins could contribute to shortening of rDNA repetitive regions during cell divisions (Ide *et al.*, 2010; Smith *et al.*, 2014).

In this study, we have found that anaphase bridges are formed in an *Ath2a.1/rat5* mutant line during mitotic and meiotic divisions. Further analysis investigating different recombination proteins immunolocalisation was carried out in order to find out which mechanisms produced these anaphase bridges.

3.5.4 *Agrobacterium tumefaciens* T-DNA integration during Floral Dipping is not dependent of AtH2A1/RAT5 but on DSB formation and processing by HR and NHEJ pathways

Genetically modified (GM) crops could be a very useful tool for the agro-economic future of developing countries. The continuous increase of the world population (from 6 to 9 billion inhabitants in 2050), the increase industrialization and thus nature pollution and the climate change would enforce an increase in the yield and nutritional improvement of crops in the next decades. Genetic engineering could be a very useful tool to provide some solutions to this problem. GM transgenic crops have been produced in the last decade such as herbicide resistant canola (Alimohammadi *et al.*, 2009; Valentine, 2003). *Agrobacterium tumefaciens* contains a Tumour Inducer (Ti) plasmid which contains the Transfer DNA (T-DNA) that would be able to be integrated into the host plant cell genome (Alimohammadi *et al.*, 2009).

The process of the T-DNA transformation from the Ti plasmid into the host plant cell requires different plasmid virulence genes in the bacteria and the use of several proteins located in the host cell (Zhu *et al.*, 2003). How the T-DNA fragment gets integrated into the plant genome is still unanswered question. The T-DNA integration is likely dependent on the DNA repair machinery and chromatin proteins like histone H2A.1 present in the plant host cell (Alimohammadi *et al.*, 2009). AtH2A.1 (RAT5) protein has been related to the T-DNA integration (Valentine, 2003). However, the exact role of AtH2A.1 in the T-DNA integration is not fully understood, whether this protein affects the chromatin compaction, interacting with VirD2 from *A. tumefaciens* in the host DNA or has a role by the interaction with other proteins that have not been yet discovered (Valentine, 2003).

AtH2A.1 (RAT5) is one of the *Arabidopsis* H2A isoforms which is a main component of the nucleosomes. AtH2A.1 seems to play a vital role in DSB repair and chromosome stability.

Chromatin remodelling and DNA accessibility can be regulated throughout post-translation modification of histone tails. For example, in budding yeast there are only 2 genes encoding for histone H2A and both code for an identical protein. This H2A protein contains a histone tail which includes an S/TQ motif which can be the target for serine/threonine phosphatidylinositol 3-kinases like ATM (Ataxia Telangiectasia Mutated) and ATR (Ataxia Telangiectasia and Rad3-related protein) with key roles in HR and DNA-PKcs (DNA-dependent Protein Kinase catalytic subunit) which is essential in NHEJ. Phosphorylation of the serine in this domain occurs rapidly after a DSB has formed (Kamakaka and Biggins, 2005; Sarma and Reinberg, 2005). The phosphorylation of the histone H2A on this S/TQ motif is relying on DNA dependent checkpoint kinases ATM, ATR and DNA-PKcs. It has been found that these kinases are surrounding the DNA damages and recruiting other proteins that are important for DNA DSB repair and processing. In higher eukaryotes, like in humans and plants like *Arabidopsis*, more histone H2A isoforms have evolved from this primordial H2A form. Higher eukaryotes have evolved in a H2A histone variant to keep this role, the H2AX variant which conserved the S/TQ motif. *Arabidopsis* genome encodes for 2 *Ath2AX* genes producing nearly identical proteins which have a key role in labelling and correctly processing DSBs during mitosis and meiosis (unpublished data, E Sanchez-Moran). Nevertheless, we cannot rule out that other histone Ath2A isoforms could not be taking part in other aspects of DSB repair and processing during mitosis and meiosis as a remnant of the H2A histone in budding yeast.

According to our results, our *Ath2a.1* mutant shows abnormalities during DSB repair/processing during meiosis visualised as connections between chromosomes, anaphase bridges, chromosome lagging and fragmentation. Furthermore, anaphase bridges, chromosome lagging and fragmentation were also observed during mitotic divisions. These

abnormal results confirm that AtH2A.1 (RAT5) plays a crucial role in the processing of DNA DSBs.

DSBs can occur as a result of an error during DNA replication or can be catalysed by proteins like SPO11 during meiosis. Higher eukaryotes have evolved two main pathways to repair DSBs: HR error free and NHEJ error prone pathway. However, DSBs in plants and humans are fundamentally repaired by NHEJ while in budding yeast mostly is repaired by HR (Jia *et al.*, 2012; Li *et al.*, 2005; Tzfira and Citovsky, 2006).

In budding yeast, *ku70* mutants (NHEJ) are able to get T-DNA integration. Furthermore, in *rad50* mutants (HR) T-DNA integration also occurred. However, when both pathways were inhibited by mutating proteins involved in both pathways, no integration of T-DNA could be observed (Tzfira and Citovsky, 2006). In Arabidopsis, an *Atku80* mutant exhibits deficient T-DNA integration in to host DNA of somatic cells (Li *et al.*, 2005; Jia *et al.*, 2012).

Several proteins from both bacterial and host cell have shown to have a role in the T-DNA integration (Gelvin, 2003; Tzfira and Citovsky, 2002). Several questions have been posed to understand the way the T-DNA single strand integrates into the plant genomic DNA. Are there any plant proteins which could play a role in choosing specific sites for the T-DNA integration? Does HR or NHEJ proteins have a role in the T-DNA integration? To answer these questions, genetic analysis using mutants for most components of the HR and NHEJ pathways were done to analyse their effect in T-DNA integration.

The virulence genes that are normally located in the Ti plasmid have been found to play an important role for transforming the T-DNA into the plants genome (Gelvin, 2003; Yanmin Zhu *et al.*, 2003). Further investigation has found that phenolic and sugar molecules could stimulate the bacteria to transfer the T-DNA when the plant cell wall had been wounded.

Therefore, the virulence proteins would trigger and guide the T-DNA from the bacteria into the plant cytoplasm as a complex and finally to the plant genome (Yanmin Zhu *et al.*, 2003).

The VirD2 and VirD1 proteins were found to play a basic function in excising the T-DNA from the Ti plasmid. The T-DNA has two borders that include around 25 bp repeated sequences in both sides. These repeat sequences are recognised by the virulence proteins that are found in the Ti plasmid. The VirD2 will join to the 5'-end after released the T-DNA single strand DNA (ssDNA) and transferred it into the plant cell. Another plant virulence protein that has been further described is VirE2 which coats the entire T-DNA and protects it from plant cell endonucleases when the T-complex (T-DNA and VirD2) enter the cell. Also, VirD2-ssDNA can be delivered into cell nucleus by dynein motor proteins and eventually target it into the plant genome (Pacurar *et al.*, 2011; Tzfira and Citovsky, 2006).

The structure of the chromatin and chromatin related proteins like histones in *A. thaliana* could affect the efficiency of T-DNA integration. Moreover, the T-DNA integration occurs randomly on the genomic sequence but normally it has more affinity for regions on the promoters, 5' and 3' untranslated domains because these regions might have a temporary unpacking state of the chromatin and it would be easier to be targeted (Alonso *et al.* 2003; Tzfira *et al.*, 2004). *Arabidopsis* root T-DNA transformation in *Ath2a1/rat5* mutant showed a deficiency in T-DNA integration. In the other hand, additional extra copies of this gene (over expression) increased 2-fold the T-DNA integration observed in the wild-type (Mysore *et al.*, 2000b).

Several studies have been conducted to identify which organs are targeted by the T-DNA integration using the Floral Dipping procedure. Some of these studies used GUS-staining as a plant marker of the T-DNA integration. This allowed the authors to identify the ovules (female gametes) were the only organ stained with the GUS-staining, proving that the ovules are the target sites for the T-DNA insertion using Floral Dipping (Bechtold *et al.*, 2000;

Desfeux *et al.*, 2000). *Agrobacterium* might pass through the pollen tube along the stigma down to the style and eventually to the ovules (Desfeux *et al.*, 2000). It was found that the developmental timing and the size of buds is also very important. The T-DNA transformation from *Agrobacterium* failed when the Floral Dipping was done 2 or more days after the anthesis and also failed 6 days prior to the anthesis. Thus, the perfect time that should be chosen for Floral Dipping is 3 days before anthesis in which the stigma cap forms at the top of the style connected to the elongated gynaecium (Desfeux *et al.*, 2000). Surprisingly, this is the time when female meiotic stages start, when DSBs are formed in the embryo sac mother cells or female meiocytes (Armstrong and Jones, 2001).

In the other hand, several studies have showed that the T-DNA integration efficiency is dependent on DSBs in the host genomic DNA (Salomon and Puchta, 1998; Windels *et al.*, 2003; Tzfira and Citovsky, 2006; Tzfira *et al.*, 2004). X-ray irradiation has been conducted to produce extra DNA breaks, and it was found that T-DNA integration frequency could be significantly increased (Tzfira *et al.*, 2004).

According to Tzfira and collaborators (2004), adding restriction cutting enzymes which could create breaks on specific sequence sites on the tobacco genome could increase T-DNA integration in these target sites. It was proposed that T-DNA ssDNA segments might be converted into a double stranded T-DNA (dsT-DNA) before getting integrated into the restriction sites (Tzfira *et al.*, 2004; Windels *et al.*, 2003).

Our results show that in absence of DSBs catalysed by AtSPO11.2, the T-DNA integration by Floral Dipping is highly reduced to 82.4% that of the wild-type (**Table 5**). This shows how important meiotic DSBs are for this T-DNA transformation method in *Arabidopsis*.

The T-DNA can be transferred into the plant cell nucleus and eventually gets integrated into the plant host genome using different DNA repair or recombinant pathways (Windels *et al.*, 2003). In budding yeast (*Saccharomyces cerevisiae*), the T-DNA is integrated into DSBs in

the host genomic DNA and relies on HR and NHEJ proteins showing that these pathways play a vital role in the T-DNA integration (Bundock and Hooykaas, 1996; Risseuw *et al.* 1996). However, plants seem to utilize the NHEJ pathway instead of HR for the T-DNA integration on roots. Nonetheless, in *S. cerevisiae*, T-DNA integration can be existed by either pathways HR and NHEJ (Tzfira and Citovsky, 2006; Windels *et al.*, 2003). In budding yeast, the deficiency of KU70 which is an essential protein for NHEJ pathway, allows the T-DNA integration to use the HR pathway. Furthermore, when the RAD52 recombinase (a key protein for the HR in yeast) is absent then the integration of T-DNA molecules can use the NHEJ pathway. Nevertheless, if both RAD52 and Ku70 are absent, then, no T-DNA integration can be successful in budding yeast (Tzfira and Citovsky, 2006; Tzfira *et al.*, 2004).

In plants, DSBs can be repaired by NHEJ pathway by recruiting different proteins like KU70, KU80, LIG4 and XRCC4. Nevertheless, the HR pathway might also be used for repairing these DSBs in plants by recruiting recombinase proteins like RPA and RAD51 (Bray and West, 2005). From these proteins, KU80 and ligases like LIG4 seemed to be the most involved in T-DNA integration (Bray and West, 2005).

According to Tzfira and collaborators (2004), the model proposed for the T-DNA integration into the host cell genome starts with T-DNA invasion of the 3'-ends as this part of this molecules are un-protected against host cell endonuclease activities while the 5'-ends are protected by the VirD2 protein. Once the T-DNA enters the cell, the T-DNA can be converted into dsDNA. During this process a few of bases can be lost from the unprotected 3'-ends. Consequently, either processes HR or NHEJ might participate in the T-DNA integration (Tzfira *et al.*, 2004). If NHEJ assists, then the VirD2 protein can be replaced by AtKU70-AtKU80 heterodimer that are responsible for joining both ends of dsDNA. During this event, H2AX would also participate for unpacking DNA as a result of DNA DSBs

response. However, HR pathway is used; Rad52 might play a similar role in plants than in budding yeast (Tzfira *et al.*, 2004). The T-DNA ends can be recognized by Rad52 which therefore would attach to the single strand 3'-ends. In this case, the VirD2 will be still attached to the 5'-ends to protect it from exonucleolytic degradation. The Rad52 (or plant orthologue –not found yet-) and MRE11 could form complexes that would attach to DNA DSBs ends before being recognized by NHEJ proteins, KU70/KU80) or by HR nucleoproteins RAD51 and DMC1 (Brunaud *et al.*, 2002; Tinland *et al.*, 1995; Van Attikum *et al.*, 2003).

Several proteins involved in DSBs repair have been confirmed to play a critical role for T-DNA integration into the host cell genome using either HR (like Spo11, Rad50, Mre11) or NHEJ (like Ku70, Ku80 and LIG4) (van Attikum *et al.* 2001; van Attikum and Hooykaas, 2003). T-DNA integration efficiency is reduced in *ku80* and *lig4* mutants in *Arabidopsis* (Windels *et al.*, 2003). Furthermore, AtLIG4 is not necessary for the T-DNA integration using the root transformation technique but seems to be required in the germ-line cells using the Floral Dipping procedure (Van Attikum *et al.*, 2003). Using these two different techniques (Floral Dipping vs. Root Tumour Formation) has revealed differences on the T-DNA integration pathway not just the target tissues (ovules vs. root cells) (Tzfira *et al.*, 2004). In *A. thaliana*, AtLIG4 seems to not play a role for the T-DNA integration while in yeast it was the most important component (Li *et al.* 2005; Van Attikum *et al.*, 2003). In this study, we have found that AtLIG4 seems to play a very important role for the T-DNA integration using Floral Dipping transformation, in its absence the T-DNA integration was reduced around 80% that of the wild-type (**Table 5**).

Atku80 mutant have shown to be deficient in T-DNA integration using the root transformation methodology (Tzfira *et al.*, 2004; Li *et al.*, 2005). Our study has showed that

both AtKU70 and AtKU80 are both required for the T-DNA integration, in their absence the T-DNA integration was reduced very similarly around 62% and 65%, respectively (**Table 5**). This reduced T-DNA integration was very similar between both AtKU70 and AtKU80, something to expect as both are part of the same heterodimer protein complex.

	Mutant	Proportion of T-DNA integration compared to wild-type %	Reduction in T-DNA integration	Role of proteins
HR	<i>Atspo11.2</i>	17.6%	82.4%	DSB formation
	<i>Atmre11</i>	11.7%	88.3%	DSB resection
	<i>Atrad51</i>	20%	80%	ssDNA invasion
	<i>Atmsh4</i>	44%	56%	dHj processing
	<i>Atmlh3</i>	32%	68%	dHj processing
NHEJ	<i>Atku70</i>	38%	62%	NHEJ
	<i>Atku80</i>	35%	65%	NHEJ
	<i>Atlig4</i>	20%	80%	NHEJ
	<i>Ath2a1/rat5</i>	64%	36%	

Table 5. Proportion of plants with T-DNA integration compared to the wild-type in different mutants of key components of HR and NHEJ.

Our results also showed that the AtMRE11 is highly important for the T-DNA integration using Floral Dipping, in its absence the reduction of T-DNA integration was around 88.3% that one of the wild-type (**Table 5**). HR recombinase AtRAD51 also seems to play an important role in T-DNA integration using Floral Dipping, in its absence the T-DNA integration was significantly reduced compared with Col about 80% (**Table 5**). According to

Tzfira and collaborators (2004), MRE11 and RAD52 are necessary for T-DNA integration in yeast but their orthologues role in plant T-DNA integration was not fully understood. This study actually proves that both AtMRE11 and AtRAD51 play a crucial role in T-DNA integration by Floral Dipping in *Arabidopsis*.

Furthermore, AtMSH4 and AtMLH3 also seem to have some roles on T-DNA integration, in their absence the efficiency of T-DNA integration was reduced to 56% and 68% that of the wild-type, respectively.

Our results illustrate that there is not significant differences among proteins involved in DSB formation (AtSPO11.2), DSB resection (AtMRE11) and ssDNA invasion (AtRAD51) in their role for T-DNA integration (Chi-square test, P-value 0.659884). Furthermore, there is not a significant difference in proteins involved in Double Holliday junction (dHj) processing (AtMSH4 and AtMLH3) in their T-DNA integration role (Chi-square text, P-value 0.427717). Nevertheless, there was significant differences between the roles of proteins involved in DSBs formation and processing (AtSPO11.2, AtMRE11, AtRAD51) and proteins involved in dHj processing (AtMSH4 and AtMLH3) (Chi-square text, P-value 0.05847). This could show that these two groups of protein could be involved in different processes of T-DNA integration. Additionally, no significant differences were observed in the T-DNA integration role of NHEJ proteins AtKU70, AtKU80 and AtLIG4 (Chi-square text, P-value 0.37296) showing that these group of proteins are likely involved in the same T-DNA integration pathway (**Figure 25**).

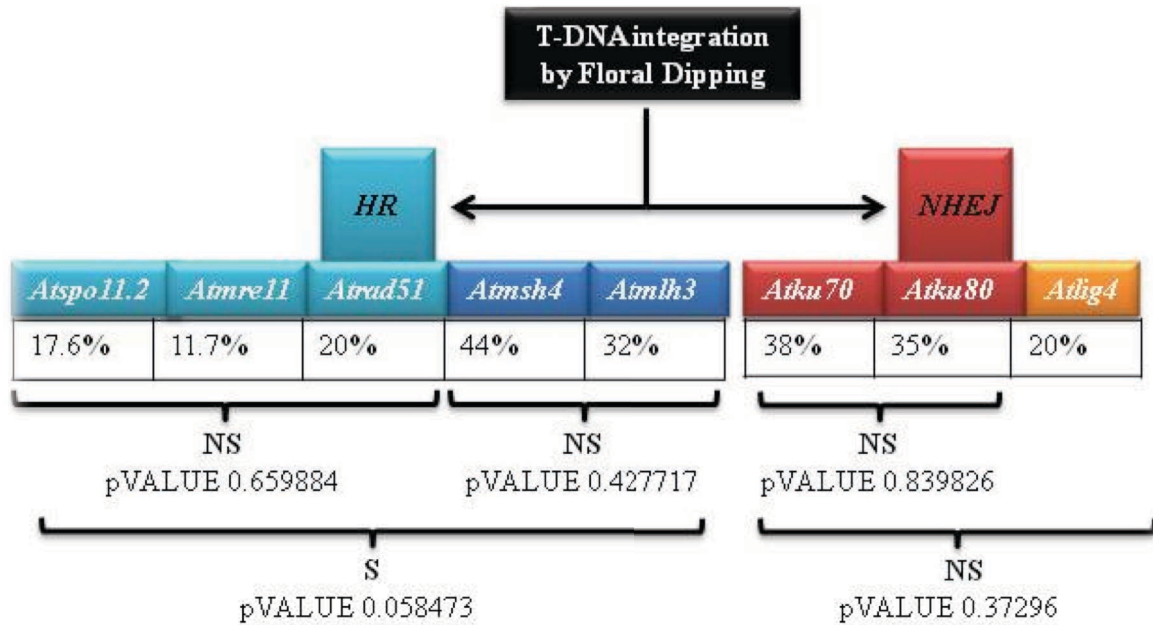


Figure 25. Diagram representing different DSB repair pathway mutants involved in T-DNA integration by Floral Dipping.

The proportion of plants with T-DNA integration compared to the wild-type is indicated. NS (non-significant) S (significant).

In summary, T-DNA integration using the Floral Dipping Transformation method is dependent of meiotic DSBs catalysed by AtSPO11.2 and the DSB processing pathways HR (AtMRE11, AtRAD51, AtMSH4 and AtMLH3) as well as NHEJ (AtKU80, AtKU70 and AtLIG4). Moreover, although AtH2A1/RAT5 has been shown to have an important role in root T-DNA integration its role using Floral Dipping does not seem to be that significant.

CHAPTER FOUR

Characterisation of *AtSSRP1*

4.1 INTRODUCTION

4.1.1 High mobility group proteins (HMG)

Chromatin is a flexible dynamic structure that interacts to a multi-complex of proteins. High mobility group (HMG) proteins are considered to be the second most abundant group of chromatin proteins after histone proteins, and seem to be architectural components of the chromatin (Catez and Hock, 2010). Recent studies have shown that HMG proteins might play an important role in the epigenetic changes as they can alter the level of histone modifications when they combine with the chromatin (Catez and Hock, 2010; Kim *et al.*, 2009). They participate in a mixture of DNA-dependent processes such as chromatin remodelling, changes of chromosomal structures during cell cycle, DNA recombination, DNA repair, apoptosis and even regulate transcription factors (Bustin, 2001; Lildballe *et al.*, 2008; Reeves and Adair, 2005).

High mobility group proteins are a heterogeneous set of nuclear proteins that have a molecular mass of less than 30 kDa (Aleporou-Marinou *et al.*, 2003; Catez and Hock, 2011). They were discovered in early 1960s by Johns and were described according to their high mobility when they were run in acidic polyacrylamide gels (Czura *et al.*, 2003). HMG proteins were found first in mammalian cells and defined as non-histone chromatin proteins since they were different than histones (Bustin, 2001; Goodwin and Johns, 1973). HMG proteins can be divided into three basic families known as HMGA, HMGB and HMGN proteins. Nevertheless, there is no evidence that HMGN proteins are present in plants (Pedersen and Grasser, 2010). HMG proteins can be classified based on their DNA-binding regions.

HMGA proteins include AT-hook domains to bind to DNA, whereas, HMGB include HMG-box domains and the HMGN proteins contain a nucleosome binding region. These main domains can be used to differentiate between HMG protein families and their role by their recognition of specific DNA sequences or not (Catez and Hock, 2011).

Broadly, HMG protein families have differences in their structures but they still share similar DNA/chromatin binding sites (known as binding motifs) and are flanked with acidic residues in their C-terminus region (Sgarra *et al.*, 2004). It has been suggested that the acidic tails are responsible for the communication with other proteins and, thus, regulate the activity of the HMG protein binding sites (Catez and Hock, 2011). The HMGA protein family consist of four variant proteins that are encoded by two different genes by alternative splicing in humans: *HMGAI* gene encodes the proteins HMGA1a (106 aa, 11.9 kDa), HMGA1b (95 amino acids, 10.6 kDa) and HMGA1c (179 aa, 19.7 kDa). Additionally, HMGA2 (108 aa, 12kDa) is encoded by a different gene, *HMG2* (Catez and Hock, 2011; Sgarra *et al.*, 2004).

The number of AT-hook motifs seems to be variable between eukaryotic organisms. These AT-hook motifs can be attached to the AT-rich regions of DNA in the minor groove of the naked double stranded DNA and the DNA surrounding by the nucleosomes. Each one of the AT-hook sequence domains consist of highly conserved positively charged amino acid domains in an specific sequence: proline, arginine, glycine, arginine and proline (PRGRP) (Catez and Hock, 2011; Sgarra *et al.*, 2004). It is supposed that the AT-hook motifs can play a crucial role of changing chromatin structure (Sgarra *et al.*, 2004). It is suggested that one of the AT-hook domains is enough to provide a binding site to DNA. Nevertheless the affinity between the HMG proteins and the DNA would increase significantly when 3 or more of the AT-hook motifs are present in the protein (Catez and Hock, 2011).

Therefore, HMGA proteins are essential molecules that associate with (SARs). These SARs contain a high abundance of AT sequences where AT-hook motifs can attach. Consequently, these could explain how chromatin can be attached to the chromosome scaffold (also known as nuclear matrix or chromosome axis) and how HMG proteins could then regulate different biological processes of the nucleus like DNA replication, transcription, or DNA repair. It has been revealed that HMGA proteins can delocalise histone H1 from SARs, so that chromatin can be unwound and transcription activities can be initiated (Sgarra *et al.*, 2004).

Indeed, several studies have been conducted to understand the function of HMGA proteins. Consequently, it has been determined that the most important functions of HMGA proteins are to produce changes in DNA activities or processes by increasing the attraction of the binding regions of transcription factors (TFs) to gene promoters as well as facilitating the interaction between nucleoproteins complexes that are responsible of controlling these activities (Sgarra *et al.*, 2004).

HMGB proteins are defined by an HMG box region in their sequence. It is found that this 80 amino acid box region can attach to the minor groove of the DNA without any specificity in the DNA sequence (Catez and Hock, 2011). The protein family called HMGN can be combined within the nucleosomes as it seems to be attached within DNA and the histone octamer (Bianchi and Agresti, 2005; Catez and Hock, 2011). Recent studies have shown that HMG proteins might play crucial roles in controlling epigenetic changes. Once they interact with the chromatin, they can facilitate changes to the histone modifications. This has been observed among HMGN and HMGB proteins (Catez and Hock, 2011).

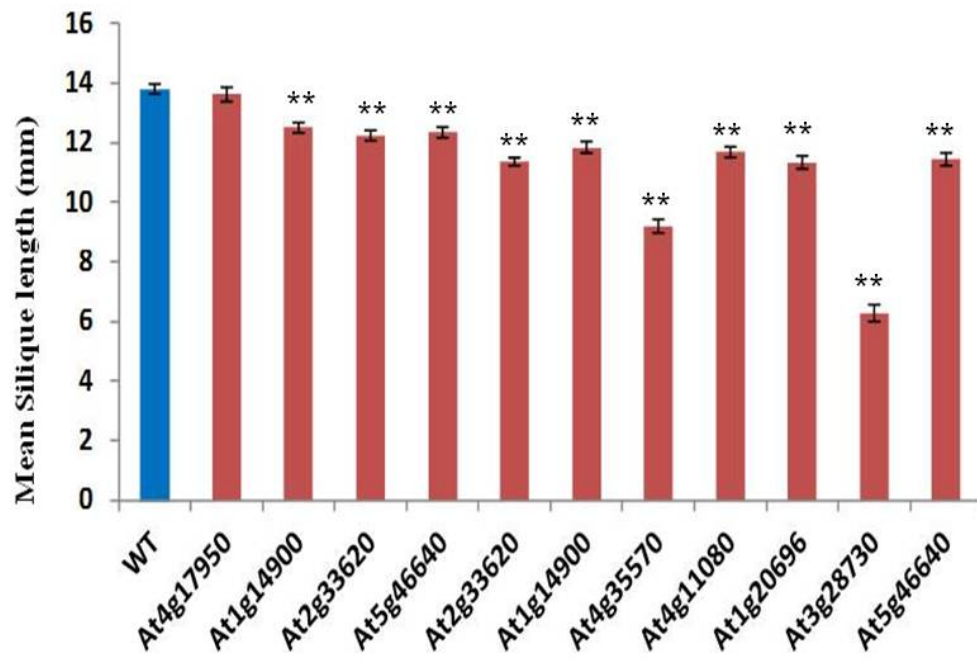
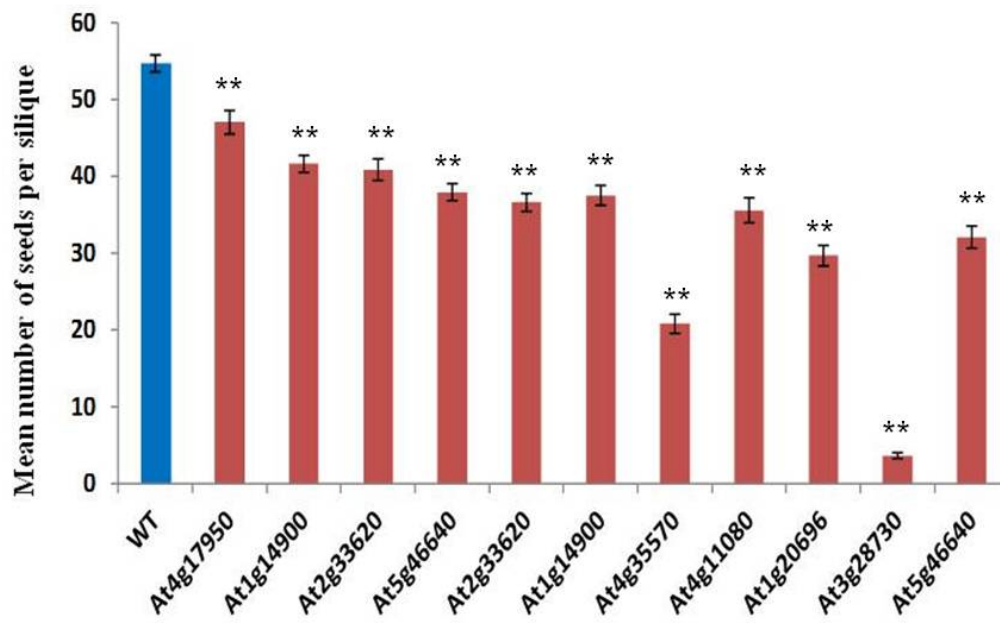
In this study, we carried out a reverse genetic analysis to find out HMG proteins that could have important roles in meiosis by using T-DNA insertion mutants and characterising their fertility and putative errors during the meiotic process.

4.2. RESULTS

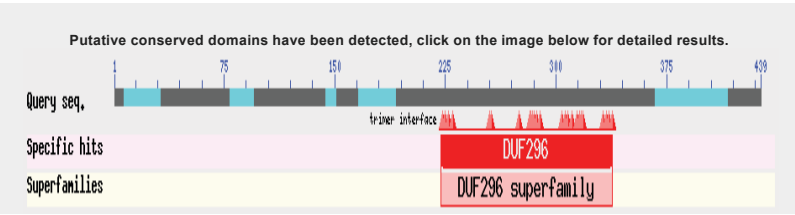
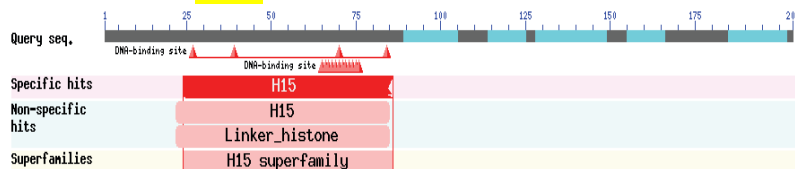
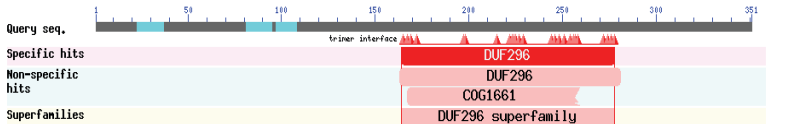
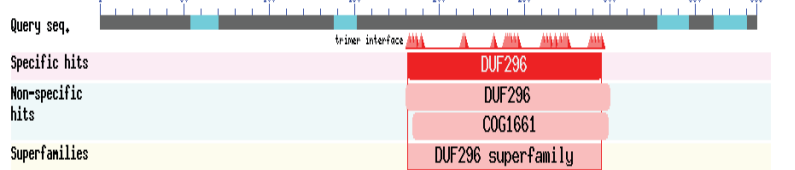
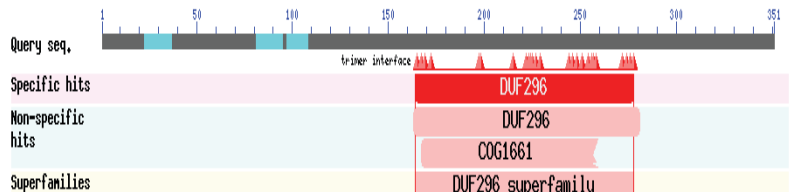
4.2.1 Fertility characterisation in *Athmg* mutants in *Arabidopsis*

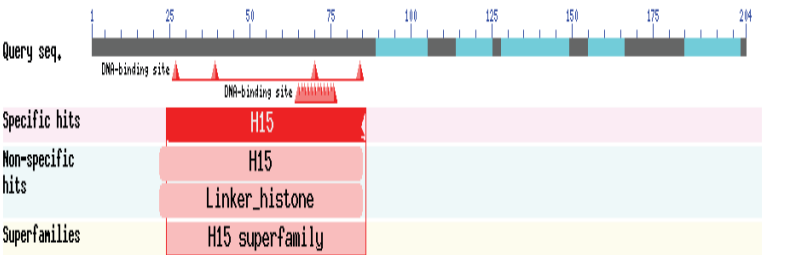
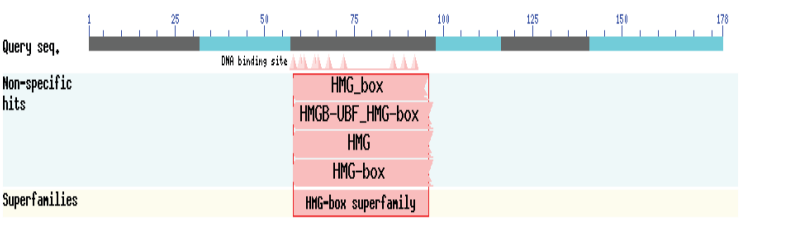
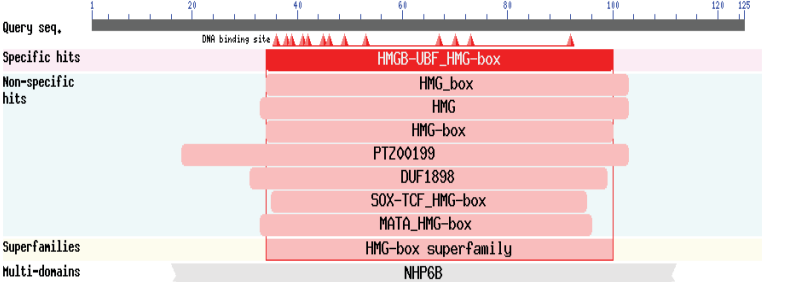
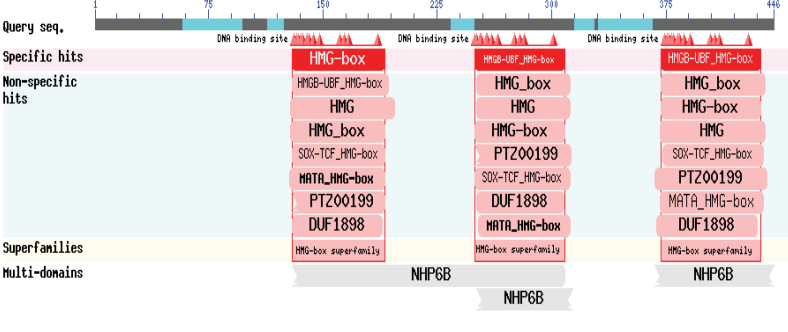
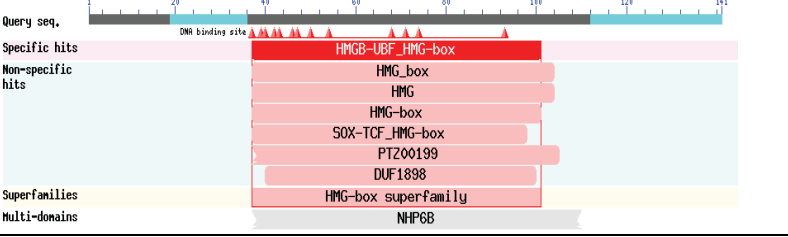
Different *Athmg* mutants (**Figure 26**) were analysed by a reverse genetic analysis in order to find if any of these genes have a role in the meiotic process. *Athmg* mutants grown at the same time and identical conditions as the wild-type (Col) showed a semi-sterile phenotype (**Figure 26D**) with more or less severity.

Measurement of the silique length and quantification of the number of seeds per silique were carried out to assess the fertility of different *Athmg* mutants comparing them to the *Arabidopsis* wild-type (Col). The mean silique length of the siliques for all the *Athmg* mutants analysed showed that all but the At4g17950 were significantly reduced (marked with 2 stars (**)) compared to the mean of 13.8 mm of the wild-type (*t*-test, $p < 0.005$) (**Figure 26A**). Furthermore, the mean number of seeds per silique for all the *Athmg* mutants were significantly reduced (marked with 2 stars (**)) compared to the 54.68 seeds/silique in the wild-type (*t*-test, $p < 0.005$) (**Figure 26B**) (N=100).

A**B**

C

Gene locus	Conserved domain	P-value of seeds number per silique
<p>At4g17950</p> <p><i>HMGA-LIKE</i></p> <p>N514014</p>	<p>MDSREIHHQQQQQQQQQQQQQQHLOQQQQPPGMLMHHNSYNRNFNAAAALMGHNTSSTQAMHQRLPFGGSMSPHQ QQHQYHHPQQQIDQKTLLESLGFDGSPSSVAATQOHSRFGIDHQQVKKKRGRPKRYAADGGGGGGGNNIALGLAPTSPL PSASNSYGGGNEGGGDSAGANANSDDPPAKRNRGRPGSGKKQLDALGGTGGVGFTHVIEVKTGEDIAKILAFNTQGP RAICILSATGAVTNVMLRQANNSNPTGTVKYEGRFEIISLGSFLNSENGTVTKGNLSVSLAGHEGRIVGGCVDGMLVAG SQVQVIVGSFVPDGRKQKQSAQRAQNTPEPASAFANMLSFGGVGGPGSPRSQQQHSSESEENESNSPLHRRSNNNNNNH GIFGNSTPQPLHQIPMQMYQNLWFGNSPQ</p> 	<p>5.15E-05</p>
<p>At1g14900</p> <p><i>HMGA3</i></p> <p>N578240</p>	<p>MAPDLHHGSADTHSSELPFSLPPYQPMIEAIESLNDKNGCNKTTIAKHISTQOTLPPSHMTLLSYHLNMQMKTGQLIM VKNNYMKPDPDAPPKRGRGRPKQKTAESDAAAAVVAATVVSTDPRGRPKPKDPSEPPQEKVITGSGRFRGRPKR FRTDSEVAEPEAAQATGERRGRGRPKVKPTVAVPGC</p> 	<p>2E-13</p>
<p>At2g33620</p> <p><i>HMGA2</i></p> <p>N655266</p>	<p>MSGSETGLMAATRESMQFTMALHQQQQHSQAQPQQSNRPLSFGGDDGTALYKQPMRSVSPQQYQPNAGENSVLNMLPGGESGGMGTGGSEPVKRR RGRPKRYGPDGEMSLGPNPAPSTVSQSSGGDGEKKRGRPGSSSKRLKQALGSGTIGFTPHVLTVLAGEDVSKIMALTHNGPRAVCVLSANG AISNVTLRQATSQGTVTYEGRFEILSLGSGFHLLENNQSRRTGGLSVLSLSPDGNVLGGVAGLLIAASPQVIVVGSFVLPDGEKPKQHVQGMGLSS PVLPRVAPQVLMTPSSPQSRGTMSSESCGGGHSPIHQSTGGPYNNINMPWK</p> 	<p>6.67E-12</p>
<p>At5g46640</p> <p><i>HMGA1-LIKE</i></p> <p>N667672</p>	<p>MDSRDI PPSHNQLQPPGMLMSHYRNPNAAAAPLMVPTSTSQPIQHPRLPFGNQSSQTFHQQQQQMDQKTLLESLGFDGDS PSSQPMRFGIDDQNLQVKKRGRPKRYTPDGSIALGLAPTSPLLSAASNSYEGGVDGSGGNGNSVDPVVKRNRGRPGS SKKQLDALGGTSGVGFTHVIEVNTGEDIAKVMFASDQGSRTICILSASGAVSRVMLRQASHSSGLVITYEGRFEIITLGS VLNVEYNGSTNRSGNLSVALAGPDGIVGGSVVGNLVAATQVQVIVGSFVAEAKPKQSSVNIARGQNPPEPASAFANMLNFG SVSQGPSSSESEENESGSPAMHRDNNNGIYGAQQQQQLPHPHQMYQHLWSNHGQ</p> 	<p>1.37E-18</p>
<p>At2g33620</p> <p><i>HMGA2</i></p> <p>N662954</p>	<p>MSGSETGLMAATRESMQFTMALHQQQQHSQAQPQQSNRPLSFGGDDGTALYKQPMRSVSPQQYQPNAGENSVLNMLNLP GESGGMGTGGSEPVKRRRGRPKRYGPDGEMSLGPNPAPSTVSQSSGGDGEKKRGRPGSSSKRLKQALGSGTIGFTPHVLTVLAGEDVS SKIMALTHNGPRAVCVLSANGAISNVTLRQATSQGTVTYEGRFEILSLGSGFHLLENNQSRRTGGLSVLSLSPDGNVLGGVAGLLIAASPQVIVV SFLPDGEKPKQHVQGMGLSSPVLPRVAPQVLMTPSSPQSRGTMSSESCGGGHSPIHQSTGGPYNNINMPWK</p> 	<p>1.4E-19</p>

<p>At1g14900</p> <p><i>HMGA1</i></p> <p>N578336</p>	<p>MAFDLHHGSASDTHSSELPFSFLPPYQPMIMEAIESLNDKNGCNKTTIAKHIESTQOTLPPSHMTLLSYHLNOMKKTGQLIM VKNYNMPPDPDAPPKRGRGRPKOKTQAESDAAAAVVAATVSTDPSPRGRPKPKDPSEPPQEKVITGSGRPRGRPKR PRDTSVVAPEPAQAQATGERGRGRPKVKPTVVAFVGC</p> 	<p>5.58E-17</p>
<p>At3g51880</p> <p><i>HMGB1</i></p> <p>N372902</p>	<p>MKTAKGDKVKTTEALKPVDDRKVGKRPKAPAEKPTRKREKKAKKDPNPKRAPSFAFFVLEDFRVTFKKNPNVKAVSAGKAGGQK WKSMSQAEKAPYEKAARKAIEYEQMDAYNNKLEEGSDESEKRSINDEDEASGEEELLEKAAGDDEEEEEEDDDDDDEED</p> 	
<p>At4g35570</p> <p><i>HMGB5</i></p> <p>N677838</p>	<p>MKDNDQTEVESRSTDDRLKVRGNKVGKTKDPNRPKPPSPFFVFLDDFRKEFNLANPDKNSVGNVGRAAGKWKMTTEEERA FFVAKSQSKKTEYAVTMQQYNMELANGKTTGDDEKQEKAAAD</p> 	<p>1.11E-07</p>
<p>At4g11080</p> <p><i>HMGB1</i></p> <p>N302986</p>	<p>MSTVSDPAHAKKSRNSRKALKQKNEIVESPVSVDGKGETKSFEKDLMEMQAMLEKMKIEKEKTEDLLKEKDEILRKRKEVEQ EKLKTTELKQLQMKFEKPNMTFAFSQSLAQTEEEKGKGGKDDCAETKRPSTPYILWCKDNWNEVKKQNPADFKETSNI AKWGI SAEEKPYEEKYQADKEAYLQVITKEKREAMKLLDDEQKQTAMELLDQYLHFVQBAEHDNKKKAKKIKDPLK KQPI SAYLLYANERRAALKGENKSVIEVAKMAGEEWKLNLSSEKAPYDQMAKKNKEIYLQEMEGYKRTKEEAMSKKEE FMKLHQEALQLKKEKTDNI IKKTETAKNKKKNENVDNPKPKPTSSYFLCKDARKSVLEHPGINNSTVTAHISLKW MELGEEKQVYNSKAAELMEAYKKEVEEYNNKTKTSS</p> 	<p>8.78E-16</p>
<p>At1g20696</p> <p><i>HMGB3</i></p> <p>N547872</p>	<p>MKGAKSAETRSTKLSVTKPKAKGAKGAADPNPKRPPSAFFVFMDFRVTYKEEHPKNKSVAAVGKAGGKWKLSLSDSEK APVYAKADKRVEYKNNMAYNKLEEGPKDEESDKSVSEVNDDEADGSEEEEDDD</p> 	<p>1.04E-25</p>

<p>At3g28730 <i>HMG-SSRP1</i> N683769</p>	<p>MADGHSFNNISLSGRGGKNPGLLKINSGGIQWKKQGGGKAVEVDRSDIVSVSWTKVTKSNQLGVKTKDGLYYKFGFRDQDV PSLSSFFQSSYGKTPDEKQLSVSGRNWGEVDLHGNTLTLFLVGSKAQFEVSLADVSQTQLQGNVDTLEPHVDDTAGANEKDS LMEISFHIPNSNTQFVGDENRPPSQVFNNTIVAMADVSPGVEDAVVTFESIAITLPRGRYNNVELHLSFLRLQGOANDFKIQY SSVVRLFLLPKSNQPHTFVVISLDPPIRKGQTMYPHIVMQFETDTVVESELSISDELMNTKFKDKLERSYKGLIHEVFTTVL RWLSGAKITPKGRSSQDGFVAVKSSLKAEDGVLYPLEKGFLLPKPPTLI LHDEIDYVEFERHAAGGANMHYFDLLIRLKT DHEHLFRNIQRNEYHNLTYTFISSKGLKIMNLGGAGTADGVAAVLGDNDDDDAVDPHLTRIRNQAADSEDEDEDFVMGEDDD GGSPTDDSGGDDSDASEGGVGEIKEKSIKKEPKKEASSKGLPPKPKRTVAADGSSKRRKPKKKKDFNAPKRAMSGMFSSQ MERDNIKKEHPGIAFGEVGVKVLGDKWRQMSADDKEPEYEAQVVKQRYKDEISDYKNPQPMNVDSGNDSSDN</p> <p>Query seq.</p> <p>Specific hits</p> <p>Superfamilies</p> <p>Multi-domains</p>	<p>6.6E-48</p>
<p>At5g46640 <i>HMGA-LIKE</i> N610363</p>	<p>MDSRDI PPSHNQLQPPPGMLMSHYRNPNAAASPLMVPTSTSQPIQHPRLPFGNQSQTFHQQQQQMDQKTLLESLFGDGS PSSQPMRFGIDDQNLQVKKKRGRRPKYTPDGSIALGLAPTSPLLSAASNSYEGGVGDSGGNGNSVDPVVKRNRGRPGS SKKQDALGCTSGVGFPHVIEVNTGEDIASKVMFSDQGSRTICILSASGAVSRVMLRQASHSSGI VTYEGRPEIITLSSGS VLNYEVNGSTNRSNLSVALAGPDGGIVGGSVVGNLVAATQVQVIVGSFVABAKPKQSSVNIARGQNPEPASAPANMLNFG SVSQGPSSSESEENESGSPAMHRDNNNGIYGAQQQQQOPLHPHQMQMYQHLWSNHGQ</p> <p>Query seq.</p> <p>Specific hits</p> <p>Non-specific hits</p> <p>Superfamilies</p>	<p>1.7E-21</p>

D

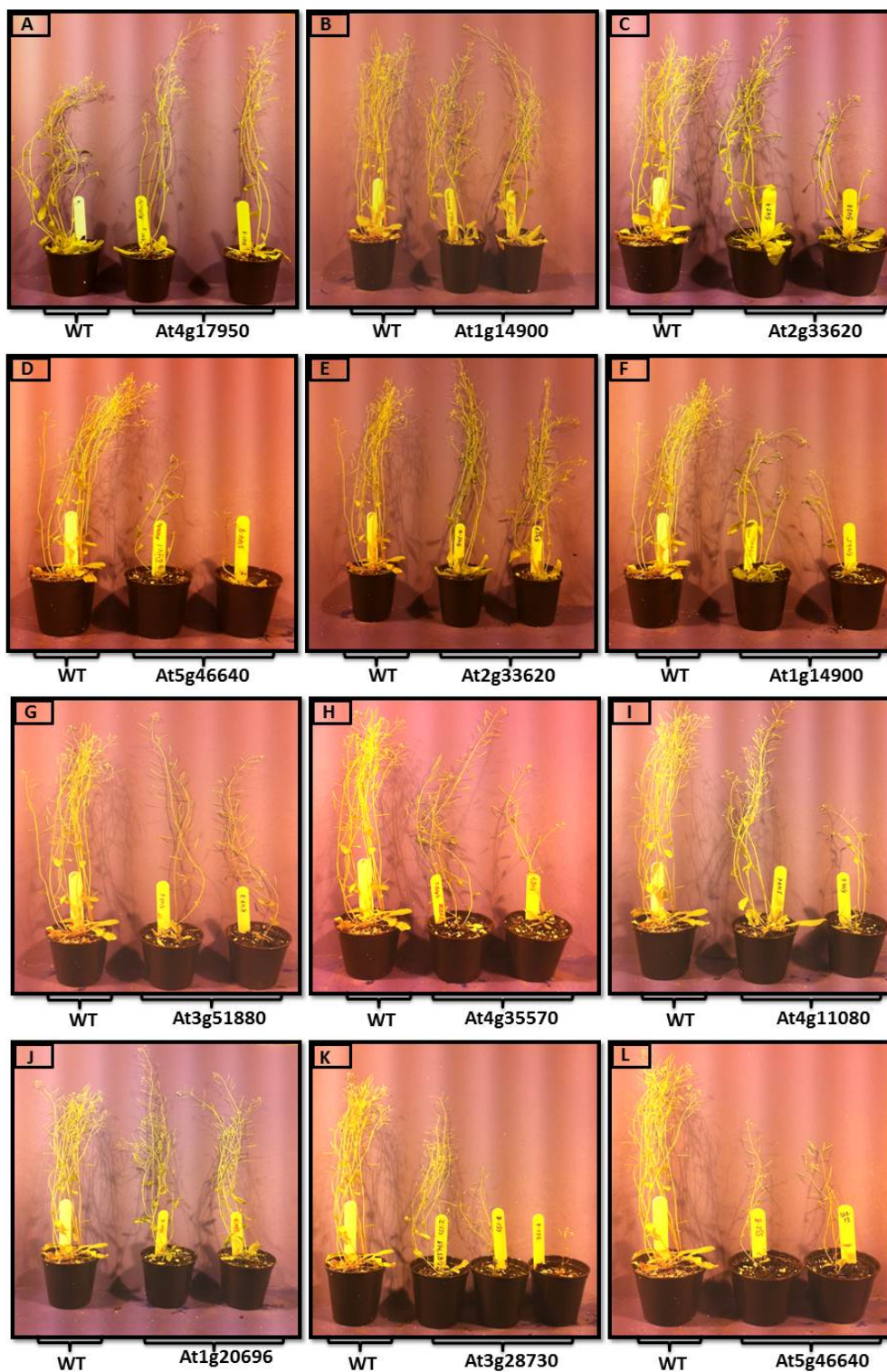


Figure 26. Fertility evaluation for *Athmg* mutants.

A Mean silique length for the wild-type (WT) and the different mutants. **B** Mean number of seeds per silique. Error bars = Standard Error of the mean. **C** Table representing the different *AthMG* genes analysed, their mutations, their protein sequence and conserved domains and their fertility p-value (*t*-test, $p < 0.005$). Yellow highlights = AT-hook motifs. **D** Photographs of the different mutants analysed next to wild-type plants grown at the same time and with the same conditions.

4.2.2 Characterisation of *Atssrp1* mutant

The *Atssrp1* mutant has been chosen for further analysis based on its defects in plant size (dwarf plants) and the severity in the reduction of fertility (decreased number of seeds). Structure Specific Recognition Protein 1 (SSRP1) is an abundant HMG protein which can bind to chromatin and seem to play a crucial role in DNA repair response, in DNA replication and elongation, and in regulation of the transcription machinery. In higher eukaryotes, SSRP1 protein contains two conserved domains. The N-terminal domain that interacts to the SSRP1 partner is known as SPT16 (Suppressor of Ty16) forming the FACT complex (Facilitates Chromatin Transcription complex). This N-terminal domain also contains a tubulin binding domain. The C-terminal domain might bind into the DNA (Kumari *et al.*, 2009; Zeng *et al.*, 2010).

SSRP1 gene seems to be necessary for microtubule growth development, maturation and formation in mitosis (Zeng *et al.*, 2010). It has been reported that this protein is also important for chromosome alignment and segregation by organizing microtubules as bundles (Zeng *et al.*, 2010). In our study, we identified an *Atssrp1* mutant which showed different chromosomal abnormalities including chromosome fragmentation during mitotic and meiotic divisions, and chromosome missegregation during meiotic Anaphase I and II stages.

AtSSRP1 gene is located in the short arm of *Arabidopsis* chromosome 3. It consists of 16 exons and 15 introns in addition of a 3' and a 5' UTRs. The T-DNA line analysed (SALK-001283C) is inserted in the exon number 14 of the *AtSSRP1* gene (At3g28730). TAIR databases and its Sequence Viewer tools have been used to represent the DNA sequence, gene structure and the position of T-DNA insertion line of *AtSSRP1* gene (**Figure 27A** and **Appendix C**).

Atssrp1 T-DNA insertion mutant seeds (SALK-001283C line) were obtained from the SALK Institute (San Diego). Mutant and wild-type seeds were planted together in identical conditions monitored at the glasshouse. DNA was extracted from plant leaves to genotype them. Two primers were designed (LP and RP) around the T-DNA insertion site in *AtSSRP1* gene and another specific primer for the left border of the T-DNA (BP) was designed and used to confirm the presence of the T-DNA insertion (**Figure 27A**).

PCR and gel electrophoresis was conducted to check the presence of the T-DNA insertion within the *AtSSRP1* gene. Additionally, wild-type plants were used as a control (**Figure 27B**). Wild-type plants showed one single band amplification of approximately 1,034 bp size as a result of amplifying the genomic sequence between LP and RP primers in *AtSSRP1* gene (**Figure 27B**). The agarose gel in **Figure 27B** shows three homozygous mutant plants with the T-DNA inserted in both homologous chromosomes. These homozygous mutants provided one single band amplification of approximately 700 bp in size as a result of amplifying the left border of the T-DNA up to the RP primer in the *AtSSRP1* genomic sequence (**Figure 27B**).

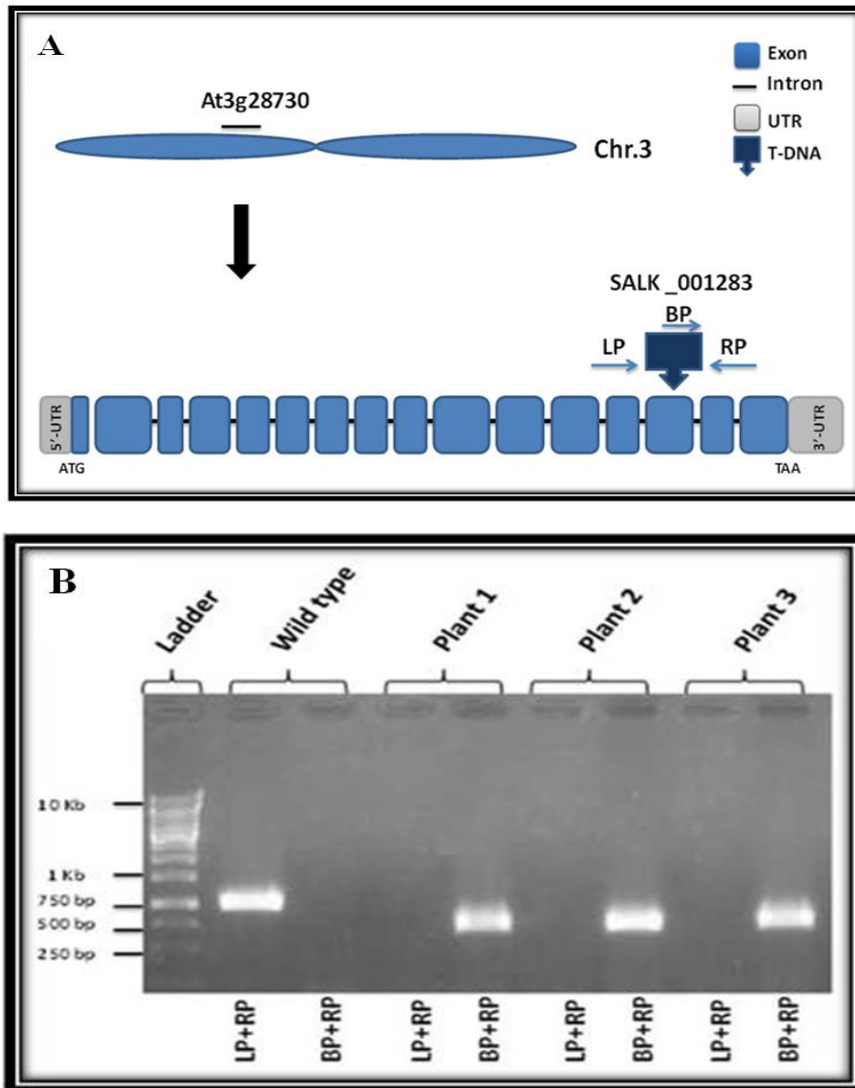


Figure 27. Schematic representation of the structure of *AtSSRP1* gene and the location of the T-DNA insertion in the mutant analysed.

A *AtSSRP1* gene includes 16 exons (blue boxes) in addition of 5' and 3'UTRs (grey boxes). The T-DNA is inserted in the exon number 14 (inverted dark blue arrow box). **B** PCR was conducted to identify the T-DNA insertional *Atssrp1* mutant plants. Agarose gel photograph showing a wild-type plant and three homozygous mutant plants.

4.2.3 Plant phenotype for *Atssrp1* mutant

Atssrp1 mutant plants showed a delayed in growth and development compared to the wild-type plants grown in the same conditions (**Figure 28**). Furthermore, the mutants displayed a semi-sterile phenotype (**Figure 28**). *Atssrp1* mutant plants showed a dwarf-like phenotype in some plants (not all 30%, N=100) and a delay and abundance of inflorescences and leaves, and a delay in flowering time compared to the wild-type (**Figure 28C**).

Fertility of *Atssrp1* mutant (Salk line 001283) and wild-type plants was assessed by measuring the silique length and counting the number of seeds per silique (N=100 siliques in 5 plants). The mean number of seeds per silique in *Atssrp1* mutant plants was significantly reduced with a mean of only 3.66 seeds/silique compared to 54.68 seeds/silique in the wild-type (*t*-test, $p=1.3 \times 10^{-47}$) (**Figure 28A**). The mean silique length for the *Atssrp1* mutant plants was also significantly reduced to 6.28 mm compared to the 13.58 mm in the wild-type (*t*-test, $p=1.52 \times 10^{-36}$) (**Figure 28B**).

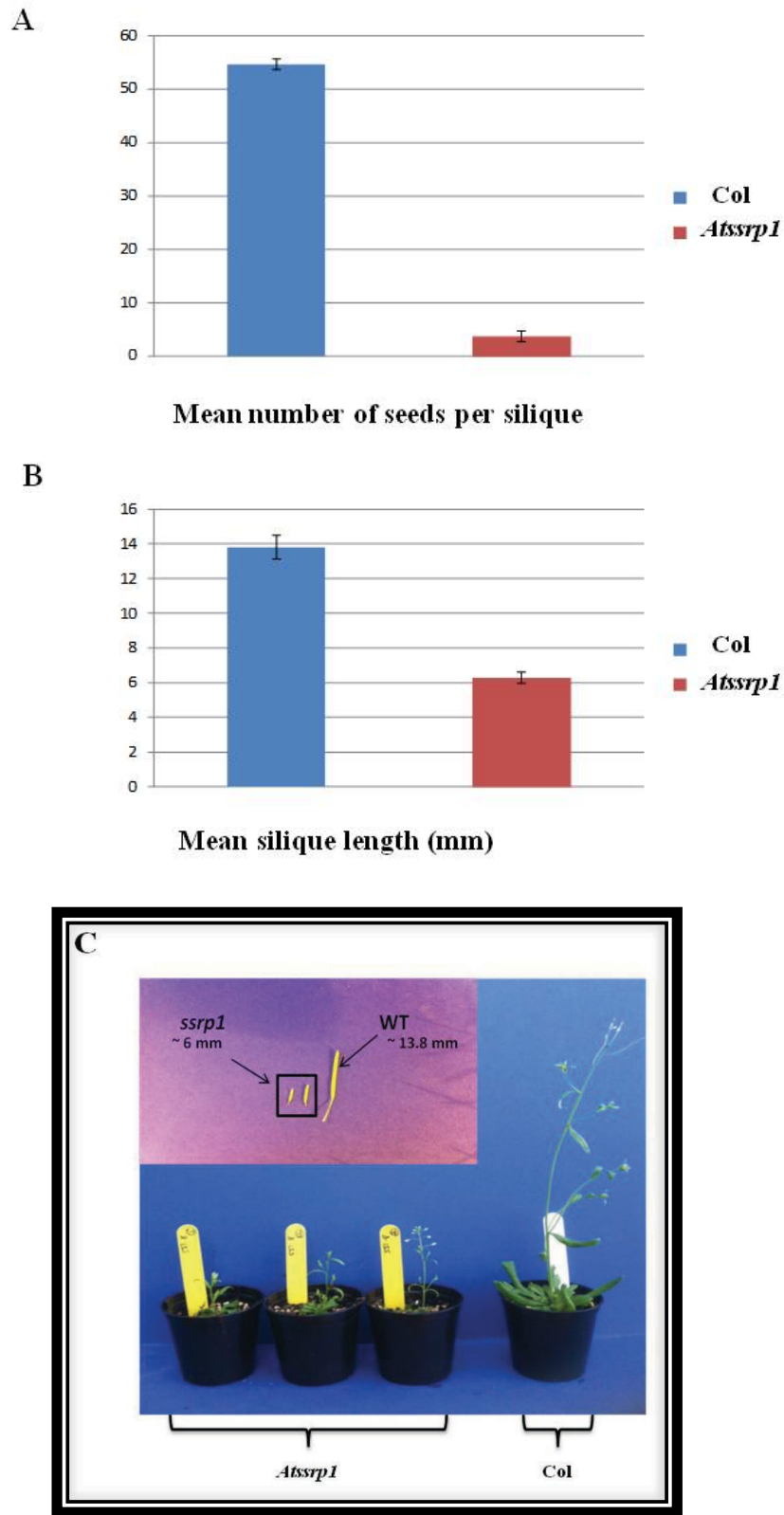


Figure 28. Plant phenotype in *Atssrp1* mutant.

A Mean number of seeds per silique. **B** Mean silique length. Error bars = Standard error of the mean. N=100 siliques. **C** Pictures of *Atssrp1* mutant and wild-type plants taken after 3 week of germination.

4.2.4 Expression of *AtSSRP1* in *Arabidopsis thaliana*

To characterise the expression of *AtSSRP1* gene and evaluate the mutant line (SALK-001283C) a Reverse Transcription Polymerase Chain Reaction (RT-PCR) was carried out. RNA was extracted from leaves and flower buds in both, the wild-type (Col) and *Atssrp1* mutant plants. Two sequence specific primers were designed to amplify approximately 200bp of the *AtSSRP1* transcript. To avoid genomic contamination the forward primer was designed against the end of exon 13 and the beginning of exon 14. The reverse primer was designed into the 3'UTR of *AtSSRP1* (sequence in Material and Methods). An RT-PCR control using primers to amplify 220bp of the *AtACTIN2* gene a known housekeeping gene was carried out. **Figure 29** shows the agarose gel with the electrophoresis separation of these RT-PCR products. The *AtACTIN2* control shows equal intensity of the 220 bp bands in the different tissues (leaf vs. bud) and the different samples (wild-type vs. *Atssrp1* mutant). *AtSSRP1* transcript is present in similar amounts in somatic (leaves) and meiotic (flower buds) wild-type tissues (**Figure 29**). Nevertheless, no band was visible for the *AtSSRP1* transcript in the *Atssrp1* mutant (**Figure 29**).

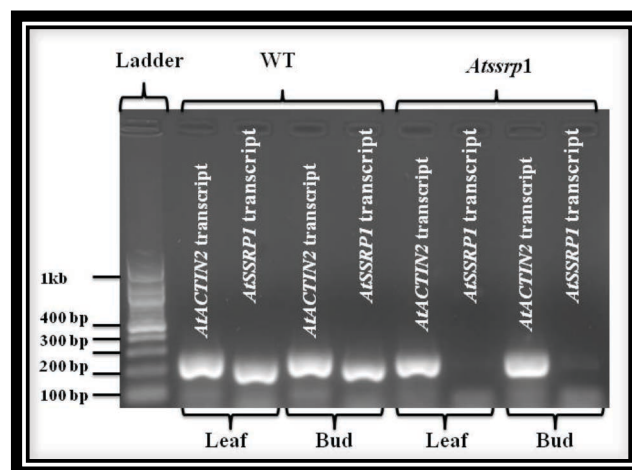


Figure 29. RT-PCR electrophoresis photograph showing the expression of *AtSSRP1* gene in wild-type and *Atssrp1* mutant tissues.

Housekeeping gene *AtACTIN2* was used as a control. RNA was extracted from leaves and flower buds. *Atssrp1* mutant plants did not show expression of *AtSSRP1* gene as expected.

4.2.5 Cytogenetic analysis of the male meiosis in *Atssrp1* mutant

Cytological analysis of chromosome behaviour during meiotic stages in pollen mother cells was carried out in *Atssrp1* mutant plants. We observed no defects during meiotic prophase I with fully complete chromosome pairing and synapsis at pachytene (**Figure 30**). However, some cells (about 15%) revealed some chromosome fragmentation during zygotene and pachytene (**Figures 30 B and D, arrows**). Furthermore, some cells showed chromosome missegregation during anaphase I which led to unequal number of chromosomes in second division cells like prophase II (**Figures 30I and J**). Subsequently, further chromosome missegregation occurred during second meiotic division (**Figures 30K, L and M**) and thus, creating unbalanced gametes with different chromosome number (**Figure 30**).

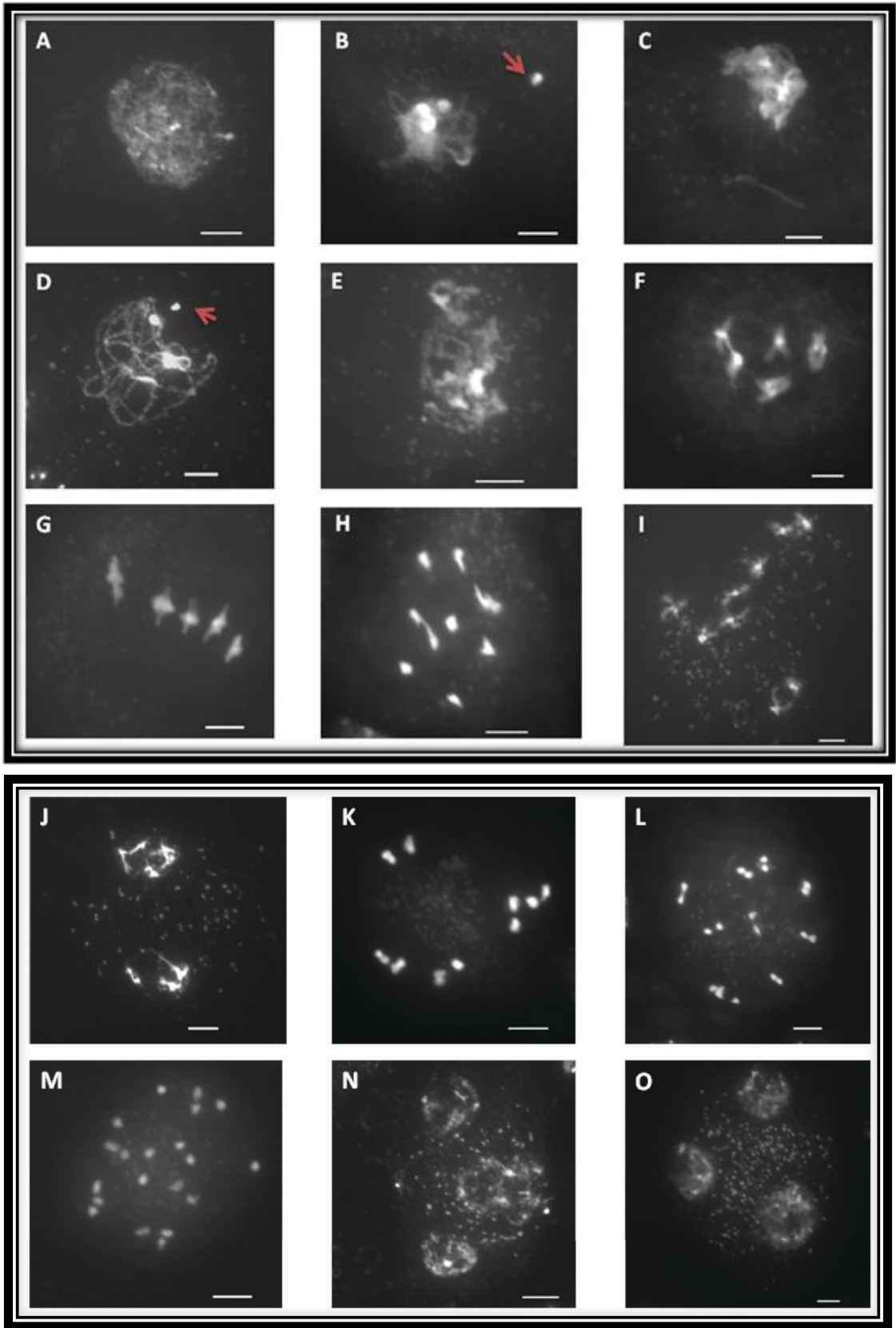


Figure 30. Meiotic stages of PMCs in *Atssrp1* mutant line (SALK-001283).

A Leptotene. **B** Pairing of homologous chromosomes starts at zygotene. **C and D** Pachytenes, with fully paired chromosomes. **E** Diakinesis. **F** Metaphase I with 5 bivalents. **G** Anaphase I with chromosomes migrating to opposite poles in an asynchronous manner. **H** Telophase I. **I and J** Prophase II, chromosomes start to condense and some cells appeared with unequal number of chromosomes in each nucleus. **K** Metaphase II, with unequal number of chromosomes in each pole (2 vs. 8 instead of the wild-type 5 vs. 5). **L and M** Anaphase II, the sister chromatids start to migrate to opposite poles. Previous missegregation and new missegregation problems accumulate and unbalance nuclei are formed. **N and O** Telophase II-Tetrad stage with unbalance number of chromosomes. Scale bar = 5µm.

4.2.6 Cytogenetic analysis of the mitotic division in *Atssrp1* mutant

Cytogenetic analysis was performed to study the mitotic chromosome behaviour in the wild-type and *Atssrp1* mutant plants. Chromosomal abnormalities were observed during anaphase in the *Atssrp1* mutant. Anaphase bridges were visualised (**Figure 31, arrows**). Furthermore, some chromosome fragmentation could be observed at this stage too (**Figure 31, arrows**). Consequently, it seems that *Atssrp1* mutants are affected in the genome stability which could explain the vegetative phenotype observed with delay growth or dwarf-like plants.

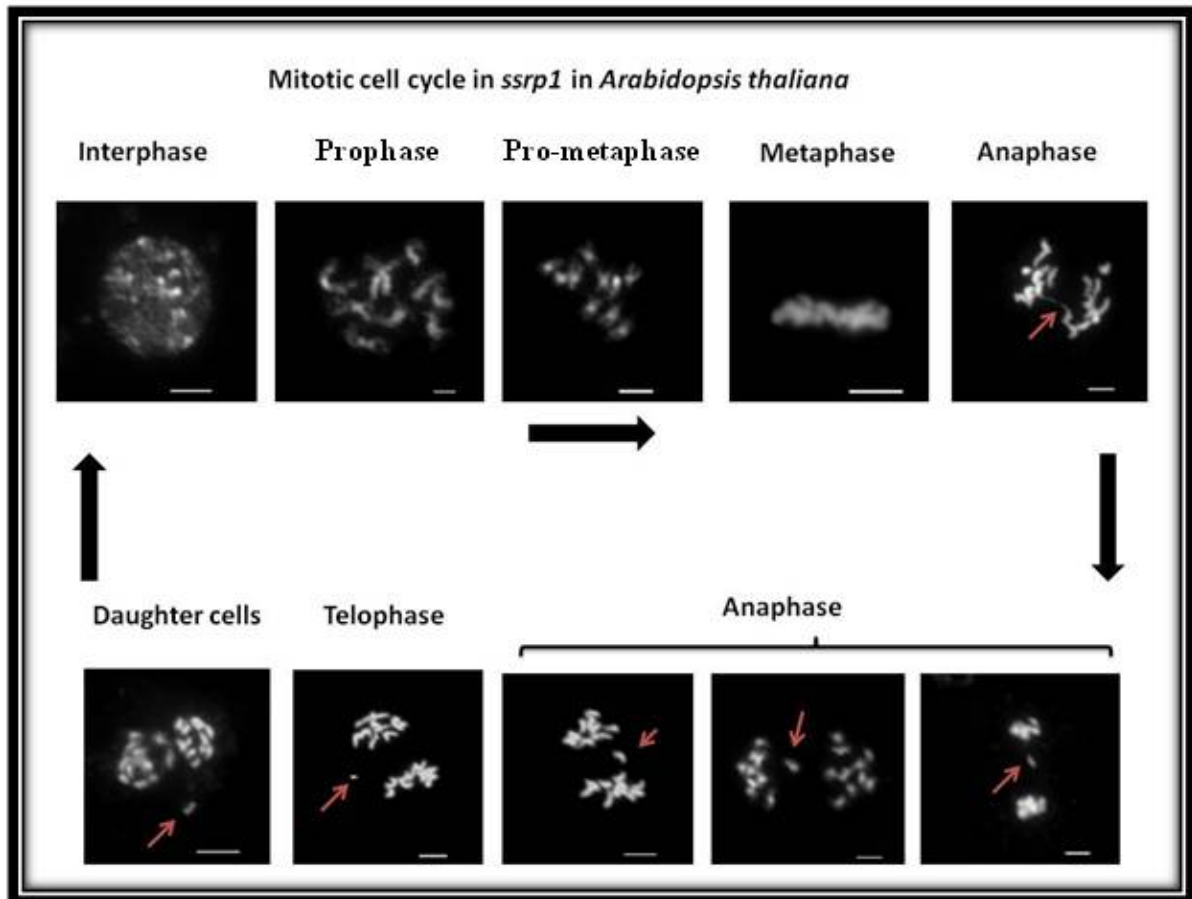


Figure 31. Cytological analysis of the mitosis in wild-type and *Atssrp1* mutant.

A cytogenetic analysis was conducted to study the mitotic cell divisions in both wild-type and *Atssrp1* mutant using DAPI staining and fluorescence microscopy. *Atssrp1* presented different chromosome abnormalities including anaphase bridges and chromosome fragmentation. Scale bar = 5 μ m.

4.2.7 Quantification of meiotic chromosome missegregation in *Atssrp1*

Meiotic chromosome segregation in wild-type (Col) and *Atssrp1* mutant has been characterised and categorised into two class: normal (accurate chromosome segregation) or abnormal (unbalanced chromosome segregation). Quantification of these two classes was carried out in first meiotic division (anaphase I to metaphase II) and second meiotic division (anaphase II-telophaseII). All the wild-type meicytes showed a balanced chromosome segregation during the first meiotic division (with 5 chromosomes segregating to opposite poles) and during second meiotic division (with 5 chromatids segregating to each pole). Nevertheless, in the *Atssrp1* mutant only 39% of the meicytes showed a correct segregation of chromosomes (N=152 meicytes) (**Figure32**). Interestingly, the abnormal chromosome segregation was more frequent during second meiotic division (92.8%) than during first meiotic division (29.2%).

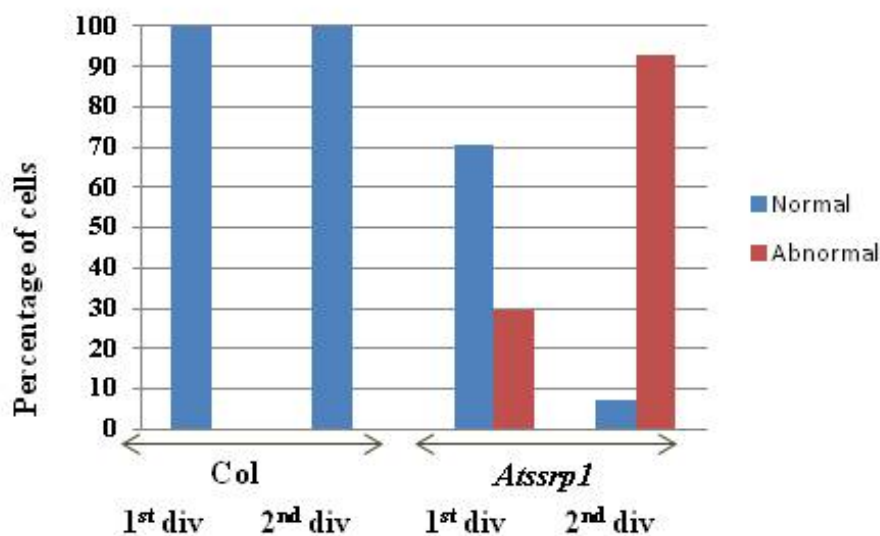
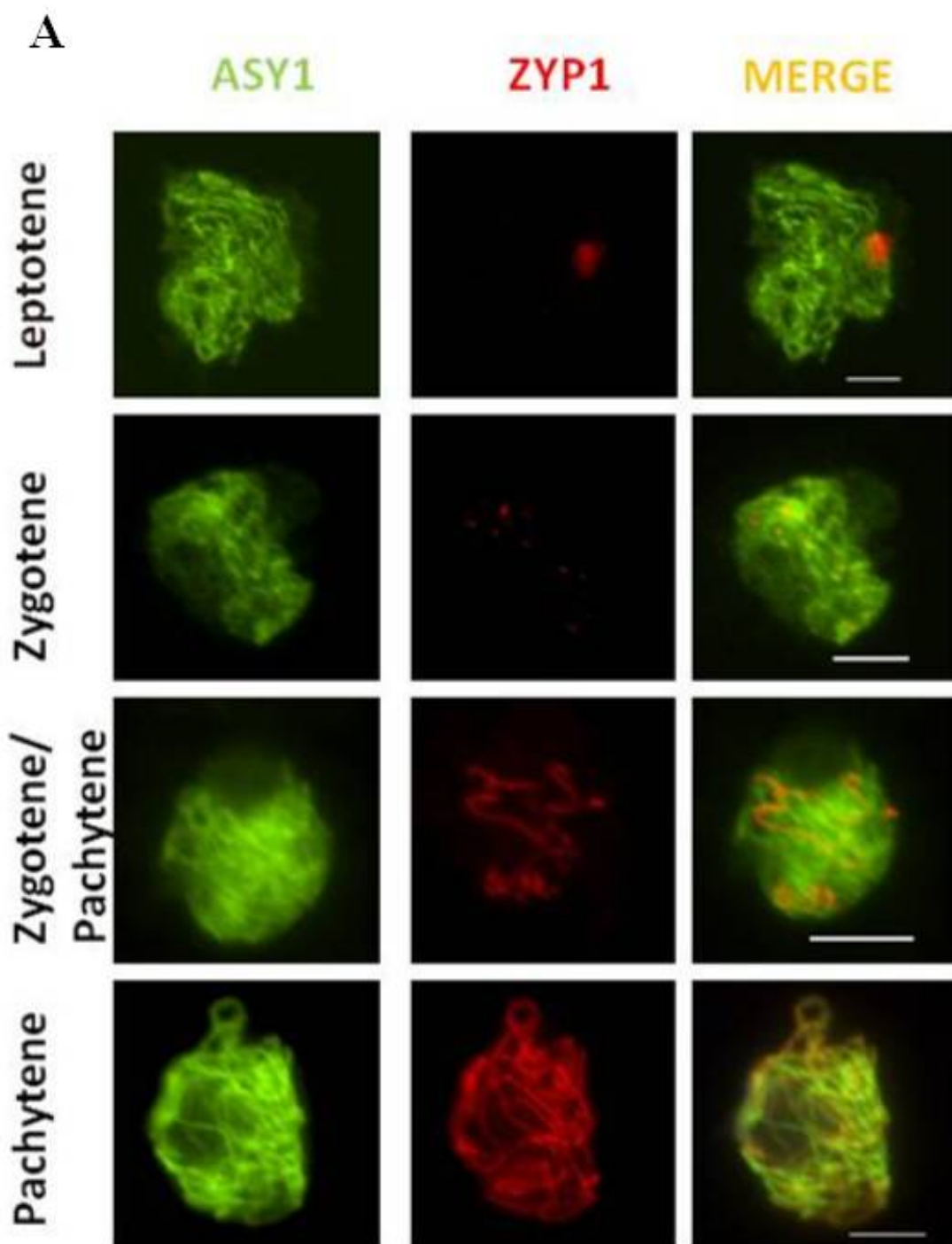


Figure 32. Proportion of normal and abnormal meiotic chromosome segregation in the wild-type and *Atssrp1* mutant.

Percentage of cells with normal and abnormal chromosome segregation during first meiotic division (AI-MII) and second meiotic division (AII-TII) in wild-type (Col) (N=200 meicytes) and *Atssrp1* mutant (N=152 meicytes).

4.2.8 Immunolocalization of AtASY1 and AtZYP1 on both wild-type and *Atssrp1* mutant

Immunolocalisation studies were conducted to study the polymerization of both AtASY1 and AtZYP1 proteins throughout meiotic prophase I in the wild-type and *Atssrp1* mutant. Our analysis showed that AtASY1 appeared at G2 as foci and around leptotene as a linear signal along the chromosome axis. AtZYP1 signal starts as foci during zygotene and polymerizes as a continuous signal at pachytene. Both AtASY1 and AtZYP1 immunolocalisation in the wild-type and in the *Atssrp1* mutant were identical (**Figure 33A and B**).



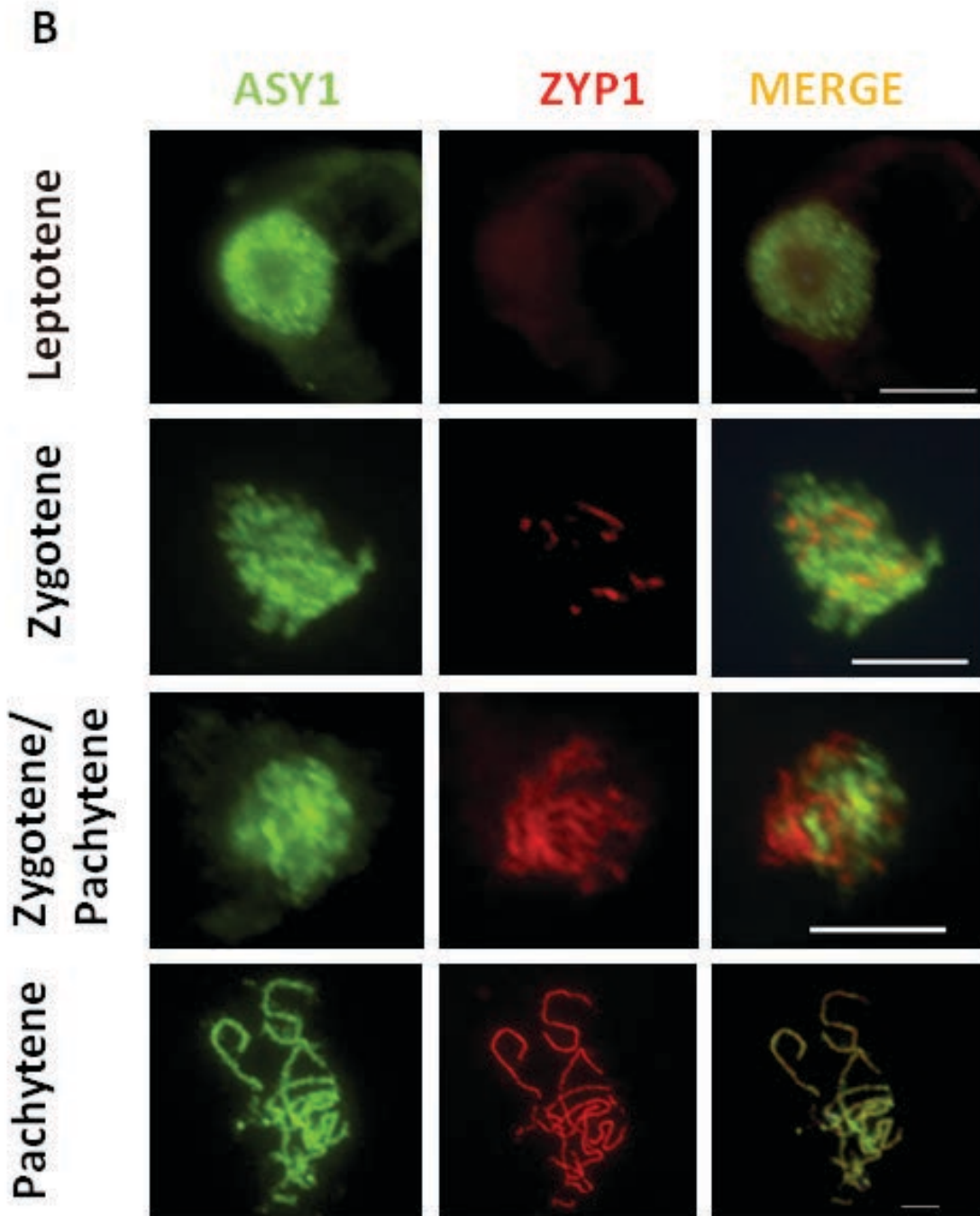


Figure 33. immunolocalisation of AtASY1 and AtZYP1 in both wild-type and *Atssrp1* mutant.

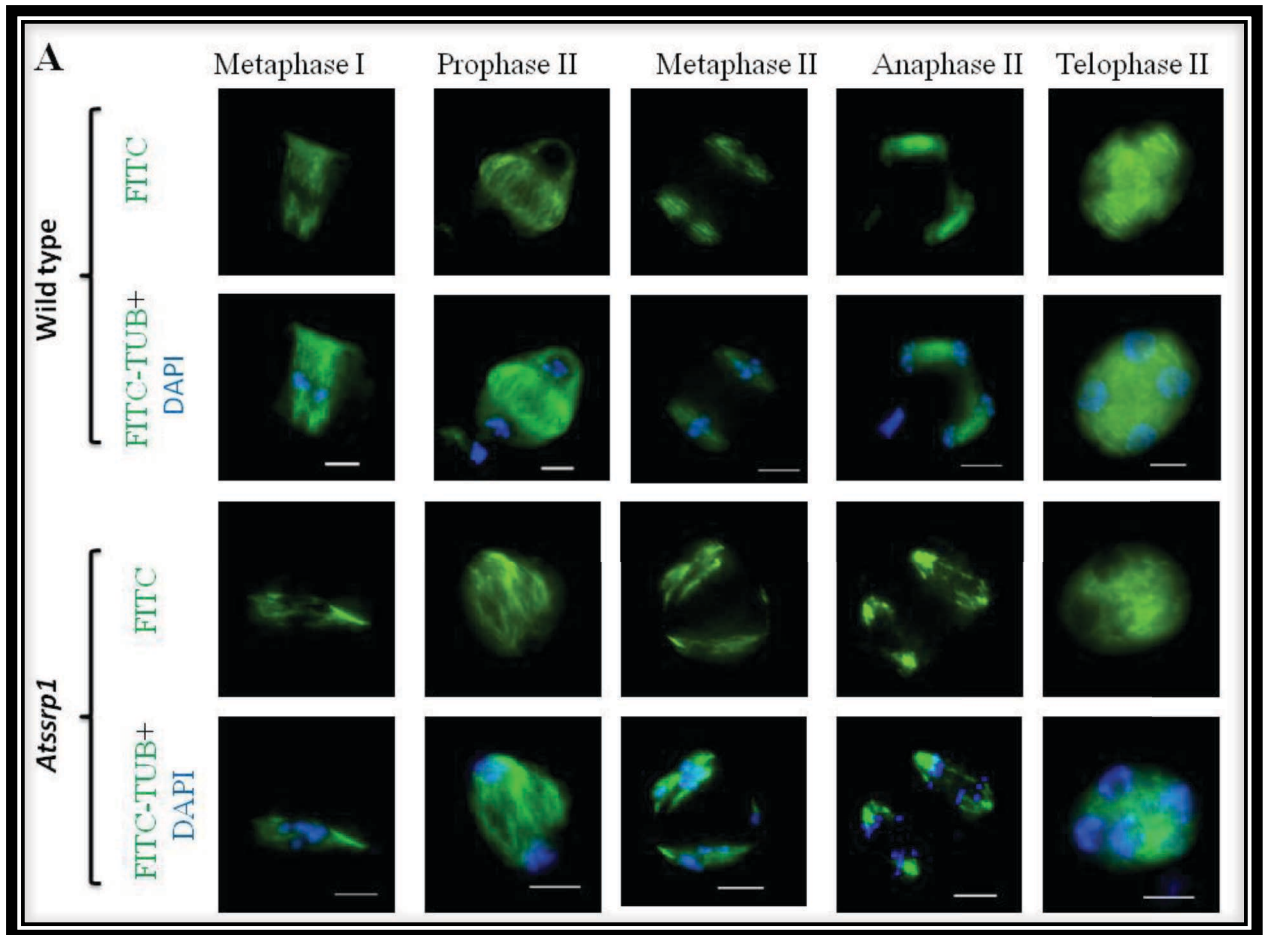
This figure shows the co-localization of AtASY1 (green) and AtZYP1 (red) in both wild-type and *Atssrp1*. **A** Immunolocalisation of AtASY1 and AtZYP1 in the wild-type. **B** Immunolocalisation of AtASY1 and AtZYP1 in the *Atssrp1* mutant. Scale bar = 5µm.

4.2.9 Localization and distribution of microtubule spindles during meiosis and mitosis in *Arabidopsis*

Immunolocalisation of beta-tubulin was carried out to study the meiotic and mitotic spindles in the wild-type (Col) and *Atssrp1* mutant in *Arabidopsis* (**Figure 34A**). Monoclonal anti-beta-tubulin antibodies raised in mouse was used to identify beta-tubulin.

Our analysis in the wild-type showed the association of microtubules on spindle at metaphase I which attached to chromosomes centromeres (**Figure 34A**). Microtubules also associated on spindles at metaphase II attaching to the centromeres of the sister chromatids to separate them to different poles. In *Atssrp1* mutant, the spindle forms at metaphase I and metaphase II similarly to that of the wild-type. Nevertheless, the spindles seem to contain less microtubules and their distribution not so orderly rearranged like in the wild-type (**Figure 34**). Eventually, these spindle defects would lead to abnormal chromosome segregation during first and second meiotic divisions.

Deferent chemical components have been identified to stabilize microtubules which have been widely used as anti-tumour drugs to arrest cell division like Taxol. Flutax1 is derivate of this drug combined with a fluorophore (fluorescein) was used in this study as a complementary technique to visualise microtubules and thus, mitotic spindles (**Figure 34B**). Flutax1 is a fluorescent taxol that associates to the microtubules preventing the microtubule de-polymerisation. Flutax1 allowed us to visualise the microtubule cytoskeleton in somatic cells and the mitotic spindle in wild-type and *Atssrp1* mutant cells (**Figure 34B**). Chromosome missegregation and micronuclei have been observed during mitotic stages at anaphase and telophase. Therefore, it seems that AtSSRP1 might play a key role in the proper distribution and/or polarization of microtubules in the mitotic spindle.



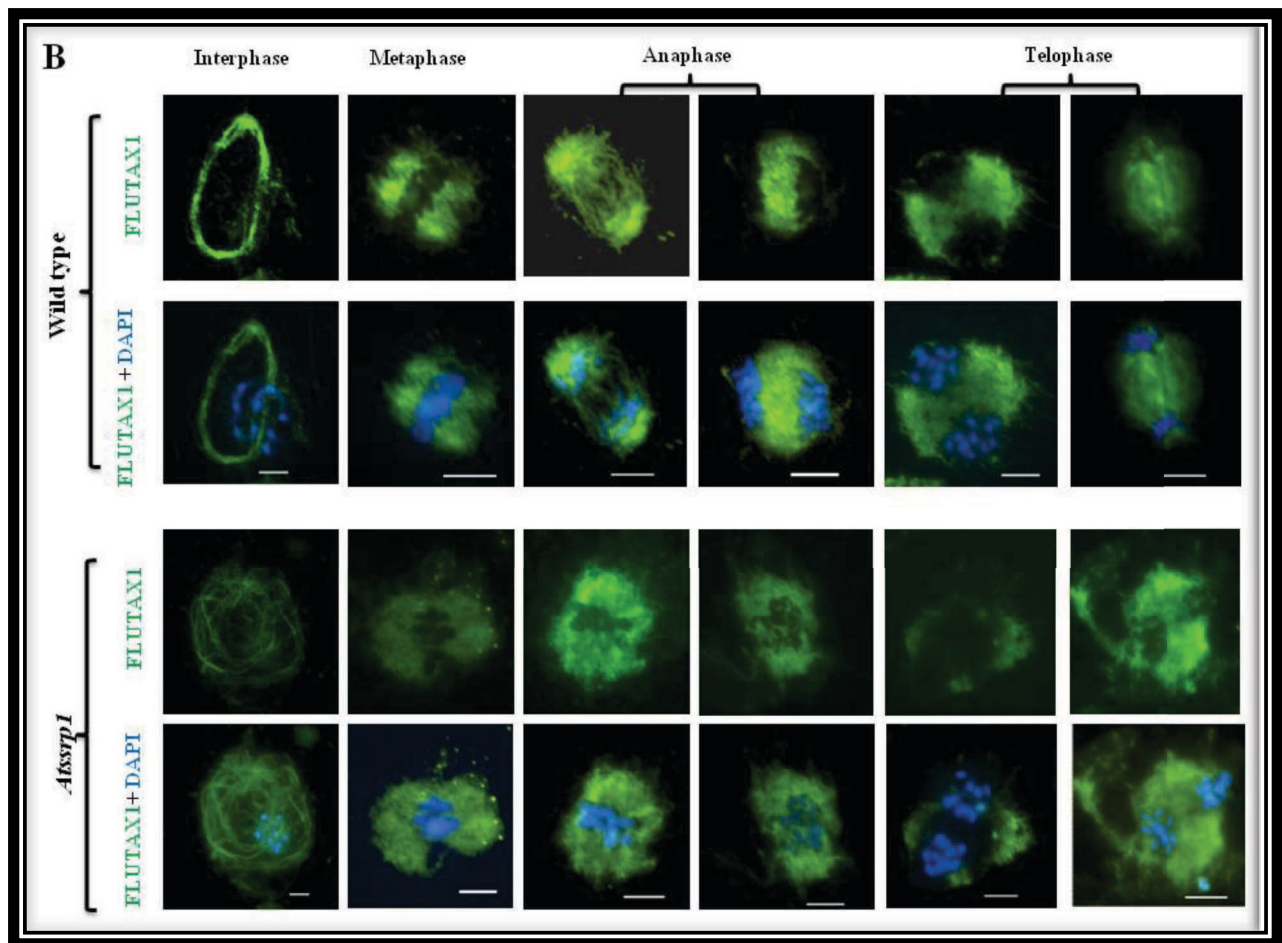


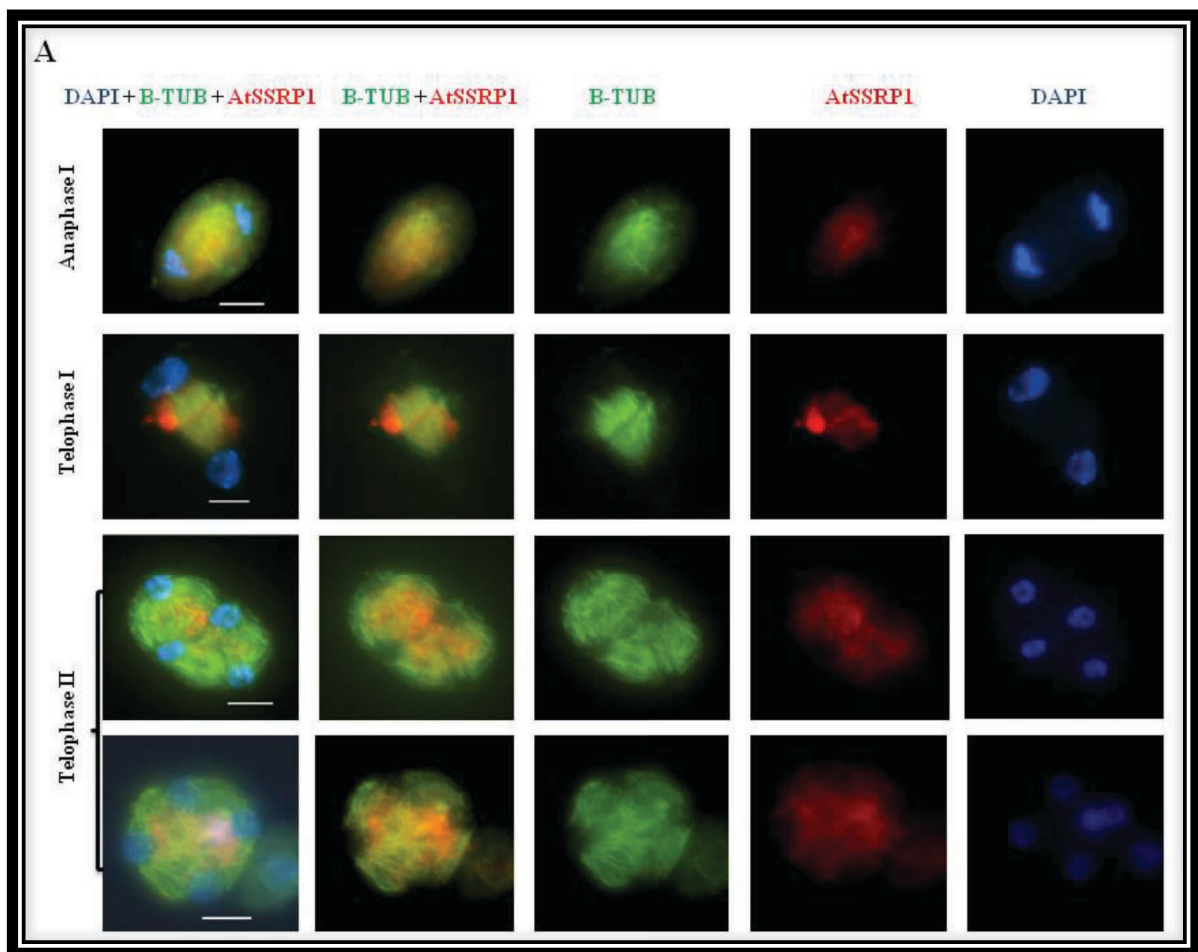
Figure 34. Staining of beta-tubulin in meiosis and mitosis in wild-type and *Atssrp1* mutant.

A Immunolocalisation of beta-tubulin during meiosis. Monoclonal mouse anti-beta-tubulin and secondary anti-mouse FITC antibodies (green) were used to identify the microtubule spindle during meiosis. **B** Flutax1 staining of mitotic spindles. Scale bar = 5µm.

4.2.10 Immunolocalisation of AtSSRP1 in wild-type and *Atssrp1* mutant

Immunolocalisation of AtSSRP1 has been conducted to study the distribution of AtSSRP1 molecules on the chromatin and spindles in *Arabidopsis* meiocytes. A polyclonal anti-hSSRP1 (human SSRP1) raised in rabbit was used together with a monoclonal anti-beta-tubulin antibody raised in mouse. Secondary antibodies anti-rabbit TRITC (red) and anti-mouse FITC (green) were used to identify the signals with an epifluorescence microscope.

This analysis showed that, in the wild-type (**Figures 35A and B**), AtSSRP1 appears as a high abundance signals that partially co-localize with microtubules in all different meiotic stages (**Figure 35A**) except at late telophase II/young pollen grains that the AtSSRP1 signal localises along the chromatin (**Figure 35B**). These observations are consistent with the possible role of AtSSRP1 in managing the correct spindle formation during meiotic stages. In the *Atssrp1* mutant line not signal of AtSSRP1 was observed (**Figures 35C and D**)



B

DAPI+B-TUB+AtSSRP1

B-TUB+AtSSRP1

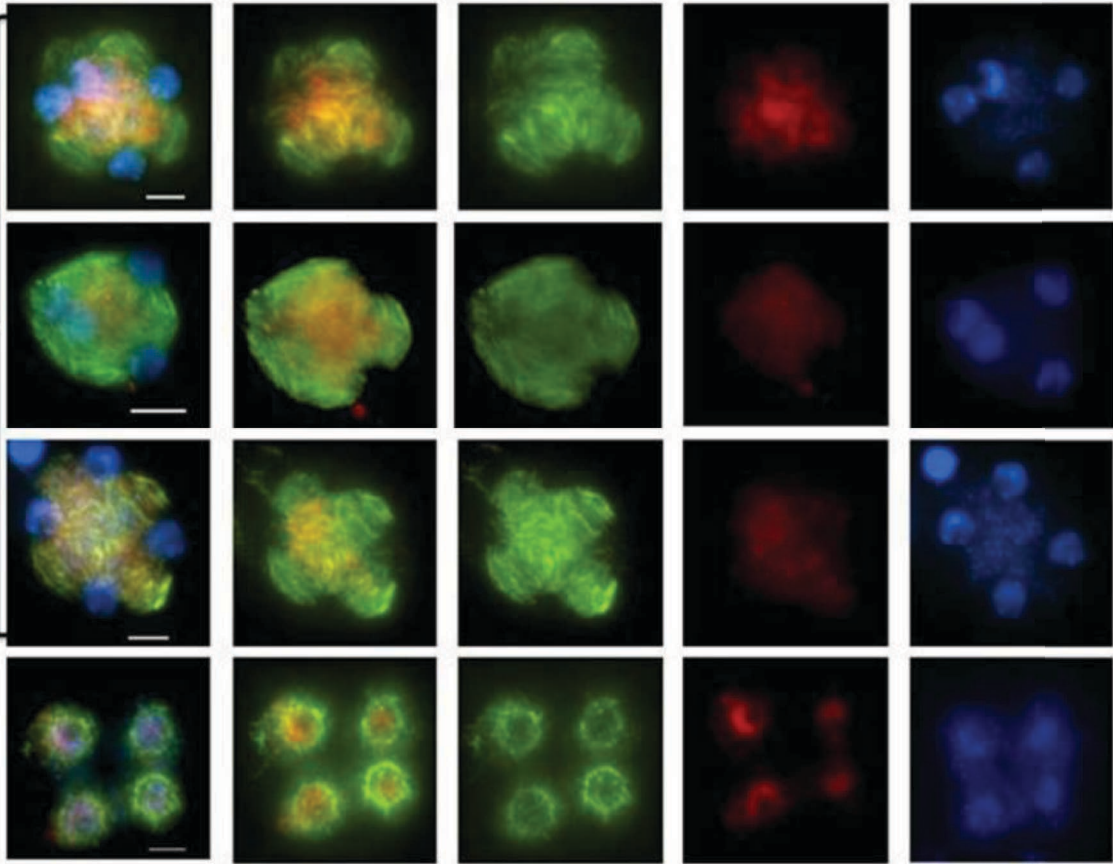
B-TUB

AtSSRP1

DAPI

Telophase II

Late Telophase II



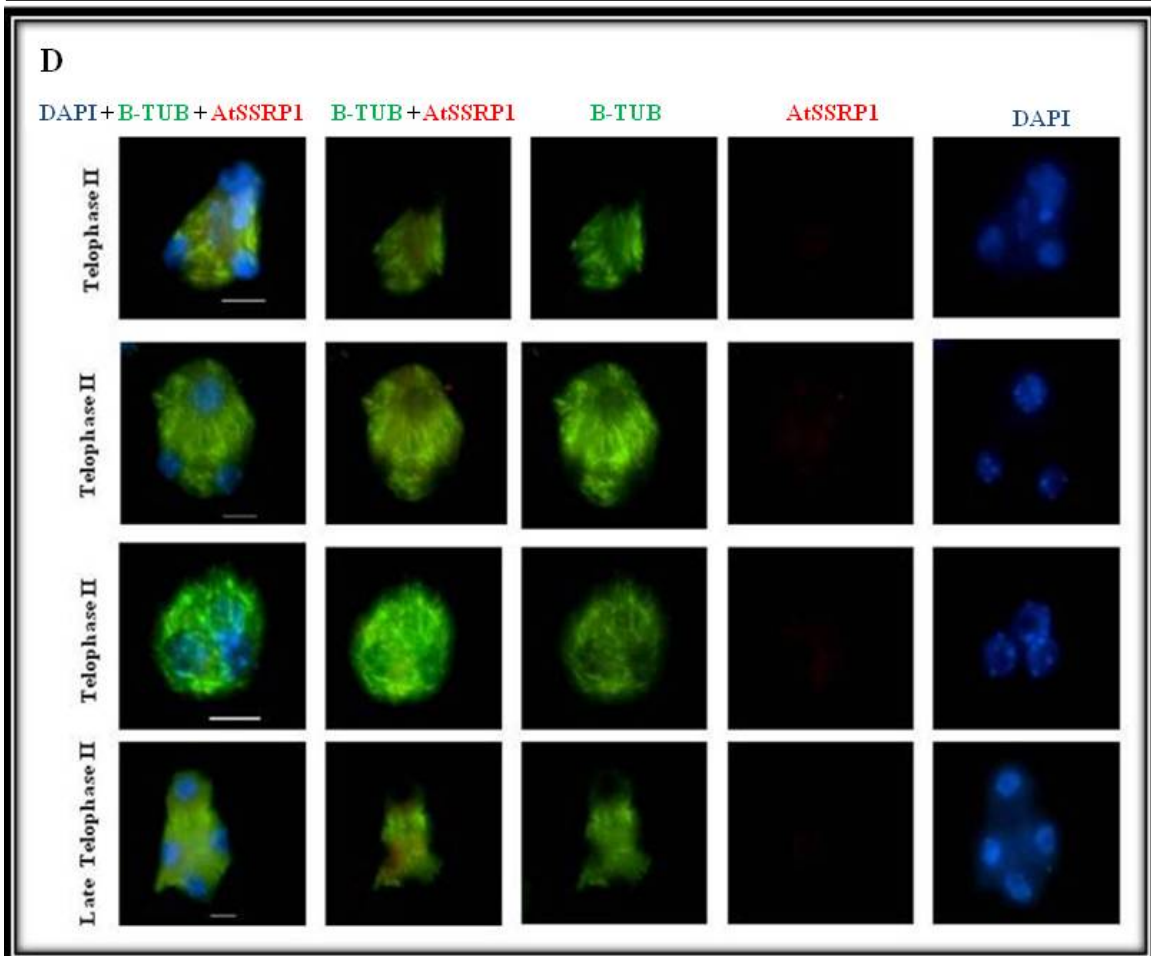
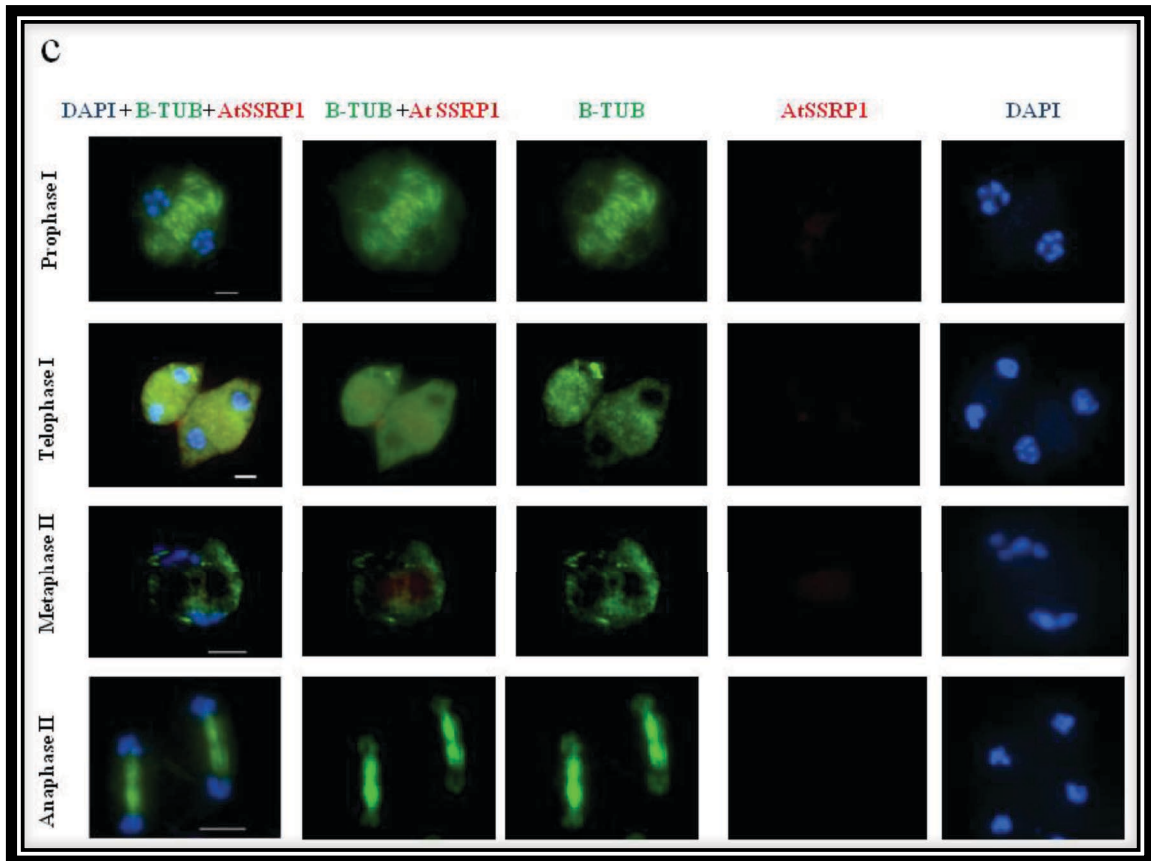


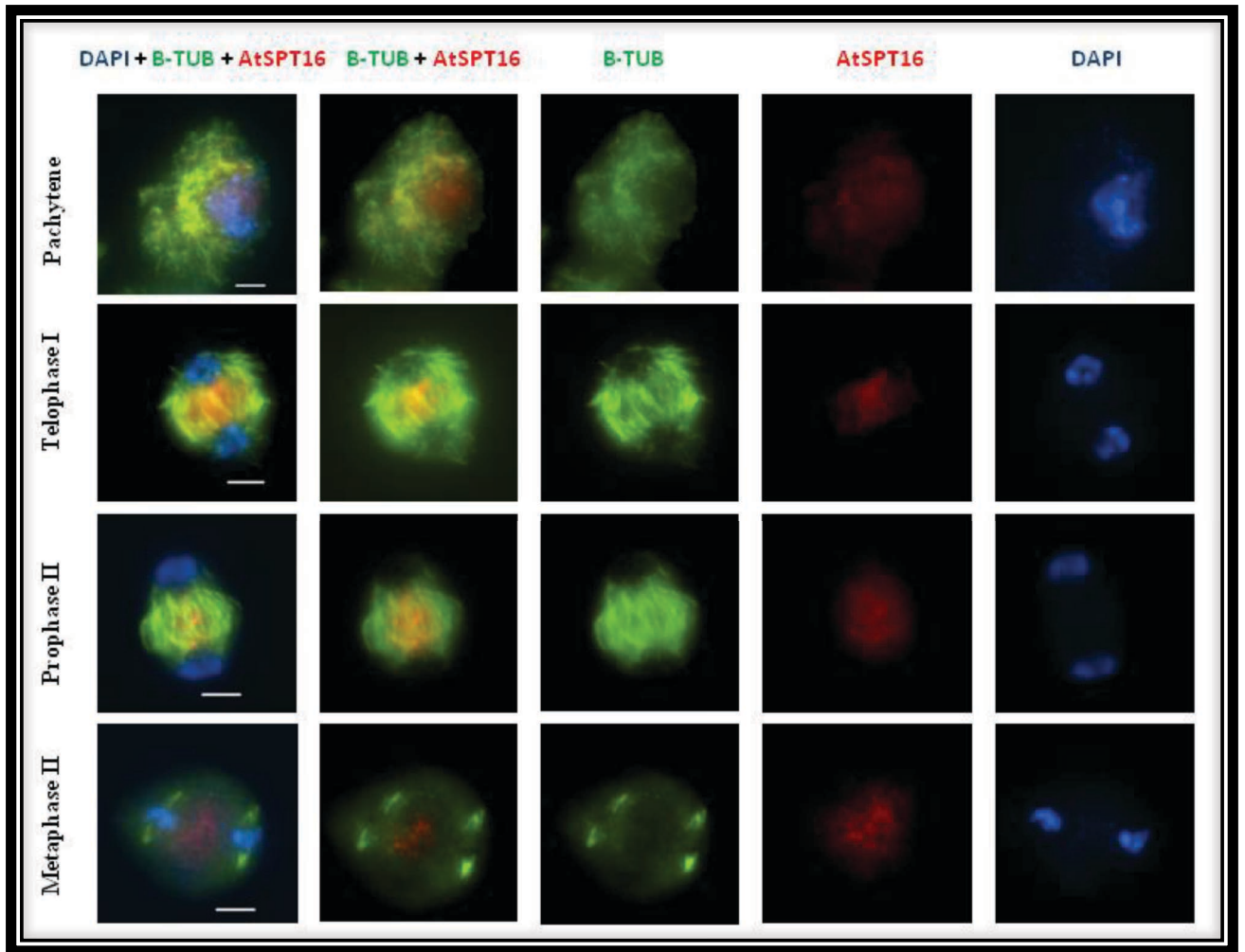
Figure 35. Dual immunolocalisation of beta-tubulin (green) and AtSSRP1 (red) during meiosis.

A and **B** Wild-type meiocytes. **C** and **D** *Atssrp1* mutant meiocytes. Scale bar = 5µm.

4.2.11 Immunolocalisation of AtSPT16 in the wild-type

Immunolocalisation of AtSPT16 was carried out using a polyclonal anti-hSPT16 antibody raised in rabbit and visualized with a secondary anti-rabbit TRITC antibody. Dual immunolocalisation with beta-tubulin antibodies was carried out in order to analyse the association of AtSPT16 with the microtubules in *Arabidopsis*.

Our analysis showed that AtSPT16 appears as a high abundance foci signal. During prophase I the signal seems to be inside the nucleus localising in the chromatin (**Figure 36**). In later stages AtSPT16 seems to co-localize with the spindles from the first meiotic division until prophase II (**Figure 36**). However, AtSPT16 seems to re-localise from the cytoplasm into the chromatin during the second meiotic division, being fully visible during Telophase II (**Figure 36**). This observation shows that AtSPT16 could have a role in the proper distribution and dynamics of microtubules in the first meiotic spindle but not during the second meiotic division where AtSPT16 seems to be more a chromatin associated.



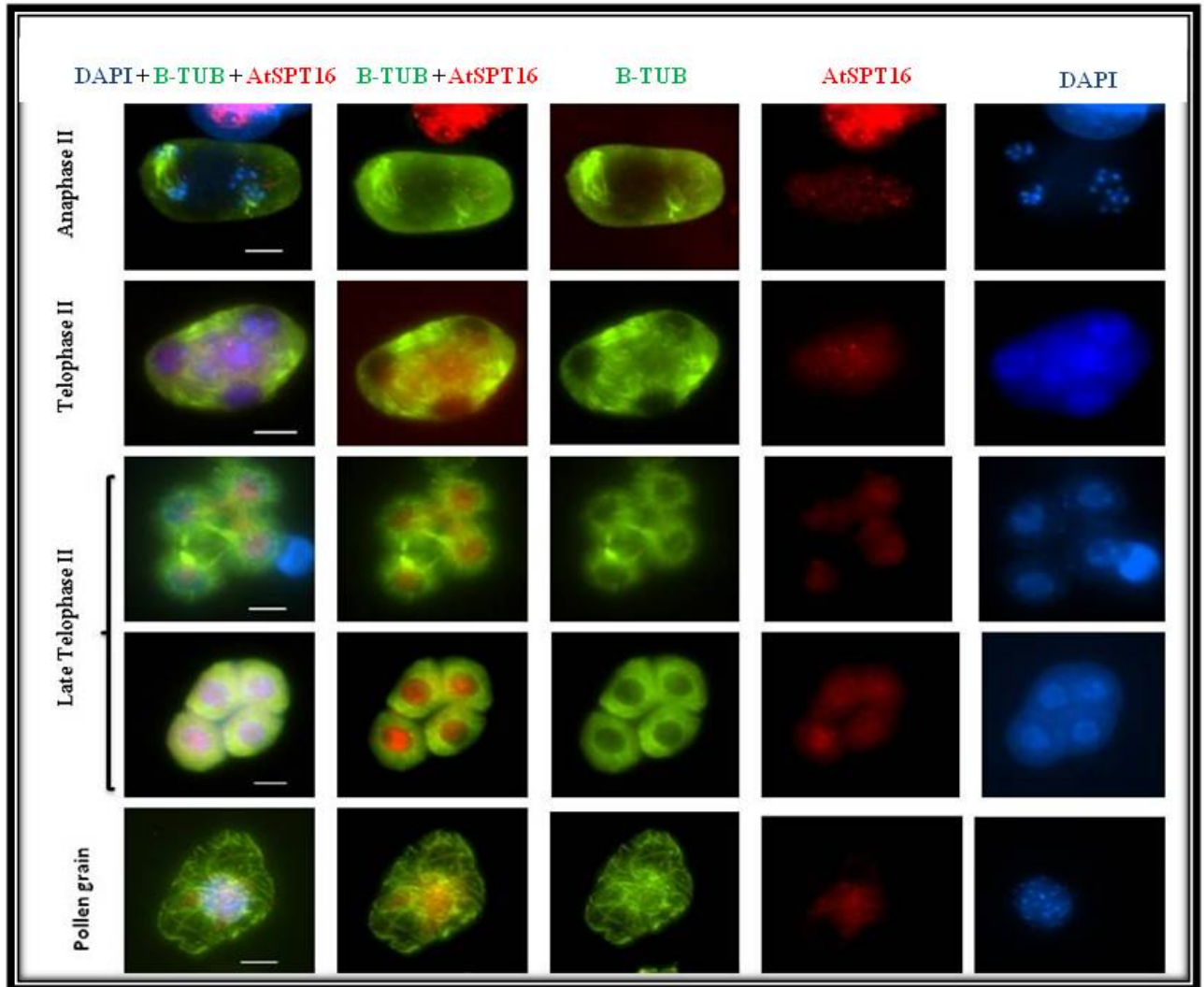
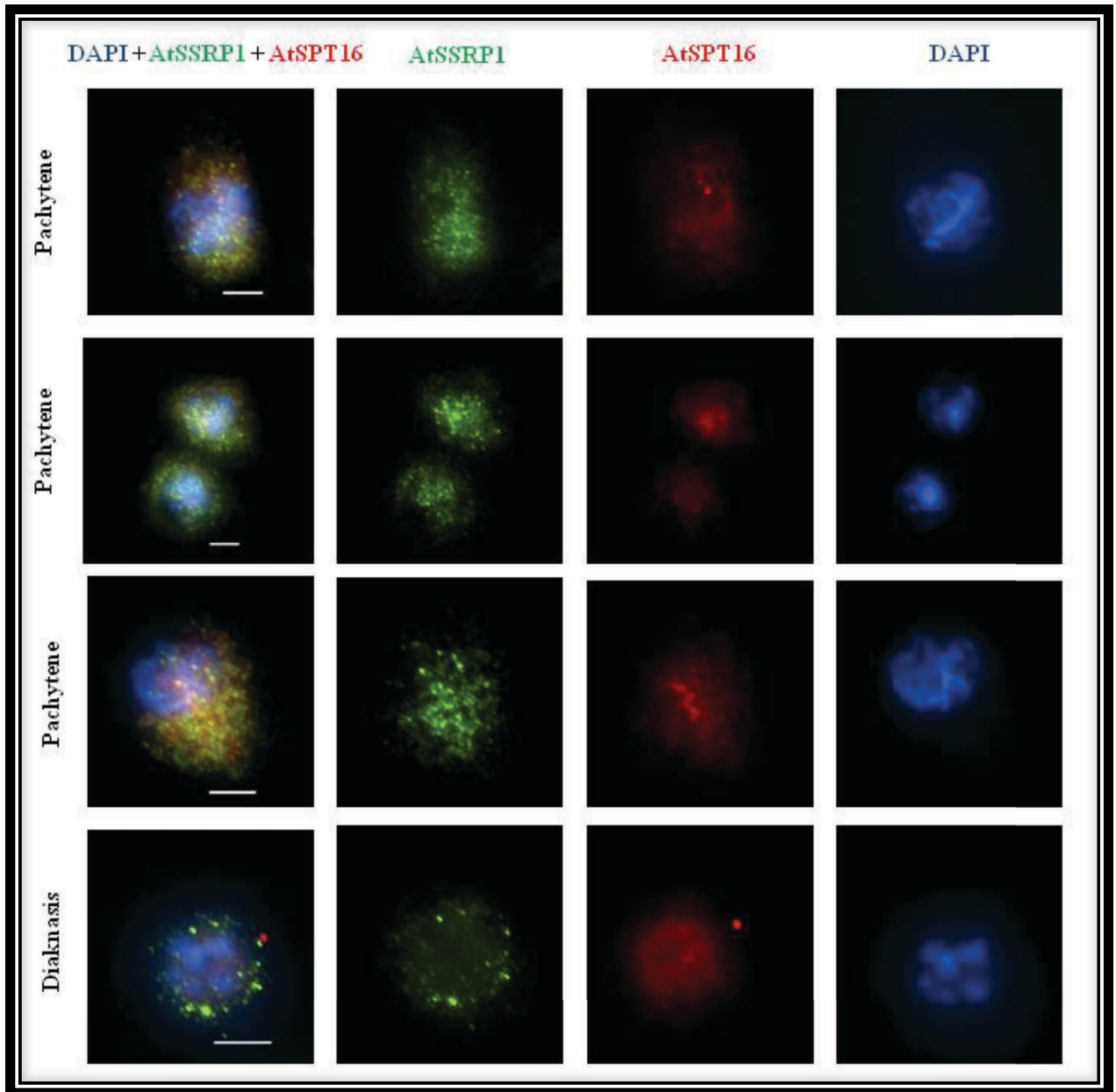


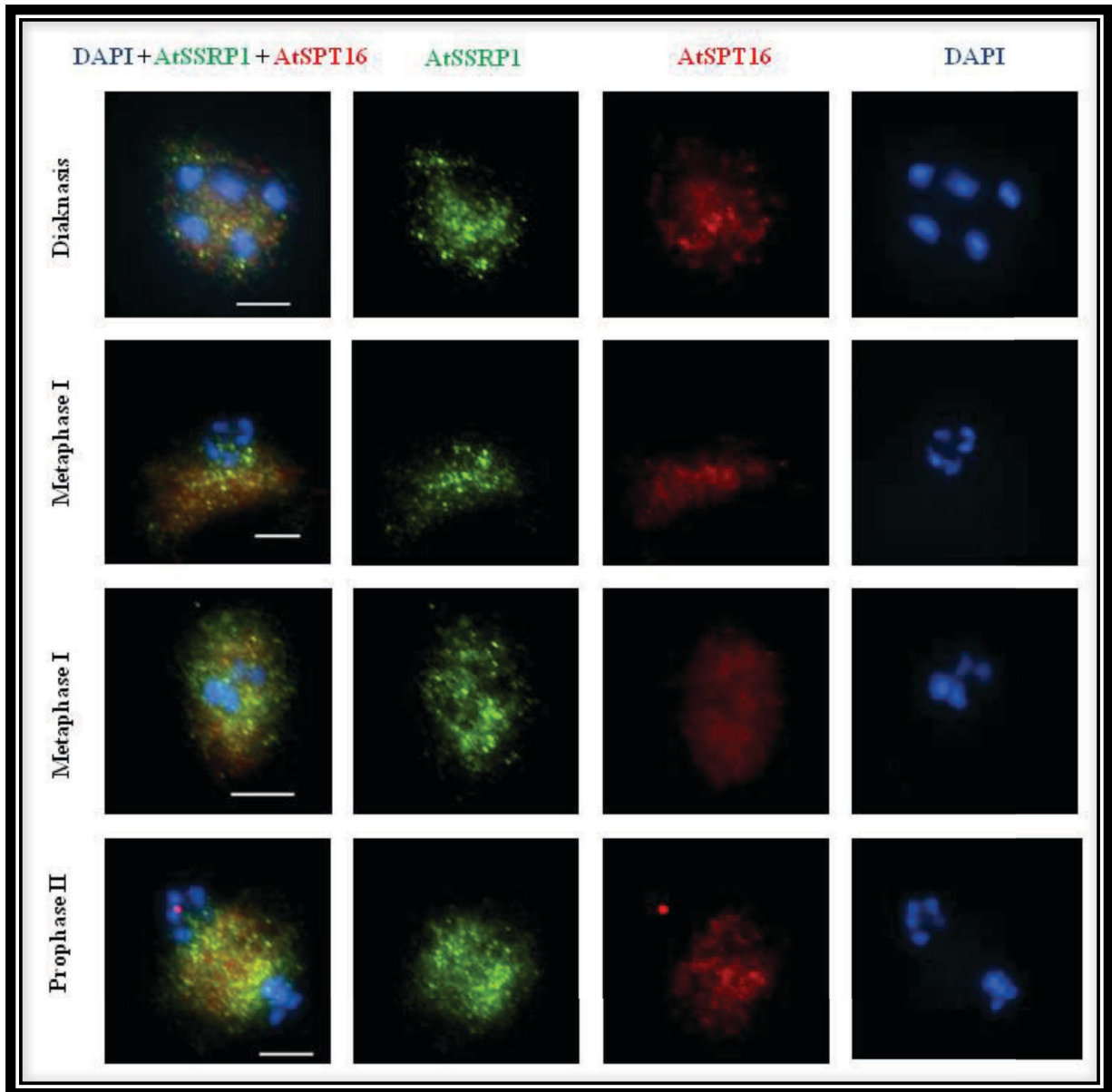
Figure 36. Dual immunolocalisation of beta-tubulin (green) and AtSPT16 (red) in wild-type meiosis.

The different meiotic stages are indicated. Scale bar = 5µm.

4.2.12 Dual immunolocalisation of AtSPT16 and AtSSRP1 in the wild-type

Dual immunolocalisation of AtSPT16 and AtSSRP1 was carried out in order to study their distribution in *Arabidopsis* meiocytes. A polyclonal anti-hSPT16 antibody raised in rabbit and a monoclonal anti-hSSRP1 antibody raised in mouse were used for the dual localisation. AtSPT16 and AtSSRP1 appeared as a high abundance signal as foci on the wild-type. During prophase I, both proteins seem to partially co-localise on the cytoplasm although there are some AtSPT16 foci localised onto the chromatin in pachytene nuclei (**Figure 37**). At diakinesis the number of AtSSRP1 foci seems to get reduced to very bright foci on the cytoplasm while the AtSPT16 signal is still present at the nucleus. From metaphase I until anaphase II, both proteins seem to co-localise at the region where the spindle is formed. At telophase II, AtSPT16 signal starts re-localising into the nucleus whereas AtSSRP1 is still present in the cytoplasm (associated to microtubules). At late telophase II/young pollen grains both proteins co-localise onto the nuclear chromatin.





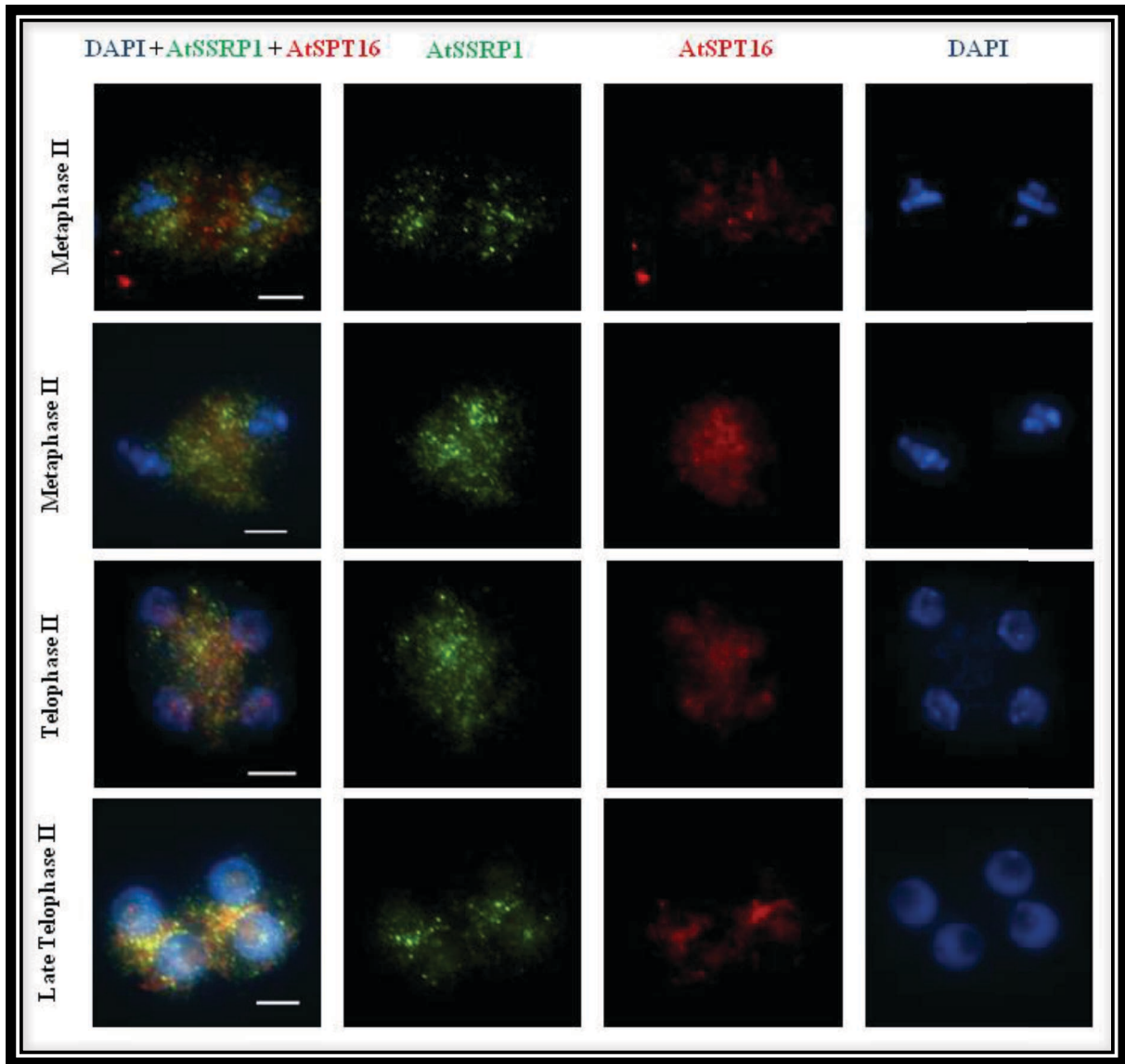


Figure 37. Dual immunolocalisation of AtSSRP1(green) and AtSPT16 (red) in wild-type pollen mother cells.

Meiotic stages are indicated. Scale bar = 5µm.

4.2.13 Characterization of *Atk1* mutant

AtK1 gene plays a clear role in microtubule maturation and organization during meiosis (Zhu *et al.*, 2012). It has been reported that this protein is also important for chromosome alignment at the second division that leads to accurate segregation by organizing microtubules as bundles (Zhu *et al.*, 2012). In this study, we have identified an *Atk1* mutant in *Arabidopsis* which has showed abnormalities during the second meiotic division and therefore leads to random chromosome segregation during anaphase II.

AtK1 gene is located in the long arm of chromosome 4 of *A. thaliana*. It consists of 17 exons and 16 introns in addition of the 3' and 5' UTRs. The T-DNA in this line (SALK-043587) is inserted in the exon number 3 of the *AtK1* gene (At4g21270). TAIR databases and the Sequence Viewer tool has been used to represent the DNA sequence, gene structure and the position of T-DNA insertion line of *AtK1* gene (**Figure 38A**).

Atk1 mutant is a T-DNA insertion line (SALK-043587) which seeds were obtained from the SALK Institute (San Diego). Mutant and wild type seeds were planted together in identical conditions monitored in the glasshouse. DNA was extracted from plant leaves to genotype them. Two primers were designed (LP and RP) around the T-DNA insertion site in *AtK1* gene and another specific primer for the left border of the T-DNA used to represent this line (BP) was designed to confirm the presence of the T-DNA insertion (**Figure 38A**).

PCR and gel electrophoresis was conducted to check the presence of the T-DNA insertion within the *Atk1* gene. Additionally, wild-type plants have been used as a control (**Figure 38B**). Wild-type plants showed one single band amplification of approximately 1,042 bp size as a result of amplifying the genomic sequence between LP and RP primers in *AtK1* gene (**Figure 38B**). The homozygous mutants provided one single band of 777 bp as a result of amplifying the left border of the T-DNA up to the RP primer in *atk1* mutant (**Figure 38B**).

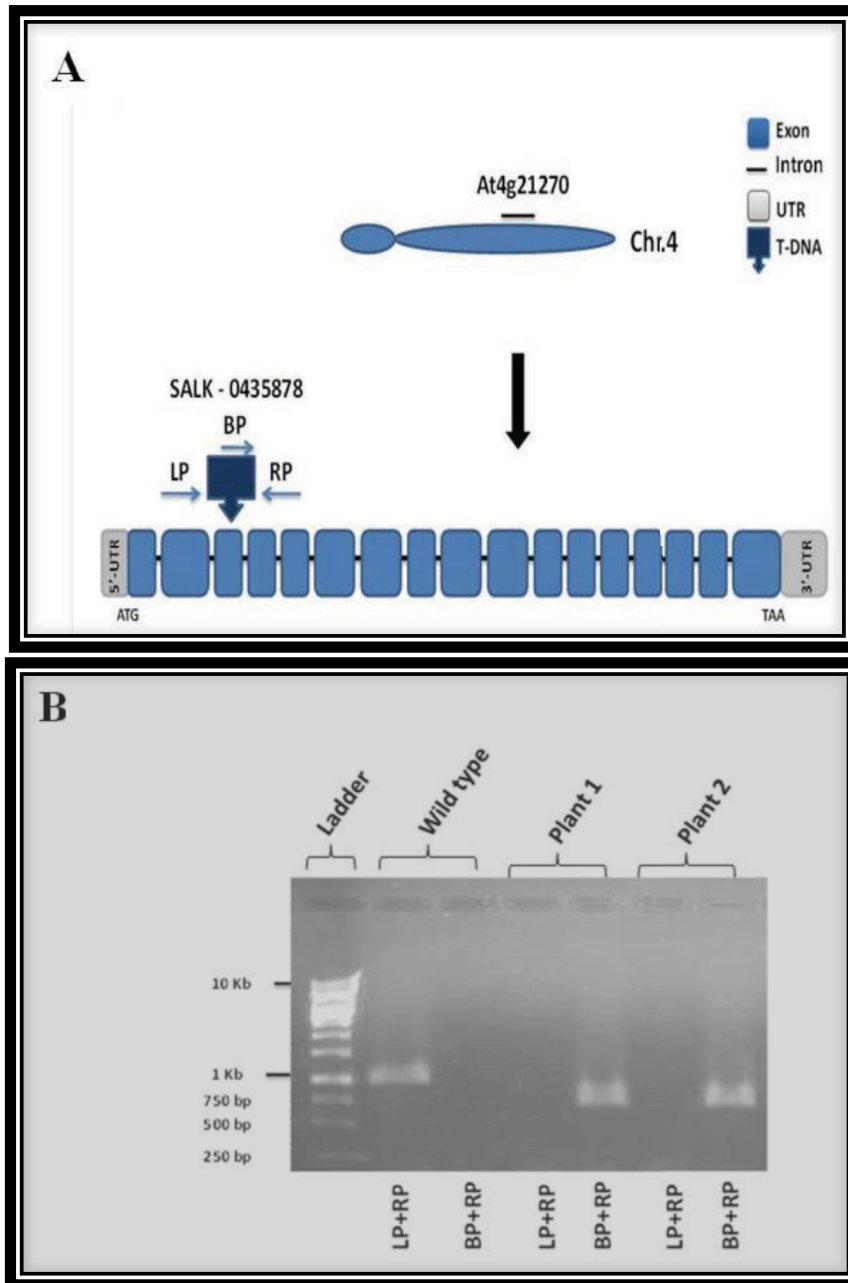
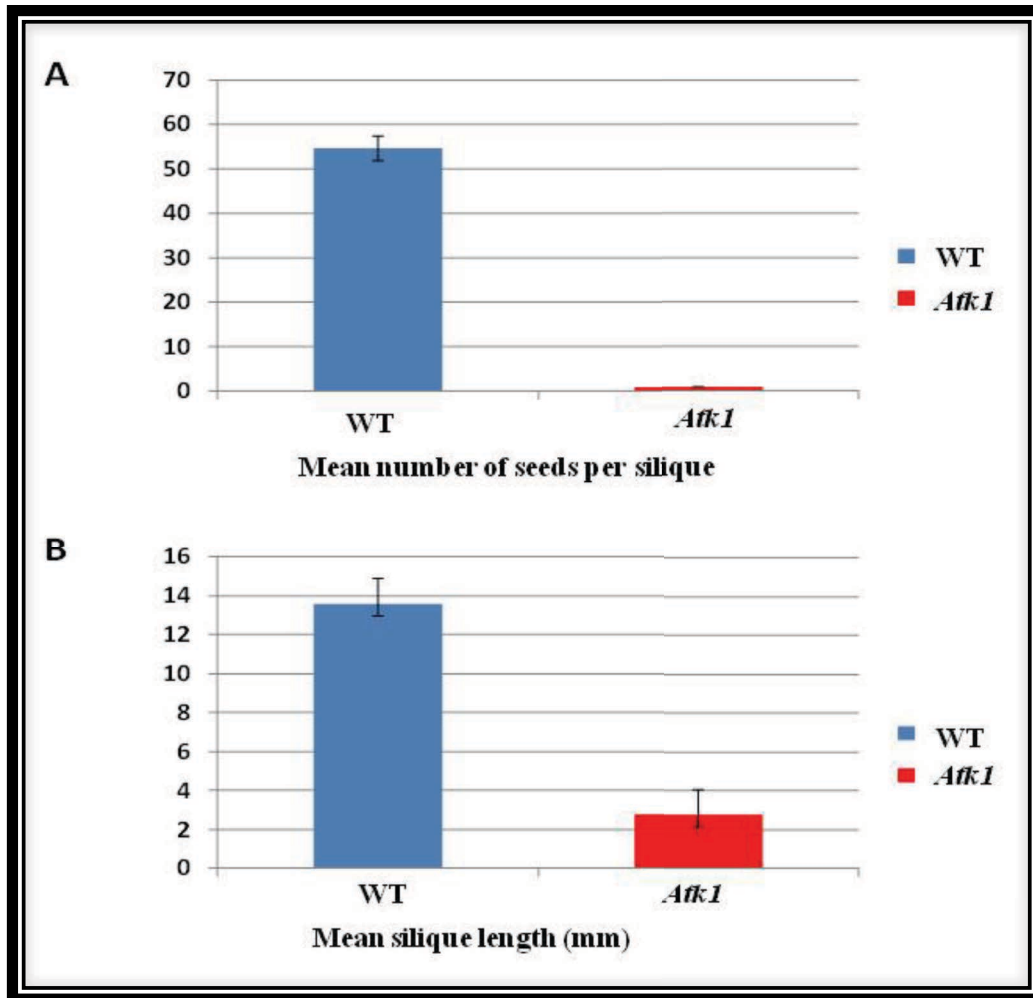


Figure 38. *ATK1* gene structure, T-DNA insertion location and plant genotyping.

A *AtK1* gene consists of 17 exons (blue boxes) in addition of 5' and 3'UTRs (grey boxes). The T-DNA is inserted in the 3rd exon (inverted dark blue arrow box). **B** Gel electrophoresis photograph showing a wild-type PCR product and two homozygous plants for the T-DNA insertion.

Atk1 mutant plants show a semi-sterile phenotype with a mean number of seeds per silique of 0.92, a very significant reduction compared to the 54.68 seeds/silique in the wild-type (*T*-test, $p=6.49 \times 10^{-44}$) (**Figure 39A**). The mean length of the silique for *atk1* mutant plants was also

significantly reduced to 2.76 mm compared to the 13.58 mm of the wild-type (*T*-test, $p=2.95 \times 10^{-59}$) (Figure 39B).



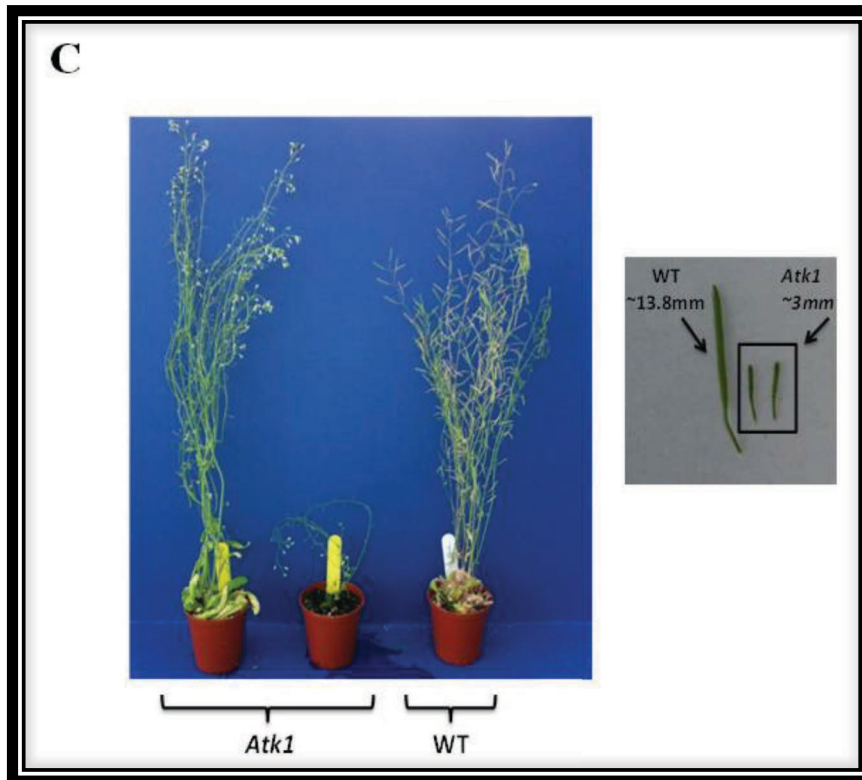


Figure 39. Semi-sterile phenotype in *Atk1* mutant.

A Mean number of seeds per silique in the wild-type and *Atk1* mutant. **B** Mean silique length. **C** Photographs of wild-type and *Atk1* mutant plants grown at the same time and conditions. The reduced size of the siliques is very clear.

Cytogenetic analysis of meiosis in the *Atk1* mutant revealed defects in chromosome segregation similar to those observed in *Atssrp1* mutants (**Figure 40**). Meiotic stages start normally in *Atk1* mutant, with chromosome pairing and synapsis fully completed at pachytene (**Figures 40A, B and C**). Chromosome condensation increased during diplotene and diakinesis showing five bivalents at metaphase I (**Figures 40D, E and F**). Nevertheless, the chromosome segregation during anaphase I showed unequal segregation of chromosomes to opposite poles (**Figure 40G**). This led to some prophase II and metaphase II cells with nuclei with unbalanced chromosome numbers (**Figures 40H, I and J**). Subsequently, further chromosome missegregation occurred at anaphase II and thus, the creation of gametes with unequal chromosome number (**Figures 40K and L**).

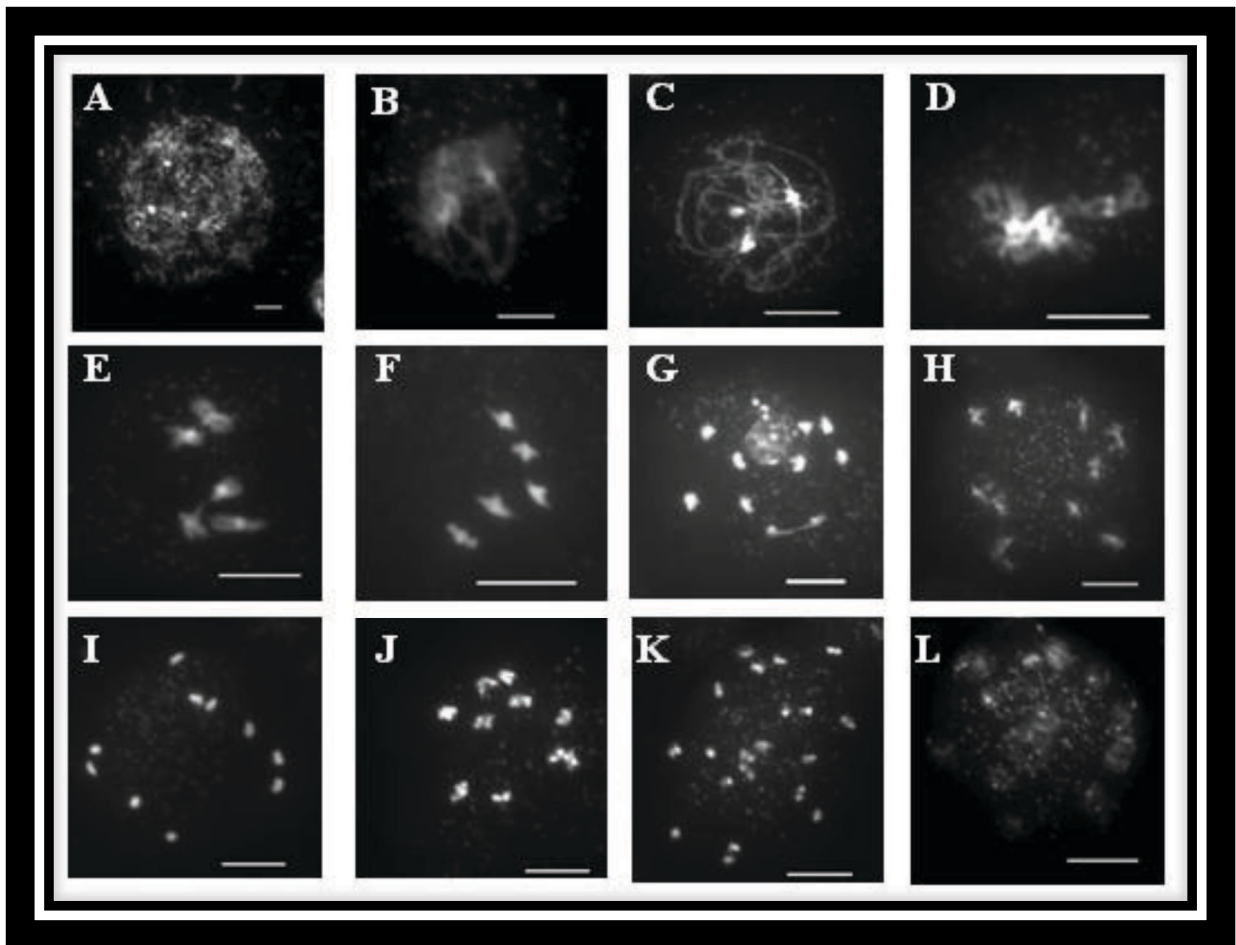


Figure 40. Cytological analysis of the meiotic process in *atk1* mutant (SALK-043587).

A Leptotene. **B** Zygotene. **C** Pachytene, homologous chromosomes are fully synapsed. **D** Diplotene. **E** Diakinesis. 5 bivalents are visible. **F** Metaphase I: five bivalents were observed aligning on the metaphase plate. **G** Anaphase I, with asynchronous segregation of chromosomes and possibly missegregation. **H** Prophase II. **I** and **J** Metaphase II. **K** Anaphase II with further chromosome missegregation. **L** Telophase II/Tetrad stage with several nuclear envelopes instead of the four observed in wild-type. Scale bar = 5 μ m.

4.3 DISCUSSION

4.3.1 HMG proteins roles

HMGA family includes HMG proteins with one or several AT-Hook DNA binding domains. A study in mouse using homozygous mutants for an *hmga* gene reported a variety of mutant phenotypes which included growth retardation, diabetes (as a result of reducing insulin receptor in all tissues) and absence of fat (Sgarra *et al.*, 2004). It has been also reported that the mouse embryos could be aborted *hmga* mutants (Bianchi and Agresti, 2005). Several lines of evidence suggest that the HMGA protein plays an important in DNA repair. Moreover, HMGA can also participate in controlling P53 in facilitating programmed cell death (apoptosis) (Fusco and Fedele, 2007).

Other studies have shown that HMGA also plays a vital role in controlling the cyclin dependant kinase 2 which regulates DSB repair machinery (Fusco and Fedele, 2007). For crossovers to take place there are several proteins that are extremely important during homologous recombination. These proteins can participate in recombination processes and thus in chiasma formation during meiosis. Therefore, HMGA proteins are very important for different nuclear processes such as DNA modulation, chromatin compaction, DNA repair and regulation of gene expression. Our results have showed that some of these HMGA proteins in *Arabidopsis* seem to have an important role in plant fertility.

HMGB proteins are another family of HMG proteins which carry an HMG-box motif with a high affinity to attach to the DNA. In mammals, four HMGB isoforms have been identified (HMGB1-4) which are very abundant and have been described as chromatin chaperones (Stros, 2010). Different functions have been found for HMGBs in mammalian and plant species. HMGB proteins are involved in transcription regulation, DNA replication,

DNA recombination and DNA repair (Schrumpfova *et al.* , 2011; Stros, 2010). HMGBs also have a role in modulating chromatin structure when they attach to the nucleosomes and change the chromatin organization.

In yeast, HMGB proteins expression is regulated by the *NHP6A/B* genes. Knockout of any one of these genes did not show any abnormal phenotype. Nevertheless, a double knockout for both genes showed different morphological defects. However, a null mutant for mouse *HMGB1* gene showed different pleiotropic defects as well as a short live span (Pedersen *et al.*, 2010).

HMGB proteins have been reported to have a role in H1 displacement which could participate in nucleosome remodelling and facilitate the nucleosomal DNA to be accessible to different transcription factors (Stros, 2010). In plants, HMGB1 plays a role in the maintenance of the length of telomeres. However, in mouse *hmgbl* mutant did not show this defect in chromosome telomeres. On other hand, losing *AtHMGB1* gene in *Arabidopsis* did not show any abnormalities in chromatin structure (Schrumpfova *et al.*, 2011).

Arabidopsis AtHMGB2/3 proteins are abundantly expressed and localised in the nucleus and cytoplasm of the cell. Whereas AtHMGB1/5 are located entirely in the nucleus which reflects the possibility of having a main role in chromatin modelling (Pedersen *et al.*, 2010). In this study, we have analysed some mutants for several of these *AtHMGB* genes showing a significant role in plant fertility.

4.3.2 AtSSRP1 role in microtubule and spindle stability and organization is important for accurate chromosome segregation

In mice, the knockout mutant for *SSRP1* gene is lethal and in humans, hSSRP1 protein seems to increase in cancerous tissues (Zeng *et al.*, 2010). Consequently, it has been suggested that this protein might play a basic role in cell cycle maturation. Knockdown mutants for *hSSRP1* have been constructed using siRNA in HeLa cells. These have shown deficiencies at mitotic progression including impaired and delayed chromosome movements, deficiency of chromosome alignments (as a result of inaccurate chromosome orientations by spindles) and therefore led to chromosome missegregation (Zeng *et al.*, 2010).

These observations indicate that SSRP1 protein might have a novel function in cell division and maturation during embryogenesis (Cao *et al.*, 2003). At interphase, SSRP1 plays a role in regulating transcription and DNA replication in the presence of another protein called SPT16 (Orphanides *et al.*, 1999). The proteins, SSRP1 and SPT16 form a heterodimer that is part of the FACT complex. However, SSRP1 seems to act independently of SPT16 in mitosis as it associates with microtubules (Skop *et al.*, 2004).

AtPS1 (*Arabidopsis thaliana* Parallel Spindle 1) gene is found to be highly conserved in higher plants (d'Erfurth *et al.*, 2008). When *Atps1* is mutated, missegregation of chromosomes occurs in meiosis II. 2N chromosomes have been observed in the male gametes which would lead to triploid plants in the subsequently generations. These abnormalities occur as a result of deficiency in spindle function, thus there is a failure of proper orientation of the chromosomes at meiosis II (d'Erfurth *et al.*, 2008).

In our study, chromosome missegregation occurred in *Atssrp1* during meiosis with serious consequences in the plant fertility. According to (Chan *et al.*, 2012), two main domains can be categorized in the centromere. The first domain is the histone H3 variant known as CENP-

A in humans or CENH3 in plants, which is a fundamental for kinetochore development. The second domain is the pericentric heterochromatin that is important for sister chromatid cohesion. Surprisingly, it has been found that the FACT complex might play a role in facilitating the deposition of CENP-A at the centromere in both human and mouse (Chan *et al.*, 2012). Thus, AtSSRP1 might also be necessary for the correct centromere formation in plant chromosomes. Nevertheless, our immunolocalisation results did not show any AtSSRP1 signal on centromeres to corroborate this hypothesis.

The heterodimer SSRP1/SPT16 forms the FACT complex and orthologues have been found in *Arabidopsis*, humans and *Drosophila* (Ikeda *et al.*, 2011). This complex has been described as a histone chaperone that is involved in histone displacements and histone modifications. It has been found that the complex plays a crucial role in remodelling the chromatin architecture, which might be necessary for DNA repair, centromere condensation and H2A-H2B displacements (Ikeda *et al.*, 2011, Tan *et al.*, 2006). As mentioned before, H2AX is a histone H2A variant that is rapidly phosphorylated at its C-terminal (S139) around a DSB. H2AX seems to be crucial for the DSB processing and repair (Hio *et al.*, 2008; Tan *et al.*, 2006). Interestingly, the FACT complex acts as a facilitator for the H2AX to reassemble or be removed from the nucleosomes (Hio *et al.*, 2008, Tan *et al.*, 2006). We identified some chromosome fragmentation as early as zygotene/pachytene but the number of fragments was very limited (maximum one per cell) as well as the number of cells with fragments (15% of cells). Meiotic recombination is initiated by the formation of DSBs catalysed by SPO11, in *Arabidopsis* around of 100-200 DSBs are formed, so if the FACT complex has a very important role in their process we should have expected to find more chromosome fragmentation in *Atssrp1* mutant. Furthermore, immunolocalisation of AtASY1 and AtZYP1 proteins showed complete synapsis in the mutant. Also, the chiasma frequency observed in

the mutant was identical to the observed in the wild-type. Thus, AtSPO11.1/2 catalysed DSBs are correctly processed through meiotic homologous recombination in *Atssrp1*.

Both mitosis and meiosis need the activity of Cyclin-Dependent Kinases (CDKs) which are important for the progression of these cell divisions (Bulankova *et al.*, 2010). CDKs are managed by a complicated complex of proteins organized throughout the cell cycle and divisions that participate in the inhibition or activation of CDKs (Bulankova *et al.*, 2010). Higher eukaryotic organisms require the activity of Cyclin A and B subunits. Some CDKs are highly abundant at metaphase after the attachment of the spindle to chromosome centromeres. During this period, the activation of the anaphase promoting complex (APC/C) takes place mediated by different CDKs. This complex plays a key role in the separation of the sister chromatids through the breakage of the Securin which it is initiated by a Separase activity that cleaves the cohesin complex. Moreover, the APC participates in the degradation of cyclins causing a decrease in CDK activity (reduction of CDK is essential for chromosome decondensation, DNA replication and transcription) (Bulankova *et al.*, 2010).

Several cyclin proteins act as regulatory partners with CDKs. TAM (Tardy Asynchronous Meiosis), TDM (Three-Division Mutation), OSD1 (Omission of Second Division) and SMG7 (Suppressor with Morphogenetic Effect on Genitalia7) have been discovered to play an important role in cell cycle progression and cell division transitions. *Arabidopsis* TAM (CYCA1, 2) and OSD1 are important for the transition of cells from meiosis I into meiosis II. Mutants of these genes cannot proceed to meiosis II, thus, two diploid gametes are formed instead of four gametes (Bulankova *et al.*, 2010; Cromer *et al.*, 2012).

It has been reported that SSRP1 is an essential protein for MT growth at prophase when MTs are polymerizing from polar centrosomes. In addition, SSRP1 found cross-link MTs keeping them organized in bundles.

It has been also reported that SSRP1 and SPT16 are working together as a heterodimer in the FACT complex in higher eukaryotes including budding yeast and mammals (Wittmeyer *et al.* 1999; Formosa *et al.* 2001). In budding yeast, SPT16 and POB3 proteins associate to the DNA polymerase (POL1). POB3 protein in budding yeast is an orthologue for mammalian SSRP1 (Wittmeyer and Formosa 1997). Nevertheless, it does not contain a DNA binding motif. POB3 associates with another chromatin component NHP6 which is an HMGA protein with a DNA binding motif (Formosa, *et al.* 2001). Thus, POB3 and NHP6 proteins may function in a similar manner to the mammalian SSRP1 protein (Brewster *et al.*, 2001).

SSRP1 in mouse have been reported to be essential for microtubule polymerization, spindle organization and stability. Furthermore, mouse SSRP1 has been found to co-localize along the whole length of microtubules (Zeng *et al.*, 2010). Nevertheless, in this study, AtSSRP1 did not localise along the microtubules but around the same region where microtubules are polymerizing in the mitotic and meiotic spindle. Furthermore, during meiosis AtSSRP1 localization on the microtubule organization regions appeared very early in prophase I and it remained throughout meiotic stages until late telophase II (**Table 6**). Interestingly, AtSPT16 localization on the same region was delayed up to late diakinesis and stayed on the meiotic microtubules up to middle telophase II re-localising into the nucleus before AtSSRP1 (**Table 6**). Both AtSSRP1 and AtSPT16 colocalised in the nucleus of late telophase II and young pollen grains (male gametes).

	P I	M I	A I	T I	P II	M II	A II	T II	Pollen
AtSPT16	■	■	■	■	■	■	■	■	■
AtSSRP1	■	■	■	■	■	■	■	■	■

Table 6. Localization of AtSPT16 and AtSSRP1 during the *Arabidopsis* meiotic process.

AtSPT16 localises on the nuclear chromatin (light blue) in early prophase I. At diakinesis, it starts to localise on the cytoplasm on microtubules (green). At metaphase I the AtSPT16 signal co-localises with the microtubule spindle. At second division the signal co-localises with microtubules until early telophase II when the signal reorganises inside the nucleus and stays during the pollen grain further development. AtSSRP1 localises with microtubules (green) throughout the meiotic process until late telophase II when re-localises inside the nucleus and stays there during the pollen grain maturation. P I; prophase I. M I; metaphase I. A I; anaphase I. T I; telophase I. P II; prophase II. M II; metaphase II. A II; anaphase II. T II; telophase II.

4.4 Kinesin AtK1 might have also an important role in accurate organization of the *Arabidopsis* spindle in mitosis and meiosis

Kinesins are a family of motor proteins which are crucial for microtubule organization (Chen *et al.*, 2002). Several kinesin proteins have been isolated and studied intensively in different organisms (Chen *et al.*, 2002). The distinct function that has been found for the kinesins is the production of forces over microtubules as a result of hydrolysing ATP (Chen *et al.*, 2002). Studies have showed that a number of kinesins have been found to play a basic function in meiosis and mitosis (Mountain and Compton, 2000). AtK1 is an *Arabidopsis* Kinesin which has an important role in microtubule movement. AtK1 contains a distinct C-terminal domain as other kinesin proteins and it seems to be also conserved in *Drosophila* and budding yeast. Non Claret Disjunctal (NCD) protein in *Drosophila* and KAR3 protein in budding yeast are kinesins involved in the assembly and managing of the structure of spindles in both mitosis and meiosis. Furthermore, in other organisms this type of kinesin is important also for the spindle assembly and their function for accurate chromosome segregation (Chen *et al.*, 2002).

In *Arabidopsis*, AtK1 is a Kinesin which plays a role in the maturation of chromosome segregation. In an *atk1* mutant, spindles failed in establishing a bipolar structure and

chromosomes failed to align at the metaphase plate leading to chromosome missegregation at anaphase (Chen *et al.*, 2002). *Drosophila ncd* mutant showed similar abnormalities to that observed in *atkl* in *Arabidopsis*, with abnormal spindle formation and inaccurate chromosome segregation. However in budding yeast *kar3* mutant spindle monopolar formation (instead of bipolar) was observed that may occur as a result of a defect in microtubule spindle assembly. Furthermore, *kar3* mutant has shown defects in chromosomes synapsis during prophase I and reduction of recombination frequency that shows that KAR3 might have more important roles (Chen *et al.*, 2002).

Interestingly, the meiotic phenotype of *Atkl* mutant is very similar to that observed in *Atssrp1* mutant. Chromosome missegregation was observed at anaphase I and at anaphase II in both mutants in *Arabidopsis*. Nevertheless, in *Atkl* mutant, no chromosome fragmentation was observed in early prophase I stages in contrast to the *Atssrp1* mutant. AtK1 kinase could be involved in a similar pathway to AtSSRP1 in order to ensure an accurate organization of microtubules in the spindle to secure correct chromosome segregation.

In conclusion, *Arabidopsis* HMG proteins seem to have an important role in ensuring plant fertility. One of these HMG proteins, AtSSRP1 might be involved in the FACT complex together with AtSPT16 in the chromatin to help in some instances to repair DSBs and possibly in gene transcription. Some fragmentation has been observed in *Atssrp1* mitotic and meiotic cells. Nevertheless, AtSSRP1 has a key role in ensuring correct microtubule organization in the mitotic and meiotic spindle. In the absence of AtSSRP1, the mitotic and meiotic spindles seem to contain less microtubules and their organization is not as tight as in the wild-type. *Atkl* kinase mutant showed a very similar meiotic phenotype to that observed in *Atssrp1*. Both mutants showed missegregation of chromosomes during first and second meiotic anaphases. This could suggest that both AtSSRP1 and AtK1 proteins are involved in the same pathway to achieve a correct microtubule spindle organization in *Arabidopsis*.

Nevertheless, the *Atk1* mutant did not show any fragmentation what shows that AtSSRP1 seems to keep a chromatin functionality perhaps together with AtSPT16 forming the FACT complex.

CHAPTER FIVE

Characterisation of human *hSSRP1* gene function

5.1 INTRODUCTION

In the previous chapter, we have seen how Arabidopsis SSRP1 protein is very important for MT organization during mitotic and meiotic divisions. SSRP1 and its role in the FACT complex has been broadly studied in different higher eukaryotes including mammals. Nevertheless, very little has been reported about SSRP1 role in MT organization and chromosome segregation. SSRP1 protein sequence is evolutionary conserved among higher eukaryotes including plants and humans. In order to analyse if this functional role of SSRP1 in plants is also conserved in humans, we decided to initiate collaboration with Mr. Klarke Sample and Professor Roy Bicknell (School of Immunity and Infection, University of Birmingham). They used cell cultures from different human tissues obtained from the Birmingham Women's Hospital: Human Umbilical Vein Endothelium Cells (HUVECs) and fibroblast cells.

Structure Specific Recognition Protein 1 (SSRP1) is a chromatin component belonging to the HMG protein family (Zeng *et al.*, 2010). This protein has different roles in several crucial different biological processes such as DNA repair, regulation of the transcription machinery as well as tubulin maintenance and organization as the protein contains a tubulin binding site (Kumari *et al.*, 2009; Zeng *et al.*, 2010).

SSRP1 protein also contains a specific domain that can bind to another partner protein called SPT16. The heterodimer association of these proteins forms the FACT (Facilitates Chromatin Transcription) complex. Human hFACT complex has been involved in several functions like cell division maturation and assembly and disassembly of histones during cell division (Kumari *et al.*, 2009, Zeng *et al.*, 2010).

SSRP1 protein has been found to be an essential nuclear protein to manage and regulate microtubule polymerization and therefore to participate in chromosomal movements

(Winkler *et al.*, 2011; Zeng *et al.*, 2010). Depletion of this protein affects spindle formation, structure organization and movement (Zeng *et al.*, 2010).

5.2 RESULTS

5.2.1 *In silico* analysis of SSRP1 protein in different species

The *Arabidopsis* AtSSRP1 amino acid sequence was used to identify homologues in other species using the Basic Local Alignment Search (BLAST) tool from NCBI and TAIR. *Arabidopsis thaliana* (*At*) (646 aa), *Drosophila melanogaster* (*Dm*) (723 aa), Human (709 aa), Mouse (708 aa) and Rat (709 aa) SSRP1 homologues were compared using the Multiple sequence alignment sequence tool (NCBI).

The conserved amino acids have been highlighted in red colour, amino residues with some similarity have been highlighted in blue (**Figure 41**). SSRP1 sequences in the mammalian species are highly conserved (99% identical). However, *Arabidopsis* AtSSRP1 sequence has only a 35% identical amino acid sequence with the human (**Figure 41**).

At 1 MADGHSFNNISLSGRGKPNGLLKINSGGIQWKQGGGKAVEVDRSDIVSVSWTKVTKSNQLGVKTKDGLYYKFVGFRRDQ 80
Dm 1 -----RLKMTQNIIFKNKTGKVEQISAEIDLINSQRFVGTWGLRVFTKGGVLRHFTGFRDS 59
Human 1 MAETLEFNDVYQEVKGSMDGRLRLSRQGIIFKNKSTGKVDNIQAGELTEGIWRRVALGHGLKLLTKNGHVYKYDGFRES 80
Mouse 1 MAETLEFNDFQEVKGSMDGRLRLSRQGIIFKNKSTGKVDNIQAGELTEGIWRRVALGHGLKLLTKNGHVYKYDGFRES 80
Rat 1 MAETLEFNDFQEVKGSMDGRLRLSRQGIIFKNKSTGKVDNIQAGELTEGIWRRVALGHGLKLLTKNGHVYKYDGFRES 80

81 DVPSLSSFFQSSYGKTPDEKQLSVSGRNWGEVDLHGNTLTLFLVGSKQAFEVSLADVSQTqLQGKNDVTLEFHVDDTAGA 163
60 EHEKLGKFIKAACSQEMVEKEMCVKGNWGTARFMGSVLSFDKESKTI FEVPLSHVSQC-VTGKNEVTLEFHQNDDAPV 137
81 EFEKLSDFFKTHYRLELMEKDLCVKGNWGTVKFGQLLSFDIGDQPVFEIPLSNVVSQC-TTGKNEVTLEFHQNDDAEV 158
81 EFEKLSDFFKTHYRLELMEKDLCVKGNWGTVKFGQLLSFDIGDQPVFEIPLSNVVSQC-TTGKNEVTLEFHQNDDAEV 158
81 EFEKLSDFFKTHYRLELMEKDLCVKGNWGTVKFGQLLSFDIGDQPVFEIPLSNVVSQC-TTGKNEVTLEFHQNDDAEV 158

164 SLMEISFHIPNSN[5]DENRPPSQVFNDTIVAMADVSPGVEDAVVTFESIAILTPRGRYNVELHLSFLRLQGQANDFKIQ 245
138 GLELMRFHIPAVE SAEEDPVDKFHONVMSKASVISASGESIAIFREIQILTPRGRYDIKIFSTFFQLHGKTFDYKIP 214
159 SLMEVRFYVPTQ EDGVDPVEAFAQNVLKADVIQATGDAICIFRELOCLTPRGRYDIRIYPTFLHLHGKTFDYKIP 235
159 SLMEVRFYVPTQ EDGVDPVEAFAQNVLKADVIQATGDAICIFRELOCLTPRGRYDIRIYPTFLHLHGKTFDYKIP 235
159 SLMEVRFYVPTQ EDGVDPVEAFAQNVLKADVIQATGDAICIFRELOCLTPRGRYDIRIYPTFLHLHGKTFDYKIP 235

246 YSSVVRFLFLPKSNOPHTFVVISLDPPIKQGOTMYPHIVMOPETDTVVESELISIDELMNTKFKDKLERSYKGLIHEVFT 325
215 MDSVLRFLFMLPHKDSROMFFVLSLDPPIKQGOTRYHYLVXLFAPDEETTIELPFSEALRDKYEGKLEKISGPVYEVMG 294
236 YTTVLRFLFLPHKQDOROMFFVVISLDPPIKQGOTRYHFLILLFSKDEDISLTLNMNEEEVEKRFEGRLTKNMSGSLYEMVS 315
236 YTTVLRFLFLPHKQDOROMFFVVISLDPPIKQGOTRYHFLILLFSKDEDISLTLNMNEEEVEKRFEGRLTKNMSGSLYEMVS 315
236 YTTVLRFLFLPHKQDOROMFFVVISLDPPIKQGOTRYHFLILLFSKDEDISLTLNMNEEEVEKRFEGRLTKNMSGSLYEMVS 315

326 TVLRWLSGAKITKPGKFRSSQDGFVAVKSLKAEDGVLYPLEKGFFFLPKPPTLILHDEIDYVEFERhaaGGANMHYFDLL 405
295 KVMKVLIGRKITGPGNFIGHSGTAAVGC SFKAAAGYLYPLERGFIIYHKPPLHIRFEEISSVNFAR---SGGSTRSFDPE 371
316 RVMKALVNRKITVPGNFQGHSGAQICITCSYKASSGLLYPLERGFIVHKPPVHIRFDEISFVNFAR---GTTTTRSFDPE 392
316 RVMKALVNRKITVPGNFQGHSGAQICITCSYKASSGLLYPLERGFIVHKPPVHIRFDEISFVNFAR---GTTTTRSFDPE 392
316 RVMKALVNRKITVPGNFQGHSGAQICITCSYKASSGLLYPLERGFIVHKPPVHIRFDEISFVNFAR---GTTTTRSFDPE 392
316 RVMKALVNRKITVPGNFQGHSGAQICITCSYKASSGLLYPLERGFIVHKPPVHIRFDEISFVNFAR---GTTTTRSFDPE 392

406 IRLKTDEHELFRNIQRNEYHNLTYFISSEKGLKIMNLGGAGTADGVAALVGDNDdDDAVDPHLTRIRNQA----- 475
372 VTLKNGTVHIFSSIEKEEYAKLFDYITQKHLVSNMG-KDKSGYKVDVDFGSDnENEPPDAYLARIKAEAREKEEDDDDDGD 450
393 IETKQGTQYTFSSIEREEYGKLFDFVNAKLNINRGLKEGMNPSYDEYADSD-EDQHDAYLERMKEEGKIREENANDSS 471
393 IETKQGTQYTFSSIEREEYGKLFDFVNAKLNINRGLKEGINPGYDDYADSD-EDQHDAYLERMKEEGKIREENANDSS 471
393 IETKQGTQYTFSSIEREEYGKLFDFVNAKLNINRGLKEGINPGYDDYADSD-EDQHDAYLERMKEEGKIREENANDSS 471

476 -DESDEFEDEFVMGEDDDGGSPTDSDGGddSDASEGGVGEIKEKSIKKEPKKEASSSKGLPPKRTVAA[10]KKKKDPN 560
451 SDEGS-TDEDFKPNENESDVAAEYDSNV--ESDS---DDSDASGGGGD----- 493
472 DDSGEETDESFNPGEEEEEDVAEEFDSNA--SASSSSNEGSDRDEKRRKQLKAKMAKDRKSRKPPVEV KKGKDPN 545
472 DDSGEETDESFNPGEEEEEDVAEEFDSNA--SASSSSNEGSDRDEKRRKQLKAKMAKDRKSRKPSSEA KKGKDPN 545
472 DDSGEETDESFNPGEEEEEDVAEEFDSNA--SASSSSNEGSDRDEKRRKQLKAKMAKDRKSRKSSSE KKGKDPN 545

561 APKRAMSGFMFFSQMERDNIKKEHPGIAFGVEGVKVLGDKWRQMSADKPEYAKAQVDKQRYKDEISDYKNPQ----- 633

546 APKRPMASAYMLWLNASREKIKSDHPGISITDLSKKAGEIWKGMSKEKKEEWRKAEDARRDYEKAMKEYEGGRGESSKRD 625
546 APKRPMASAYMLWLNASREKIKSDHPGISITDLSKKAGEIWKGMSKEKKEEWRKAEDARRDYEKAMKEYEGGRGESSKRD 625
546 APKRPMASAYMLWLNASREKIKSDHPGISITDLSKKAGEIWKGMSKEKKEEWRKAEDARRDYEKAMKEYEGGRGESSKRD 625

634 -----PMNVDSGN 641

626 KSKKKKKVKVMEKSTPSRGSSSKSSSRQLSESFKSKEFVSSDESSSGENKSKKKRRRSEDSseEEELASTPPSSSEDAS 705
626 KSKKKKKVKAKMEKSTPSRGSSSKSSSRQLSDSFKSKEFVSSDESSSGENKSKKKRRRSEDS-EEELASTPPSSSEDAS 704
626 KSKKKKKVKAKLEKSTPSRGSSSKSSSRQLSDSFKSKEFVSSDESSSGENKSKKKRRRSEDSdEEELASTPPSSSEDAS 705

642 DSDSn 646

706 GSDE- 709
705 GSDE- 708
706 GSDE- 709

Figure 41. Multiple amino acid sequence alignment of SSRP1 homologues in *Arabidopsis*, *Drosophila* and other mammalian species (human, mouse and rat).

SSRP1 protein sequences of *Arabidopsis thaliana* (*At* - 646 aa), *Drosophila melanogaster* (*Dm* - 723 aa), Human (709 aa), Mouse (708 aa) and Rat (709 aa) were aligned using the multiple sequence alignment tool at NCBI. Identical amino acid residues have been highlighted in red and similar amino acid residues in blue.

5.2.2 hSSRP1 and hSPT16 localisation in different human somatic cells

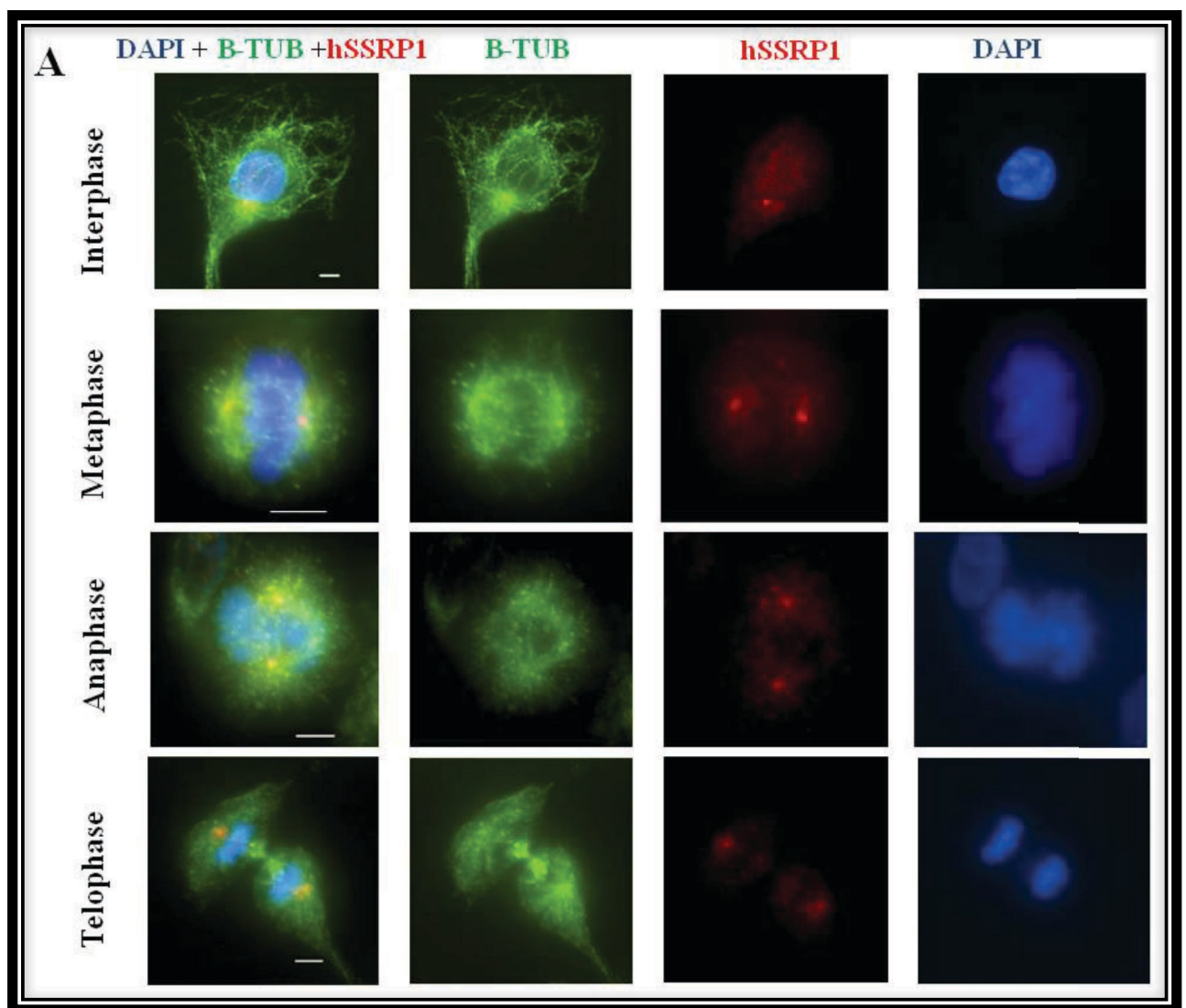
In order to identify the functions of human hSSRP1 protein we used immunolocalisation studies to localise the presence of this protein in different human cell types. Two different anti-hSSRP1 antibodies were used in these experiments. A mouse monoclonal anti-hSSRP1 antibody (Santa Cruz Biotechnologies ^{INC.} SC-74536) and a rabbit polyclonal anti-hSSRP1 antibody (SC-25382) were both raised against the N-terminal 1-300 amino acids of human hSSRP1. We also used a rabbit polyclonal anti-hSPT16 antibody (SC-28734) raised against a C-terminal peptide (748-1,047 amino acids) of human hSPT16 protein.

Furthermore, to identify the microtubules we used another two different beta-tubulin antibodies. A goat polyclonal anti-beta-tubulin antibody (SC-12841) and a mouse monoclonal anti-beta-tubulin antibody (SC-166729) were both raised against a C-terminal amino acid peptide from *Arabidopsis* At β -TUB4.

5.2.2.1 hSSRP1 localisation in human endothelium cells

Dual immunolocalisation for hSSRP1 and beta-tubulin was conducted in human endothelium cells (**Figure 42A**). Human hSSRP1 protein appears as discrete small foci on the nuclear chromatin and at a specific site at the cytoplasm close to the nuclear membrane (**Figure 42A**). At mitotic metaphase, two distinct signals were observed in the Microtubule Organizer

Centres (MTOCs) of the cell (**Figure 42A**). These two main signals persisted throughout anaphase and telophase divisions around the MTOCs. Each signal would be distributed into the daughter cells after the mitotic division. After this stage, the signal would be divided to form smaller discrete foci as in the interphase cells. The localization of hSSRP1 was identical using both a mouse monoclonal and a rabbit polyclonal anti-hSSRP1 antibody (**Figure 42**). This suggests that the signal observed in these cells is highly specific. We also conducted a control of the secondary antibodies (**Figure 42C**) to confirm specificity. There was not signal in these cells indicating the primary Abs were working fine.



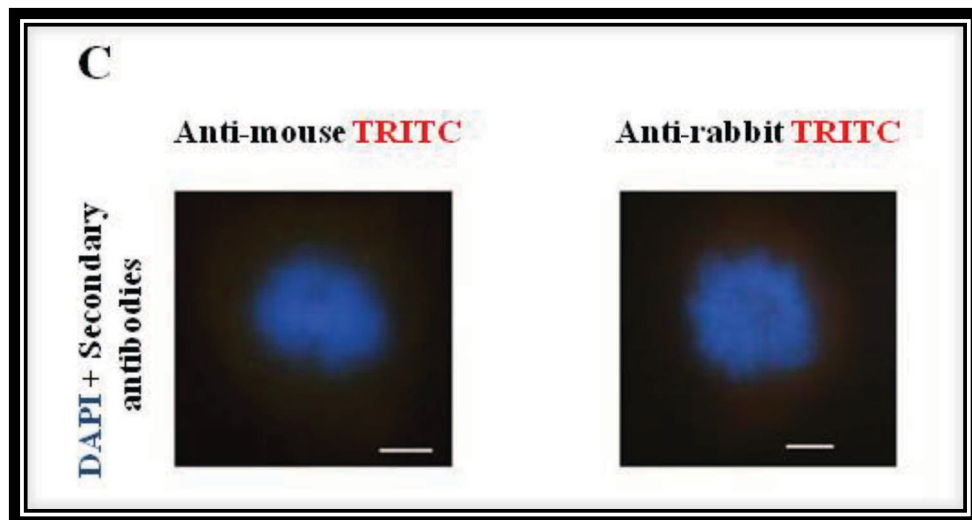
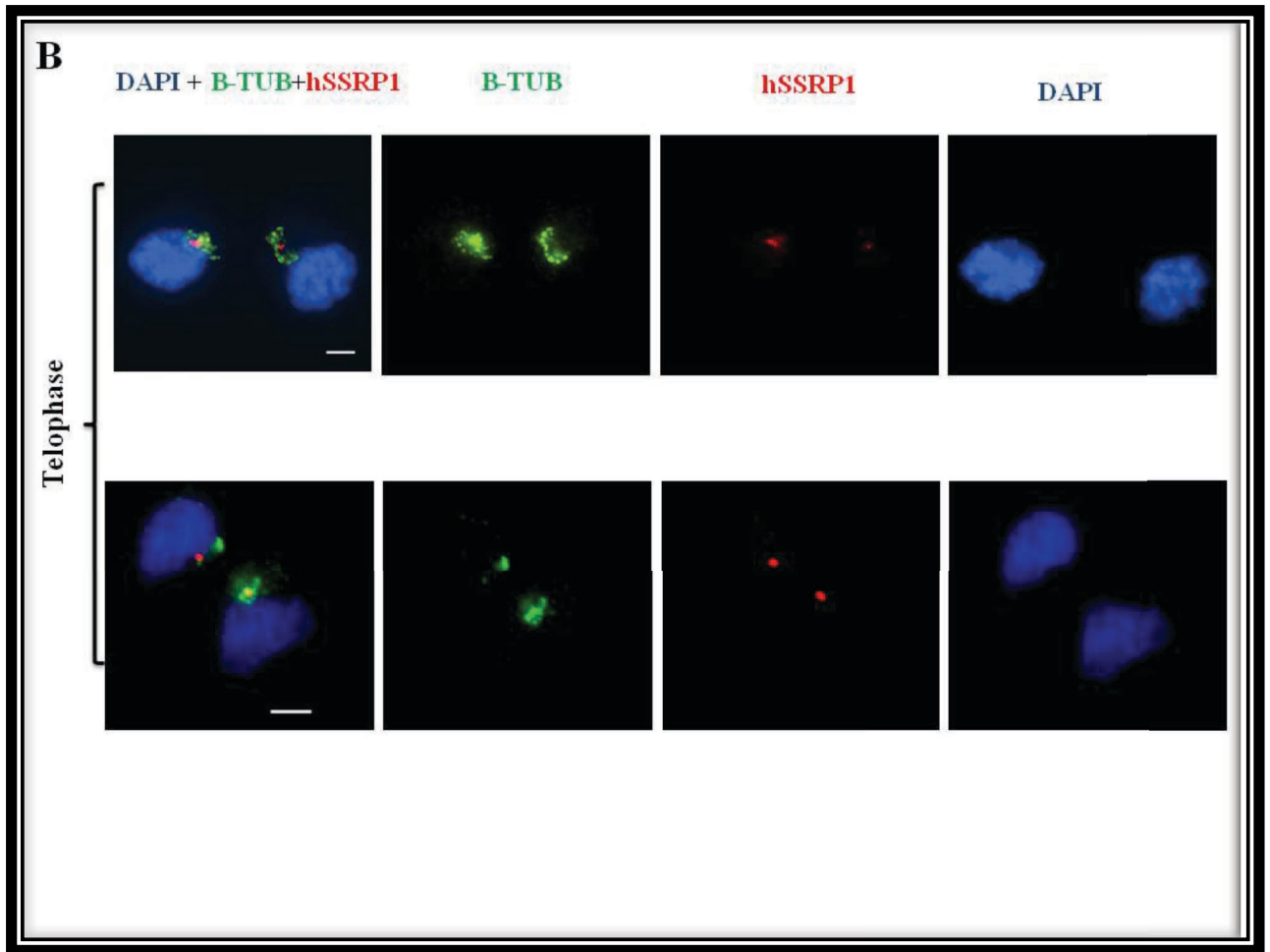


Figure 42. Dual immunolocalisation for hSSRP1 and Beta-Tubulin in Human endothelium cells.

A Immunolocalisation using a mouse monoclonal anti-hSSRP1 (red) and a goat polyclonal anti-beta-tubulin (green) antibodies. **B** Immunolocalisation using a rabbit polyclonal anti-hSSRP1 (red) and a goat polyclonal anti-beta-tubulin (green) antibodies. **C** Control immunolocalisation using the secondary antibodies anti-mouse TRITC and anti-rabbit TRITC. No signal is detected at mitotic metaphase. Scale bar =5 μ m.

Some images were obtained by a compilation of Z-stack images obtained from the same cell using the epifluorescence microscope (**Figure 43**). The maximum intensity combination of the stacks was created using NIS-Elements AR (NIKON). Three examples of these Z-stack sets are provided in **Figure 43** using the two different antibodies recognising hSSRP1 in endothelium cells. This method allows different focal planes of the cell to be obtained, production of 3-dimensional (3D) images and a high resolution maximum intensity combination of the stack. Surprisingly, each signal of hSSRP1 observed at both poles of metaphase/anaphase cells could be individualized into another two signals in the MTOCs regions (**Figure 43**). This suggests that hSSRP1 might be part of human centrioles.

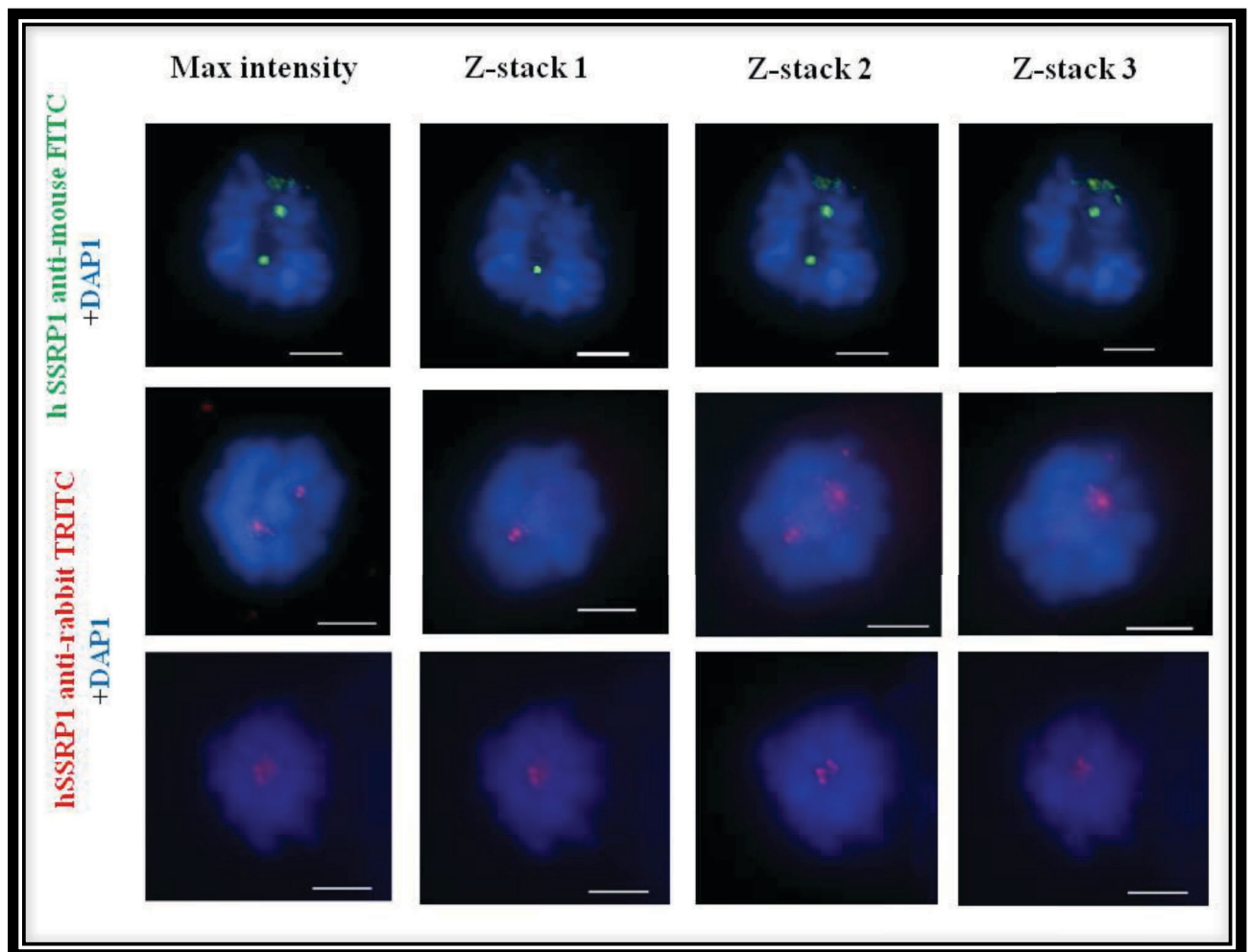


Figure 43. Immunolocalisation of hSSRP1 using a Z-stack acquisition of images for SSRP1 in endothelium cells.

Different antibodies recognising the hSSRP1 in endothelium cells (hSSRP1 anti-mouse-FITC and hSSRP1 anti-rabbit TRITC) and each signal of hSSRP1 localize on both poles of metaphase/anaphase cells. Scale bar =5 μ m.

5.2.2.2 hSSRP1 localisation in human fibroblast cells

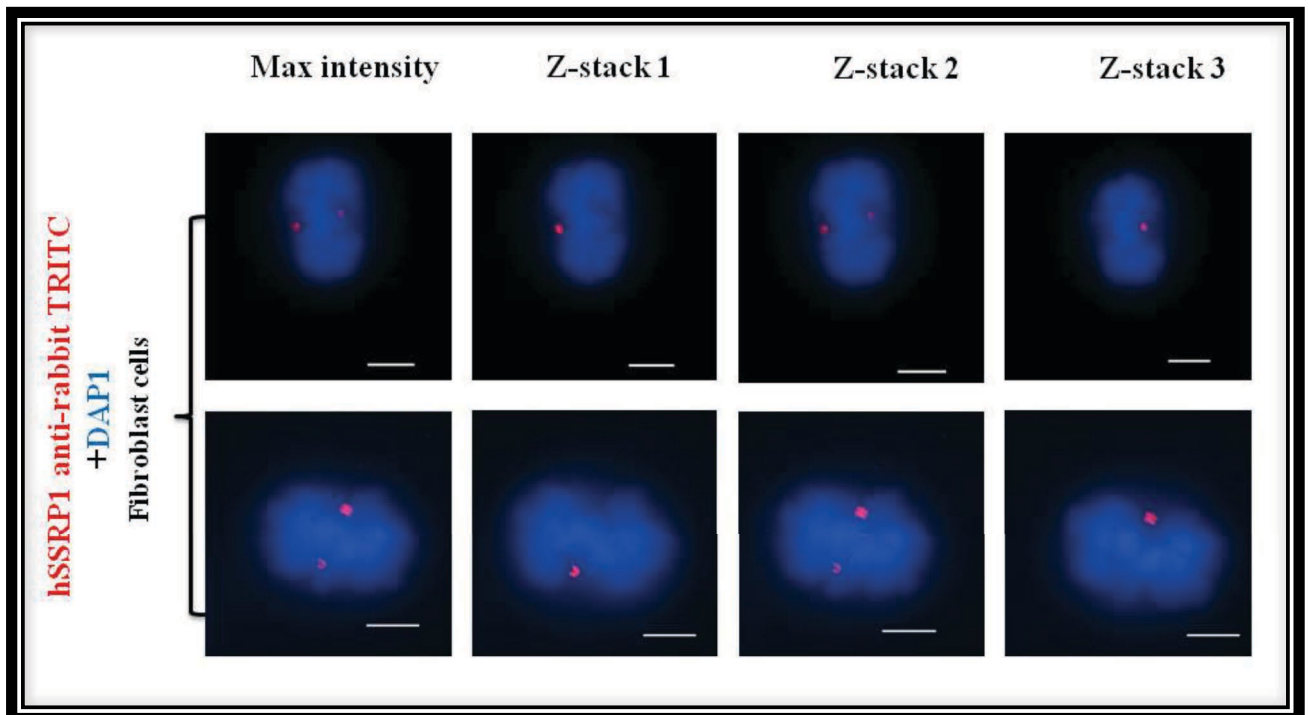


Figure 44. Immunolocalisation of hSSRP1 on human fibroblasts.

A rabbit polyclonal anti-hSSRP1 antibody was used to recognise the localisation of hSSRP1 on to structures suggesting they might be the centrioles. Scale bar =5 μ m.

5.2.2.3 hSPT16 localisation in human endothelium cells

Immunolocalisation of hSPT16 was carried out in human endothelium cells. A rabbit polyclonal anti-hSPT16 antibody and a mouse monoclonal anti-beta-tubulin antibody were used for dual immunolocalisation (**Figure 45**). At mitotic metaphase hSPT16 localises on the MTOCs as small discrete foci.

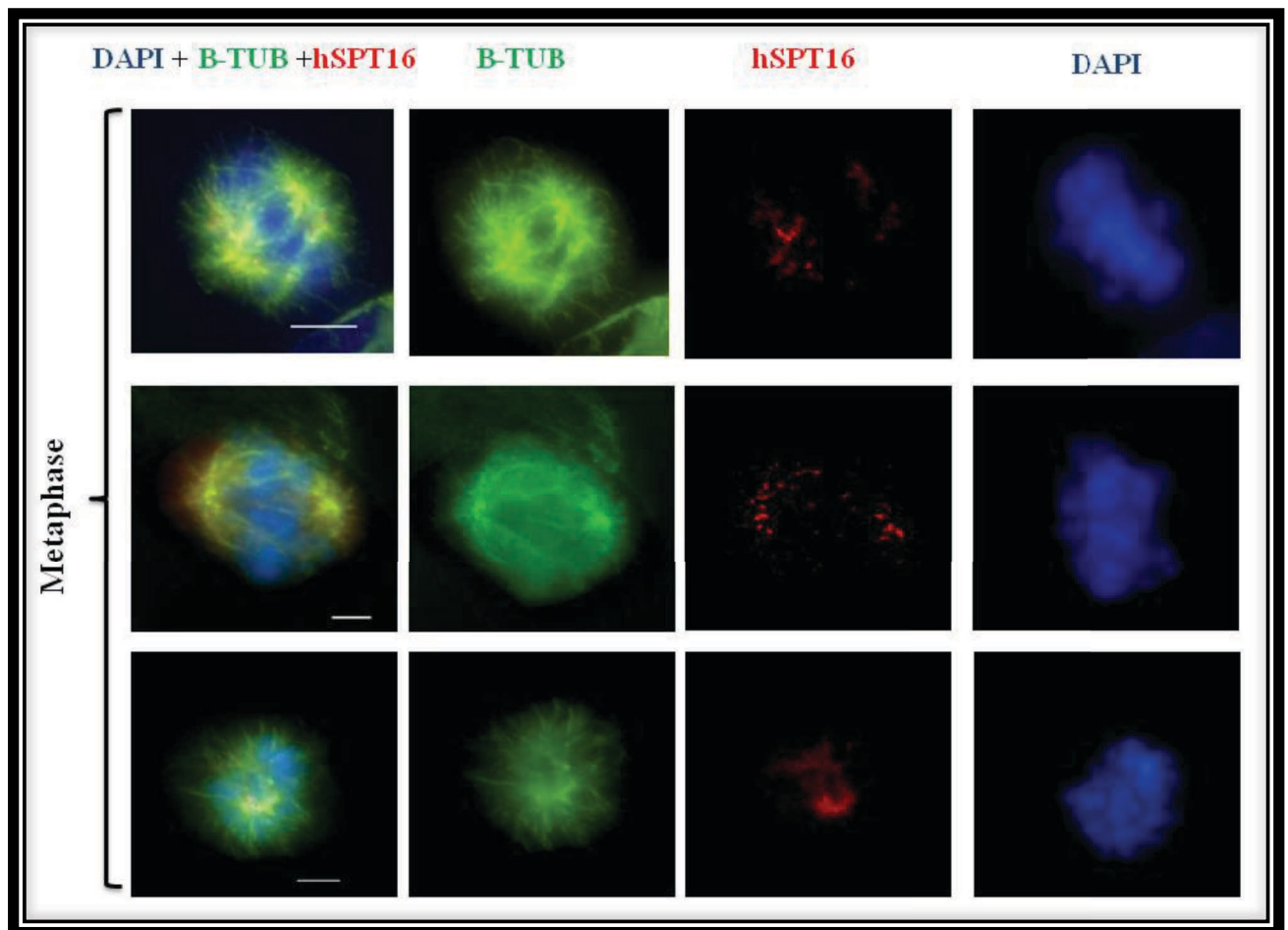


Figure 45. Dual immunolocalisation for hSPT16 and Beta-Tubulin in human endothelium cells.

Anti-hSPT16 TRITC (red) and anti-beta-tubulin FITC (green) immunolocalisation on mitotic metaphase cells. Scale bar = 5 μ m.

5.2.2.4 Co-localisation of hSSRP1 and hSPT16 in human endothelium cells

Dual immunolocalisation was conducted to study the co-localization and distribution of both hSSRP1 and hSPT16 proteins in human endothelium cells (**Figure 46**). hSSRP1 and hSPT16 localized on the MTOCs regions of the mitotic cells. Nevertheless, hSSRP1 signal recognised a specific structure on the MTOCs, the centrioles. Whereas, hSPT16 appeared as small foci around the MTOCs in the endothelium cells. Furthermore, hSPT16 signals also appeared on the nuclear chromatin.

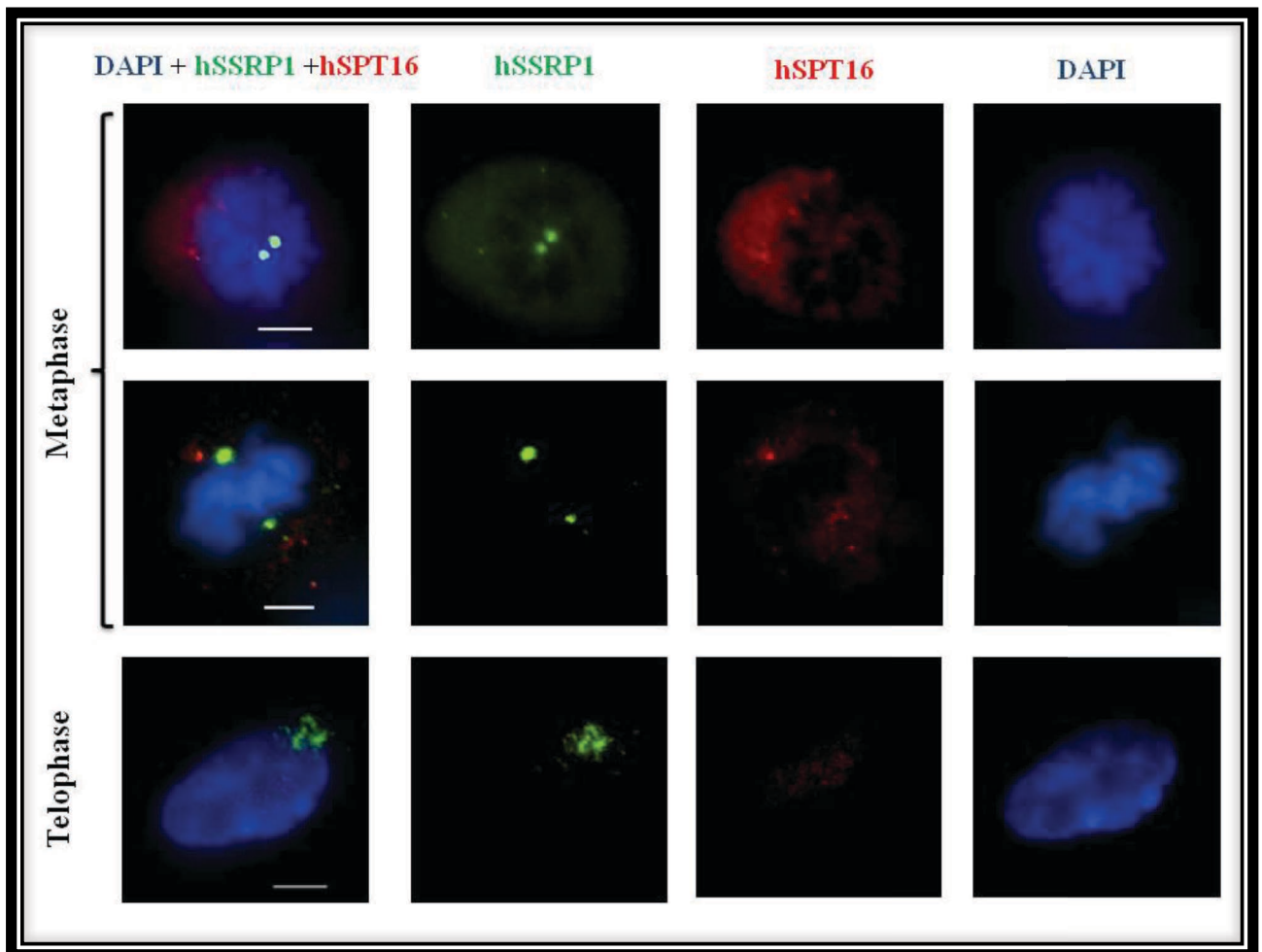


Figure 46. Immunolocalisation of hSSRP1 and hSPT16 in human endothelium cells.

A mouse monoclonal anti-hSSRP1 FITC (green) and a rabbit polyclonal anti-hSPT16 TRITC (red) antibodies were used. Scale bar =5 μ m.

5.2.3 Characterisation of siRNA *hssrp1* knockdown mutants in human endothelium cells

5.2.3.1 Design of siRNA constructs for *hSSRP1*

hSSRP1 gene is located in the “q” arm of chromosome 11 in the human genome. The gene structure consists of 15 exons and 14 introns in addition of the 3’ and 5’ UTRs. Two siRNAs were obtained from Life Technology (Invitrogen), siRNA0 and siRNA1 are targeting exon 6 and exon 3 respectively (**Figure 47**). NCBI Sequence Viewer tool has been used to produce an overview of the gene structure. The sequence for the mRNA of the gene can be found in the **Appendix D**. **Table 7** shows the different siRNA oligo sequences designed for this experiment.

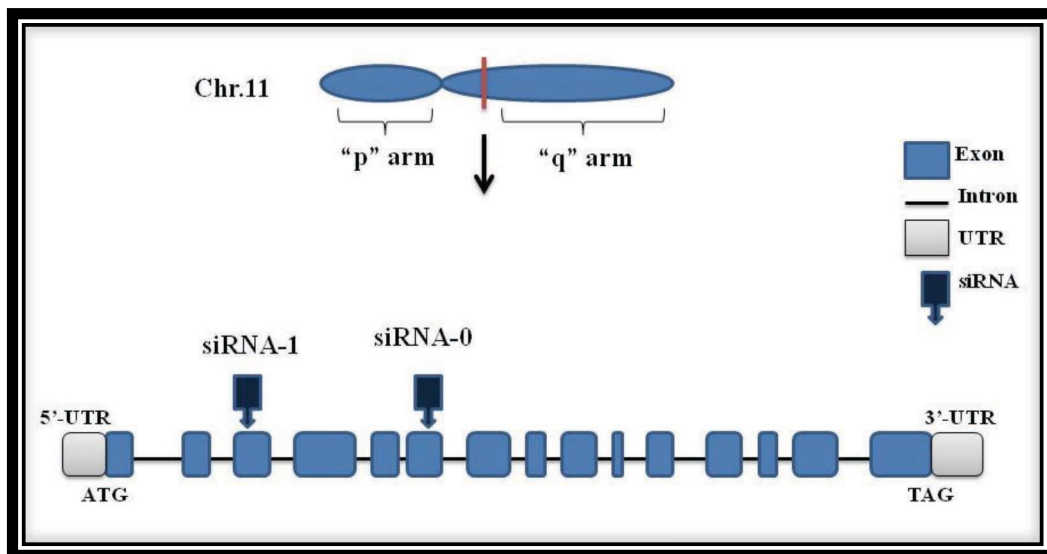


Figure 47. Schematic representation of the structure of *hSSRP1* gene and the target location for the designed siRNAs.

hSSRP1 gene includes 15 exons (blue boxes) in addition of 5’ and 3’UTRs (grey boxes). The siRNA0 and siRNA1 target regions (inverted dark blue arrow box) are located at exon 6 and exon 3, respectively.

Oligo siRNA	Duplex siRNA	Target	Duplex name
S13490 Sense GCAAGACCUUUGACUACAATT S13490 Antisense TTGTAGTCAAAGGTCTTGCCA	GCAAGACCUUUGACUACAATT ACCGUUCUGGAAACUGAUGTT	S13490 DUPLEX Targeted EXON 6	SiRNA-0
S13491 Sense GGACUAAAACUGCUUACAATT S13491 Antisense UUGUAAGCAGUUUAAGUCCAT	GGACUAAAACUGCUUACAATT TACCUGAAUUUGACGAAUGUU	S13491 DUPLEX Targeted EXON 3	SiRNA-1

Table 7. siRNA oligo sequences to target *hSSRP1*.

siRNA-0 and siRNA-1 sense and antisense oligos are indicated.

5.2.3.2 Q-PCR analysis of *hssrp1* knockdown mutant cells

The efficiency of the siRNA oligos to knockdown *hSSRP1* in Human Umbilical Vein Endothelial Cells (HUVEC) was confirmed using reverse transcriptase quantitative PCR (qPCR) (**Figure 48**). Both siRNA oligo sets, siRNA0 (D0) and siRNA1 (D1) were successful in reducing the *hSSRP1* RNA level observed in cells by about 90% compared with the control duplex (NCD). Anything above a 70% knockdown value is considered acceptable in human molecular research (Litzenburger *et al.* 2013).

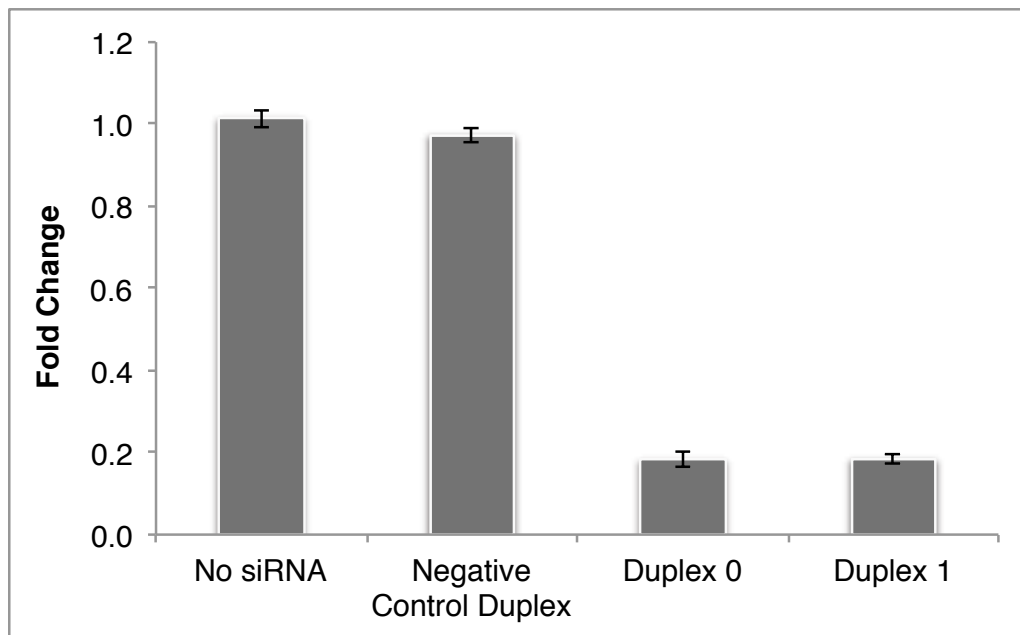


Figure 48. Relative Expression of *hSSRP1* by qPCR in HUVEC.

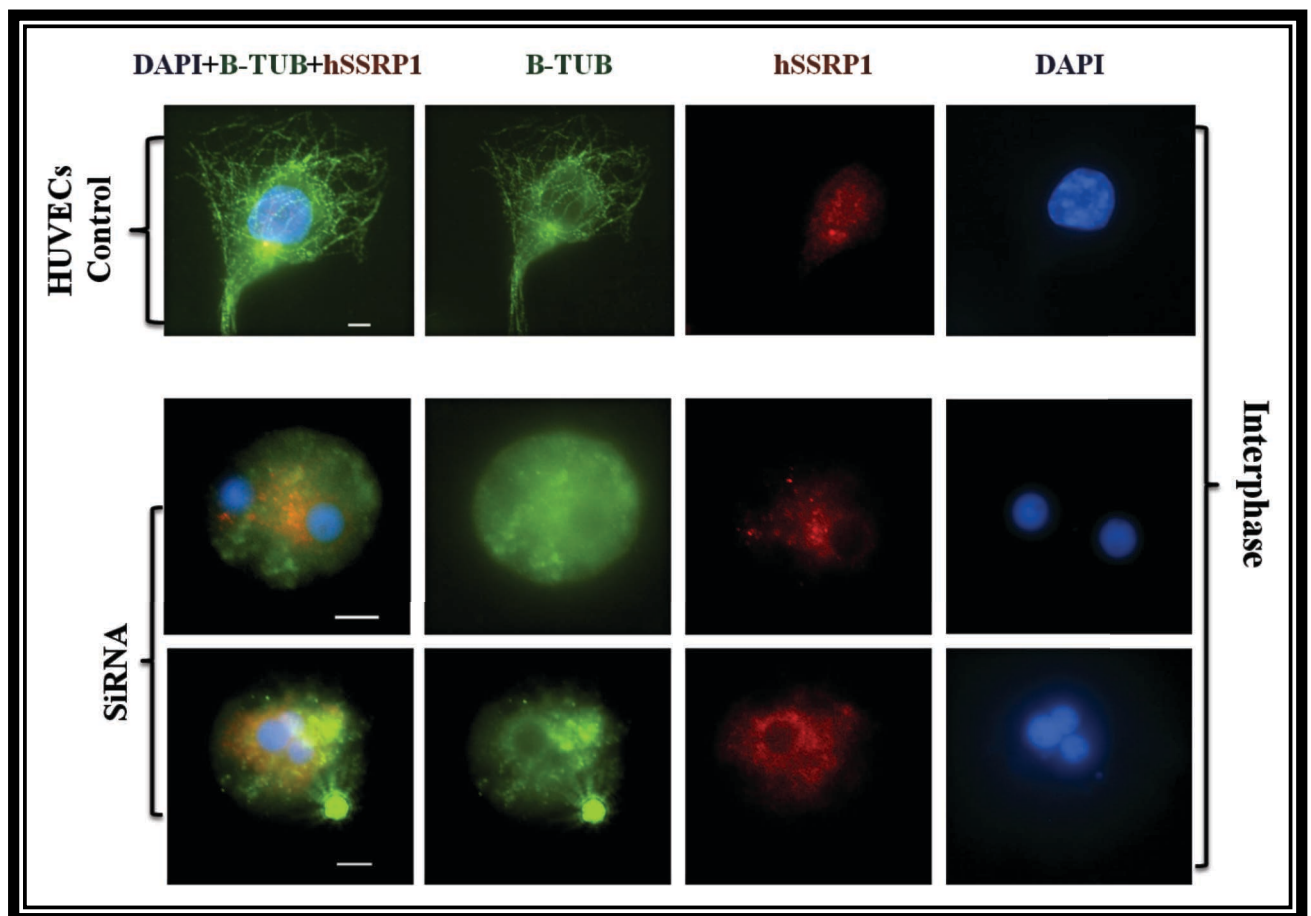
Relative expression was compared to the expression of beta-actin (*ACTB* gene). NCD; cells treated with the control duplex. D0; siRNA0. D1; siRNA1 (mean ± SEM).

5.2.3.3 Cytological analysis of *hssrp1* knockdown mutant cells

Immunofluorescence localization of hSSRP1 in HUVECs treated and untreated was carried out to validate the effect of the siRNA oligos (**Figure 49**).

Our results showed that both, siRNA0 and siRNA1, resulted in similar cytological abnormalities in HUVECs (**Figure 49**). The first observation is that both siRNAs contribute to knockdown the hSSRP1 protein level in these cells as observed by immunolocalisation of hSSRP1. The hSSRP1 signal was hugely reduced compared to the controls (**Figure 49**). This was expected from the previous Q-PCR data. We observed that the signal from microtubules (beta-tubulin) was also highly affected. Less microtubules were observed in the siRNA treated cells in both, cytoskeleton and mitotic spindle (**Figure 49**). Several multi-nucleated cells could be easily found in the knockdown cells (see interphase cells in **Figure 49**).

Furthermore, the low amount of beta-tubulin in the spindle also coincided with a poor alignment of the chromosomes at the metaphase plate probably leading to missegregation of chromosomes and formation of micronuclei (see metaphase in **Figure 49**). Cells in telophase seem to have problems in the cytokinesis (**Figure 49**) judging by the increased number of cells accumulated in this stage on the cell culture. These defects in cytokinesis of the mitotic products could explain the presence of multinuclear cells.



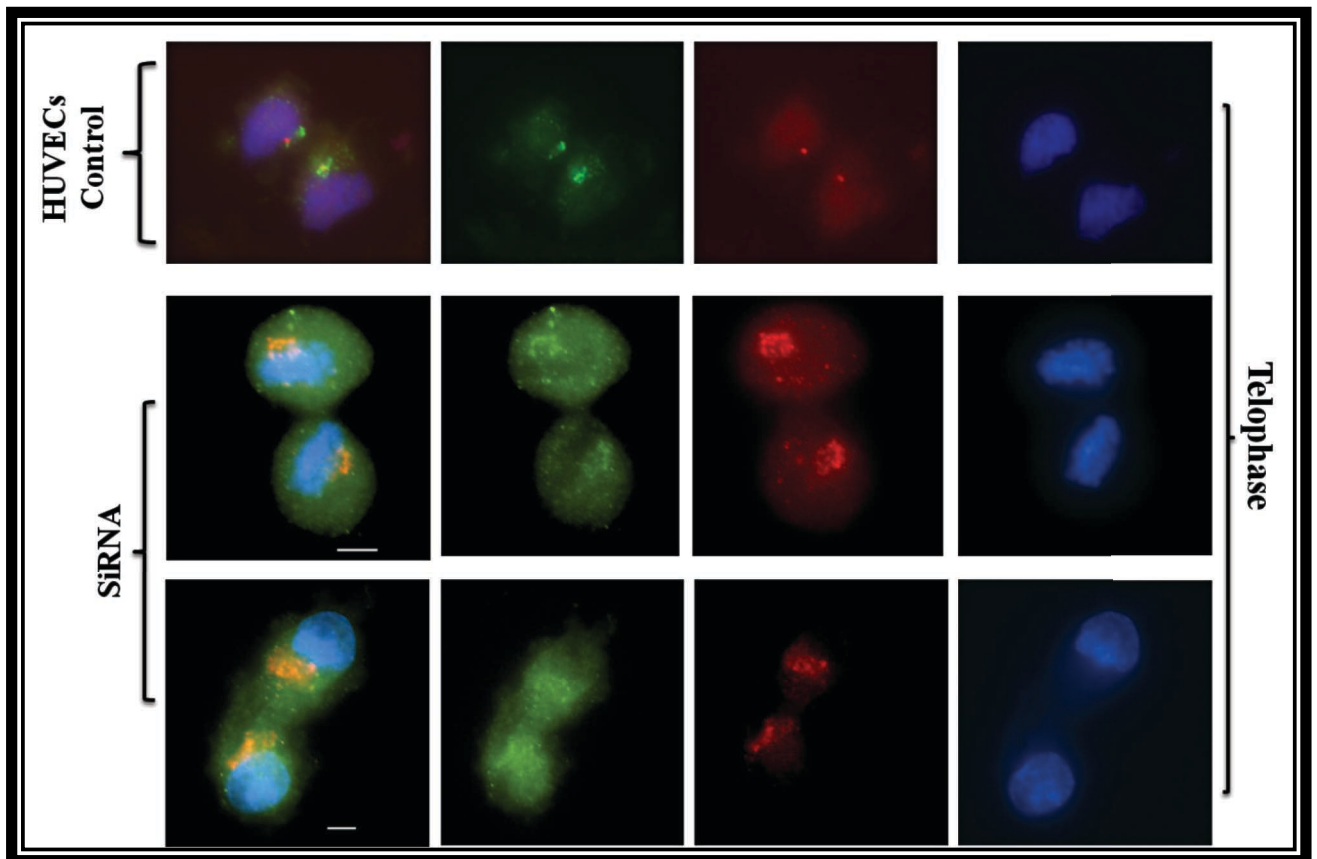
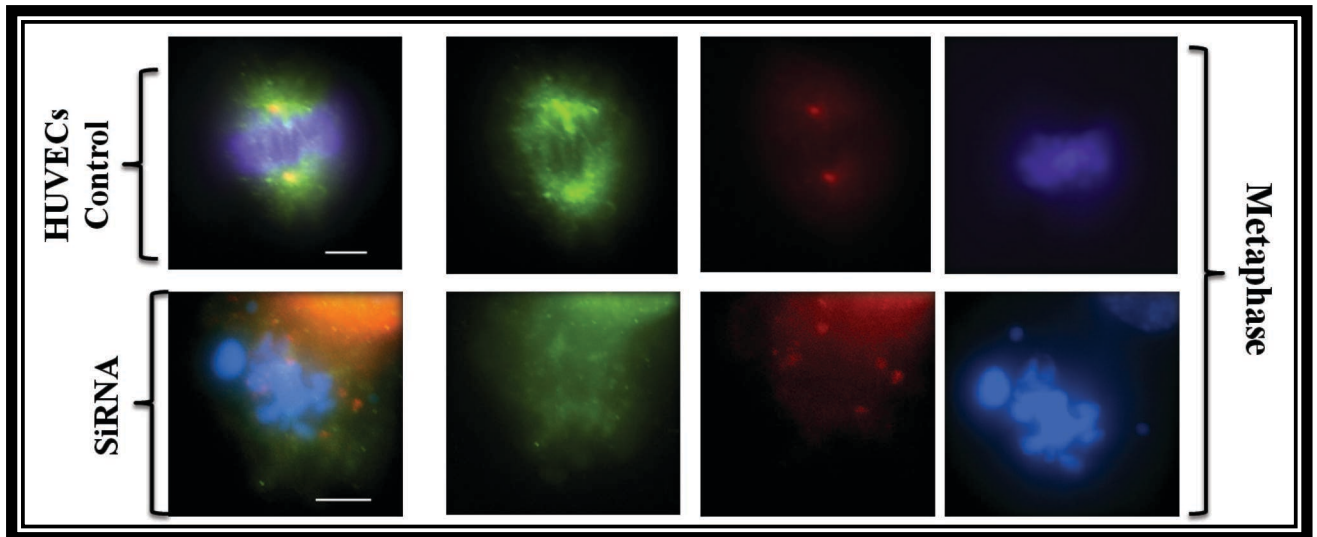


Figure 49. Dual immunolocalisation of hSSRP1 and beta-tubulin in *hssrp1* knockdown and control cells (HUVEC).

siRNA0 and siRNA1oligos were used to knockdown *hSSRP1* gene in HUVECs. A rabbit polyclonal anti-hSSRP1 TRITC antibody (red) and a mouse monoclonal anti-beta-tubulin FITC antibody (green) were used. SiRNA0 and siRNA1 treated and untreated HUVECs at interphase and mitotic stages (metaphase and telophase) are shown. Scale bar =5 μ m.

5.3 DISCUSSION

5.3.1 hSSRP1 and hSPT16 localise on chromatin and centrosome regions

In mouse, SSRP1 seems to associate with microtubules and is required for microtubule growth (Zeng *et al.*, 2010). According to Zeng and collaborators (2010), the SSRP1 signal covers all the main body of microtubules at the mitotic spindle. However, our results have shown a different localization of hSSRP1 in the cell. In human endothelium and fibroblast cells, hSSRP1 protein appears as discrete foci distributed along the microtubules at cytoskeleton of the cell but accumulated in a specific region of the cell during interphase. Once mitosis is started, hSSRP1 signal appears in two structures in located in both opposite poles of the mitotic spindle where the centrosomes or microtubule organization centres (MTOCs) should be. High resolution images using reconstruction of 3D Z-stacks of images have shown us that hSSRP1 could be labelling the human centrioles.

Surprised with these results we carried out several immunolocalisation controls, using two different antibodies against hSSRP1 and different combination of primary and secondary antibodies showing us that the signal was very specific. Furthermore, the siRNA knockdown cells showed that these hSSRP1 signals disappeared or got highly reduced in these treated cells.

The centrosome is a cytoplasmic organelle which is essential for the growth of microtubules. It represents the Microtubule Organization Centre (MTOC) that appears as an astral like component on the opposite poles of the cell division (Bornens, 2012; Hodges *et al.*, 2010). The centrosome maintains and organizes the microtubule cytoskeleton which is important for

giving the cell structure and shape and also participates in several cellular processes including cell motility, adhesion and polarity (Azimzadeh and Bornens, 2007).

The centrosome is duplicated at the beginning of S-phase which of them will migrate to each different cell pole. They arrange and organize the mitotic microtubule spindle (Azimzadeh and Bornens, 2007).

The centrosome consists of a pair of a cylindrical structure called centrioles which orientate one to each other at a 90 degree angle. The centrioles are highly conserved among some eukaryotes and each one is formed of 9 microtubule triplets organized as a symmetrical array (Hodges *et al.*, 2010). These pairs of centrioles are joined together on their proximal sites by coiled-coil proteins that are part of the pericentriolar material (PCM) (Azimzadeh and Bornens, 2007; Azimzadeh, 2014). Two different centrioles have been detected: mother centriole mature and daughter centriole immature. The daughter centriole is smaller in size (80% the size of the mother centriole). Furthermore, the mother centriole consist of two sets of appendages on its distal regions which are the attachment of the centrioles into the plasma membrane of the cell (Azimzadeh and Bornens, 2007 ; Azimzadeh, 2014; piel *et al.*, 2000). It has been reported that these centrioles are embedded within a huge amount of protein mixture known as the pericentriolar material (PCM) and both form the centrosome.

Plants and fungi do not have a centrosome but a different structure with different mixture of proteins which play a role for microtubule polymerization (Azimzadeh, 2014; Hodges *et al.*, 2010). In this study, we have found that hSSRP1 seem to be part of human centrioles and its role seems to allow the formation and organization of microtubules in the mitotic spindle.

SPT16 associates with SSRP1 to form the FACT complex that has been involved in the regulation and elongation of transcription factors as well as in DNA replication and repair (Duina *et al.*, 2007). According to Zeng and collaborators (2010) during the mitotic process

SPT16 seems to act independently from SSRP1 as SPT16 does not localize within the mitotic spindle as SSRP1 does in mouse.

Our results showed that hSPT16 localises as discrete foci into the nuclear chromatin in human interphase cells and around the centrosome region or MTOCs but not on the centrioles during the mitotic division. These results clearly distinguish between both FACT components suggesting different roles during mitosis for hSSRP1 and hSPT16.

In HELA cells, it was shown that SSRP1 is not associated to SPT16 as expected (Li *et al.*, 2006). Nevertheless, in human lung small cell carcinoma (H1299), SSRP1 and SPT16 are associated as a heterodimer during DNA replication and the transcriptional elongation. However, there is no evidence found that the SSRP1 and SPT16 co-localize together in during mitosis. SSRP1 has been shown to localize with microtubules whereas SPT16 has never been associated with the microtubules at the mitotic spindle (Li *et al.*, 2007; Zeng *et al.*, 2002; Skop *et al.*, 2004).

Surprisingly, in mice, SSRP1 is also working independently to SPT16 during mitosis (Zeng *et al.*, 2010). However, these authors showed that SSRP1 co-localised with tubulin along the whole length of the microtubules present on the mitotic spindle in mouse and we have shown a completely different picture in human cells. hSSRP1 seems to localise on the centrioles at the centrosomes and not along the microtubules in human cells.

5.3.2 siRNA *hssrp1* knockdown mutant cells possess an aberrant spindle and chromosome segregation

Our results showed that siRNA *hssrp1* knockdown cells had disorganized and deficient mitotic spindles that lead to inaccurate chromosome movements and segregation during anaphase and the formation of multinucleate cells.

The organization, growth and development of microtubules is a fundamental biological process that is essential for the accurate mitotic cell division (Zeng *et al.*, 2010). Several proteins have been found to play a role in the maturation of microtubules like SSRP1. Mouse knockout mutants for SSRP1 are lethal, but the siRNA knockdown cells have shown deficiencies and disorganization of the mitotic spindle (Zeng *et al.*, 2010). Furthermore, SSRP1 protein levels have been shown to be increased in human and mouse cancer cells with high mitotic proliferation.

However, it was reported that it was difficult to analyse the mouse *ssrp1* knockdown cells because most of the cells went into apoptosis and only a few of them over passed the mitotic checkpoints to be able to complete to mitotic later stages (Zeng *et al.*, 2010). In this case, only around 4% of 200 mitotic cells revealed inaccurate mitotic cell division (Zeng *et al.*, 2010). Similarly, we encountered similar problems in our siRNA treated HUVECs.

Other genes have been found to play an important role in the maturation of microtubules in the mitotic spindles like MuMA, Aurora kinases (Bowman *et al.*, 2006). MuMA has been found to be an essential protein for spindle regulation and orientation in humans and *Drosophila* (Bowman *et al.*, 2006). Mammalian MuMA attaches to microtubules and helps them to polymerize. *Drosophila* Mud protein is a homologue to MuMA that is also important in microtubule polymerization (Du *et al.*, 2002). Depletion of this protein leads to defects on the polarity of the mitotic spindle (Bowman *et al.*, 2006; Du *et al.*, 2002).

Aurora kinases have been also found to be important for the maturation of the mitotic spindle. These kinases are highly conserved among species. A dysfunction in Aurora kinase leads to chromosome instability by errors in the role of the centrosome. Consequently, defects on centrosome activity lead to defects in the mitotic spindle assembly and metaphase chromosomes fail to align and eventually abnormal chromosome segregation and defects in cytokinesis occur (Fu *et al.*, 2007). Similar results were observed in our siRNA *hSSRPI* knockdowns.

CHAPTER SIX

General Discussion and Conclusions

6.1 The importance of studying chromatin components

The chromatin contains DNA and proteins in order to pack the DNA molecules (chromosomes) inside the cell nucleus but this compaction has to be highly dynamic to allow several vital biological processes to occur (Sanchez-Moran, 2013). The different levels of DNA compaction and the chromatin proteins involved are evolutionary conserved among higher eukaryotes suggesting its importance. In this study, we have studied some of these chromatin components revealing their roles in DNA repair (AtH2A1, AtSSRP1) and chromosome segregation during mitosis and meiosis (AtSSRP1, AtK1 and hSSRP1).

In the first instance we identified these components in the plant model species *Arabidopsis thaliana* expecting that in roles chromatin would be similar, if not identical to other species as their protein sequence seemed to be evolutionary conserved. We have confirmed this hypothesis in chapters 4 and 5 where we characterised the chromatin component SSRP1 showing that AtSSRP1 is similar to humans (hSSRP1) even though their structure localization has been found out to have some important differences. Both proteins seem to organize and maintain an accurate spindle to ensure correct chromosome segregation. Nevertheless, the location of hSSRP1 is in the centrioles whereas AtSSRP1 cannot be located in these structures as plants lack centrioles. Nevertheless, AtSSRP1 is located in the similar functional region that organizes the microtubules in the spindle (MTOCs). These results emphasize the importance in studying chromatin components not only in human but in other model species as their functional role is more likely to be similar and basic knowledge could have enormous benefits for human health, especially, in matters involving genome instability and cell cycle (cancer), fertility and DNA recombination technologies (gene therapy).

6.2 *Arabidopsis* Histone AtH2A isoforms

The first level of eukaryotic chromatin organization is the nucleosome fibre. At this level, DNA (~147 bp) associates to an octamer of histone proteins forming the nucleosome. The nucleosome octamer is formed of two copies of these histones: H2A, H2B, H3 and H4 (Maeshima *et al.*, 2010).

Budding yeast genome contains two genes for each of these histones which encode for identical proteins. Nevertheless, during evolution higher eukaryotes have accumulated different gene copies for each histone (histone families). These histone families contain different histone isoforms, some of them identical copies and others just sharing some similarities at the amino acid sequence. During evolution some of these copies have accumulated mutations so the sequence of some isoforms has varied. For example, in the *Arabidopsis* genome there are 13 H2A isoforms, 11 isoforms for H2B, 15 isoforms for H3 and 8 isoforms for H4 (Sanchez-Moran, 2013). The 8 *Arabidopsis* H4 genes encode identical H4 proteins (the amino acid sequence remained identical). It is interesting to notice that H4 histone amino acid sequence has remained very similar even among different species. For instance, there are only 2 amino acid difference between the H4 histones in *Arabidopsis* and humans (Sanchez-Moran, 2013).

In this study, we have analysed mutants in 8 of the 13 isoforms of H2A (AtH2A1, AtH2A2, AtH2A3, AtH2A5, AtH2A6, AtH2A10, AtH2A12 and AtH2A13). The AtH2A isoform sequence shows the highest diversity among the histones, especially at their C-terminal region which seems to be involved in different chromatin remodelling functions (Bonisch and Hake, 2012). Histone isoforms have been differentiated between histone core proteins and histone variants. Histone variants have been described in histones H2A and H3 and they have

been classified like this because they have shown different functions and in some cases they are located in specific locations in the chromatin. Histone core isoforms have similar sequences if not identical like in AtH4 and are deposited into the nucleosome during the DNA replication. On the other hand, histone variants can be deposited at different stages of the cell cycle.

The H2AZ variant seems to be involved in controlling gene expression by regulating the DNA access to the transcription machinery (Segal and Widom, 2009). Nucleosomes which contain the H2AZ are more tightly attached to the associated DNA; therefore, the RNA polymerase II cannot get access to the DNA (Hodges *et al.*, 2009; Segal and Widom, 2009). Absence of H2AZ resulting in embryo lethality in mouse, and its reduction have revealed abnormalities in cell division including chromosome lagging, anaphase bridges and chromosome fragmentation in mouse and *Xenopus* (Faast *et al.*, 2001; Rangasamy *et al.*, 2004).

In plants, H2AZ might act as a temperature sensor at the level of the chromatin. When the temperature increases the eviction of H2AZ from nucleosomes at promoter regions of repressed genes and, thus, allows their expression in order to accommodate the plant to this temperature changes (Kumar and Wigge, 2010). Furthermore, H2AZ has been shown to share the position of meiotic crossovers in *Arabidopsis* (AtRAD51 and AtDMC1) suggesting to have a role in the formation or processing of DSBs (Choi *et al.*, 2013). In *Arabidopsis*, there are 3 genes coding for H2AZ variant: *AtH2A8*, *AtH2A9* and *AtH2A11*. In this study we did not analyse these variants but a double mutant *Ath2a8xAth2a11* has shown aberrations in reproductive growth which has been previously reported (Kumar and Wigge, 2010).

H2AX is another important histone variant that seems to be highly conserved in higher eukaryotes. This variant represents around 2-25% of all the H2A histone forms in the cell. It

has a distinct C-terminal domain ST/Q motif in which the serine residue gets rapidly phosphorylated in a region where a DSB has occurred. The phosphorylated H2AX known as γ H2AX, signals the DSB formation and might have an important role in producing chromatin changes to recruit DNA repair proteins to the site (see review Sanchez-Moran, 2013). In this study, we analysed the two copies of H2AX present in the *Arabidopsis* genome (*AtH2A3* and *AtH2A5*). Mutants for both genes showed a significant reduction in fertility that correlates with the meiotic errors observed by Sanchez-Moran and collaborators (unpublished data).

Another group of *Arabidopsis* histone AtH2A isoforms with similar sequences containing another phosphorylation motif (SPKK) are: AtH2A6, AtH2A7 and AtH2A12. This SPKK motif could associate to A/T rich sites of the minor groove of the DNA and the phosphorylation of its serine residue could potentially regulate the association/disassociation to DNA. Phosphorylation of this site could participate in chromatin remodelling and assembly during DNA replication (Green, 2002). Interestingly, this motif is only present in histone H2A in plants not in mammals, insects or yeast (Yi *et al.*, 2006). In this study, we analysed mutants for *AtH2A6* and *AtH2A12* genes that showed a semi-sterile phenotype. Further cytological analysis should be carried out in the future to understand the function of this group of histones AtH2A.

The remaining AtH2A histones in *Arabidopsis* could be classified as the core AtH2A histone group which includes: AtH2A1, AtH2A2, AtH2A4, AtH2A10 and AtH2A13. We have analysed mutants for all of them except AtH2A4 and found that they have a semi-sterile phenotype. We also analysed some RNAi mutants for *AtH2A10* and *AtH2A13* genes which RNAi construct could affect the other histone isoforms of the same group due to similarities to their DNA sequence and they showed a proper reduction in fertility as it was expected.

In summary, *Arabidopsis* histones AtH2A might have different roles involving fertility in plants.

6.3 AtH2A1 (RAT5) is involved in DNA repair and recombination

We have analysed in more detail the histone isoform AtH2A1 in this study. AtH2A1 has been previously related with T-DNA integration. The *rat5* (*Ath2a1*) mutant have been found to be very important in T-DNA integration in *Arabidopsis*. Using root transformation methods, it was shown that in *Ath2a1/rat5* mutant there was a clear deficiency in T-DNA integration. RAT5 stands for Resistant to *Agrobacterium tumefaciens*-mediated transformation 5 (Mysore *et al.*, 2000). Furthermore, the overexpression of AtH2A1 increased the susceptibility of T-DNA integration in *Arabidopsis* (Tenea *et al.*, 2009).

However, in this study, evaluating the T-DNA integration using the Floral Dipping procedure have shown that *Ath2A1/rat5* mutant have no significant reduction in T-DNA integration compared to the wild-type. This might show that AtH2A1 histone is required for T-DNA integration in some type of cells/organs and not in others (see further discussion in **6.4**).

A thorough cytological analysis of the *Ath2a1/rat5* mutant has showed that the isoform could be involved in DNA repair during mitotic and meiotic divisions. We found chromosome lagging, anaphase bridges, and chromosome missegregation and fragmentation during mitosis and meiosis. This DNA repair role for AtH2A1 might explain why is so important during T-DNA integration in roots transformation and not in Floral Dipping methodologies.

6.4 Decoding the mechanisms of T-DNA integration using Floral Dipping

GM transgenic crops have been used very often to transform crops with herbicide resistance genes (Alimohammadi *et al.*, 2009; Valentine, 2003). *Agrobacterium tumefaciens* transfers the T-DNA from its Ti plasmid (tumour inducer plasmid) into the plant genome. There are different T-DNA transformation methods: Transformation of protoplasts, callus culture cells, or other isolated plant cells (Gelvin and Schilperoort, 1998), Transformation of leaf mesophyll cells or other cells within intact plants (Tang *et al.*, 1996), Transformation of seeds (Feldman and Marks, 1987), “Clip ‘n squirt” method (Chang *et al.*, 1994), Transformation by “vacuum infiltration” (Bechtold *et al.*, 1993) and Floral Dipping transformation (Clough and Bent, 1998). The most frequently used method to transform *Arabidopsis thaliana* is the Floral Dipping Transformation method. In the first T-DNA transformation offspring (T1) the transformed seeds bear the T-DNA insertion in heterozygosis (Feldmann, 1992; Bechtold *et al.*, 1993). This means that the T-DNA integration during Floral Dipping must occur after the beginning of male/female gametogenesis within a flower; in the pollen mother cells, ovules or fertilized embryos. It has been demonstrated by different authors that the primary target for T-DNA integration using the Floral Dipping Method is the female germ-line (ovule) (Ye *et al.*, 1999; Bechtold *et al.*, 2000; Desfeux *et al.*, 2000).

In this study, we have evaluated the role of different proteins in T-DNA integration using the Floral Dipping approach. Previous similar analyses have been carried out using the root transformation methods, where they found that T-DNA integration was dependent of different DNA DSB repair pathways. The most important seemed to be HR and NHEJ. According to Windels and collaborators (2003), the T-DNA integration efficiency is reduced in *Atku80* and *Atlig4* mutants in *Arabidopsis*. However, other studies have mentioned that AtLIG4 is not necessary for the T-DNA integration (Van Attikum *et al.*, 2003). In our study,

we have found that AtLIG4 plays an important role for the T-DNA integration. These difference in results might be explained because the different mutant line used in some studies (Van Attikum *et al.*, 2003) had the T-DNA insertion in the *AtLIG4* gene inserted in intron one which might reduce the amount of AtLIG4 protein but not produce a null mutant, whereas in our study we used a T-DNA insertional mutant with the T-DNA inserted in exon one and therefore producing a complete null mutant.

Furthermore, Ku70, Rad50 and Mre11 proteins have been found to be essential for the T-DNA integration in yeast as well as in plants (van Attikum *et al.* 2001; van Attikum and Hooykaas, 2003). *Arabidopsis Atku80* mutant is deficient in T-DNA integration into the host plant DNA in somatic cells (Li *et al.*, 2005). In this study, we have shown that both AtKU70 and AtKU80 are required for T-DNA integration in *Arabidopsis* using the floral dipping approach. These observations show that NHEJ components (AtKU70, AtKU80 and AtLIG4) are required for T-DNA integration using Floral Dipping in *Arabidopsis*. On the other hand, HR recombination proteins MRE11 and RAD52 are required for T-DNA integration in yeast (Tzfira *et al.*, 2004). In our study, we presumed that if HR was important for T-DNA integration during Floral Dipping then meiotic HR components should have key roles. Thus, we analysed different mutants involved in different aspects of this pathway: *Atspo11.2* (formation of DSBs), *Atmre11* (resection of DSBs), *Atrad51* (single strand DNA invasion), *Atmsh4* and *Atmlh3* (maturation of dHJs). Interestingly, all these components are essential for T-DNA integration in *Arabidopsis thaliana* using the Floral Dipping approach.

The highest reduction in T-DNA integration was found in *Atspo11.2* mutant suggesting that meiotic DSBs are a clear target for T-DNA integration. It has been reported that DSBs also increased the T-DNA integration in somatic cells (Salomon and Puchta, 1998). Nevertheless, DSBs by itself are not sufficient for T-DNA integration as it requires processing by HR

components, such as DSB resection by AtMRE11, single strand invasion by the recombinase AtRAD51, and dHj maturation and processing by AtMSH4 and AtMLH3.

Surprisingly, in absence of AtH2A1 (RAT5) there is not significant reduction in T-DNA integration using Floral Dipping. AtH2A1 (RAT5) has been previously demonstrated to be necessary for T-DNA integration using root transformation methods (Mysor *et al.*, 2000; Yi *et al.*, 2002). The differences could be because of the different plant cells that are targeted for the T-DNA transformation (roots *vs.* ovules). We have shown that AtH2A1 seems to be involved in a DNA repair pathway in somatic cells, explaining its importance for the root transformation method. Whereas, it might not be so important for the ovule transformation which seems to use the meiotic DSB processing proteins involving in HR and NHEJ.

6.5 High Mobility Group (HMG) proteins and their role in plant fertility

Higher-order chromatin loops are associated to the chromosome axis or chromosome scaffold providing a higher level of chromatin compaction. Scaffold association regions (SARs) or Matrix attachment regions (MARs) are the physical attachment regions in the DNA sequence where the chromatin axis proteins bind. The SARs/MARs regions are rich in AT nucleotides (Cook, 2010; Dean, 2011; Naeshima and Eltsov, 2008). These attachments domains have been found to be important for chromatin dynamics and remodelling to facilitate gene transcription and DNA replication (Hart and Laemmli, 1998; Laemmli *et al.*, 1992). This structure is highly conserved during evolution in higher eukaryotes. In *Arabidopsis*, SARs seem to be very important for the regulation of the transcription machinery (Tetko *et al.*, 2006).

The chromosome axis components compose a large number of different protein families involved in several biological processes. One of these protein families is the High Mobility Group (HMG) family which are the most abundant proteins after histones in the chromatin and seem to play a crucial role in chromatin remodelling (Bustin, 2001; Lildballe *et al.*, 2008; Reeves and Adair, 2005).

The HMGA proteins have been studied to identify their roles in chromatin behaviour. These proteins have important roles in DNA biological activities including the increase in the affinity of transcription factors to the gene promoters and targeting other nuclear protein complexes into these domains (Sgarra *et al.*, 2004). The HMGA proteins are differentiated from other HMG proteins because their sequence includes one or several AT-hook motifs. These are DNA binding motifs that associate to AT-rich regions of the genome at the base of the chromatin loops attached to the chromosome axis (Cook, 2010; Dean, 2011; Naeshima and Eltsov, 2008).

In our study several *Athmga* mutants have been studied including *Athmga1*, *Athmga2*, *Athmga3* and other *Athmga*-likes that contain AT-hook motifs. All of them possessed a semi-sterile phenotype showing that they might have a role in plant fertility.

The HMGB proteins contain an HMG box motif that binds to DNA. This specific domain seems to attach to the minor groove of the DNA without any specificity in the DNA sequence. Also it has been revealed that HMG proteins might have a role in meiosis (Bianchi and Agresti, 2005; Catez and Hock, 2011). In this study, we analysed several *Athmgb* mutants in order to understand their role in *Arabidopsis*. Our analysis included *Athmgb1*, *Athmgb3*, *Athmgb5*, *Atssrp1*. All mutants showed a semi-sterile phenotype. However the highest reduction of fertility was observed in the *Athmgb* mutant *Atssrp1*. Several abnormalities were observed for this mutant including defects in DNA repair and abnormal

segregation of chromosomes in both meiotic and mitotic divisions. Further cytological analysis should be carried out in the future to understand the function of this group of *AtHMGB* genes. In summary, *Arabidopsis* HMG family might have different roles by involving in plants fertility.

6.6 *Arabidopsis* AtSSRP1 is involved in DNA repair and chromosome segregation during mitosis and meiosis

Structure specific recognition protein 1 (SSRP1) is one component of non-histone protein, HMG protein family that has been identified in different species. It plays a vital role in DNA repair, DNA replication and elongation, and in regulation of the transcription machinery (Kumari *et al.*, 2009; Zeng *et al.*, 2010). SSRP1 protein includes different conserved domains. The N-terminal region contains a domain that interacts with SPT16 forming the Facilitate Chromatin Transcription complex (FACT complex) as well as a tubulin binding domain. The C-terminal region contains another domain that includes an HMG-box domain which is a DNA binding domain (Kumari *et al.*, 2009, Zeng *et al.*, 2010).

It has been found that SSRP1 protein has a clear role in DNA repair (Kumari *et al.*, 2009). A knockdown mutant for *SSRP1* gene in mammalian cells showed an increase in the number of H2AX and RAD51 foci, thus, an increase in the activation of the HR process. Interestingly, over-expression of SSRP1 led to an apparent reduction of H2AX and RAD51 foci and, thus, a reduction in the HR events of the cells exposed to hidroxiurea (which creates DNA breaks).

The FACT complex is formed by the heterodimer SSRP1/SPT16 and it has been found in *Arabidopsis*, humans and *Drosophila* (Ikeda *et al.*, 2011). This complex has been described as a histone chaperone complex that plays an important role in histone displacement and

histone deposition in nucleosomes during the DNA replication, the chromatin remodelling and the DNA repair (Ikeda *et al.*, 2011).

Furthermore, SSRP1 has been found to play an essential function in cell division and maturation during embryogenesis (Cao *et al.*, 2003). However, there was no study conducted to investigate the role of SSRP1 in *Arabidopsis*. Our analysis has showed that AtSSRP1 has an essential role in mitosis and meiosis. In absence of AtSSRP1 the mitotic and meiotic spindles do not form or organize correctly producing chromosome missegregation errors. Immunolocalization of AtSSRP1 and AtSPT16 shows that they co-localise during some stages of meiosis where they could be working in the formation and organization of microtubules in the spindle, together as FACT complex or independently. The fact that AtSPT16 is located on the chromatin throughout prophase I whereas AtSSRP1 is already localised on the microtubules, shows that their role could be independent.

Chromosome fragmentation has been observed in the mutant during mitosis and meiosis which indicates shows that AtSSRP1 is important in DNA repair perhaps associated with AtSPT16 in the FACT complex as previously reported in other species.

6.7 Human hSSRP1 localises in the centrioles and is essential for the correct mitotic spindle formation and organization

The correct formation and organization of microtubules is a fundamental biological process that is essential for the mitotic cell cycle (Zeng *et al.*, 2010). Depletion of SSRP1 using siRNA approaches in mice have shown to be lethal. Nevertheless, in human cell knockdowns it was observed that it produced a deficient and disorganised spindle main body.

In this study, we had similar results when we carried out siRNA knockdown mutants in HUVECs. siRNA *hssrp1* mutants showed a reduction in the amount of microtubules involved in the mitotic spindle and disorganized spindles that produced errors in the chromosome segregation and even in the cell cytokinesis leading to multinuclear cells. Furthermore, immunolocalization analysis of hSSRP1 during mitosis showed us that the protein is localised in the centrioles (spindle organizers). This is different from previously published data where SSRP1 protein co-localised with tubulin along the microtubules in mice (Zeng *et al.*, 2010). We carried out several controls using different antibodies to corroborate our results and also we have shown that our siRNA knockdown mutants reduced the signal observed of hSSRP1 as expected.

6.8 Evolutionary differences in spindle organization between plants and mammals

Microtubules are essential in plants in different biological processes including cell division, cell polarity, phragmoplast assembly, mitosis, cytokinesis and meiosis. Plant microtubules nucleation is different to that in animals as they lack the structure called centriole (Eckardt, 2006; Lemmon and Brown, 2007). Plants comprise an anastral mitotic spindle in which the microtubules are nucleated in the lack of centrosomes while animals contain centrosomes which are a type of Microtubule Organizer Centres (MTOCs). Plants do not seem to have atypical MTOC (Azimzadeh *et al.*, 2008; Lemmon and Brown, 2007; Smirnova and Bajer, 1992). Nevertheless, γ -tubulin is essential for microtubule growth in all higher eukaryotes including plants (Lemmon and Brown, 2007).

The centrosome in animals and the spindle body in yeast nucleate microtubules. Nevertheless, the plants microtubules are polymerized from diffuse nucleating domains, the

γ -TuRCs (γ -tubulin ring complexes) (Erhardt *et al.*, 2002). The γ -TuRC have two molecules of γ - tubulin (GCP2-GCP3) that joined together to form γ -tubulin small complex (γ -TuSC). However, there are other (GCP4-GCP6) create γ -TuSC-like complexes. Consequently, the assembly between two complexes (γ -TuSC and γ -TuSC-like sub-complex) would participate in producing inactive γ -TuRC. Therefore, In the presence of other activating proteins and other targeting factors (sub-cellular molecules) to γ -TuRC, would lead to activate and initiate the polymerization of microtubules (Erhardt *et al.*, 2002 Hashimoto, 2013; Pastuglia, 2006). It has been found that the presence of γ -tubulin is necessary for the microtubule nucleation in plants (Murata *et al.*, 2005).

Our results have shown how important SSRP1 is in organizing the correct mitotic and meiotic spindles in *Arabidopsis* and the correct mitotic spindle in humans. hSSRP1 is located in the centrioles showing its importance in microtubule formation and organization in human mitosis. Nevertheless, plants do not have centrioles but the signal of AtSSRP1 localises in the region where mitotic and meiotic spindles are formed. In both cases, mutations in *SSRP1* genes produces aberrations in spindle formation and chromosome missegregation showing that although the localization is different, its function seems to be conserved among plants and humans. This shows that although centrioles are not evolutionary conserved, some of its components like hSSRP1 seem to be essential even in plants.

6.9 GENERAL CONCLUSIONS

- In this study, we have carried out a genetic analysis of different chromatin components in *Arabidopsis thaliana* which have resulted to have essential roles in fertility, DNA repair and chromosome segregation.
- T-DNA insertional mutants for different Arabidopsis histone *AtH2A* isoforms have shown a reduction in fertility compared to the wild-type. From histone core *AtH2A* isoforms (*AtH2A1*, *AtH2A2*, *AtH2A10* and *AtH2A13*) to histone variants like *AtH2AX* (*AtH2A3* and *AtH2A5*) and *AtH2A* isoforms bearing the SPKK DNA binding motif (*AtH2A6* and *AtH2A12*). This shows the importance of these histones *AtH2A* isoforms in plant fertility.
- A detailed cytogenetic analysis was carried out for one of these mutants (*Ath2a1*) showing the presence of chromosome aberrations during mitosis and meiosis.
- About 50% of mitotic anaphases presented one chromosome bridge or fragmentation in *Ath2a1* mutant. This shows that *AtH2A1* might have a very important role in DNA repair.
- In meiosis, about 16% of diakinesis meiocytes had interconnections between non-homologous chromosomes and 87% of anaphase I cells presented an average of 2.5 chromosome bridges. This shows that *AtH2A1* might have an important role in DNA DSB processing during meiosis.
- In absence of *AtH2A1* it has been previously reported the unviability of the T-DNA to get integrated in the plant genome by *Agrobacterium tumefaciens* using root transformation. Nevertheless, we have demonstrated that *Ath2a1* mutant is not resistant to the T-DNA integration using Floral Dipping transformation approaches. This shows that T-DNA integration might use diverse pathways involving different

chromatin proteins depending of the tissues or cells that *Agrobacterium* is targeting for the transformation.

- A detailed genetic analysis of different components of HR and NHEJ has shown that both pathways are required for the T-DNA integration using Floral Dipping.
- The absence of meiotic DSBs catalysed by AtSPO11 heterodimer decreases significantly the frequency of T-DNA integration via Floral Dipping. This shows the importance of DSBs in the T-DNA integration using this approach.
- Similarly, DSB resection (AtMRE11) and ssDNA strand invasion (AtRAD51) are as important as the presence of these DSBs for the T-DNA to be integrated on the plant genome using Floral Dipping.
- dHjs processing (AtMSH4 and AtMLH3) also have a significant role in T-DNA integration via Floral Dipping.
- Furthermore, NHEJ components (AtKU70, AtKU80 and AtLIG4) also have a very important role in T-DNA integration using Floral Dipping transformation.
- T-DNA insertional mutants for different *High Mobility Group (HMG)* genes in Arabidopsis have shown a reduction in fertility compared to the wild-type. From HMGA family members (with AT-hook DNA binding motifs) to HMGB family members (with a HMG-box DNA binding motif). This shows the importance of these HMG proteins in plant fertility.
- A detailed cytogenetic analysis was carried out for one of these mutants (*Atssrp1*) showing the occurrence of chromosome fragmentation and missegregation during mitosis and meiosis.
- Chromosome fragmentation and chromosome lagging during mitotic anaphase was observed in *Atssrp1* showing its importance in DNA repair and chromosome

segregation. These chromosome aberrations could explain the delayed development/dwarf size of the mutant plants.

- Similar chromosome behaviour was found during meiosis. Chromosome fragmentation could be visualised as early as pachytene stage. Whereas, chromosome missegregation was observed during anaphase I (29.2% of the cells) and anaphase II (92.8%). AtSSRP1 might be important in DSB processing and in meiotic chromosome segregation. This meiotic phenotype could explain the reduced fertility in the mutant.
- The FACT complex is formed by the heterodimer SSRP1/SPT16 in higher eukaryotes and it has been reported to have a key role in DNA repair. Arabidopsis AtSSRP1 and AtSPT16 colocalise with the chromatin during interphase/S phase stages in mitosis and meiosis showing that both could be involved in the FACT complex and thus in the DNA repair of any errors produced during the DNA replication.
- Meiotic chromosome formation (AtASY1) and synapsis (AtZYP1) seem to be completely normal in *Atssrp1* so the fragmentation errors seem to be independent of DSBs processing and meiotic recombination.
- The reduced number of microtubules and their different organization in, both, the meiotic and mitotic spindles could explain the problems in chromosome segregation.
- The use of Flutax1, a fluorescein tagged taxol, has proved to be a good alternative to microtubule immunolocalisation in *Arabidopsis thaliana*.
- In Arabidopsis, AtSPT16 colocalises in the nucleus with AtSSRP1 only late telophase II. Whereas, localises around the microtubules from late prophase I onwards. This might hint that FACT complex might be also involved in the formation and organization of the meiotic spindle.

- *Arabidopsis* kinase *Atk1* mutant has been reported to have chromosome missegregation errors during meiosis. In this study, we have shown that the meiotic chromosome missegregation is very similar to that one observed in *Atssrp1* mutant. This shows that both proteins could be involved in a similar pathway of chromosome segregation.
- Nevertheless, *Atk1* has not shown chromosome fragmentation which shows that AtSSRP1 has an independent role in DNA repair.
- We have shown that human hSSRP1 localises on the centrosomes at the centrioles.
- We have carried out a siRNA experiment to knockdown hSSRP1 in HUVECs showing its important role in DNA repair as well as in microtubule formation and organization in human mitotic spindle and therefore, its role in chromosome segregation and cytokinesis.
- The analysis of SSRP1 in plants and humans has showed the conservation of its functional roles in DNA repair and spindle organization even when the structural location has changed during evolution (plants have not centrioles).

6.10 Future Work

- We would further cytologically analyse the meiotic process in all the different semi-sterile mutants for *Ath2a* and *Athmg*.
- We would identify and characterise the chromosome regions involved in the anaphase bridges and fragmentation observed in *Ath2a1* and in *Atssrp1* mutants by Fluorescence *in situ* hybridization (FISH) using rDNA, telomere and centromere probes.
- We would like to increase the number of single mutants used to quantify the T-DNA integration in *Arabidopsis* using Floral Dipping. Some of these mutants would be: *Atspo11.1*, *Atrad50*, *Atdmc1*, *AtMus81*,... As well as to do it using double mutants (e.g.: *Atspo11.2xAtlig4*) in order to identify if HR and NHEJ are using the same or different pathways for the T-DNA integration.
- We would like to characterise a null *Atspt16* mutant to compare its phenotype to *Atssrp1* and try to differentiate if the DNA repair and chromosome segregation functionalities are FACT dependent or just by itself. At the moment, we have identified heterozygous mutants for a T-DNA insertion in *AtSPT16* but every time we grow the offspring not homozygous mutants appear, showing that the mutation could be lethal in *Arabidopsis*. Further analyses would be carried out to demonstrate this.
- We have tried to use different antibodies to identify the centrioles, centrosomes and MTOCs in human and plant cells but we have not been very successful. We would like to colocalise our SSRP1 protein with a protein known to be in this regions.

REFERENCES

Acilan, C., Potter, D. M. and Saunders, W. S. (2007) DNA repair pathways involved in anaphase bridge formation. *Genes Chromosomes Cancer*, **46**, 522-31.

Albertson, R., Riggs, B. and Sullivan, W. (2005) Membrane traffic: a driving force in cytokinesis. *Trends Cell Biol*, **15**, 92-101.

Albini, SM. and Jones, GH. (1984) Synaptonemal complex-associated centromeres and recombination nodules in plant meiocytes prepared by an improved surface-spreading technique. *Exp cell Res*, **155**,5888-592.

Aleporou-Marinou, V., Marinou, H. and Patargias, T. (2003) A mini review of the high mobility group proteins of insects. *Biochem Genet*, **41**, 291-304.

Alimohammadi, Mohammad and Mohammad B. Bagherieh-Najjar. (2009) Agrobacterium-Mediated Transformation of Plants: Basic Principles and Influencing Factors. *African Journal of Biotechnology*, **20**, 5142-5148.

Allfrey, V. G., Faulkner, R. and Mirsky, A. E. (1964) Acetylation and Methylation of Histones and Their Possible Role in the Regulation of Rna Synthesis. *Proc Natl Acad Sci U S A*, **51**, 786-94.

Alonso, J. M., Stepanova, A. N., Leisse, T. J., Kim, C. J., Chen, H., Shinn, P., Stevenson, D. K., Zimmerman, J., Barajas, P., Cheuk, R., Gadrinab, C., Heller, C., Jeske, A., Koesema, E., Meyers, C. C., Parker, H., Prednis, L., Ansari, Y., Choy, N., Deen, H., Geralt, M., Hazari, N., Hom, E., Karnes, M., Mulholland, C., Ndubaku, R., Schmidt, I., Guzman, P., Aguilar-Henonin, L., Schmid, M., Weigel, D., Carter, D. E., Marchand, T., Risseuw, E., Brogden, D., Zeko, A., Crosby, W. L., Berry, C. C. and Ecker, J. R. (2003) Genome-wide insertional mutagenesis of *Arabidopsis thaliana*. *Science*, **301**, 653-7.

Armstrong, S. J., Caryl, A. P., Jones, G. H. and Franklin, F. C. (2002) Asy1, a protein required for meiotic chromosome synapsis, localizes to axis-associated chromatin in *Arabidopsis* and *Brassica*. *J Cell Sci*, **115**, 3645-55.

Ausio, J. and Abbott, D. W. (2002) The many tales of a tail: carboxyl-terminal tail heterogeneity specializes histone H2A variants for defined chromatin function. *Biochemistry*, **41**, 5945-9.

- Ausio, J., Dong, F. and Van Holde, K. E.** (1989) Use of selectively trypsinized nucleosome core particles to analyze the role of the histone "tails" in the stabilization of the nucleosome. *J Mol Biol*, **206**, 451-63.
- Azimzadeh, J., Nacry, P., Christodoulidou, A., Drevensek, S., Camilleri, C., Amiour, N., Parcy, F., Pastuglia, M. and Bouchez, D.** (2008) Arabidopsis TONNEAU1 proteins are essential for preprophase band formation and interact with centrin. *Plant Cell*, **20**, 2146-59.
- Azimzadeh, J. & Bornens, M.** (2007) Structure and duplication of the centrosome. *J Cell Sci*, **120**, 2139-42.
- Azimzadeh, J., Nacry, P., Christodoulidou, A., Drevensek, S., Camilleri, C., Amiour, N., Parcy, F., Pastuglia, M. & Bouchez, D.** (2008) Arabidopsis TONNEAU1 proteins are essential for preprophase band formation and interact with centrin. *Plant Cell*, **20**, 2146-59.
- Bechtold N, Ellis J, Pelletier G** (1993) In planta Agrobacterium-mediated gene transfer by infiltration of adult Arabidopsis thaliana plants. *C R Acad Sci Paris Life Sci* **316**: 1194–1199.
- Belmont, A. S.** (2006) Mitotic chromosome structure and condensation. *Curr Opin Cell Biol*, **18**, 632-8.
- Bleuyard, J. Y. & White, C. I.** (2004) The Arabidopsis homologue of Xrcc3 plays an essential role in meiosis. *EMBO J*, **23**, 439-49.
- Bleuyard JY, Gallego ME, Savigny F, White CI.** (2005) Differing requirements for the Arabidopsis Rad51 paralogs in meiosis and DNA repair. *Plant Journal* **41**: 533–545.
- Ross-Macdonald P, Roeder GS.** (1994) Mutation of a meiosis-specific MutS homolog decreases crossing over but not mismatch correction. *Cell* **79**: 1069–1080.
- Bianchi, M. E. and Agresti, A.** (2005) HMG proteins: dynamic players in gene regulation and differentiation. *Curr Opin Genet Dev*, **15**, 496-506.
- Bisgrove, S. R., Hable, W. E. and Kropf, D. L.** (2004) +TIPs and microtubule regulation. The beginning of the plus end in plants. *Plant Physiol*, **136**, 3855-63.
- Blow, J. J. & Tanaka, T. U.** (2005) The chromosome cycle: coordinating replication and segregation. Second in the cycles review series. *EMBO Rep*, **6**, 1028-34.

- Bonenfant, D., Towbin, H., Coulot, M., Schindler, P., Mueller, D. R. and Van Oostrum, J.** (2007) Analysis of dynamic changes in post-translational modifications of human histones during cell cycle by mass spectrometry. *Mol Cell Proteomics*, **6**, 1917-32.
- Bonisch, C. & Hake, S. B.** (2012) Histone H2A variants in nucleosomes and chromatin: more or less stable? *Nucleic Acids Res*, **40**, 10719-41.
- Bornens, M.** (2012) The centrosome in cells and organisms. *Science*, **335**, 422-6.
- Bonner, W. M., Redon, C. E., Dickey, J. S., Nakamura, A. J., Sedelnikova, O. A., Solier, S. and Pommier, Y.** (2008) GammaH2AX and cancer. *Nat Rev Cancer*, **8**, 957-67.
- Bowman, S. K., Neumuller, R. A., Novatchkova, M., Du, Q. and Knoblich, J. A.** (2006) The Drosophila NuMA Homolog Mud regulates spindle orientation in asymmetric cell division. *Dev Cell*, **10**, 731-42.
- Brown, R. C. and Lemmon, B. E.** (2007) The Pleiomorphic Plant MTOC: An Evolutionary Perspective. *Journal of Integrative Plant Biology*, **49**, 1142-1153.
- Bulankova, P., Rihs-Kearnan, N., Nowack, M. K., Schnittger, A. and Riha, K.** (2010) Meiotic progression in Arabidopsis is governed by complex regulatory interactions between SMG7, TDM1, and the meiosis I-specific cyclin TAM. *Plant Cell*, **22**, 3791-803.
- Bundock, P. and Hooykaas, P.** (2002) Severe developmental defects, hypersensitivity to DNA-damaging agents, and lengthened telomeres in Arabidopsis MRE11 mutants. *Plant Cell*, **14**, 2451-2462.
- Bustin, M.** (2001) Chromatin unfolding and activation by HMGN chromosomal proteins. *Trends Biochem Sci*, **26**, 431-7.
- Cai, G.** (2010) Assembly and disassembly of plant microtubules: tubulin modifications and binding to MAPs. *Exp. Botany*, **61**, 623-626.
- Cao, S., Bendall, H., Hicks, G. G., Nashabi, A., Sakano, H., Shinkai, Y., Gariglio, M., Oltz, E. M. and Ruley, H. E.** (2003) The High-Mobility-Group Box Protein SSRP1/T160 Is Essential for Cell Viability in Day 3.5 Mouse Embryos. *Molecular and Cellular Biology*, **23**, 5301-5307.
- Catez, F. and Hock, R.** (2010) Binding and interplay of HMG proteins on chromatin: lessons from live cell imaging. *Biochim Biophys Acta*, **1799**, 15-27.

- Chan, F. L., Marshall, O. J., Saffery, R., Kim, B. W., Earle, E., Choo, K. H. and Wong, L. H.** (2012) Active transcription and essential role of RNA polymerase II at the centromere during mitosis. *Proc Natl Acad Sci U S A*, **109**, 1979-84.
- Chang SS, Park SK, Kim BC, Kang BJ, Kim DU, Nam HG** (1994) Stable genetic transformation of *Arabidopsis thaliana* by *Agrobacterium* inoculation in planta. *Plant J* **5**:551–558.
- Chan, G. K. and Yen, T. J.** (2003) The mitotic checkpoint: a signaling pathway that allows a single unattached kinetochore to inhibit mitotic exit. *Prog Cell Cycle Res*, **5**, 431-9.
- Clough SJ, Bent AF.** (1998) Floral dip: a simplified method for *Agrobacterium*-mediated transformation of *Arabidopsis thaliana*. *Plant J* **16**: 735–743.
- Cook, P. R.** (2010) A model for all genomes: the role of transcription factories. *J Mol Biol*, **395**, 1-10.
- Cromer, L., Heyman, J., Touati, S., Harashima, H., Araou, E., Girard, C., Horlow, C., Wassmann, K., Schnittger, A., De Veylder, L. and Mercier, R.** (2012) OSD1 promotes meiotic progression via APC/C inhibition and forms a regulatory network with TDM and CYCA1;2/TAM. *PLoS Genet*, **8**, e1002865.
- Czura, C. J., Yang, H. & Tracey, K. J.** (2003) High mobility group box-1 as a therapeutic target downstream of tumor necrosis factor. *J Infect Dis*, 187 Suppl 2, S391-6.
- D'erfurth, I., Jolivet, S., Froger, N., Catrice, O., Novatchkova, M., Simon, M., Jenczewski, E. and Mercier, R.** (2008) Mutations in AtPS1 (*Arabidopsis thaliana* parallel spindle 1) lead to the production of diploid pollen grains. *PLoS Genet*, **4**, e1000274.
- De, D. N.** (2002) Protein constitution of the chromosome axis. *Chromosoma*, **111**, 69-79.
- Dernburg, A.F., McDonald, K., Moulder, G., Barstead, R., Dresser, M. and Villeneuve, A.M.** (1998) Meiotic recombination in *C-elegans* initiates by a conserved mechanism and is dispensable for homologous chromosome synapsis. *Cell*, **94**, 387-398.
- De Muyt, A., Pereira, L., Vezon, D., Chelysheva, L., Gendrot, G., Chambon, A., Laine-Choinard, S., Pelletier, G., Mercier, R., Nogue, F. and Grelon, M.** (2009) A high throughput genetic screen identifies new early meiotic recombination functions in *Arabidopsis thaliana*. *PLoS Genet*, **5**, e1000654.

- Dean, A.** (2011) In the loop: long range chromatin interactions and gene regulation. *Brief Funct Genomics*, **10**, 3-10.
- Desfeux, C., Clough, S. J. and Bent, A. F.** (2000) Female reproductive tissues are the primary target of Agrobacterium-mediated transformation by the Arabidopsis floral-dip method. *Plant Physiol*, **123**, 895-904.
- Diqui, N.U., Rusyniak, S., Hasenkampf, C.A. and Riggs, C.D.** (2006) Disruption of the Arabidopsis SMC4 gene, AtCAP-C, compromises gametogenesis and embryogenesis. *Planta*, **223**, 990-997.
- Doxsey, S.** (2001) Re-evaluating centrosome function. *Nat Rev Mol Cell Biol*, **2**, 688-98.
- Duina, A. A., Ruffange, A., Bracey, J., Hall, J., Nourani, A. and Winston, F.** (2007) Evidence that the localization of the elongation factor Spt16 across transcribed genes is dependent upon histone H3 integrity in *Saccharomyces cerevisiae*. *Genetics*, **177**, 101-12.
- Edlinger, B. and Schlogelhofer, P.** (2011) Have a break: determinants of meiotic DNA double strand break (DSB) formation and processing in plants. *J Exp Bot*, **62**, 1545-63.
- Erhardt, M., Stoppin-Mellet, V., Campagne, S., Canaday, J., Mutterer, J., Fabian, T., Sauter, M., Muller, T., Peter, C., Lambert, A. M. and Schmit, A. C.** (2002) The plant Spc98p homologue colocalizes with gamma-tubulin at microtubule nucleation sites and is required for microtubule nucleation. *J Cell Sci*, **115**, 2423-31.
- Faast, R., Thonglairoam, V., Schulz, T. C., Beall, J., Wells, J. R., Taylor, H., Matthaei, K., Rathjen, P. D., Tremethick, D. J. and Lyons, I.** (2001) Histone variant H2A.Z is required for early mammalian development. *Curr Biol*, **11**, 1183-7.
- Fache, V., Gaillard, J., Van Damme, D., Geelen, D., Neumann, E., Stoppin-Mellet, V. and Vantard, M.** (2010) Arabidopsis kinetochore fiber-associated MAP65-4 cross-links microtubules and promotes microtubule bundle elongation. *Plant Cell*, **22**, 3804-15.
- Falck, J., Coates, J. and Jackson, S. P.** (2005) Conserved modes of recruitment of ATM, ATR and DNA-PKcs to sites of DNA damage. *Nature*, **434**, 605-11.
- Feldmann K.** (1992) T-DNA insertion mutagenesis in Arabidopsis: seed infection transformation. In C Koncz, N-H Chua, J Schell, eds, *Methods in Arabidopsis Research*. World Scientific, Singapore, pp 274–289.

- Feldmann KA, Marks MD** (1987) Agrobacterium-mediated transformation of germinating seeds of *Arabidopsis thaliana*: a non-tissue culture approach. *Mol Gen Genet* **208**: 1–9.
- Ferdous, M., Higgins, J. D., Osman, K., Lambing, C., Roitinger, E., Mechtler, K., Armstrong, S. J., Perry, R., Pradillo, M., Cunado, N. and Franklin, F. C.** (2012) Inter-homolog crossing-over and synapsis in *Arabidopsis* meiosis are dependent on the chromosome axis protein AtASY3. *PLoS Genet*, **8**, e1002507.
- Fosket, D. and Morejohn, L.** (1992) Structural and functional organization of tubulin. *Annu. Rev. Plant Physiol. Plant Mol. Biol.*, **43**, 201-240.
- Fu, J., Bian, M., Jiang, Q. and Zhang, C.** (2007) Roles of Aurora kinases in mitosis and tumorigenesis. *Mol Cancer Res*, **5**, 1-10.
- Fusco, A. and Fedele, M.** (2007) Roles of HMGA proteins in cancer. *Nat Rev Cancer*, **7**, 899-910.
- Gelvin SB, Schilperoort RA.** (1998) *Plant Molecular Biology Manual*. Kluwer Academic Publishers, Dordrecht, The Netherlands physical interaction of AvrPto and Pto kinase. *Science* **274**: 2060–2063.
- Gerton, J. L. and Hawley, R. S.** (2005) Homologous chromosome interactions in meiosis: diversity amidst conservation. *Nat Rev Genet*, **6**, 477-87.
- Glotzer, M.** (2005) The molecular requirements for cytokinesis. *Science*, **307**, 1735-9.
- Goodwin, G. H. and Johns, E. W.** (1973) Isolation and characterisation of two calf-thymus chromatin non-histone proteins with high contents of acidic and basic amino acids. *Eur J Biochem*, **40**, 215-9.
- Grelon, M., Vezon, D., Gendrot, G. and Pelletier, G.** (2001) AtSPO11-1 is necessary for efficient meiotic recombination in plants. *EMBO J*, **20**, 589-600.
- Gupta, R., Webster, C. I., Walker, A. R. and Gray, J. C.** (1997) Chromosomal location and expression of the single-copy gene encoding high-mobility-group protein HMG-I/Y in *Arabidopsis thaliana*. *Plant Mol Biol*, **34**, 529-36.
- Hamant, O., Ma, H. and Cande, W. Z.** (2006) Genetics of meiotic prophase I in plants. *Annu Rev Plant Biol*, **57**, 267-302.

- Hamoir, G.** (1992) The discovery of meiosis by E. Van Beneden, a breakthrough in the morphological phase of heredity. *Int J Dev Biol*, **36**, 9-15.
- Hart, C. M. and Laemmli, U. K.** (1998) Facilitation of chromatin dynamics by SARs. *Curr Opin Genet Dev*, **8**, 519-25.
- Hashimoto, T.** (2013) A ring for all: gamma-tubulin-containing nucleation complexes in acentrosomal plant microtubule arrays. *Curr Opin Plant Biol*, **16**, 698-703.
- Heo, K., Kim, H., Choi, S. H., Choi, J., Kim, K., Gu, J., Lieber, M. R., Yang, A. S. and An, W.** (2008) FACT-mediated exchange of histone variant H2AX regulated by phosphorylation of H2AX and ADP-ribosylation of Spt16. *Mol Cell*, **30**, 86-97.
- Higgins, J. D., Sanchez-Moran, E., Armstrong, S. J., Jones, G. H. and Franklin, F. C.** (2005) The Arabidopsis synaptonemal complex protein ZYP1 is required for chromosome synapsis and normal fidelity of crossing over. *Genes Dev*, **19**, 2488-500.
- Higgins, JD, Armstrong, SJ, Franklin, FCH and Jones, GH** (2004) The Arabidopsis MutS homolog AtMSH4 functions at an early step in recombination: evidence for two classes of recombination in Arabidopsis, *Genes & Development*, vol. 18, no. **20**, pp. 2557-70.
- Hirota, T., Gerlich, D., Koch, B., Ellenberg, J. and Peters, J.M.** (2004) Distinct functions of condensin I and II in mitotic chromosome assembly. *J Cell Sci*, **117**, 6435-6445.
- Hirst, M. and Marra, M. A.** (2009) Epigenetics and human disease. *Int J Biochem Cell Biol*, **41**, 136-46.
- Hodges, C., Bintu, L., Lubkowska, L., Kashlev, M. and Bustamante, C.** (2009) Nucleosomal fluctuations govern the transcription dynamics of RNA polymerase II. *Science*, **325**, 626-8.
- Hodges, M. E., Scheumann, N., Wickstead, B., Langdale, J. A. & Gull, K.** (2010) Reconstructing the evolutionary history of the centriole from protein components. *J Cell Sci*, **123**, 1407-13.
- Hoffelder, D. R., Luo, L., Burke, N. A., Watkins, S. C., Gollin, S. M. and Saunders, W. S.** (2004) Resolution of anaphase bridges in cancer cells. *Chromosoma*, **112**, 389-97.

Horn, P. J. and Peterson, C. L. (2002) Molecular biology. Chromatin higher order folding--wrapping up transcription. *Science*, **297**, 1824-7.

Ikeda, Y., Kinoshita, Y., Susaki, D., Ikeda, Y., Iwano, M., Takayama, S., Higashiyama, T., Kakutani, T. and Kinoshita, T. (2011) HMG domain containing SSRP1 is required for DNA demethylation and genomic imprinting in Arabidopsis. *Dev Cell*, **21**, 589-96.

Inoue, N., Ikawa, M., Isotani, A. and Okabe, M. (2005) The immunoglobulin superfamily protein Izumo is required for sperm to fuse with eggs. *Nature*, **434**, 234-8.

Ishibashi, T., Dryhurst, D., Rose, K. L., Shabanowitz, J., Hunt, D. F. and Ausio, J. (2009) Acetylation of vertebrate H2A.Z and its effect on the structure of the nucleosome. *Biochemistry*, **48**, 5007-17.

Islam, M. N., Paquet, N., Fox, D., 3rd, Dray, E., Zheng, X. F., Klein, H., Sung, P. & Wang, W. (2012) A variant of the breast cancer type 2 susceptibility protein (BRC) repeat is essential for the RECQL5 helicase to interact with RAD51 recombinase for genome stabilization. *J Biol Chem*, **287**, 23808-18.

Jia, Q., Bundock, P., Hooykaas, P. J. J. and De Pater, S. (2012) Agrobacterium tumefaciens T-DNA Integration and Gene Targeting in Arabidopsis thaliana Non-Homologous End-Joining Mutants. *Journal of Botany*, **2012**, 1-13.

Kaloriti, D., Galva, C., Parupalli, C., Khalifa, N., Galvin, M. and Sedbrook, J. (2007) Microtubule associated proteins in plants and the processes they manage. *J. Integrative Plant Biol.*, **49**, 1164-1173.

Kamakaka, R. T. and Biggins, S. (2005) Histone variants: deviants? *Genes Dev*, **19**, 295-310.

Keeney, S. (2008) Spo11 and the Formation of DNA Double-Strand Breaks in Meiosis. *Genome Dyn Stab*, **2**, 81-123.

Keeney, S., Giroux, C. N. & Kleckner, N. (1997) Meiosis-specific DNA double-strand breaks are catalyzed by Spo11, a member of a widely conserved protein family. *Cell*, **88**, 375-84.

- Kim, Y. C., Gerlitz, G., Furusawa, T., Catez, F., Nussenzweig, A., Oh, K. S., Kraemer, K. H., Shiloh, Y. and Bustin, M.** (2009) Activation of ATM depends on chromatin interactions occurring before induction of DNA damage. *Nat Cell Biol*, **11**, 92-6.
- Komaki, S., Abe, T., Coutuer, S., Inze, D., Russinova, E. and Hashimoto, T.** (2010) Nuclear-localized subtype of end-binding 1 protein regulates spindle organization in Arabidopsis. *J Cell Sci*, **123**, 451-9.
- Kumar, S. V. and Wigge, P. A.** (2010) H2A.Z-containing nucleosomes mediate the thermosensory response in Arabidopsis. *Cell*, **140**, 136-47.
- Kumari, A., Mazina, O. M., Shinde, U., Mazin, A. V. and Lu, H.** (2009) A role for SSRP1 in recombination-mediated DNA damage response. *J Cell Biochem*, **108**, 508-18.
- La Cour LF, Wells B.** (1971) The chromomeres of prepachytene chromosomes. *Cytologia*, **36**, 111-120.
- Laemmli, U. K., Kas, E., Poljak, L. and Adachi, Y.** (1992) Scaffold-associated regions: cis-acting determinants of chromatin structural loops and functional domains. *Curr Opin Genet Dev*, **2**, 275-85.
- Laurentino, E. C., Taylor, S., Mair, G. R., Lasonder, E., Bartfai, R., Stunnenberg, H. G., Kroeze, H., Ramesar, J., Franke-Fayard, B., Khan, S. M., Janse, C. J. and Waters, A. P.** (2011) Experimentally controlled downregulation of the histone chaperone FACT in *Plasmodium berghei* reveals that it is critical to male gamete fertility. *Cell Microbiol*, **13**, 1956-74.
- Lee, J. Y. and Orr-Weaver, T. L.** (2001) The molecular basis of sister-chromatid cohesion. *Annu Rev Cell Dev Biol*, **17**, 753-77.
- Lejeune, E., Bortfeld, M., White, S. A., Pidoux, A. L., Ekwall, K., Allshire, R. C. and Ladurner, A. G.** (2007) The chromatin-remodeling factor FACT contributes to centromeric heterochromatin independently of RNAi. *Curr Biol*, **17**, 1219-24.
- Lemmens, B. B., Johnson, N. M. and Tijsterman, M.** (2013) COM-1 promotes homologous recombination during *Caenorhabditis elegans* meiosis by antagonizing Ku-mediated non-homologous end joining. *PLoS Genet*, **9**, e1003276.

- Li J, Krichevsky A, Vaidya M, Tzfira T. and Citovsky V.** (2005) Uncoupling of the functions of the Arabidopsis VIP1 protein in transient and stable plant genetic transformation by *Agrobacterium*. *Proceedings of the National Academy of Sciences of the United States of America*, **102**, 5733-5738.
- Li, J., Vaidya, M., White, C., Vainstein, A., Citovsky, V. and Tzfira, T.** (2005) Involvement of KU80 in T-DNA integration in plant cells. *Proc Natl Acad Sci U S A*, **102**, 19231-6.
- Lildballe, D. L., Pedersen, D. S., Kalamajka, R., Emmersen, J., Houben, A. and Grasser, K. D.** (2008) The expression level of the chromatin-associated HMGB1 protein influences growth, stress tolerance, and transcriptome in Arabidopsis. *J Mol Biol*, **384**, 9-21.
- Litzenburger, B. D., Uray, I. P., Hill, J., Keyomarsi, K and Brown, P. H** (2013) Mechanism-based chemoprevention of triple-negative breast cancer by blockade at multiple cell cycle regulatory points. *Cancer Prev*, **6**, 1940-6215.
- Liu, B., Marc, J., Joshi, H. C. and Palevitz, B. A.** (1993) A gamma-tubulin-related protein associated with the microtubule arrays of higher plants in a cell cycle-dependent manner. *J Cell Sci*, **104** (Pt 4), 1217-28.
- Li, Y., Zeng, S. X., Landais, I. & Lu, H.** (2007) Human SSRP1 has Spt16-dependent and -independent roles in gene transcription. *J Biol Chem*, **282**, 6936-45.
- Lolas, I. B., Himanen, K., Gronlund, J. T., Lynggaard, C., Houben, A., Melzer, M., Van Lijsebettens, M. and Grasser, K. D.** (2010) The transcript elongation factor FACT affects Arabidopsis vegetative and reproductive development and genetically interacts with HUB1/2. *Plant J*, **61**, 686-97.
- Luger, K., Mader, A. W., Richmond, R. K., Sargent, D. F. and Richmond, T. J.** (1997) Crystal structure of the nucleosome core particle at 2.8 Å resolution. *Nature*, **389**, 251-60.
- Ma, H.** (2006) A molecular portrait of Arabidopsis meiosis. *Arabidopsis Book*, **4**, e0095.
- Macqueen, A. J., Colaiacovo, M. P., McDonald, K. and Villeneuve, A. M.** (2002) Synapsis-dependent and -independent mechanisms stabilize homolog pairing during meiotic prophase in *C. elegans*. *Genes Dev*, **16**, 2428-42.

- Madigan, J. P., Chotkowski, H. L. and Glaser, R. L.** (2002) DNA double-strand break-induced phosphorylation of *Drosophila* histone variant H2Av helps prevent radiation-induced apoptosis. *Nucleic Acids Res*, **30**, 3698-705.
- Maeshima, K., Hihara, S. and Eltsov, M.** (2010) Chromatin structure: does the 30-nm fibre exist in vivo? *Curr Opin Cell Biol*, **22**, 291-7.
- Maguire, M. P., Riess, R. W. and Paredes, A. M.** (1993) Evidence from a maize desynaptic mutant points to a probable role of synaptonemal complex central region components in provision for subsequent chiasma maintenance. *Genome*, **36**, 797-807.
- Mao, Z., Bozzella, M., Seluanov, A. and Gorbunova, V.** (2008) DNA repair by nonhomologous end joining and homologous recombination during cell cycle in human cells. *Cell Cycle*, **7**, 2902-6.
- McKim, K.S., Green-Marroquin, B.L., Sekelsky, J.J., Chin, G., Steinberg, C., Khodosh, R. and Hawley, R.S.** (1998) Meiotic synapsis in the absence of recombination. *Science*, **279**, 876-878.
- Miller KR.** (2000) Anaphase. *Biology* (5 ed.). Pearson Prentice Hall. pp. 169–70.
- Molinier, J., Stamm, M. E. and Hohn, B.** (2004) SNM-dependent recombinational repair of oxidatively induced DNA damage in *Arabidopsis thaliana*. *EMBO Rep*, **5**, 994-9.
- Murata, T., Sonobe, S., Baskin, T. I., Hyodo, S., Hasezawa, S., Nagata, T., Horio, T. and Hasebe, M.** (2005) Microtubule-dependent microtubule nucleation based on recruitment of gamma-tubulin in higher plants. *Nat Cell Biol*, **7**, 961-8.
- Mysore, K. S., Nam, J. and Gelvin, S. B.** (2000) An *Arabidopsis* histone H2A mutant is deficient in *Agrobacterium* T-DNA integration. *Proc Natl Acad Sci U S A*, **97**, 948-53.
- Nasmyth, K. and Haering, C. H.** (2005) The structure and function of SMC and kleisin complexes. *Annu Rev Biochem*, **74**, 595-648.
- Okada, M., Okawa, K., Isobe, T. and Fukagawa, T.** (2009) CENP-H-containing complex facilitates centromere deposition of CENP-A in cooperation with FACT and CHD1. *Mol Biol Cell*, **20**, 3986-95.

- Orphanides, G., Wu, W. H., Lane, W. S., Hampsey, M. and Reinberg, D.** (1999) The chromatin-specific transcription elongation factor FACT comprises human SPT16 and SSRP1 proteins. *Nature*, **400**, 284-8.
- Page, S. L. and Hawley, R. S.** (2001) c(3)G encodes a Drosophila synaptonemal complex protein. *Genes Dev*, **15**, 3130-43.
- Pastuglia, M., Azimzadeh, J., Goussot, M., Camilleri, C., Belcram, K., Evrard, J. L., Schmit, A. C., Guerche, P. and Bouchez, D.** (2006) Gamma-tubulin is essential for microtubule organization and development in Arabidopsis. *Plant Cell*, **18**, 1412-25.
- Pawlowski, W. P., Golubovskaya, I. N., Timofejeva, L., Meeley, R. B., Sheridan, W. F. and Cande, W. Z.** (2004) Coordination of meiotic recombination, pairing, and synapsis by PHS1. *Science*, **303**, 89-92.
- Pedersen, D. S. and Grasser, K. D.** (2010) The role of chromosomal HMGB proteins in plants. *Biochim Biophys Acta*, **1799**, 171-4.
- Puizina, J., Siroky, J., Mokros, P., Schweizer, D. and Riha, K.** (2004) Mre11 deficiency in Arabidopsis is associated with chromosomal instability in somatic cells and Spo11-dependent genome fragmentation during meiosis. *Plant Cell*, **16**, 1968-1978.
- Rabini, S., Franke, K., Saftig, P., Bode, C., Doenecke, D. and Drabent, B.** (2000) Spermatogenesis in mice is not affected by histone H1.1 deficiency. *Exp Cell Res*, **255**, 114-24.
- Rangasamy, D., Greaves, I. and Tremethick, D. J.** (2004) RNA interference demonstrates a novel role for H2A.Z in chromosome segregation. *Nat Struct Mol Biol*, **11**, 650-5.
- Redon, C., Pilch, D., Rogakou, E., Sedelnikova, O., Newrock, K. and Bonner, W.** (2002) Histone H2A variants H2AX and H2AZ. *Curr Opin Genet Dev*, **12**, 162-9.
- Reeves, R. and Adair, J. E.** (2005) Role of high mobility group (HMG) chromatin proteins in DNA repair. *DNA Repair (Amst)*, **4**, 926-38.
- Rhoades MM.** (1961) Meiosis. In *The cell*, ed. J Brachet, AE Mirsky, pp. 3:1-75. New York: Academic.

- Roeder, G. S.** (1990) Chromosome synapsis and genetic recombination: their roles in meiotic chromosome segregation. *Trends Genet*, **6**, 385-9.
- Rogakou, E. P., Pilch, D. R., Orr, A. H., Ivanova, V. S. and Bonner, W. M.** (1998) DNA double-stranded breaks induce histone H2AX phosphorylation on serine 139. *J Biol Chem*, **273**, 5858-68.
- Ross, K. J., Fransz, P., Armstrong, S. J., Vizir, I., Mulligan, B., Franklin, F. C. and Jones, G. H.** (1997) Cytological characterization of four meiotic mutants of *Arabidopsis* isolated from T-DNA-transformed lines. *Chromosome Res*, **5**, 551-9.
- Sanchez-Moran, E., Armstrong, S. J., Santos, J. L., Franklin, F. C. and Jones, G. H.** (2002) Variation in chiasma frequency among eight accessions of *Arabidopsis thaliana*. *Genetics*, **162**, 1415-22.
- Sanchez-Moran, E., Santos, J. L., Jones, G. H. and Franklin, F. C.** (2007) ASY1 mediates AtDMC1-dependent interhomolog recombination during meiosis in *Arabidopsis*. *Genes Dev*, **21**, 2220-33.
- Sanchez Moran, E., Armstrong, S. J., Santos, J. L., Franklin, F. C. and Jones, G. H.** (2001) Chiasma formation in *Arabidopsis thaliana* accession Wassileskija and in two meiotic mutants. *Chromosome Res*, **9**, 121-8.
- Sanchez-Moran E.** (2013) Genomics and chromatin packaging. *Annual Plant Reviews*, **46**, 123-156.
- Sand-Dejmek, J., Adelmant, G., Sobhian, B., Calkins, A. S., Marto, J., Iglehart, D. J. and Lazaro, J. B.** (2011) Concordant and opposite roles of DNA-PK and the "facilitator of chromatin transcription" (FACT) in DNA repair, apoptosis and necrosis after cisplatin. *Mol Cancer*, **10**, 74.
- Santisteban, M. S., Kalashnikova, T. and Smith, M. M.** (2000) Histone H2A.Z regulates transcription and is partially redundant with nucleosome remodeling complexes. *Cell*, **103**, 411-22.
- Sarma, K. and Reinberg, D.** (2005) Histone variants meet their match. *Nat Rev Mol Cell Biol*, **6**, 139-49.

- Salomon, S And Puchta, H.** (1998) Capture of genomic and T-DNA sequences during DSB repair in somatic plant cells. *EMBO J*, **17**, 6086-6095
- Schwarzacher, T.** (2003) Meiosis, recombination and chromosomes: a review of gene isolation and fluorescent in situ hybridization data in plants. *J Exp Bot*, **54**, 11-23.
- Sedbrook, J. C.** (2004) MAPs in plant cells: delineating microtubule growth dynamics and organization. *Curr Opin Plant Biol*, **7**, 632-40.
- Segal, E. and Widom, J.** (2009) From DNA sequence to transcriptional behaviour: a quantitative approach. *Nat Rev Genet*, **10**, 443-56.
- Siaud, N., Dray, E., Gy, I., Gerard, E., Takvorian, N. and Doutriaux, M.P.** (2004) Brca2 is involved in meiosis in *Arabidopsis thaliana* as suggested by its interaction with Dmc1. *EMBO J*, **23**, 1392-1401.
- Sgarra, R., Rustighi, A., Tessari, M. A., Di Bernardo, J., Altamura, S., Fusco, A., Manfioletti, G. and Giancotti, V.** (2004) Nuclear phosphoproteins HMGA and their relationship with chromatin structure and cancer. *FEBS Lett*, **574**, 1-8.
- Shrivastav, M., De Haro, L. P. and Nickoloff, J. A.** (2008) Regulation of DNA double-strand break repair pathway choice. *Cell Res*, **18**, 134-47.
- Sirotkin, A.M., Edelman, W., Cheng, G., Klein-Szanto, A., Kucherlapati, R., and Skoultchi, A.I.** (1995). Mice develop normally without the H1(0) linker histone. *Proc Natl Acad Sci U S A*, **92**, 6434-6438.
- Skop, A. R., Liu, H., Yates, J., 3rd, Meyer, B. J. & Heald, R.** (2004) Dissection of the mammalian midbody proteome reveals conserved cytokinesis mechanisms. *Science*, **305**, 61-6.
- Smirnova, E. A. and Bajer, A. S.** (1992) Spindle poles in higher plant mitosis. *Cell Motil Cytoskeleton*, **23**, 1-7.
- Smith, S. J., Osman, K. & Franklin, F. C.** (2014) The condensin complexes play distinct roles to ensure normal chromosome morphogenesis during meiotic division in *Arabidopsis*. *Plant J*, **80**, 255-68.

- Stack, S. M. and Anderson, L. K.** (2001) A model for chromosome structure during the mitotic and meiotic cell cycles. *Chromosome Res*, **9**, 175-98.
- Struk, S. and Dhonukshe, P.** (2014) MAPs: cellular navigators for microtubule array orientations in Arabidopsis. *Plant Cell Rep*, **33**, 1-21.
- Swarbreck, D., Wilks, C., Lamesch, P., Berardini, T. Z., Garcia-Hernandez, M., Foerster, H., Li, D., Meyer, T., Muller, R., Ploetz, L., Radenbaugh, A., Singh, S., Swing, V., Tissier, C., Zhang, P. and Huala, E.** (2008) The Arabidopsis Information Resource (TAIR): gene structure and function annotation. *Nucleic Acids Res*, **36**, D1009-14.
- Tamura, K., Adachi, Y., Chiba, K., Oguchi, K. and Takahashi, H.** (2002) Identification of Ku70 and Ku80 homologues in Arabidopsis thaliana: evidence for a role in the repair of DNA double-strand breaks. *Plant J*, **29**, 771-81.
- Tan, B. C., Chien, C. T., Hirose, S. and Lee, S. C.** (2006) Functional cooperation between FACT and MCM helicase facilitates initiation of chromatin DNA replication. *EMBO J*, **25**, 3975-85.
- Tang X, Frederick RD, Zhou J, Halterman DA, Jia Y, Martin GB** (1996) Initiation of plant disease resistance by physical interaction of AvrPto and Pto kinase. *Science* **274**:2060–2063.
- Tenea, G. N., Spantzel, J., Lee, L. Y., Zhu, Y., Lin, K., Johnson, S. J. and Gelvin, S. B.** (2009) Overexpression of several Arabidopsis histone genes increases agrobacterium-mediated transformation and transgene expression in plants. *Plant Cell*, **21**, 3350-67.
- Tetko, I. V., Haberer, G., Rudd, S., Meyers, B., Mewes, H. W. and Mayer, K. F.** (2006) Spatiotemporal expression control correlates with intragenic scaffold matrix attachment regions (S/MARs) in Arabidopsis thaliana. *PLoS Comput Biol*, **2**, e21.
- Turner, B. M.** (2005) Reading signals on the nucleosome with a new nomenclature for modified histones. *Nat Struct Mol Biol*, **12**, 110-2.
- Tzfira T, Li J, Lacroix B. and Citovsky V** (2004) Agrobacterium T-DNA integration: molecules and models. *Trends Genet* , **20**, 375-383
- Tzfira, T. and Citovsky, V.** (2006) Agrobacterium-mediated genetic transformation of plants: biology and biotechnology. *Curr Opin Biotechnol*, **17**, 147-54.

Uanschou, C., Siwiec, T., Pedrosa-Harand, A., Kerzendorfer, C., Sanchez- Moran, E., Novatchkova, M., Akimcheva, S., Woglar, A., Klein, F. and Schlogelhofer, P. (2007) A novel plant gene essential for meiosis is related to the human CtIP and the yeast COM1/SAE2 gene. *EMBO J*, **26**, 5061-5070.

Valentine, L. (2003) *Agrobacterium tumefaciens* and the plant: the David and Goliath of modern genetics. *Plant Physiol*, **133**, 948-55.

Valls, E., Sanchez-Molina, S. and Martinez-Balbas, M. A. (2005) Role of histone modifications in marking and activating genes through mitosis. *J Biol Chem*, **280**, 42592-600.

Van Attikum, H., Bundock, P. and Hooykaas, P. J. (2001) Non-homologous end-joining proteins are required for *Agrobacterium* T-DNA integration. *EMBO J*, **20**, 6550-8.

Van Attikum, H., Fritsch, O., Hohn, B. and Gasser, S. M. (2004) Recruitment of the INO80 complex by H2A phosphorylation links ATP-dependent chromatin remodeling with DNA double-strand break repair. *Cell*, **119**, 777-88.

Van Damme, D. and Geelen, D. (2008) Demarcation of the cortical division zone in dividing plant cells. *Cell Biol Int*, **32**, 178-87.

Van Damme, D., Vanstraelen, M. and Geelen, D. (2007) Cortical division zone establishment in plant cells. *Trends Plant Sci*, **12**, 458-64.

Varga-Weisz, P. D. and Becker, P. B. (2006) Regulation of higher-order chromatin structures by nucleosome-remodelling factors. *Curr Opin Genet Dev*, **16**, 151-6.

Vazquez, J., Belmont, A. S. and Sedat, J. W. (2002) The dynamics of homologous chromosome pairing during male *Drosophila* meiosis. *Curr Biol*, **12**, 1473-83.

Wang, Z., Zang, C., Cui, K., Schones, D. E., Barski, A., Peng, W. and Zhao, K. (2009) Genome-wide mapping of HATs and HDACs reveals distinct functions in active and inactive genes. *Cell*, **138**, 1019-31.

Wasteneys, G. O. and Ambrose, J. C. (2009) Spatial organization of plant cortical microtubules: close encounters of the 2D kind. *Trends Cell Biol*, **19**, 62-71.

Waterworth, W.M., Altun, C., Armstrong, S.J., Roberts, N., Dean, P.J., Young, K., Weil, C.F., Bray, C.M. and West, C.E. (2007) NBS1 is involved in DNA repair and plays a

synergistic role with ATM in mediating meiotic homologous recombination in plants. *Plant J*, **52**, 41-52.

Wang, W. (2012) A variant of the breast cancer type 2 susceptibility protein (BRC) repeat is essential for the RECQL5 helicase to interact with RAD51 recombinase for genome stabilization. *J Biol Chem*, **287**, 23808-18.

West, C. E., Waterworth, W. M., Sunderland, P. A. and Bray, C. M. (2004) Arabidopsis DNA double-strand break repair pathways. *Biochem Soc Trans*, **32**, 964-6.

Wierzbicki, A. T. and Jerzmanowski, A. (2005) Suppression of histone H1 genes in Arabidopsis results in heritable developmental defects and stochastic changes in DNA methylation. *Genetics*, **169**, 997-1008.

Windels, P., De Buck, S., Van Bockstaele, E., De Loose, M. and Depicker, A. (2003) T-DNA integration in Arabidopsis chromosomes. Presence and origin of filler DNA sequences. *Plant Physiol*, **133**, 2061-8.

Winey, M., Mamay, C. L., O'toole, E. T., Mastronarde, D. N., Giddings, T. H., Jr., McDonald, K. L. and McIntosh, J. R. (1995) Three-dimensional ultrastructural analysis of the *Saccharomyces cerevisiae* mitotic spindle. *J Cell Biol*, **129**, 1601-15.

Winkler, D. D. and Luger, K. (2011) The histone chaperone FACT: structural insights and mechanisms for nucleosome reorganization. *J Biol Chem*, **286**, 18369-74.

Woodcock, C. L. and Dimitrov, S. (2001) Higher-order structure of chromatin and chromosomes. *Curr Opin Genet Dev*, **11**, 130-5.

Yelagandula, R., Stroud, H., Holec, S., Zhou, K., Feng, S., Zhong, X., Muthurajan, U. M., Nie, X., Kawashima, T., Groth, M., Luger, K., Jacobsen, S. E. & Berger, F. (2014) The histone variant H2A.W defines heterochromatin and promotes chromatin condensation in Arabidopsis. *Cell*, **158**, 98-109.

Yi, H., Mysore, K. S. and Gelvin, S. B. (2002) Expression of the Arabidopsis histone H2A-1 gene correlates with susceptibility to Agrobacterium transformation. *Plant J*, **32**, 285-98.

Yi, H., Sardesai, N., Fujinuma, T., Chan, C. W., Veena and Gelvin, S. B. (2006) Constitutive expression exposes functional redundancy between the Arabidopsis histone H2A gene HTA1 and other H2A gene family members. *Plant Cell*, **18**, 1575-89.

Yu, H.G. and Koshland, D. (2005) Chromosome morphogenesis: Condensin dependent cohesin removal during meiosis. *Cell*, **123**, 397-407.

Yu, H.G. and Koshland, D.E. (2003) Meiotic condensin is required for proper chromosome compaction, SC assembly, and resolution of recombination-dependent chromosome linkages. *J Cell Biol*, **163**, 937-947.

Zeng, S. X., Li, Y., Jin, Y., Zhang, Q., Keller, D. M., Mcquaw, C. M., Barklis, E., Stone, S., Hoatlin, M., Zhao, Y. and Lu, H. (2010) Structure-specific recognition protein 1 facilitates microtubule growth and bundling required for mitosis. *Mol Cell Biol*, **30**, 935-47.

Zhang, L., Tao, J., Wang, S., Chong, K. and Wang, T. (2006) The rice OsRad21-4, an orthologue of yeast Rec8 protein, is required for efficient meiosis. *Plant Mol Biol*, **60**, 533-54.

Zhang, S. B., Huang, J., Zhao, H., Zhang, Y., Hou, C. H., Cheng, X. D., Jiang, C., Li, M. Q., Hu, J. and Qian, R. L. (2003) The in vitro reconstitution of nucleosome and its binding patterns with HMG1/2 and HMG14/17 proteins. *Cell Res*, **13**, 351-9.

Zalevsky J, MacQueen AJ, Duffy JB, Kempfues KJ, Villeneuve AM. (1999) Crossing over during *Caenorhabditis elegans* meiosis requires a conserved MutS-based pathway that is partially dispensable in budding yeast. *Genetics* , **153**, 1271–1283.

Zeng, X. S., Dai, Mu-Shui., Keller, M. D., Lu, M. D. (2002) SSRP1 functions as a coactivator of the transcriptional activator p63. *EMBO J*, **21**, 5487-5497.

Zhu, Y., Nam, J., Humara, J. M., Mysore, K. S., Lee, L. Y., Cao, H., Valentine, L., Li, J., Kaiser, A. D., Kopecky, A. L., Hwang, H. H., Bhattacharjee, S., Rao, P. K., Tzfira, T., Rajagopal, J., Yi, H., Veena, Yadav, B. S., Crane, Y. M., Lin, K., Larcher, Y., Gelvin, M. J., Knue, M., Ramos, C., Zhao, X., Davis, S. J., Kim, S. I., Ranjith-Kumar, C. T., Choi, Y. J., Hallan, V. K., Chattopadhyay, S., Sui, X., Ziemienowicz, A., Matthyse, A. G., Citovsky, V., Hohn, B. and Gelvin, S. B. (2003) Identification of *Arabidopsis* rat mutants. *Plant Physiol*, **132**, 494-505.

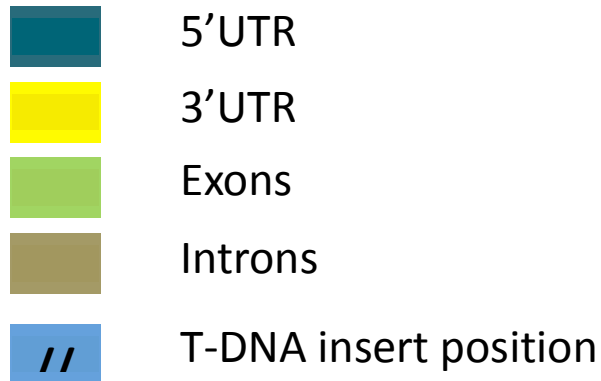
Zickler, D. and Kleckner, N. (1999) Meiotic chromosomes: integrating structure and function. *Annu Rev Genet*, **33**, 603-754.

APPENDIX

Appendix A: Full genomic DNA of H2A1 gene (RAT5) (At5g54640)

Other names:

HTA1, RAT5, ATHTA1, MRB17.14, MRB17_14, HISTONE H2A 1, RESISTANT TO AGROBACTERIUM TRANSFORMATION 5



Full genomic DNA:

```

GTACATCAATATTTTGCATTATCTCTGTTCCCTAATAAAGTAACACTGTAGTATTTACATCATATCGACTTCAAAACATGAAGGAATGGATGA
CAATAACAGTTTCGTAAATGATCAAAACACAATAACTCTAATCTGAATTTGTGAGTTTGTCAAACCTTGAAAGTGCAATTTATTACGAATGTAGA
TATCGCAAAGGGTAGATAATGGAAGTAGGTGTGGGTGTCGTTATAGCCATATTGAATTCAAAAGGAAAGACATTAATAGAAATGAATTTT
GAAACATGTTGATAGATCATGTCCTTCTTCTGGGTTACCCAGTTTTCGCCATAAACCTAAAACCAACAGGACCATCATTTTCGACCTCAGCCACA
TTGACTGGTCTGCCCAATCTAGCTATGATATCTTAATTTCCGTATGACTTGGATCCATAAATATTGAAATAGATTTGGTGAACACAATTT
ACTCTTAAAACCTTCTTCTTTCATGCAATGTTCTTTTCTCACTTAAACATTTTTATATAGTGACATTTTATAGTAATCCAACGTTATTTATAT
GATAGTAATTCATCAAATTTATATAGTGATAAAATCCACAATGGTTGTCAATAAAAAATATGAACAACACAATAGAAATAGTAAAAGTGAC
TATGTTAAATCATTTTCTTCGCTGGGTTTGGTGGCGAGTTCATAACCCATAAGCGGCCCATTTACTTCGTAACCTCAATTCGATTTGTTCA
GCGTCCCAAGCCATAATATATTTCAAGGGCATAAAATAAATGAGGTTTATATGAAAAATTTGAAATTTCCCTCGTCCAGAAGAAACCAA
CAAAACGCAAAAGTTCAAGCGTGGGAGAAAAACTTCAGATCGTAGCCATTCATTAATTAATCAACGGTTTAAACCTCTTCGATCCG
CGTACTCTATTCTTATTGGTCAAATAACTTAA
TCCTCCAACATATATAACAACAATCAGATTTCTCTCTGTTAATTTTCGTCAGAAAAAAATTCGATTTTTTTGCG
GCTCTTTGTGGGTTGTTGTTGTTGAAAATGCTGGTCTGGAAAAACTCTGGATCCCGTGGGGCGAAGAAAGCTACATCTCGGAGTAGCAAAG
CCGGTCTTCAATTTCCCGTGGGTCGTATCGCTCGTTTCTTAAAAGCCGGTAAATACGCCGAACGTTGGTGGCCGGTCTCCGGTTATCTCGC
CGCCGTTCTCGAATATTTGGCCGCC dna GAGGTAAAATTACATCGTCTTTTCTCTCTTTCCCATCCGTTTCCGATCTTATTCGTCTGACTCT
GTTTTTGGCTGATCGATTACGAATCTAGGTTCTTACATTTTCCGAATTTGACATGCAAAAAATGAAATTAGATTCTGTTTGAATGAATGTT
GTAGTTCTGTAATGACCTAATTTGGGTTGTTCTGATTGGTTGATGGTAATCGAGATCATATGAATCGTTGTAGTTTCTCGCAAGATTCTA
AATTTTTTCAATTATGGTAACCAATTTGATTTGAGTTGTTAAAGTCTCAAATTTGAAAGTTTGTATCATGAATTTGTGTGTTTTGAATTTGTT
CAGGTCTTGAATTAGCTGGAAACGCAGCAAGAGACAACAAGAAGACAGTATTTGTTCTCGTCACATTCAGCTTGGCGTCAGAAACGATGAGG
AGCTAAGCAAGCTTCTTGGAGATGTGACGATTGCTAATGGAGGAGTGATGCCTAACATCCACAATCTCCTTCTCCCTAAGAAGGCTGGTGTCTC
AAAGCCTCAGGAAGAT TAGGTCTTTTAAACACAATGATATAGAACCGTCTCTCTTTTGGCTTTAGATCTAATAACCTAATAACTAGCTAGATGT
TTTCACTTTTTGTATCTTTGCTTTTTTAAATTCCTTTAGGATTTGTTTCTTCCGTTTCTGTTTTCGACATGTTTCTGTTTTGTGAATAT
ATGAAAGTATTTTGCAGAAATATGAATGATAATGTCTTTCAAAA

```

CDS:

```

ATGGCTGGTCTGGAAAAACTCTGGATCCGGTGGGGCGAAGAAAGCTACATCTCGGAGTAGCAAAGCCGGTCTCAATCCCGGTGGGTCGTATCGCTC
GTTCTTAAAAGCCGGTAAATACGCCGAACGTGTTGGTGGCGGTGCTCCGTTTATCTCGCCCGTTCTCGAATATTTGGCCCGGAGGTTCTGAATTA
GCTGAAACGCAGCAAGAGACAACAAGAAGACAGTATTGTTCTCTGTCACATTACGCTTGGGTGTCAGAAACGATGAGGAGCTAAGCAAGCTCTTGA
GATGTGACGATTGCTAATGGAGGAGTGATGCCTAACATCCACAATCTCTTCTCCCTAAGAAGGCTGGTCTTCAAGCCTCAGGAAGATTAG

```

Full length of cDNA:

```

GTTAATTTTCGTCAGAAAAAAATTCGATTTTTTGGCTCTTTGTTGGGTTGTTGTTGTTGAAAAATGGCTGGTCTGGAAAAACTCTGGATCCGGTGGGGC
GAAGAAAGCTACATCTCGGAGTAGCAAAGCCGGTCTTCAATCCCGTGGGTCGTATCGCTCGTTTCTAAAAGCCGGTAAATACGCCGAACGTTGGT

```

```
GCCGGTGCTCCGGTTATCTCGCCCGCTTCTCGAATATTTGGCCCGGAGGTTCTTGAATTAGCTGGAAACGCAGCAAGAGACAACAAGAAGACACGTA
TTGTTCTCGTACATTCAGCTTGCAGTTCAGAAACGATGAGGAGCTAAGCAAGCTTCTGGAGATGTGACGATTGCTAATGGAGGAGTGATGCCTAACAT
CCACAATCTCCTTCCCTAAGAAGGCTGGTGCTCAAAGCCTCAGGAAGATTAGGTCTTTAACACAATGATATAGAACACGTCTCTCTTTGGCTTTAGA
TCTAATAACCTAATAACTAGCTAGATGTTTTCACTTTTGTATCTTTGCTTTTTTAATTCCTTAGGGATTGTTTTCTTCCGTTTCTGTTTCGACATGTTGTT
CTGTTTTGTGAATATATGAAAGTATTTTGGCAAATATGAATGATAATGTCTTTCAAAAA
```

>SALK_040809.18.50.x

```
AAAAATCAATGTTTTTTCGCTCTTTGGGGGGGAGTTGTTGTTGAACTGGCTGGACATGGAA
CACCTCTTGGATACGGTGGGGCCAATAATGCTACATCTCTGAGTGGCTACCCGGTCTTCA
ATTCTCTGCGGGCGCTATCACTTCTGTCTTATAGCCGGTATCTACTCCAAACGGGATGGT
GCCGGTGCTCCGGTTTACCTCGCCCGCTTCTCGACCATTGGCCGCC
```

```
SALK_040809.18.50.x PRODUCT_SIZE 1014 PAIR_ANY_COMPL 0.00 PAIR_3'_COMPL
0.00 DIFF_TM 0.23 LP CACACCACATTGACTGGTCTG Len 21 TM 60.06 GC 52.38
SELF_ANY_COMPL 0.23 3'_COMPL 0.00 RP ATTTTTGCATGTCAAATTCGG Len 21 TM
59.82 GC 33.33 SELF_ANY_COMPL 0.23 3'_COMPL 0.00 Insertion chr5
22196495 BP+RP_PRODUCT_SIZE 468-768
```

Appendix B: pEarleGate PEG205 vector

This vector is Kan resistant in Bacteria and Basta resistant in Plant. It was used for the transformation of the T-DNA integration from *Agrobacterium tumefaciens* into plants (*Arabidopsis*). Insertion sequence is shown as follows:

>PrsS1, poppy pistil S1

```
ATG AACATATTTTATGTTATTGTGCTGCTATCGTTCTTCTGTCCAAGTCAAGCGGT TTC TTTCTGTTATTGAGGTGCGTATAATGAACAGAA
GAGGTAACGGGA EGAGCATTGGCATCCATGCCC ATCCAAAGATAATGATCTTCAAACCAAACAGTGACATCTGGTCATGACATGAGTTTTTC
ATTTAGGGAAGATTTTTCCATACAACCTCACTTCTATTGTGACCTACAATGGGATAAAGAAACAAAGTTCGGGTTTTATTCTATCAGGCAAAG
AGGGATGATGACGGTAGGTGCTCTT CCAGTGCCTCTGGAAAGATAATGC ATGATGGTTTATACGGTTTTGATCAGGAGCATCAGATCTGGCAGA
TTTACCATTTGATAAAGAAAGAAAGGAAGGAAGGTCGAACC TGA
```


CTAAGTTATGGCATGTAGTAAACGTTGGACCTTTAGTTGTTTGGAGTTAACCAGATTTTTCTCTTTGACCTTAAAGATCTGTGTACTTCTTA
 GAAAAGAAGAGCCTGTCTTTACCTCAAAATATAGAGTACTCTGGTAAGGCCATAGCTAAGAAGCAACAAAACAGATCGTGTCTTATCGAAATT
 GTTATACAAGAGGTTCTGTATGATGAAAGTTATGGACAAGAAGCATCTAAAACCTTATGGACAATGGGACGAGCTTTACACATAGCTTGCAACG
 ATGTAGCTTTTCGCATTTGTGGTCTCTTTTCACCTTCTCTCATGTCTAGATACTTTTCTCAACCTCTCCCACCTCAAAACATTTGGACCAATGA
 TCCAAGAGCCAAAGTCACTAGCCGTTGAGCTAGCCCTGAACCAGGGCAAGATCGTCTCAATCCCAAATGGCATCAACTTTTTATCCTCTCCT
 TTTTCTCAAACCTCTCCGGCTTAAATTTTCTGGCTCTTCCATAACTTTGGATCTCTATGGATGGCCCATGC

CDS for *SSRP1* gene

ATGGCGGACGCCACTCCTTCAATAATATCTCTCTCAGCGGTTCGCGGTGGAAAGAACCCGGGTTTACTTAAAATCAATTCTGGAGGAATTCAAT
 GGAAGAAACAAGTGGTGGAAAAGCTGTGGAAGTTGATAGATCTGATATTGTAAGTGTAGTTGGACGAAAGTGACAAAGAGTAATCAATTGGG
 AGTCAAAACCAAGATGGATTGTACTACAAGTTCGTTGGATTTCGAGATCAGGATGTTCCAAGTCTGTCTAGCTTTTCCAAAGTCTTATGGA
 AAAACACCGGATGAGAAGCAATTATCAGTTAGTGGTCTAATTTGGGAGAGGTGGATTTACACGGGAATACACTAACCTTTTGGTTGGATCAA
 AACAGCTTTTGAAGTATCTTTAGCTGATGTTTACAGACTCAGCTTCAAGGGAAAAATGATGTTACTTTGGAGTTTCATGTTGATGATACTGC
 TGGTGCTAATGAGAAAGACTCGCTGATGGAGATTAGTTTTCATATTCCTAATTCACACTCAGTTTGTGGTGATGAAAACCGTCCACCTTCT
 CAAGTTTTCAATGACACAATCGTTGCAATGGCTGATGTTAGTCTGGAGTTGAGGATGCGGTCGTCACATTTGAGAGTATTGCAATCCTCACAC
 CCAGGGGTCGGTACAATGTGGAACCTTCACTTTTCTTTCTTACGATTGCAAGGACAAAGCTAATGACTTTAAAATCCAGTACAGTAGCGTTGTCCG
 TTTGTTCTTGCTTCCAAAGTCAAAACCAACCACACAGTTTGTGTTATCTCTCTAGACCCACCAATCCGGAAAGACCGTTGTCGAAAGTGAAC
 GTCATTAGTGTGAACTTATGAATACAAAGTCAAGGACAAGCTGGAGCGATCATATAAGGGTCTCATTCATGAAGTATTCACCACCGTGTG
 CGTTGGCTGTCTGGTGCAAGATCACTAAACCTGGGAAGTTCCGAGTTCCTCAAGATGGGTTTGAGTGAATCGTCTCTCAAGGAGAAAGATG
 GGGTCTTTATCCACTCGAGAAGGGATTTTCTTCTTACCTAAACCTCCAACGCTTATACTTACGATGAGATTGACTATGTCGAGTTTGAAG
 GCATGCTGCTGGTGGTGCATACATGCTTACTTTGATCTTCTCATAAGACTGAAAACCTGACCATGAACATCTGTTCCGTAACATTCAAAGAAAT
 AGTATCACAATCTTATACCTTATAAGCTCTAAGGGTTTGAAGATTATGAACCTTGGAGGTGCGGGTACCCGACAGCGGTGTTGCTGCTGTT
 TTGGGATAAATGATGATGATGATGCTGTTGACCTCATCTTACGCGTATCAGAAAACCAAGCTGCTGATGAGAGTATGAGGAGGACGAAGACTT
 TGTATGGGTGAGGATGATGATGGTGGTTCACCAACTGATGATCTGCGGGGACGACTCTGATGCTAGTGAAGGCGGTGAGGAGAGATAAAA
 GAGAAATCTATCAAGAAGGAACCTAAGAAAAGAGCTTCGTCATCGAAAGGATTGCCTCCTAAGAGGAAAACCTGTAGCCGACAGCAAGGCAGTA
 GTAAGAGGAAGAAGCCGAAGAAGAAGAAGGATCCCAACGCACCAAAAAGACCAATGTCTGGTTTCATGTTCTTTTCCAAATGGAAGAGATAA
 CATAAAGAAGGAACCCAGGAATAGCATTTGGAGAGGTGGGAAAGGTGCTTGGAGATAAGTGGCGTCAAATGCTGCTGATGATAAAGAGCCA
 TATGAAGCAAGGCTCAAGTCGACAAGCAGGATACAAGGATGAGATCAGTGATTACAAGAACCCTCAGCCGATGAATGTGGACTCAGGAAACG
 ATCCGATAGTAACATA

>SALK_001283.13.60.x

AAAGCAGTGGGTTATTCAGGGCTGCGGTGCAGGCCTCGTTGAACAATTACCATGGCCTTT
 GGGGGCGGATTTGTAGGGGGATTGATGGGAGCTCCATGACTTATACATCGTGCCCGCCCG
 GCCGCTTCGCATGGGGGTGGGCGGGGGGTGCGGTCCCGTCCCGCGGGGCTGGTGTGC
 GAGCGTCACGGGGGGGGGGTGGTGGGGGGGGGAGGGCGGTGCGGTGGGCGCGGCACGC
 TGGGTGGGGGGGGTGGGCGTGTGCCCGGTGGGGGGTGGCGGGTGGGGGGTGGATGG
 GGGGGGTCCCAGAGCGCGGGTGGCCCGGTGGGGGGCCGGAGTGTGGGCGGGC
 GGGCCGTTGCGGTGTGCGGGGGGCGGTGGGGTGGGTGGCGGGTGGGGTGTGCGCCGCG
 GGGTGTGGCGGCACGAGAGATGTGGCGGTGTGCGGTG

Appendix D: Full genomic DNA of *hSSRP1* gene in human

>gi|28416943|ref|NM_003146.2| Homo sapiens structure specific recognition protein 1 (SSRP1), mRNA

GTACGGCTTCCGGTGGCGGGACGCGGGGCCGCGCACGCGGGAAAAGCTTCCCCGGTGTCCCCCATCCCCCTCCC
 CGCGCCCCCCCCCGGTCCCCCAGCGCGCCACCTCTCGCGCCGGGGCCCTCGCGAGGGCCGACGCTGAGGAGAT
 TCCCAACCTGCTGAGCATCCGCACACCCACTCAGGAGTTGGGGCCAGCTCCCAGTTTACTTGGTTTCCCTTGTG
 CAGCCTGGGGCTCTGCCAGGCCACCACAGGCAGGGTTCGACATGCGAGAGACACTGGAGTTCAACGACGTCTAT
 CAGGAGGTGAAAGGTTCCATGAATGATGGTCTGACTGAGGTTGAGCCGTCAGGCATCATCTTCAAGAATAGCAAG
 ACAGGCAAAGTGGACAACATCCAGGCTGGGGAGTTAACAGAAGGTATCTGGCGCGGTGTTGCTCTGGGCCATGGA

CTTAAACTGCTTACAAAGAATGGCCATGTCTACAAGTATGATGGCTTCCGAGAATCGGAGTTTGAGAACTCTCT
GATTTCTTCAAACACTACTATCGCCTTGAGCTAATGGAGAAGGACCTTTGTGTGAAGGGCTGGAACGGGGGACA
GTGAAATTTGGTGGCAGCTGCTTTTCTTTGACATTGGTGACCAGCCAGTCTTTGAGATACCCCTCAGCAATGTG
TCCCAGTGCAACCACAGGCAAGAATGAGGTGACACTGGAATTCACCAAAAACGATGACGCAGAGGTGTCTCTCATG
GAGGTGCGCTTCTACGTCCCACCCACCCAGGAGGATGGTGTGGACCCTGTTGAGGCCCTTGCCCAAGATGTGTTG
TCAAAGGCGGATGTAATCCAGGCCACGGGAGATGCCATCTGCATCTTCCGGGAGCTGCAGTGTCTGACTCCTCGT
GGTCGTTATGACATTCCGATCTACCCACCTTTCTGCACCTGCA TGGCAAGACCTTTGACTACAA GATCCCTAC
ACCACAGTACTGCGTCTGTTTTTGTACCCACAAGGACCAGCGCCAGATGTTCTTTGTGATCAGCCTGGATCCC
CCAATCAAGCAAGGCCAAACTCGCTACCACTTCTTGATCCTCCTCTTCTCCAAGGACGAGGACATTTTCGTTGACT
CTGAACATGAACGAGGAAGAAGTGGAGAAGCGCTTTGAGGGTTCGGCTCACCAAGAACATGTCAGGATCCCTCTAT
GAGATGGTCAGCCGGGTTCATGAAAAGCACTGGTAAACCGCAAGATCACAGTGCCAGGCAACTTCCAAGGGCACTCA
GGGGCCAGTGCATTACCTGTTCTACAAGGCAAGCTCAGGACTGCTCTACCCGCTGGAGCGGGGCTTCATCTAC
GTCCACAAGCCACCTGTGCACATCCGCTTCGATGAGATCTCCTTTGTCAACTTTGCTCGTGGTACCCTACTACT
CGTTCCTTTGACTTTGAAATTGAGACCAAGCAGGGCACTCAGTATACCTTCAGCAGCATTGAGAGGGAGGAGTAC
GGGAAACTGTTTGATTTTGTCAACGCGAAAAAGCTCAACATCAAAAAACCGAGGATTGAAAGAGGGCATGAACCCA
AGCTACGATGAATATGCTGACTCTGATGAGGACCAGCATGATGCCTACTTGGAGAGGATGAAGGAGGAAGGCAAG
ATCCGGGAGGAGAATGCCAATGACAGCAGCGATGACTCAGGAGAAGAAACCGATGAGTCAATCAACCCAGGTGAA
GAGGAGGAAGATGTGGCAGAGGAGTTTGACAGCAACGCCTCTGCCAGTCTCCTCCAGTAATGAGGGTGACAGTGAC
CGGGATGAGAAGAAGCGGAAACAGCTCAAAAAGGCCAAGATGGCCAAGGACCGCAAGAGCCGCAAGAAGCCTGTG
GAGGTGAAGAAGGGCAAAGACCCCAATGCCCCAAGAGGCCCATGTCTGCATACATGCTGTGGCTCAATGCCAGC
CGAGAGAAGATCAAGTCAGACCATCCTGGCATCAGCATCACGGATCTTTCCAAGAAGGCAGGCGAGATCTGGAAG
GGAATGTCCAAAGAGAAGAAAGAGGAGTGGGATCGCAAGGCTGAGGATGCCAGGAGGGACTATGAAAAAGCCATG
AAAGAATATGAAGGGGGCCGAGGCGAGTCTTCTAAGAGGGACAAGTCAAAGAAGAAGAAGAAAGTAAAGGAAAGA
TGAAAAGAAATCCACGCCCTCTAGGGGCTCATCATCCAAGTCGTCTCAAGGCAGCTAAGCGAGAGCTTCAAGA
GCAAAGAGTTTGTGTCTAGTGATGAGAGCTCTTCGGGAGAGAACAAGAGCAAAAAGAAGGGAGGAGGAGCGAGGA
CTCTGAAGAAGAAGAACTAGCCAGTACTCCCCCAGCTCAGAGGACTCAGCGTCAGGATCCGATGAGTAGAAACG
GAGGAAGGTTCTCTTTGCGCTTGCCTTCTCACACCCCCGACTCCCCACCATATTTTGGTACCAGTTTCTCCTC
ATGAAATGCAGTCCCTGGATTCTGTGCCATCTGAACATGCTCTCCTGTTGGTGTGTATGTCACTAGGGCAGTGGG
GAGACGTCTTAACTCTGCTGCTTCCCAAGGATGGCTGTTTATAATTTGGGGAGAGATAGGGTGGGAGGCAGGGCA
ATGCAGGATCCAAATCCTCATCTTACTTTCCCGACCTTAAGGATGTAGCTGCTGCTTGTCTGTTCAAGTTGCTG
GAGCAGGGGTCTATGTGAGGCCAGGCCTGTAGCTCCTACCTGGGGCTATTTCTACTTTTCATTTTGTATTTCTGGT
CTGTGAAAATGATTTAATAAAGGGAAGTACTTTGGAAACCAAAAAA

S13490 Sense GCAAGACCUUUGACUACAATT

S13490 Antisense TTGTAGTCAAAGGTCTTGCCA

s13490 DUPLEX TARGETED EXON 6

GCAAGACCUUUGACUACAATT

|||||

ACCGUUCUGGAAACUGAUGTT

S13491 Sense GGACUAAACUGCUUACAATT

S13491 Antisense UUGUAAGCAGUUUAAGUCCAT

S13491 DUPLEX TARGETED EXON 3

GGACUAAACUGCUUACAATT

|||||

TACCUGAAUUGACGAAUGUU

Participation in International Scientific Conferences:

1. UK Plant Science 2012 Meeting, on 18th and 19th April 2012. **“Role of high mobility group protein (HMG) in eukaryotes”**. (*Poster Presentation*).
2. British Meiosis Group Meeting, on 28th March 2012 in Norwich. **“Role of high mobility group protein (HMG) in eukaryotic organisms”**. (*Poster Presentation*).
3. 5th British Meiosis Conference at the University of Cambridge, on 27th and 28th March 2013. **“H2A.X role in homologous recombination in eukaryotic”**. (*Invited Speaker*).
4. PhD students Open Day at the University of Birmingham, on 2nd Jun 2012. (*Poster Presentation*).
5. Postgraduate Open Day, on Tuesday 20th November 2012. (*Poster Presentation*).
6. Student Symposium 15th – 16th April 2013 at University of Birmingham. **“Chromosome axis protein (HMGA-like), SSRP1 and H2A1 have essential role in recombination and fertility”**. (*Invited speaker*).
7. Cell Division Conference at the School of Biosciences University of Birmingham, on Monday 10th June 2013. **“Chromosome axis protein (HMGA-like), SSRP1 and H2A1 have essential role in recombination and fertility”**. (*Poster Presentation*).
8. EMBO Meiosis Meeting in Dresden (Germany), on 14th to 19th September 2013. **“Essential roles of two chromatin proteins (H2A.1 and SSRP1 in eukaryotic fertility”**. (*Poster Presentation*).
9. British Meiosis Meeting at the university of Edinburgh, on 24-25 March 2014. **“Structure-Specific Recognition Protein 1 (SSRP1) has an essential role in DNA repair and meiotic chromosome segregation in humans and plants”**. (*Poster Presentation*).
10. 20th International Chromosome Conference (50th Anniversary) at the university of Kent, Canterbury, UK, on 1st-5th September 2014. **“Essential roles of two chromatin proteins in *Arabidopsis thaliana* fertility and humans”**. (*Poster Presentation*).
11. British Meiosis Meeting at the university of Newcastle, on 23-24 February 2015. **“The role of some chromatin components in chromosome dynamic in humans and plants”**. (*Poster Presentation*).

Other scientific activities

Co-organizer for the student chromatin research symposium, 2011, University of Birmingham, UK.